NOTE TO USERS

This reproduction is the best copy available.

From intracellular localization to proteolytic cleavage - functional significance of protein tyrosine phosphatase PEST regulatory mechanisms

Maxime Hallé

A thesis submitted to McGill University in partial fulfillment of the requirements of the degree of Doctor of Philosophy

Department of Biochemistry

McGill Cancer Center

McGill University

Montréal, Québec, Canada

Your file Votre référence
ISBN: 978-0-494-66305-9
Our file Notre référence
ISBN: 978-0-494-66305-9

ABSTRACT

Altered cytoskeletal regulation impacts numerous physiological phenomena: cell motility, apoptosis, oncogenic transformation and parasitic infection. The protein tyrosine phosphatase (PTP)-PEST contains multiple motifs mediating its recruitment to signalling components, and is required for actin filament organization. However, little is known regarding either the importance of PTP-PEST subcellular localization, or the role of PTP-PEST in either parasitic infection or apoptosis. My doctoral research was therefore focussed on elucidating the effect of subcellular distribution on PTP-PEST activity, specifically with respect to regulation of p130Cas (a PTP-PEST substrate), as well as on the involvement of PTP-PEST in both host-pathogen relations and apoptosis. First, PTP-PEST was found both within the cytosol and at the plasma membrane. Using *PTP-PEST -/-* rescued cell lines, I observed that tyrosine phosphorylation-dependent p130Cas interactions were controlled primarily by cytosolic PTP-PEST. Secondly, infection of fibroblasts with *Leishmania major* was observed to induce dramatic actin rearrangements, and to alter the phosphorylation state of numerous proteins. Importantly, both PTP-PEST and p130Cas were processed by the parasitic protease GP63 during infection. GP63 was also required for the cleavage of additional host proteins: cortactin, TC-PTP and caspase-3. Of note, *Leishmania* parasites mediated p38 inactivation, correlating with the proteolysis of its upstream activator TAB1, in a GP63-dependent manner. These results indicate that GP63 plays a key role in a number of biochemical events, potentially contributing to *Leishmania* infectivity. Finally, PTP-PEST was found to relocalize to the edges of retracting membrane ruffles of apoptotic cells. Surprisingly, PTP-PEST was specifically cleaved by caspase-3 at the ^{549}DSPD motif during apoptosis; leading to modification of catalytic activity and scaffolding properties, and sensitizing cells to Fas-mediated detachment. As this data demonstrated a potential role for caspase cleavage in PTP regulation, I also investigated the presence of conserved putative caspase-cleavage sites in other family members. In summary, the data presented herein links PTP-PEST with various biological processes: oncogenic signalling,

host-pathogen interactions, and apoptosis. In addition to demonstrating the involvement of PTP-PEST in diverse signalling pathways, these studies underscore the importance of subcellular localization and proteolysis in the regulation of this PTP.

RÉSUMÉ

Les modifications dans la dynamique du cytosquelette ont un impact sur de nombreux phénomènes physiologiques tels que la mobilité cellulaire, l'apoptose, l'oncogenèse et le parasitisme. La protéine tyrosine phosphatase (PTP)-PEST contient plusieurs motifs permettant le recrutement de composantes signalétiques. Celle-ci est requise pour l'organisation du réseau d'actine. Toutefois, l'importance fonctionnelle de la localisation cellulaire de la PTP-PEST, ainsi que son rôle dans les infections parasitaires et l'apoptose ont été peu décrits. Les travaux présentés dans cette thèse portent sur la compréhension des effets de la distribution cellulaire de PTP-PEST sur son activité régulatrice de son substrat p130Cas. De plus, l'implication de la PTP-PEST dans la relation pathogènes/cellules hôtes et dans l'apoptose a été étudiée. Dans un premier temps, des études de localisation ont permis d'observer la présence de PTP-PEST dans le cytosole et à la membrane plasmique. La réintroduction de différents variants de PTP-PEST dans les lignées *PTP-PEST* -/- suggère que les interactions dépendantes de la phosphorylation de p130Cas sont majoritairement contrôlées par la fraction cytosolique de PTP-PEST. En second lieu, mes travaux ont montré que l'infection de fibroblastes par le parasite Leishmania major altère la structure du cytosquelette et affecte le patron de phosphorylation de la cellule infectée. Au cours de l'infection, GP63, une protéase du parasite, dégrade les protéines PTP-PEST et p130Cas et est responsable du clivage d'autres protéines de la cellule hôte: cortactin, TC-PTP et caspase-3. De plus, GP63 est requise pour promouvoir l'inactivation de la p38 et la dégradation de son régulateur TAB1. Ces résultats suggèrent que la GP63 joue un rôle prépondérant dans de nombreux événements biochimiques qui pourraient contribuer à la virulence du parasite. Finalement, mes recherches ont démontré que PTP-PEST est relocalisée vers les membranes de rétractions des cellules entrant en apoptose. De manière surprenante, la caspase-3 clive PTP-PEST spécifiquement au motif ^{549}DSPD au cours de l'apoptose. Ce processus module l'activité catalytique et les interactions de PTP-PEST qui facilitent le

détachement cellulaire. Ces données démontrent le rôle potentiel joué par les caspases dans la régulation protéolytique des PTPs. Corrélativement, l'analyse des gènes murins et humains des PTPs souligne la présence de sites potentiellement reconnus par les caspases, suggérant que d'autres PTPs pourraient être des substrats des caspases. L'ensemble de mes résultats associe PTP-PEST à des processus biologiques variés: l'oncogenèse, les interactions pathogènes/cellules hôtes et l'apoptose. En plus de démontrer l'implication de PTP-PEST dans différents sentiers de signalisation, ces études illustrent l'importance de la localisation intracellulaire et du clivage comme moyens de régulation de cette enzyme.

TABLE OF CONTENT

LIST OF FIGURES

CHAPTER 1

CHAPTER 2

CHAPTER 3

CHAPTER 5

A, Ala	Alanine
Abl	Abelson
Apaf-1	Apoptotic protease-activating factor-1
Arp2/3	Actin related protein 2/3
BAK	Bcl-2 homologous antagonist/killer
BAX	Bcl-2 associated X protein
BCAR1	Breast cancer antiestrogen resistance 1
BCL-2	B-cell lymphoma-2
BH	BCL-2 homology
BID	BH3 interacting death domain agonist
BSA	Bovine serum albumin
C/Cys	Cysteine
CAKβ/PYK2	Cell adhesion kinase β
CARD	Caspase-recruitment domain
CD (CD45)	Cluster of differentiation
CH (domain)	Collagen homology domain
CHO	Chinese hamster ovary
C/S	Cysteine mutated in serine
Csk	C-terminal src kinase
CTH	COOH-terminal homology
CTL	Cytotoxic T lymphocytes
Crk	CT10 regulator of kinase
D/Asp	Aspartic acid
D/A	Aspartic acid mutated in alanine
DAPI	4',6-diamidino-2-phenylindole
DD	Death domain
DED	Death effector domain
DISC	Death-inducing signalling complex
DMEM	Dulbecco's modified Eagle's medium
DH	Dbl homology domain
DISC	Death-inducing signalling complex
DOCK180	Dedicator of cytokinesis 180
DSPs	Dual-specific phosphatases
E	Glutamic acid

EGF	Epidermal growth factor
EGFP	Enhanced green fluorescence protein
EGF-R	Epidermal growth factor-receptor
ER	Endoplasmic reticulum
ERK 1/2	Extracellular signal-regulated kinase 1/2
ES cells	Embryonic stem cells
EV	Empty vector
FADD	Fas-associated protein with death domain
FAK	Focal adhesion kinase
FAP1	Fas-associated phosphatase-1
FasL	Fas ligand
FCH	Fer kinase and CIP4 homology domain
FN	Fibronectin
FRET	Fluorescence resonance energy transfer
GAPs	GTPase-activating proteins
GDP	Guanosine diphosphate
GEFs	Guanine nucleotide exchange factors
Glu	Glutamine
Gln	Glycine
GPI	Glycosylphosphatidylinositol
Grb-2	Growth factor receptor binding protein-2
GST	Gluthathione S-transferase
GTP	Guanosine triphosphate
HB	Homogenisation buffer
Hic-5	Hydrogen peroxide inducible clone-5
IB	Immunoblot
IBMX	Isobutyl methyl xanthine
IL	Interleukin
Ile	Isoleucine
ILK	Integrin-linked kinase
iNOS	Inducible nitric oxide synthase
IP	Immunoprecipitation
JNK	c-Jun NH_2-terminal kinase
L.	*Leishmania*
LAR	Leukocyte common antigen related
LPA	Lysophosphatidic acid
LD	Leucine-rich motif

LIM	Lin-11, isl-1, mec-3
LPG	Lypophosphoglycan
Lys	Lysine
MAPK	Mitogen activated protein kinase
MAYP	Macrophage actin-associated tyrosine-phosphorylated protein
mDia	Diaphanous-related formin
MARCKS	Myristoylated alanine-rich C kinase substrate
MEFs	Murine embryonic fibroblasts
MLC2	Myosin light chain 2
mRNA	Messenger RNA
MRP	MARCKS-related protein
MSP	Major surface protease
MST3	Mammalian sterile 20-like kinase 3
NK	Natural killer
NO	Nitric oxyde
NRPTPs	Non-receptor PTPs
N-WASP	Neural WASP
OMM	Outer mitochondrial membrane
ODC	Ornithine decarboxylase
P/Pro	Proline
p130Cas	Crk-associated substrate
PAGE	Polyacrylamide gel electrophoresis
PBS	Phosphate-buffered saline
PCR	Polymerase chain reaction
PDGF	Platelet derived growth factor
PDGF-R	Platelet derived growth factor receptor
PEP	PEST-enriched phosphatase
PEST	Proline, glutamic acid, serine, threonine amino acid enriched sequence
PFA	Paraformaldehyde
PH	Pleckstrin homology domain
PKC	Protein kinase C
PKL	Paxillin kinase linker
PMA	Phorbol 12-myristate 13-acetate
P-MEFs	Primary mouse embryonic fibroblasts
PPARγ	Peroxisome proliferator-activated receptor γ
PSTPIP	Proline serine threonine phosphatase interacting protein
PTB	Phosphotyrosine binding

PTKs	Protein tyrosine kinases
PTPs	Protein tyrosine phosphatases
PTP-1B	Protein tyrosine phosphatases 1B
PTP-HSCF	Hematopoietic stem cell fraction PTP
PTP-PEST	Protein tyrosine phosphatase PEST
PVDF	Polyvinylidene difluoride
R-PTP	Receptor-like PTP
RTKs	Receptor tyrosine kinases
ROCK	Rho-associated coiled-coil-containing protein kinase
Q/Glu	Glutamine
Q/A	Glutamine mutated in alanine
S/Ser	Serine
SD	p130Cas substrate domain
SBD	Shc binding domain
SH2	Src homology 2
SH3	Src homology 3
SHP1	SH2 domain-containing protein tyrosine phosphatase 1
SHP2	SH2 domain-containing protein tyrosine phosphatase 2
TAB1	TAK-1-binding protein
TAK-1	TGF-beta-activated kinase 1
tBID	Truncated BID
TC-PTP	T-cell PTP
Thr	Threonine
TNF	Tumour necrosis factor
Val	Valine
VCA	Verprolin-homology (V), cofilin-homology domain (C), acidic domain (A)
VEGF	Vascular endothelial growth factor
WAS	Wiskott-Aldrich syndrome
WASP	Wiskott-Aldrich syndrome protein
WAVE	WASP verproline homologous
WPD	Tryptophan, proline, aspartic acid
WT	Wild type
X	Any amino acids
Y/Tyr	Tyrosine

ACKNOWLEDGEMENTS

First, would like to thank my supervisor, Dr. Michel L. Tremblay, for giving me the opportunity to work on the PTP-PEST project in his laboratory. I would like to thank him for the freedom, support, enthusiasm and encouragement he provided. The large number of talented and enthusiastic researchers present in his laboratory is a testament to his leadership in the field of protein tyrosine phosphatases. It was an unforgettable experience.

During my graduate studies, I benefited from a number of scholarships (Rolande and Marcel Gosselin Graduate Studentship, McGill Graduate Studies Fellowship, Arthur S. Hawkes Fellowship and Bourses FRSQ-FCAR SANTÉ) and awards (Defi Corporatif Canderel Travel Award, Richard Collier Fitzgerald Travel Award, FASEB Summer Research Conferences Poster Award). I am grateful to the above agencies for their generous financial support.

Over the course of my doctoral research, I had the opportunity to collaborate with several dynamic groups. I wish to thank my collaborators Dr. Martin Olivier and Dr. Tzu-Ching Meng, and the members of my research advisory committee, Dr. Nathalie Lamarche-Vane and Dr. Imed Gallouzi, for their time and expertise.

Michel's laboratory is like a big family, in which creativity, stimulating discussions and the exchange of information are encouraged. I would like to thank all present and past members of the lab, working with you was wonderful!

I am grateful to the PTP-PEST group: Jean-François Côté, Adam Scott and Hidehisa Shimizu, for their discussions and excellent suggestions. I wish to specially thank Dr. Christophe Blanchetot for his generous help while I was selecting the PTP-PEST rescued clones, and Jean-François Théberge for his outstanding professionalism, wise advice, and for being so helpful.

I would like to acknowledge Matthew Stuible for his patience in reviewing my manuscripts, and for his scientific advice, and Hannah Heath-Engel for the energy she put into proofreading my thesis (!). Thanks to Dr. Marie-Claude Gingras for proof-reading my "résumé" and for being an assiduous rock-climbing partner.

Many thanks to Dr. Feng Gu and Dr. Mounib Elchebly for their interesting discussions, encouragement and advices. I wish to thank Dr. Serge Hardy for his help in organization of the apoptosis manuscript, and Adelaida Gomez for her help with the *L. major* project.

I would like to thank Jacinthe Sirois, Janice Penney, Michelle Read and Sandrine Herbin for maintaining the good organization of the lab.

I would like to thank Laurent Lessard, Mélanie Chagnon, Karen Doody, Dr. Brent Townshend, Dr. Yves Boiclair, Dr. Pankaj Tailor, Isabelle Aubry, Ailsa Lee Loy, Dr. Nadia Dubé, Dr. Krista Heinonen, Dr. Annie Bourdeau, Amar S.W. Ozer Hassan, Chia-Lun Wu,

Dr. Allison Haggarty, Dr. Karim Elkouhen and Dr. Noriko Uetani for their enthusiastic discussions, and for creating such a stimulating work atmosphere.

I also want to thank Stephanie and all my friends for their encouragement along this long road. Special thanks to Martin Calille, who made the data search software I used to analyze putative caspase cleavage sites, and to Serge Morin, who generously helped me with the cell animations formatting.

And last, but not least, I wish to thank my parents, Lise and André, for their constant and unlimited support; and for believing in me, even during the most difficult periods...

CONTRIBUTION OF AUTHORS.

Publications arising from thesis work

M. Hallé, C. Blanchetot, J.-F. Théberge and M. L. Tremblay
PTP-PEST is found in cytosolic and membrane compartments, and regulates LPA-mediated p130Cas phosphorylation-dependent interactions. In preparation; Chapter 2

C. Blanchetot provided help during the selection of stable clones. J.-F. Théberge made the vector encoding PTP-PEST ΔPro3, ΔSBD and ΔPro4.

M. Hallé, M. A. Gomez, M. Stuible, H. Shimizu, W. R. McMaster, M. Olivier and M. L. Tremblay
The *Leishmania* Surface Protease GP63 Cleaves Multiple Intracellular Proteins and Actively Participates in p38 Mitogen Activated Protein Kinase Inactivation. Manuscript accepted for publication in *J. Biol. Chem.*; Chapter 3.

M. A. Gomez maintained the parasites in culture between experiments. M. Stuible provided significant help and critical input during the editing of the manuscript. H. Shimizu generated initial data on the regulation of p38 that helped me to generate the results shown on Supp. Fig. 7. W. R. McMaster provided the GP63 mutant strains of *Leishmania major*. M. Olivier provided access to his laboratory in order to perform the parasitic infections and supervised the work of M. A. Gomez.

M. Hallé, Y.-C. Liu, S. Hardy, J.-F. Théberge, C. Blanchetot, A. Bourdeau, T.-C. Meng and M. L. Tremblay
Caspase-3 Regulates Catalytic Activity and Scaffolding Functions of the Protein Tyrosine Phosphatase-PEST, a Novel Modulator of the Apoptotic Response. *Mol. Cell. Biol.*, 2007, 27 (3): 1172-1190; Chapter 4

Y.-C. Liu prepared figure 4 a, b and c; figure 5 a; figure 6 b and figure 8 a. For figure 4 d, I performed the stimulation and prepared the extract. The analysis via in gel phosphatase assay was done by Y.-C. Liu. S. Hardy performed the experiment shown in figure 2c with my assistance, and helped with organisation of the manuscript text. J.-F. Théberge generated, with my assistance, some of the PTP-PEST mutants used in this study (^{549}ASPA; ^{549}ASPA-^{604}ADSA-^{740}AKKA) in the vector pcDNA3.1Zeo. C. Blanchetot helped with the generation of cell lines used for figure 2B, which are the

same as those described in chapter 2. A. Bourdeau provided technical assistance with flow cytometry, during the generation of the data presented in figure 10. Experiments performed by Y.-C. Liu were done under the supervision of T.-C. Meng.

M. Hallé, M. L. Tremblay and T.-C. Meng
Protein Tyrosine Phosphatases: Emerging Regulators of Apoptosis. *Cell Cycle*, 2007, 6 (22): 2773-2781; Chapter 5.

I wrote the manuscript and analyzed the presence of putative caspase cleavage sequences within genes encoding PTPs. This work was done under the co-supervision of M. L. Tremblay and T. -C. Meng.

Unless stated above, I designed and performed the experiments producing all the data shown in this thesis. I also analysed and interpreted their significance, and wrote every manuscript presented herein. Work was done under the supervision of M. L. Tremblay.

Non-thesis related publications.

J. S. Jamieson, D. A. Tumbarello, **M. Hallé**, M. C. Brown, M. L. Tremblay and C. E. Turner
Paxillin is Essential for PTP-PEST-Dependent Regulation of Cell Spreading and Motility: a Role for Paxillin Kinase Linker. *J. Cell. Sci.*, 2005,118: 5835-5847.

I provided the *PTP-PEST* -/- cell lines, as well as assistance in setting up the co-immunoprecipitation conditions and in editing the manuscript.

C. Blanchetot, M. Chagnon, N. Dubé, **M. Hallé** and M. L. Tremblay
Substrate-Trapping Techniques in the Identification of Cellular PTP Targets. *Methods*, 2005, 35: 44-53.

I provided assistance with Table 1 and in writing the manuscript.

J. -F. Côté, P. L. Chung, J. -F. Théberge, **M. Hallé**, S. Spencer, L. A. Lasky, and M. L. Tremblay
PSTPIP Is a Substrate of PTP-PEST and Serves as a Scaffold Guiding PTP-PEST Toward a Specific Dephosphorylation of WASP. *J. Biol. Chem.*, Vol. 277, Issue 4, 2973-2986, January 25, 2002.

I generated the results shown in figure 3, as well as the immunoblot for Fyn and Lyn shown in figure 4B. In addition, I generated the vector pEGFP-PTP-PEST WT and pEGFP-PTP-PEST ΔPro5 used in this study. I was also actively involved in the writing and editing of the manuscript.

H. Shimizu*, **M. Hallé*** and M. L. Tremblay
PTP-PEST regulates p130Cas mediated oncogenic signalling leading to cell migration, proliferation, and invasion. In preparation. ***Co-first author**.

I generated the *PTP-PEST* rescue cell lines used in this study, the EGFP-PTP-PEST fusion constructs, the adenovirus vector cloning strategy, and, data on p130Cas phosphorylation-dependent signalling and on PTP-PEST subcellular localization. I also organized the study structure.

À Mamie,
elle dont la générosité n'a aucune limite.

THESIS OVERVIEW

Cytoskeletal elements provide a framework which supports the plasma membrane, and therefore defines the morphology adopted by a cell. The activity of the different components involved in assembling and regulating the architecture of the cytoskeletal network is critical for cell adhesion and spreading, as well as for directed motility. As cytoskeletal components directly impact cell shape, their modification during apoptosis results in dramatic morphological changes, such as membrane blebbing, and cellular detachment and rounding. These morphological changes are considered hallmarks of apoptosis (77, 222). Programmed cell death is of fundamental importance for normal embryogenesis and for the clearance of virally infected cells. Since cytoskeletal regulatory components are also required for endocytosis and phagocytosis, these molecules are targeted by several intracellular parasites (276, 309). For example, the parasite *Leishmania* targets the actin regulatory machinery for its entry within the host cell, and, once intrenalized, for polymerization of an actin coat in its host cell (212, 237).

When I began my graduate studies in the laboratory of Dr. Tremblay, his group, as well as that of Dr. Nicolas K. Tonks, had recently demonstrated the importance of PTP-PEST in the control of cell migration (11, 120). Their studies, and others, exemplified the role of PTP-PEST in regulation of the actin cytoskeleton. Although PTP-PEST was known to interact with multiple signalling molecules proposed to target the enzyme to discrete protein complexes, little was known about the effect of its subcellular localization on its function. In addition, the possible role of PTP-PEST in the relationship between host cells and intracellular pathogens was obscure. Moreover, although our laboratory had data demonstrating the requirement of PTP-PEST in normal embryogenesis (305), the potential role of this enzyme in apoptosis remained poorly documented.

The initial objective of my study was to determine the subcellular localization of PTP-PEST, and to evaluate the impact of subcellular localization on PTP-PEST functions. In addition, I was to determine whether PTP-PEST is involved in host-pathogen relationships. Over the course of a series of experiments performed on the parasite *Leishmania*, I noticed that PTP-PEST and its substrate p130Cas were both cleaved in infected cells. Interestingly, p130Cas had been previously shown to be processed by caspase-3 during apoptosis (189). Therefore, I initially believed that PTP-PEST could have been cleaved by caspases during the infection. Although further studies demonstrated that both PTP-PEST and p130Cas were in fact degraded by a protease of parasitic origin, and not by cellular proteases (including caspases), examination of the apoptotic cells prepared as a positive control revealed the proteolysis of PTP-PEST during apoptosis. My third objective was therefore to investigate the contribution of PTP-PEST to the apoptotic program, and its regulation by caspases in this cellular process. In this thesis, I present the data I have generated pertaining to the above topics, and the possible implications of my results with respect to the functional significance of PTP-PEST regulatory mechanisms.

CHAPTER 1

INTRODUCTION

1.1 PROTEIN TYROSINE PHOSPHATASES

The phosphorylation of tyrosine residues is a reversible and targeted protein modification essential for a great number of physiologic phenomena. Phosphorylation/dephosphorylation cycles modulate the catalytic activity of a variety of enzymes, affect protein structure and conformation, and stabilize the open or closed configurations of diverse proteins, thereby directly regulating surface exposure of various domains. Some protein modules, such as the Src homology 2 region (SH2) and the phosphotyrosine-binding domain (PTB), have affinity for tyrosine phosphorylated sequences (293). During the activation of signalling cascades, tyrosine phosphorylation of select proteins triggers the assembly of large complexes containing multiple enzymatic and scaffolding molecules interconnected via the interaction between tyrosine phosphorylated sites and domains recognizing these sites. Accordingly, the occurrence and regulation of this modification acts as a molecular language responsible for intra and intercellular communication, and its tight regulation is critical for cellular processes including cytoskeletal rearrangement, growth, proliferation, survival, motility, differentiation and death (219). Tyrosine phosphorylation/dephosphorylation contributes to several biologic phenomena, including embryogenesis, organogenesis, activation of the immune system and homeostasis (5), and, disregulation of this process is involved in cellular transformation, cancer progression, immune disorders and infectious diseases (5, 239, 248, 255). Tyrosine phosphorylation and dephosphorylation result, respectively, from the action of two enzymatic antitheses: the protein tyrosine kinases (PTKs) and the protein tyrosine phosphatases (PTPs).

The viral form of Src (v-Src) was the first protein tyrosine kinase identified (159). Isolated as a phosphorylated protein, and therefore named pp60, pp60v-Src was

observed to phosphorylate casein, a protein rich in tyrosine (104, 207). The epidermal growth factor receptor (EGF-R) was subsequently identified as the first receptor tyrosine kinase (76). The number of identified tyrosine kinases then rapidly expanded. Today, the 90 PTKs are considered part of the protein kinase superfamily (518 genes in human and 540 in mouse), which is considered as being one of the largest gene families, consisting of 2 to 4% of all genes (5, 47, 219).

1.1.1 Historical context of PTP discovery.

The PTKs were intensively investigated for several years before identification of the PTPs (158). Approximately ten years after the discovery of v-Src, Tonks et al. (1988) purified the first protein tyrosine phosphatase, PTP-1B (336). Analysis of the partial amino acid sequence of this protein revealed its similarity to the intracellular tandem homologous domains of CD45, a large transmembrane protein expressed on the surface of hematopoietic cells (52). It was then found that CD45 has intrinsic phosphatase activity (335). This was an important discovery, as it implied the existence of receptor-like PTPs, which could be modulated by putative ligands in order to regulate signalling cascades (333). In order to identify other PTPs, synthetic oligonucleotides were derived from the sequence of PTP-1B and used to screen a human peripheral T-cell cDNA library (81). This analysis resulted in the identification of T-cell PTP (TC-PTP) (81). Similar approaches involving PCR were used to identify several other PTPs, including PTP-PEST, which will be discussed in detail below (56, 321, 365).

1.1.2 Mechanism of dephosphorylation.

While PTKs catalyze the addition of a phosphate group to, or phosphorylate, tyrosine residues, PTPs catalyzes the removal of this modification: dephosphorylation. The catalytic domain of PTPs is composed of 280 amino acids, among which 22 are

invariant and 42 are highly conserved (10). PTPs are defined by a well conserved signature motif ([I/V]HCXXGXXR[S/T]), found in the phosphate binding site, also known as the P-loop (333). Notably, the superimposition of crystal structures of the PTP domains of PTP-1B, R-PTPα, R-PTPμ, LAR, SHP1 and SHP2 reveals significant homology in their folding and backbone organisation (10). This also suggests that PTPs process their substrates via a common mechanism. Structural studies done on the first identified PTP, PTP-1B (considered as the prototypic PTP), provided important insight into the mechanism of PTP-catalyzed dephosphorylation (333). The catalysis of phosphate removal from a tyrosine-phosphorylated substrate takes place by a two step mechanism (Fig. 1). In the catalytic pocket microenvironment, the invariant cysteine (Cys 215 in PTP-1B) of the signature motif is found at the base of a cleft and is maintained in a thiolate form, competent to initiate the enzymatic reaction (333). The sides of the cleft are formed by three motifs: the WPD loop, which contains the invariant aspartic acid residue (Asp 181 in PTP-1B), the Q loop, containing a catalytically important glutamine residue (Gln 262 in PTP-1B), and the pTyr loop (Tyr 46 in PTP-1B), which defines the depth of the cleft and is responsible for the exclusive specificity of PTP-1B for tyrosine phosphorylated substrates (333). The first catalytic step involves the sulfur atom of the thiolate cysteine side chain, which performs a nucleophilic attack on the substrate phosphate and leads to formation of an enzyme-phosphate-substrate intermediate (333). The arginine (Arg221 in PTP-1B) residue of the signature motif plays a role in stabilization of the cysteine-phosphate intermediate (330). Binding of the substrate induces a conformational change which closes the WPD loop around the substrate phosphotyrosine, and positions the conserved aspartic acid, which subsequently acts as a general acid to protonate the oxygen of the tyrosine leaving group (317, 333). The dephosporylated substrate is thereby released. In the second step, the phospho-cysteine intermediate is hydrolyzed to yield free cysteine. In this step, Asp181 acts as a general base that increases the nucleophilic potential of a water molecule coordinated by the glutamine residue of the Q loop. This triggers a second nucleophilic attack on the cysteinyl-phosphate (333). The WPD loop obstructs the opening of the active site and

isolates the cysteinyl-phosphate intermediate with water molecules (333). This prevents the transfer of the phosphate group to alternative acceptors, and provides a mechanism by which the PTP dephosphorylates its substrate without phosphorylating other proteins (333). To summarize, the first step catalyzes the removal of the phosphate modification on the substrate, and the second step allows regeneration of the active form of the enzyme.

Figure 1. PTP-1B dephosphorylates substrates via a two-steps mechanism. In the first step, the invariant cysteine found in its thyolate form at the base of the catalytic pocket initiates a nucleophilic attack on the phosphorylated substrate, leading to the formation of an enzyme-substrate intermediate. The invariant aspartic acid of the WPD loop acts as a general acid that protonates the oxygen-phosphate bond and allows release of the substrate. This results in the formation of a phosphocysteine enzyme intermediate. In the second step, the invariant aspartic residue behaves as a general base, promoting a second round of nucleophilic attack toward the cysteinyl-phosphate, which involves a water molecule positioned by the invariant glutamine of the Q loop. This reaction results in liberation of the dephosphorylated substrate, production of inorganic phosphate, and regeneration of the active enzyme.

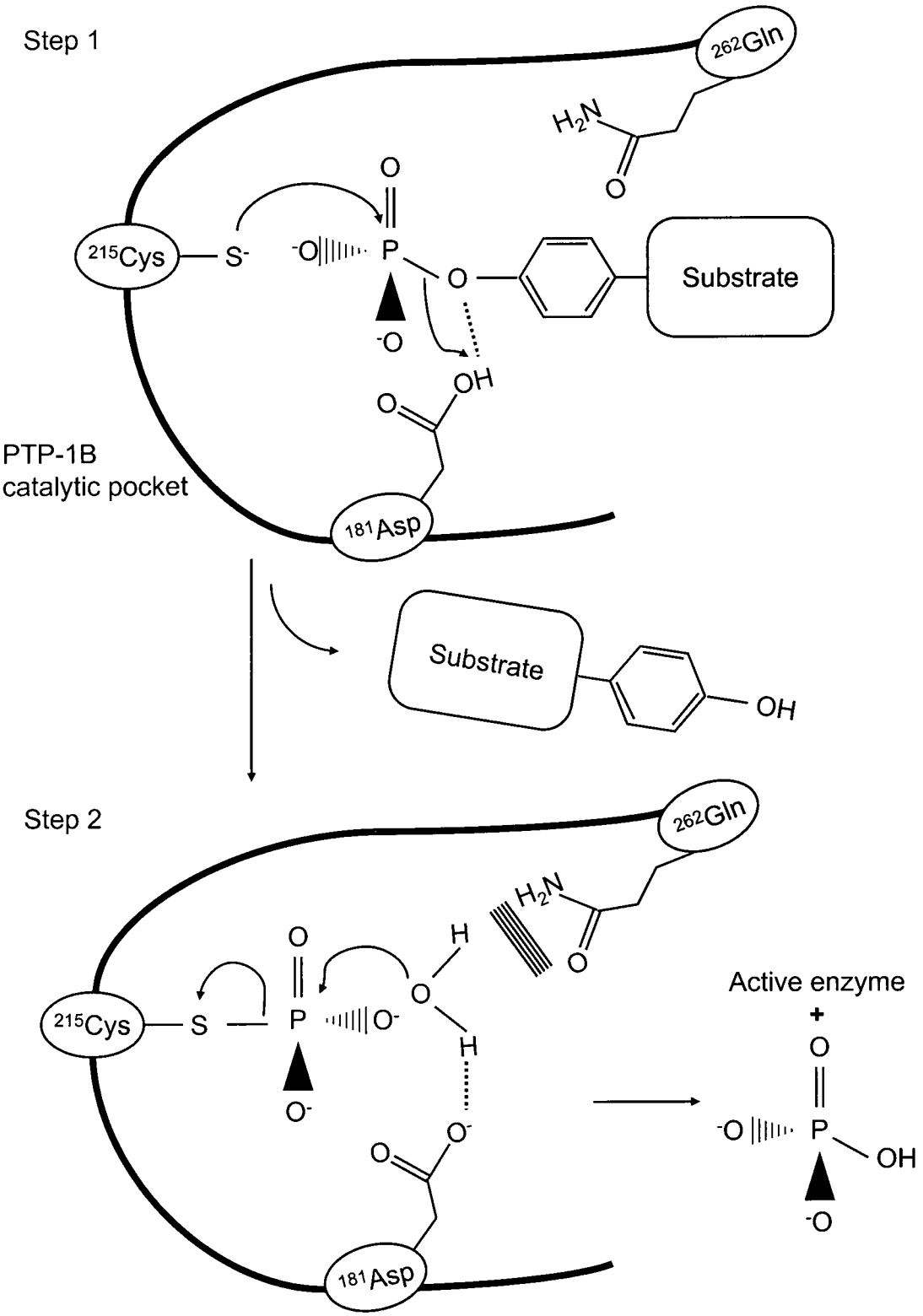
Step 1
262Gln
H2N
O
O
215Cys
S-
-O
P
O
-O
Substrate
OH
O
PTP-1B
catalytic pocket
181Asp
Substrate
OH
Step 2
262Gln
H2N
O
O
H
215Cys
S
P
O-
O
H
O-
O
181Asp
Active enzyme
+
O
-O
P
OH
-O

FIG. 1

1.1.3 Mutation of residues critical for catalysis inactivates the enzyme and generates substrate-trapping variants.

Investigation of the PTP catalytic mechanism led to the development of methods allowing the identification of specific PTP substrates. Mutation select invariant amino acids within the enzymatic domain abrogates catalytic activity, without affecting substrate recognition. These inactive enzymes are called *"substrate-trapping"* mutants (113). Mutation of the invariant cysteine residue (typically to serine, C215S for PTP-1B and C231S for PTP-PEST) blocks the nucleophilic attack and enzymatic activity (330, 333). In contrast, enzymes with mutations of the invariant aspartic residue (usually to alanine, D181A for PTP-1B and D199A for PTP-PEST) are still capable of nucleophilic attack, but are not able to remove the phosphate group from the substrate, which stabilizes the enzyme-substrate complex (113). This mutation has proven to be more effective than the C/S mutation in increasing the cellular content of in phosphorylated molecules, and in the affinity-based isolation of putative substrates (113). Mutating the glutamine residue of the Q loop, in conjunction with the D/A mutation (D/A, Q/A double mutant), further enhances substrate trapping capability due to abrogation of residual activity present in the D/A single mutant (330). Substrate trapping techniques have been extremely useful in the identification of substrates for a significant number of PTPs (25). Using this approach, Garton et al. 1996 observed, in a variety of cell lines, a 130 kDa tyrosine-phosphorylated protein with affinity for PTP-PEST (D199A), and, to a lesser extent, for PTP-PEST (C231S) (118). This candidate substrate was identified as p130Cas (118). The substrate trapping system was also used for the identification and the characterization of additional PTP-PEST substrates, including PSTPIP, paxillin kinase linker (PKL), p190RhoGAP, and cell adhesion kinase β (CAKβ or PYK2) (85, 172, 216, 287).

1.1.4 PTPs are remarkably diverse enzymes.

Genes encoding PTPs have been observed in all kingdoms, from bacteria to mammals. For example, the virulence factor YopH of *Yersinia pestis*, the causative agent of Bubonic plague, is a PTP (40). Similar to PTKs, PTPs represent a large and diverse family of genes. Analysis of human genome databases reveals the existence of 107 genes encoding PTPs enzymes (5). These have been subdivided into four classes, which are grouped accordingly to sequence homology, but, show different substrate specificity (5). A small number of molecules have been classified in the class II, III and IV (termed Asp-Based PTPs) (5). These three classes have, respectively, one (low molecular weight PTP, LMPTP), three (CDC25) and four (EyA) members (5). Class I, which contains the largest number of proteins (99), is further subdivided into classical PTPs and dual-specific phosphatases (DSPs, or VH1-like) (5). The DSPs show a high degree of diversity with respect to substrate specificity with various members having the ability to dephospohrylate mRNA, phospholipids, or serine, threonine and tyrosine residues (5). In contrast, classical PTPs show remarkable specificity for phosphorylated tyrosine residues (5). Among the 38 classical PTPs, 21 genes encode receptor-like PTPs (R-PTPs), and 17 encode intracellular non-receptor enzymes (NRPTPs) (5). The large number of genes encoding PTPs raises the possibility that the different enzymes play complementary functions. The NRPTPs show a high degree of diversity within the extra-catalytic motifs, and these regions play a critical role in subcellular localization, substrate targeting and function (5, 330). The PEST family members PTP-PEP, PTP-HSCF and PTP-PEST are all non-receptor classical class I PTPs (5).

1.1.5 PTPs can both promote and inhibit tyrosine phosphorylation cascades: Src as an example.

Although PTPs catalyze dephosphorylation reactions, it does not mean that they exclusively down-regulate signalling cascades. In the case of proteins that are inhibited by phosphorylation, dephosphorylation by PTPs is presumably an activating event. The kinase Src is involved in the phosphorylation of multiple substrates, and its aberrant activity promotes cellular transformation and cancer (164). Consequently, the activation of Src is tightly regulated. Members of the Src family possess a similar domain organisation: a membrane targeting sequence (usually myristoylation and in some cases palmitoylation) is present within the highly variable N-terminal region, and is followed by a Src homology 3 domain (SH3), an SH2 domain, a kinase domain (also termed SH1) and a C-terminal sequence containing a Src inhibitory phosphorylation site (tyrosine 527 in the mouse form of Src) (163). Intramolecular interactions involving the binding of the SH3 domain to a polyproline sequence found in the linker between the SH2 domain and the catalytic domain, as well as the association of the SH2 domain with the phosphorylated C-terminal inhibitory site, both stabilize Src in an inactive form (163). A second mode of Src inhibition occurs at the level of its catalytic domain. In this region, the A-loop, in its un-phosphorylated form, folds over and obstructs the substrate binding site (163). Several PTPs, including PTP-1B, SHP-1 and SHP-2, as well as several RPTPs (CD45, PTPα, PTPε and PTPλ), can dephosphorylate the C-terminal inhibitory site (Y527) and thereby favour Src activation (163, 275, 313). Activation is also enhanced by phosphorylation of the A-loop (Y416 in the mouse), which stabilizes the active conformation (163, 275). Conversely, PTP-BL (the mouse homologue of human FAP-1/PTP-BAS) inactivates Src via dephosphorylation at Y416 (275). Interestingly, Shp-1 was observed to dephosphorylate the activation loop of the Src family member Lck (68). Therefore, dependent on both substrate and site specificity, PTPs play a critical role in both promotion and inhibition of signal transduction.

1.2 PTP-PEST

Human and murine cDNA encoding PTP-PEST have been isolated and described by a number of different groups (56, 98, 321, 365, 375). These investigators were used similar approaches to clone novel PTPs, which resulted in the identification of PTP-PEST from a variety of sources. Typically, fragments of putative phosphatases were amplified by polymerase chain reaction (PCR) using a mixture of degenerated oligonucleotides derived from conserved sequences found in the catalytic domain of PTPs. Reaction products were then used to screen cDNA libraries, leading to the identification of novel enzymes. Research done on a human adult colon tissue cDNA library identified a candidate encoding a 780 amino acids protein, predicted to have a molecular mass of 88 kDa and designated PTPG1 (321). The N-terminal catalytic domain of PTPG1 is followed by a long carboxyl terminal extension containing two imperfect proline-rich repeats as well as four PEST motifs; regions enriched in proline, glutamic acid, serine and threonine residues (272, 321). The presence of PEST motifs correlated with accelerated protein degradation, and, therefore, the C-terminal segment of PTPG1 was termed the regulatory domain (272, 321). Interestingly, the amino acid sequence also contained three additional proline-rich motifs later described in the murine form of PTP-PEST (84, 321). An independent study using a HeLa cell cDNA library led to the identification of a similar enzyme containing 510 amino acids and predicted to be 60 kDa (365). A distinctive characteristic of the sequence of this protein, named PTP-PEST, was the presence of two PEST regions (365). Since PTP-PEST expression was observed to be increased following insulin stimulation, the PEST motifs were thought to play a critical role in the regulation of this enzyme (365). Pulse-chase experiments, however, showed that PTP-PEST has a half-life of more than four hours, underscoring its stability (56). Both of the above described proteins were predicted to have a cytosolic localization, based on the absence of hydrophobic/transmembrane domains (321, 365). Whether the differences observed between these two reported sequences was a result of alternative splicing requires additional investigations (321, 365).

Over the course of my studies in the laboratory of Dr. Michel L. Tremblay, I worked with the murine form of PTP-PEST (m-PTP-PEST). m-PTP-PEST was originally cloned from a murine embryonic kidney cDNA library (56). The complete m-PTP-PEST cDNA sequence encodes a 775 amino acids protein with a predicted molecular weight of 87 kDa, but which is resolved by electrophoresis at 112 kDa (56). Similar to the human form identified by Takekawa et al in 1992 (321), the carboxy-terminal tail of m-PTP-PEST contains four PEST sequences, whose involvement in accelerating protein degradation remains to be demonstrated, as well as several interaction-mediated motifs (see below) (Fig. 2). Located on chromosome 5 in the mouse genome, the m-PTP-PEST gene covers over 90 kb and is composed of 18 exons (55). The catalytic domain is encoded by exons 2 to 11 and the C-terminal non-enzymatic segment is encoded by exon 11 to 18 (55). For the remainder of this document, species designations will not be used for PTP-PEST, except in cases where the concept is important for interpretation of the material presented.

Figure 2. Structural organization of PTP-PEST domains. PTP-PEST, a 775-amino acids (mouse) protein comprises a amino phosphatase domain specific for phosphorylated tyrosine and multiple interacting motifs in its C-terminus. The proline-rich domains (P1, P2, P3, P4 and P5/CTH) and the Shc binding domain (SBD) recruit PTP-PEST to a variety of interacting partners. Proteins labelled in black are monitored in the current thesis. Amino acids sequences of each interacting motifs as well as PTP-PEST signature motifs are identified (53, 56, 84).

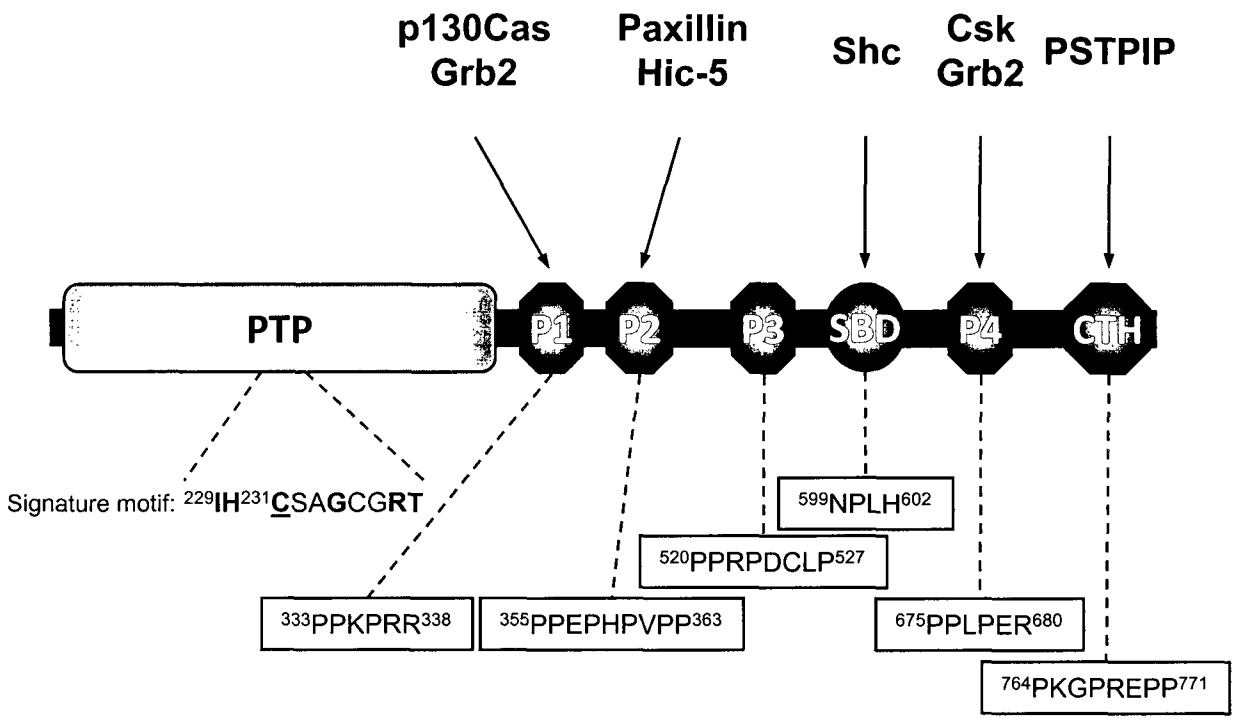
p130Cas
Grb2
Paxillin
Hic-5
Shc
Csk
Grb2
PSTPIP
PTP
P1
P2
P3
SBD
P4
CTH
Signature motif: 229IH231CSAGCGRT
599NPLH602
520PPRPDCLP527
333PPKPRR338
355PPEPHPVPP363
675PPLPER680
764PKGPREPP771

FIG. 2

1.2.1 Expression pattern of PTP-PEST

Early genetic studies led to the identification of three novel putative PTPs expressed in murine myeloid cells (375). Among these putative PTPs, the fragment termed PTPty43, which corresponds to PTP-PEST, displayed a unique ubiquitous expression pattern, in contrast to the restricted profiles observed for the six other PTPs (375). This ubiquitous tissue distribution was later confirmed at the protein level through immunoblot analysis (85, 86, 94, 95). To date, expression of PTP-PEST has been observed in a variety of tissues and organs, including oviduct, ovary, testes, intestine, stomach, skeletal muscle, heart, liver, lung, kidney, brain, thymus, spleen, fetal liver, fetal intestine and fetal brain, as well as in a variety of cell lines and lineages, such as gastric cancer, colorectal cancer, hepatocellular carcinoma, pancreatic cancer, fibroblasts, myeloid leukemia, thymocytes, splenic T-, T-, pro-B-, splenic B-, B-, bone marrow derived mast, natural killer (NK) and macrophage cells (85, 86, 94, 95, 321, 375). Interestingly, elevated levels of PTP-PEST were found in the spleen and thymus, as well as in hemopoietic cells, while only low levels were seen in kidney tissue (85, 94, 95).The ubiquitous expression of PTP-PEST suggests a fundamental biologic role for this enzyme.

1.2.2 Functions of PTP-PEST.

Analysis of whole embryo extracts revealed that PTP-PEST is expressed early during murine development (56). In situ hybridisation probing for PTP-PEST mRNA revealed the presence of this phosphatase throughout embryos from E8.0 to E12.0, as well as in extra-embryonic structures (305). The maintenance of PTP-PEST expression throughout embryonic development indicates a potential regulatory role for the enzyme during this process.

In order to investigate the role of PTP-PEST in mammals, exons 6 to 9 of the *PTP-PEST* gene, which correspond to the catalytic domain, were deleted by homologous recombination in embryonic stem (ES) cells (305). The loss of one functional *PTP-PEST* allele was not detrimental, as heterozygous animals exhibited no apparent phenotype, and had normal lifespan and fertility (305). Live *PTP-PEST* -/- homozygous mutant pups, however, could not be generated through interbreeding of *PTP-PEST* +/- mice (305). Complete ablation of the *PTP-PEST* gene resulted in embryonic lethality between E9.5 and E10.5 (305). Inactivation of *PTP-PEST* was also associated with impaired liver development and vascularisation (305). Although manipulation of the *PTP-PEST* gene did not affect gastrulation and embryonic development up to E7.5 (305), *PTP-PEST* -/- embryos failed to progress through later developmental stages due to morphologic defects such as growth retardation, inability to turn, incomplete somites formation, and impaired vasculogenesis and liver development (305). The above observations underscore the crucial role played by PTP-PEST in embryogenesis. In order to gain further insight into the physiological function of PTP-PEST, our laboratory, as well as others, conducted a variety of tissue culture based experiments. In comparison to control cells, *PTP-PEST*-/- fibroblasts displayed significantly decreased motility (11). In addition, cells over-expressing PTP-PEST exhibited a migration defect on fibronectin (120). These results suggest that balanced expression of PTP-PEST is required for optimal cellular movement. Interestingly, micro-injection of *xPTP-PESTr* (*X. lavis* PTP-PEST related) in *Xenopus* blastomeres resulted in defective gastrulation (88). In this particular model, xPTP-PESTr promoted spreading and decelerated migration of ectodermal cells induced by the mesoderm activating factor activin-A (88). The above described studies demonstrate that manipulation of PTP-PEST expression in both murine and *Xenopus* systems disrupts the tight regulation of cell migration necessary for complete embryonic development.

Cell migration is a complex phenomenon integrating the formation of membrane protrusions at the leading edge, recycling of adhesion structures, contraction of the cell

body, and detachment-retraction of the trailing end (266, 287). These processes are dependent on the coordination between dynamic cytoskeletal rearrangements and localized actin polymerization/depolymerisation, and are regulated by a vast number of proteins. *PTP-PEST* null cells seeded on fibronectin displayed both accelerated spreading (11) and assembly of a greater number of focal adhesions and stress fibres across their cell body (Maxime Hallé and Michel L. Tremblay, un-published data, Fig. 3) (11). PTP-PEST also plays a role in the inhibition of membrane protrusion (172, 286). In addition to its role in cytoskeletal rearrangement, PTP-PEST was also shown to prevent the relocalization of p130Cas at the leading edge of migrating cells, and to reduce p130Cas phosphorylation in response to fibronectin stimulation (120). p130Cas was among the first identified PTP-PEST substrates (84, 118), is required for completion of the mammalian developmental program (153), is able to associate with xPTP-PESTr (88) and is hyperphosphorylated *PTP-PEST* -/- embryos and fibroblasts (11, 305). However, p130Cas is likely not the sole route through which PTP-PEST fulfills its physiologic role. PTP-PEST was, in fact, found to associate with several other cytoskeletal components and signalling molecules, including Sin, Hef-1, leupaxin, Hic-5, paxillin, FAK, Pyk2 (also referred as cell adhesion kinase β (CAKβ)), Grb-2, Shc, filamin-A, Csk, PSTPIP, WASP, Abl, gelsolin, and receptors such as the PDGF-receptor (Fig. 2) (53, 54, 60, 79, 84-86, 94, 131, 216, 220, 243, 257). Among these, the association of PTP-PEST with paxillin was suggested to provide a link with adhesion signalling (86), while binding to PSTPIP connected it to regulators of actin polymerisation (18, 85), which supported a dual role for PTP-PEST in cytoskeletal modulation. Nevertheless, a large number of PTP-PEST substrates and interactors implies several alternative avenues integrating PTP-PEST in cytoskeletal signalling and could expand its activities to additional biologic phenomena. With respect to these additional biological processes, the abundance of pycnotic cells observed in *PTP-PEST* -/- embryos (305) may results from disregulation of apoptotic pathways, and points to a potential role for this enzyme in programmed cell death. In addition, several intracellular pathogenic microorganisms subvert the machinery controlling the actin cytoskeleton of their host (237, 276, 309). The possible involvement

and/or regulation of PTP-PEST in programmed cell death and/or in host-pathogen interaction, however, has yet to be determined.

Figure 3. PTP-PEST regulates the formation of actin stress fibres and focal adhesions in cells seeded on fibronectin. PTP-PEST heterozygous, null and null-rescued fibroblasts were held in suspension for 20 minutes and deposited for the indicated times on fibronectin coated-slides. Cells were fixed, permeabilized, and stained for polymerized actin (F-actin) and vinculin as previously described (11). Radom field images were acquired by confocal microscopy (Zeiss LSM 510-NLO). All cell lines were able to adhere to fibronectin within 20 min. Following a three hours incubation, PTP-PEST +/- cells displayed a few focal adhesions localized at the cell periphery in conjunction with cortical F-actin. In contrast, PTP-PEST -/- cells displayed a great number of adhesion structures and stress fibres dispersed throughout the cells. This phenomenon was dependent on the expression of PTP-PEST since its re-introduction in the -/- cells was sufficient to rescue the phenotype. These observations were statistically confirmed by evaluating the average number of focal adhesions detected per cell plated on fibronectin for three hours. Red: F-actin; green: vinculin.

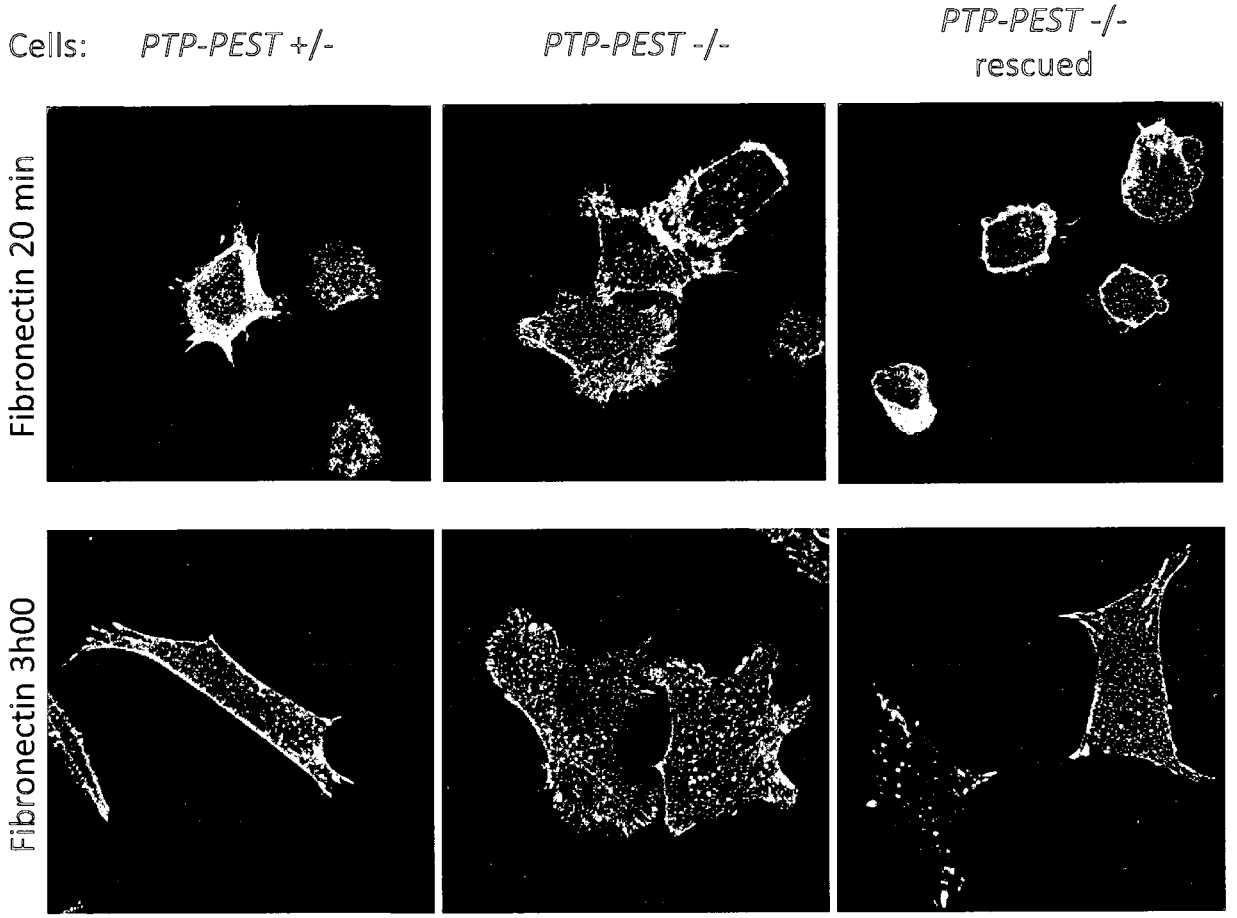
Cells:
PTP-PEST +/-
PTP-PEST -/-
PTP-PEST -/-
rescued
Fibronectin 20 min
Fibronectin 3h00

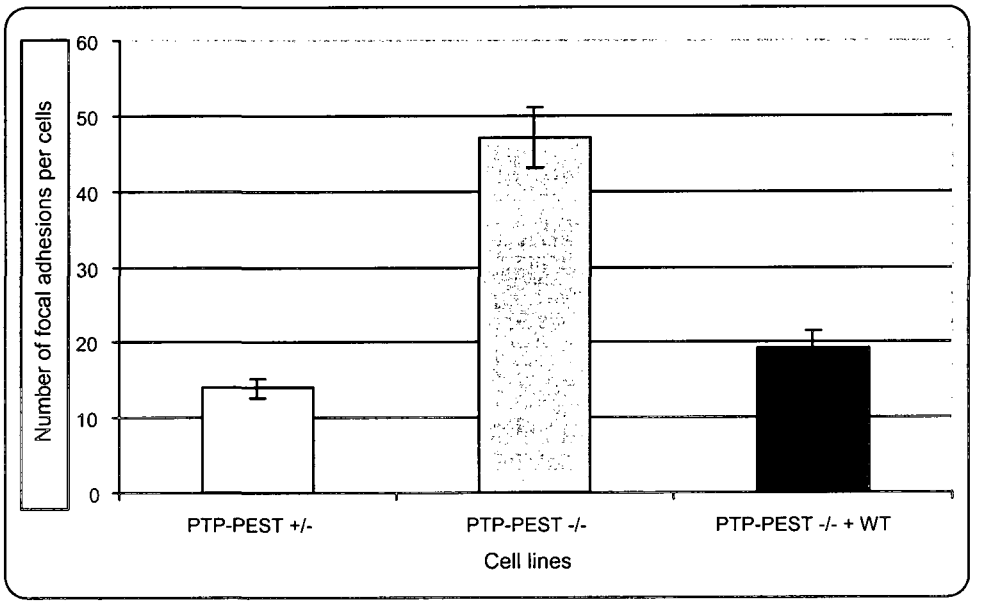
Number of focal adhesions per cells
60
50
40
30
20
10
0
PTP-PEST +/-
PTP-PEST -/-
PTP-PEST -/- + WT
Cell lines

FIG. 3

1.3 p130Cas

Identified as a major phosphorylated species in cells transformed by v-src or v-crk oncogenes, the 130 kDa Crk-associated substrate (p130Cas) is a multidomain scaffolding protein (Fig. 4) (32, 282). The N-terminal SH3 domain plays an important role in the phosphorylation-dephosphorylation cycle of p130Cas, via interactions with the PTKs FAK and CAKβ/PYK2 (14, 142), and with the PTPs PTP-1B and PTP-PEST (117, 209). The N-terminal SH3 domain is followed by a region containing 15 YXXP motifs; known as the substrate domain (SD or $(YXXP)_{15}$ on Fig. 4). The SD is characterized by its ability to accumulate multiple phosphorylation modifications. Once phosphorylated, the p130Cas SD recruits a variety of SH2 containing molecules such as Crk and Nck (188, 290). In addition to the multiple YXXP motifs, p130Cas can also be phosphorylated on its C-terminus within a Src-binding domain (SBD or R^{639}PLPSPP...Y^{668}DYV on Fig. 4), characterized by a proline-rich sequence and two tyrosine phosphorylation sites, which interact, respectively, with the SH3 and SH2 domains of Src, a PTK involved in promoting the phosphorylation of p130Cas (240). Although FAK can phosphorylate p130Cas SD, Src phosphorylation seems to be much more efficient (277), and, while activity of individual kinases results in modest phosphorylation levels, maximum phosphorylation of p130Cas seems to require cooperation between FAK and Src (277). Biochemical studies performed by Ruest et al (2001) indicate that, following recruitment to the p130Cas SH3 domain, FAK acts as an adaptor protein that binds Src (277). Following recruitment to p130Cas via FAK, Src then phosphorylates the p130Cas SD (277).

p130Cas is an important adaptor molecule, typically phosphorylated in response to the activation of integrin in order to stimulate the transmission of cell survival and migratory signals to downstream effectors. Stimuli such as lysophosphatidic acid (LPA) (50), epidermal growth factor (EGF) (246) and vascular endothelial growth factor (VEGF) (16) modulate the phosphorylation of p130Cas. Both expression and phosphorylation of

p130Cas are required to promote cell attachment and motility (152, 157). Phosphorylation of p130Cas permits the assembly of a p130Cas-Crk-DOK180 complex, which drives the activation of Rac, leading to actin polymerization and lamellipodia formation (70, 187).

Some intracellular pathogens exploit p130Cas in order to remodel the cytoskeletal architecture of their host cells. For example, *Salmonella typhimurium* recruits p130Cas in complex with FAK and paxillin in order to reorganize the actin cytoskeleton of the host cell during bacterial internalization (301). In addition to its importance in cytoskeletal architecture, p130Cas also plays a role in adhesion-mediated survival signalling and is cleaved by caspase-3 during apoptosis (189). In fact, over-expression of an SD deleted mutant of p130Cas leads to increased apoptosis, while phosphorylation of p130Cas was increased in anoikis resistant tumour cells (352). It therefore appears that signals regulating apoptosis/survival, cytoskeletal organization (either physiological or pathogen mediated) and migration all converge at the level of p130Cas. As PTP-PEST was previously identified as a regulator of p130Cas phosphorylation, it is tempting to speculate that PTP-PEST may be involved in p130Cas-linked biological functions.

Figure 4. Domain structures of PTP-PEST associated partners. A graphic depiction of the structural organization of adaptor ptoteins p130Cas, paxillin, Shc (p52 and p66) and PSTPIP as well as of the tyrosine kinase Csk is illustrated accordingly to previous descriptions (32, 38, 71, 72, 85, 262). The domains of each molecules involved in their binding to PTP-PEST are underlined.

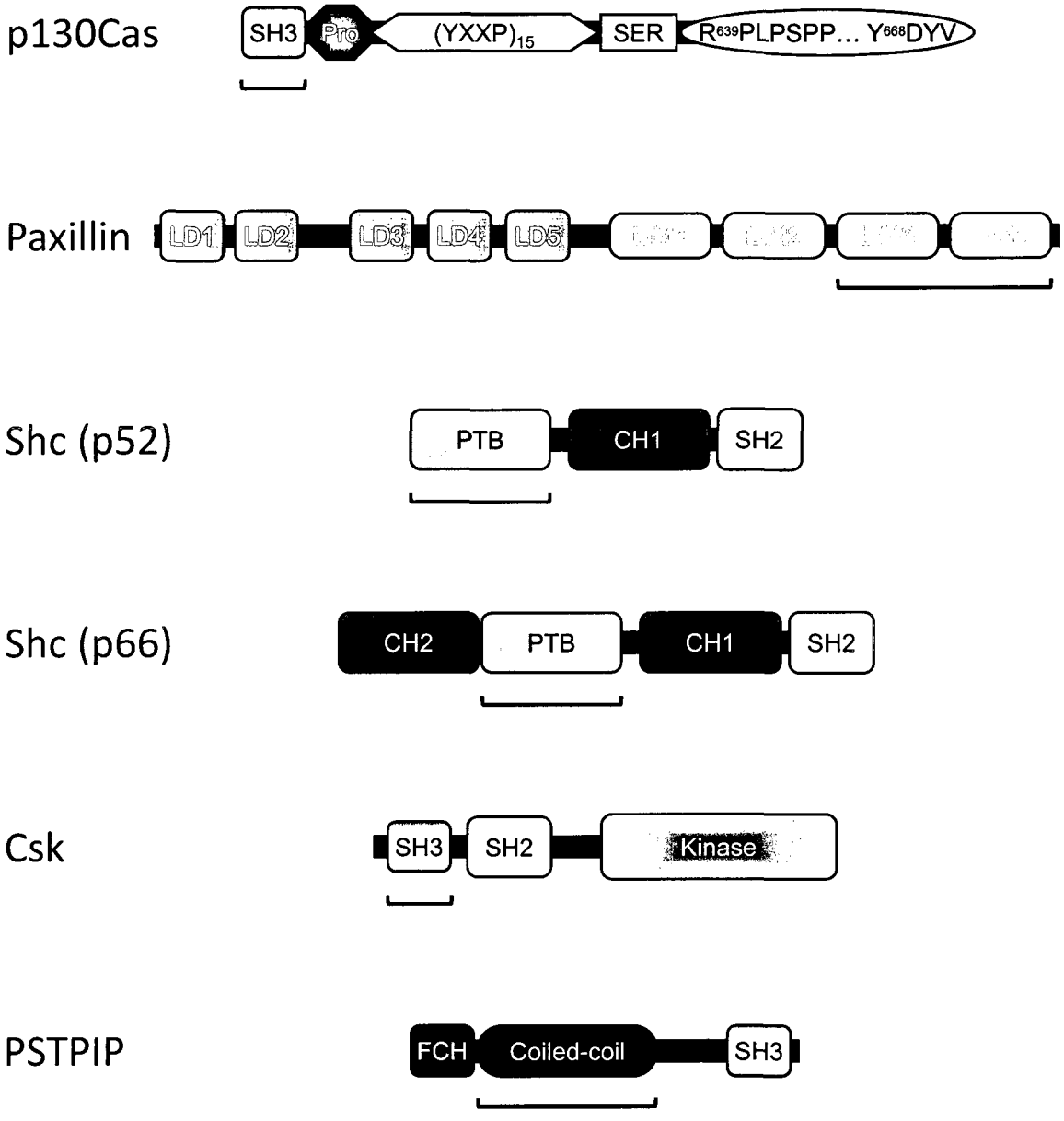
p130Cas
SH3
Pro
(YXXP)15
SER
R639PLPSPP... Y668DYV
Paxillin
LD1
LD2
LD3
LD4
LD5
Shc (p52)
PTB
CH1
SH2
Shc (p66)
CH2
PTB
CH1
SH2
Csk
SH3
SH2
Kinase
PSTPIP
FCH
Coiled-coil
SH3
Area binding to PTP-PEST

FIG. 4

1.4 PAXILLIN

In chicken embryo (CE) cells, expression of FAK leads to phosphorylation of multiple proteins, but only in the presence of PTP inhibitor; indicating that FAK could be associated with a PTP controlling its activity (289, 300). Shen et al (1998) described four FAK-interacting PTPs, of which one was later identified as a PTP-PEST (300). The association of PTP-PEST with FAK was not direct, but was mediated by paxillin via formation of FAK-paxillin-PTP-PEST complexes (300). PTP-PEST has also been reported to associate with other paxillin family members, including Hic-5 (hydrogen peroxide inducible clone-5) and Leupaxin (131, 243). The LIM 3 and 4 domains of paxillin and the LIM 3 domain of Hic-5 are necessary for binding to PTP-PEST (86, 243), and the paxillin/Hic-5 recognition site is contained within the second poly-proline rich motif of the non-catalytic segment of PTP-PEST (86, 243).

Paxillin is a multidomain adaptor molecule, which contains five leucine-rich regions (LD motifs) as well as several phosphorylation sites on its amino-terminal portion and four lin-11, isl-1, mec-3 (LIM) domains on the carboxy terminus (Fig. 4) (38). The high abundance of paxillin found in adhesion structures has led to the use of this protein as a marker of focal adhesion, or, more precisely, of focal contact (378). Genetic manipulation of paxillin expression in murine models has illustrated the importance of paxillin in cellular processes dependent on tight control of the cytoskeleton. Cells isolated from *paxillin*-null embryos showed altered morphology of both focal adhesions and of the cortical actin cytoskeleton (134). Architectural defects of the actin network caused delayed spreading and migration in *paxillin* -/- fibroblast cells (134). Inactivation of *paxillin* in embryonic stem (ES) cells also impeded their spreading following attachment to fibronectin (349). In both cases, altered FAK activation was correlated with the absence of paxillin (134, 349). In addition to FAK, paxillin also interacts with a variety of other signalling and cytoskeletal proteins, including, for example, vinculin, Crk, Csk, α4 and α9 integrins, integrin-linked kinase (ILK), p85 subunit of PI3K, actopaxin, and

paxillin kinase linker (p95PKL) (38). By mediating the association of these proteins, paxillin acts as a platform integrating adhesion and growth factor-initiated signals, in order to sustain cell migration (38, 362).

Interestingly, mutation of the PTP-PEST binding site of paxillin retarded its relocalization to focal adhesion sites of CHO.K1 cells plated on fibronectin (39). In addition, overexpression of the LIM3-LIM4 domain of paxillin stimulated cellular spreading and lamellipodia formation (39). The tandem LIM3-LIM4 engineered protein allows binding to PTP-PEST, but not to other paxillin binding partners, and may work as a functional dominant negative for the paxillin-PTP-PEST interaction. Finally, and of particular importance, paxillin is required for PTP-PEST-mediated Rac inhibition and PKL dephosphorylation, which are necessary for the control of cell spreading and migration (172). In addition to it's role in cell motility, the PTP-PEST/paxillin association may be involved in other physiological processes. This possibility, however, has not yet been investigated.

1.5 Shc

PTP-PEST was identified as a binding partner for Shc in a yeast two hybrid screen for proteins interacting with $p52^{Shc}$ (133). Three Shc encoding genes have been identified in mammals: ShcA, ShcB and ShcC (262). The ShcA protein is present as three isoforms (46, 52 and 66 kDa), as a result of either splicing or alternative translational initiation (253, 262). PTP-PEST interacts with the p52 and p66 isoforms of Shc, but not the p46 isoform (133). Shc is a scaffolding molecule consisting of an N-terminal phosphoryrosine-binding domain (PTB) and a C-terminal SH2 domain, separated by a collagen homology domain (CH1) (Fig. 4) (262). The p66Shc isoform also contains a second CH domain (termed CH2) found at the N-terminus of the protein (Fig. 4) (253).

Activation of the Ras-MAPK cascade plays a crucial role in both survival and proliferation, and is aberrantly activated in several types of cancers. Stimulation of a variety of receptors, including the receptor tyrosine kinases (RTKs), leads to the recruitment of Shc via its PTB and phosphorylation of several conserved tyrosine residues within its CH1 (Y239, Y240 and Y317 in $p52^{Shc}$) (262). Phosphorylated Shc has a high affinity for Grb2 SH2, which, in turn, interacts with Sos, a Ras guanine nucleotide exchange factor, through its SH3 domains (262). Assembly of the Shc/Grb2/Sos complex at the membrane leads to the activation of Ras and of downstream MAPKs (262). Shc, as a key component of this molecular machinery, plays a crucial role in signalling pathways sustaining cell survival and proliferation. In parallel, hyperphosphorylation of Shc was noted in a number of tumour cell lines (251). Also, inactivation of ShcA leads to major disturbances in adhesive-cytoskeletal structures, causing a phenotypic shift from normal/elongated to a radial cellular morphology (199). PTP-PEST was proposed to dephosphorylate Shc, dependent on an interaction between NPLH motif of PTP-PEST and the PTB domain of Shc (53, 95, 133). Although PTP-PEST can inactivate the Ras-MAPK pathway (95), the precise function of the PTP-PEST-Shc interaction remains obscured. However, given the importance of Shc in the formation/function of the actin network, and in cell survival/proliferation, it seems likely that the Shc/PTP-PEST interaction plays a role in these processes.

1.6 Csk

Csk is a 50 kDa protein tyrosine kinase composed of an amino-terminal SH3 domain followed by an SH2 domain and a catalytic domain (Fig. 4) (72). A yeast two hybrid screen using Csk as a bait provided primary evidences for its interaction with a PTP, PTP-PEP (74). Subsequent investigations identified a proline-rich domain within the PTP-PEP non-catalytic region as the site of interaction with the Csk SH3 domain (74, 126). This segment, of PTP-PEP was found to be practically identical to the fourth proline-rich motif (Pro4 or P4 on Fig. 2, previously identified as P2 (94)) within the PTP-

PEST non-catalytic carboxy terminal region. Further examination confirmed a direct interaction occurring between the SH3 domain of Csk and the Pro4 domain of PTP-PEST (94). Although Csk plays a significant role in the inactivation of Src family members, the participation of PTP-PEST in this phenomenon remains to be demonstrated. Nevertheless, Csk is required for LPA-induced G protein-coupled receptor-mediated actin stress fibres formation (214), and, of particular note, Csk binds to the phosphorylated *Helicobacter pylori* protein CagA, and attenuates the effect of the bacterial protein on cell survival and morphology, and allows the infection to persist (341). Csk could therefore represent a potential molecular link for the integration of PTP-PEST into less characterized and under-appreciated biological functions.

1.7 PSTPIP

A yeast two-hybrid search for PTP-HSCF interacting species, using a C221S inactive mutant of the enzyme as bait, led to the identification of a novel protein named proline serine threonine phosphatase interacting protein (PSTPIP) (307). The amino terminus of PSTPIP displays significant homology to the yeast protein CDC15p (85, 307). The latter contains a Fer kinase and CIP4 homology (FCH) domain and a coiled-coil domain (85). The similarity between the amino terminal portion of murine PSTPIP and FBP17 (Human), Toca-1 (Human), CIP4 (Mouse), PSTPIP2 (Mouse, also termed macrophage actin-associated tyrosine phosphorylated protein [MAYP]), Sydapin1 (Human), Syndapin2 (Human), Nostrin (Human), FER (Human) and CDC15p (*S. pombe*) following the FCH domain was proposed to work as a functional unit termed extended FC (EFC) domain (340). The carboxy-terminus of PSTPIP contains an SH3 domain (307), which is absent from PSTPIP2 (Fig. 4) (363, 374). Unexpectedly, the recruitment of PSTPIP to the C-terminal proline-rich motif of PTP-HSCF did not depend on its SH3 domain, but rather on its coiled-coil region (307), in which a trypophan residue in position 232 was critical for the interaction (100). Interestingly, the C-terminal poly-

proline motifs, referred to as CTH domains, of PTP-HSCF, PTP-PEP and PTP-PEST are highly conserved (100). In addition, the coiled-coil domain of PSTPIP also interacts with the CTH region of PTP-PEST (85).

In 3T3 cells, PSTPIP co-localizes with actin-rich structures, and its overexpression drives the formation of extended filopodia (307). Additioinally, PSTPIP is present in the actin ring forming the cleavage furrow of dividing cells, as are its yeast homologues imp2 and CDC15 (97, 307). The above evidence indicates that PSTPIP may recruit or modulate proteins that regulate cytoskeletal architecture and dynamics. Of note, the SH3 domain of PSTPIP interacts with two poly-proline regions of WASP, and inhibits WASP-induced actin bundling in cells (364). In addition, the coiled-coil arm of PSTPIP interacts with PTP-PEST, which brings PTP-PEST and WASP into close proximity (85) thereby allowing the dephosphorylation of WASP and the subsequent inhibition of its actin polymerization promoting activity (18, 85). PSTPIP has also been found in an analogous complex with PEST-type PTPs (PTP-PEST or PTP-HSCF) and Abl, leading to dephosphorylation and inactivation of this PTK (79). Finally, PSTPIP is capable of scaffolding Fas Ligand (FasL) and PTP-PEST, which implicates PTP-PEST in apoptosis induced by cytotoxic T-cells and Natural Killer (NK) cells (21). PSTPIP clearly works as a scaffolding molecule which connects PTP-PEST with multiple substrates, and thereby potentially connects PTP-PEST to a variety of additional biological pathways. However, the potential role of PSTPIP/PTP-PEST in apoptosis remains unclear, and, although WASP, as well as several of its binding partners, are targeted by intracellular microorganisms (125, 212, 308), the involvement of PTP-PEST, and/or a PTP-PEST/PSTPIP interaction, in these events has not yet been examined.

1.8 *LEISHMANIA*

The infection and propagation cycles of intracellular pathogenic microorganism often involve the subversion of host cell signalling and cytoskeletal machinery. Among those, the protozoa *Leishmania* has developed an arsenal of strategies to infiltrate and persist within their host. The genus *Leishmania* is part of the phylum *Sarcomastigophora*, in the order *Kinetoplastida* and the family *Trypanosomatidae*. This genus has been subdivided into two subgenera: *Leishmania* and *Viannia* (270).

1.8.1 Pathologies

It is thought that leishmaniasis may have afflicted people as far back in human history as 650 BC (183), and the disease is represented in pre-Inca pottery from Peru and Ecuador. Disfiguring lesions depicted by artists from this period on pre-Inca pottery during the first century could likely be attributed to *Leishmania* infection (183). The pathogen *Leishmania* causes a variety of clinical symptoms that can be separated into three types: cutaneous, mucocutaneous and visceral.

Cutaneous leishmaniasis can give rise to numerous lesions, in some cases up to 200 (359). Lesions initially appear as small red papules, which progress into nodules and ulcerated plaques characterized by a depression surrounded by an indurated edge (148). Although lesions usually heal within months to a year, leaving unpigmented scars (270), they commonly persist, and can be accompanied by secondary bacterial infections (148, 270). In addition to the physical suffering, afflicted patients are often victims of social prejudice (359).

Parasites of the subgenus *Viannia* (ex: *L. braziliensis*) cause the mucocutaneous form of leishmaniasis; also known as espundia or uta. Initial symptoms arising at the site

of inoculation (small red cutaneous papules) are similar to those observed with other species of *Leishmania* (270). Amastigotes then migrate or disperse, via the lymphatic system, to the buccal and nasal mucosa (90, 148). These secondary infections lead to the degeneration of cartilaginous and soft tissues (90, 270), and results in disfiguring ulceration of the lips, nose, palate and pharynx, as well as loss of the voice via infection of the larynx, trachea and vocal cords (90, 270). Patients can survive for several years with these painful symptoms, and death could result from secondary bacterial infections, malnutrition or respiratory complications (90, 270). Living with this disfiguring disease is also socially detrimental for the afflicted patients (359).

Visceral leishmaniasis initially manifests as low grade fever and mild discomfort (270), leading, in later stages, to more severe symptoms, including fever, cachexia, and abdominal swelling due to splenomegaly and inflammation of the liver (148, 270). Failure to administer the proper treatment results in 100% mortality within two years (148, 270, 359). This disease is predominantly caused by *L. donovani* in the Old World and by *L. chagasi* in the New World (90). Degeneration of *L. infantatum* infection can also lead to visceral leishmaniasis (90).

1.8.2 Parasitic life cycle of Leishmania

The protozoa *Leishmania* is transmitted between vertebrates by phlebotomine sand flies. This disease can be either a zoonosis, involving domestic or wild animals, or an anthroponosis, in which humans act as reservoir (182, 359)). Among the 400 reported different sandfly species, only 50 were implicated in the transmission of the parasite *Leishmania* (182). Following aspiration of infected blood, amastigotes (form of the parasite found in the mammalian host, see below) move to the abdominal (posterior) gut of the sandfly, where they are enveloped by a peritrophic membrane (made of proteins and glycoproteins tight together by chitinous microfibrils) secreted by gut

epithelial cells (182, 281). The parasite will spend between six and nine days within the sand fly to complete its development (182).

Amastigotes initially differentiate into small, ovoid and minimally motile procyclic promastigotes with short flagella (182). Over a period of 24-48 hours, procyclic promastigotes undergo rapid division, prior to their development into narrow elongated promastigotes termed nectomonads (182). This process occurs approximately 2-3 days following ingestion of infected blood (182). The degeneration of the peritrophic membrane liberates nectomonads in the lumen of the gut, where they adhere to the mid-gut epithelial cells and migrate towards the thoracic (anterior) mid-gut (182). At about day four, nectomonads differentiate into a shorter form named leptomonads, which undergo a second round of multiplication, resulting in considerable infection of the anterior mid-gut at day 5-7 (182). Haptomonads, the origin of which (nectomonads/leptomonads) remains to be determined, are non-motile parasites with a leaf-like morphology and a short flagellum (182). Haptomonads accumulate at the stomodeal valve and form a ring blocking passage through the valve (182). Leptomonads present in the anterior mid-gut differentiate into metacyclic promastigotes that aggregate behind the stomodeal valve (182). The non-dividing metacyclic promastigotes have a long flagellum attached at their compact cell body, which allows fast and efficient movement (182). The metacyclic promastigotes have several characteristics, including resistance to complement-mediated lysis (see below), which make them the most virulent form of *Leishmania* (182). In addition, leptomonads secrete a gel-like matrix, termed, "promastigote secretory gel", which fills and obstructs the lumen of the thoracic mid-gut (182). This matrix contributes to the transmission of the parasite because the congested fly tries repeatedly to collect blood; each time releasing metacyclic promastigotes (182).

Following inoculation of the vertebrate host, promastigotes are phagocytosed by mononuclear phagocytic cells (monocytes and macrophages) (Fig. 5) (147).

Phagocytosed metacyclic promastigotes are incorporated in phagolysosomes, where they lose their flagella, becoming 2-5 μm spheroids (90, 147). This differentiated form of parasite, termed the amastigote, then multiplies within the macrophage, via binary fission (147). Heavily infected macrophages explode and liberate their amastigotes, which will then colonise other macrophages. Depending on the *Leishmania* species, amastigotes may remain localized in a define area, causing dermal lesions near the site of inoculation (ex: cutaneous leishmaniasis caused by *L. major*); or may migrate to other tissues and cause more severe symptoms.

Figure 5. Life cycle of *Leishmania* parasites. Following their inoculation in a vertebrate host, *Leishmania* promastigotes are phagocytosed by host macrophages. Within macrophages, *Leishmania* promastigotes undergo differentiation into amastigotes, which multiply and accumulate until the cell bursts and they are released. Released amastigotes then go on to infect other macrophages. Ingestion of contaminated blood by the sandfly allows transmission of the disease between vertebrates.

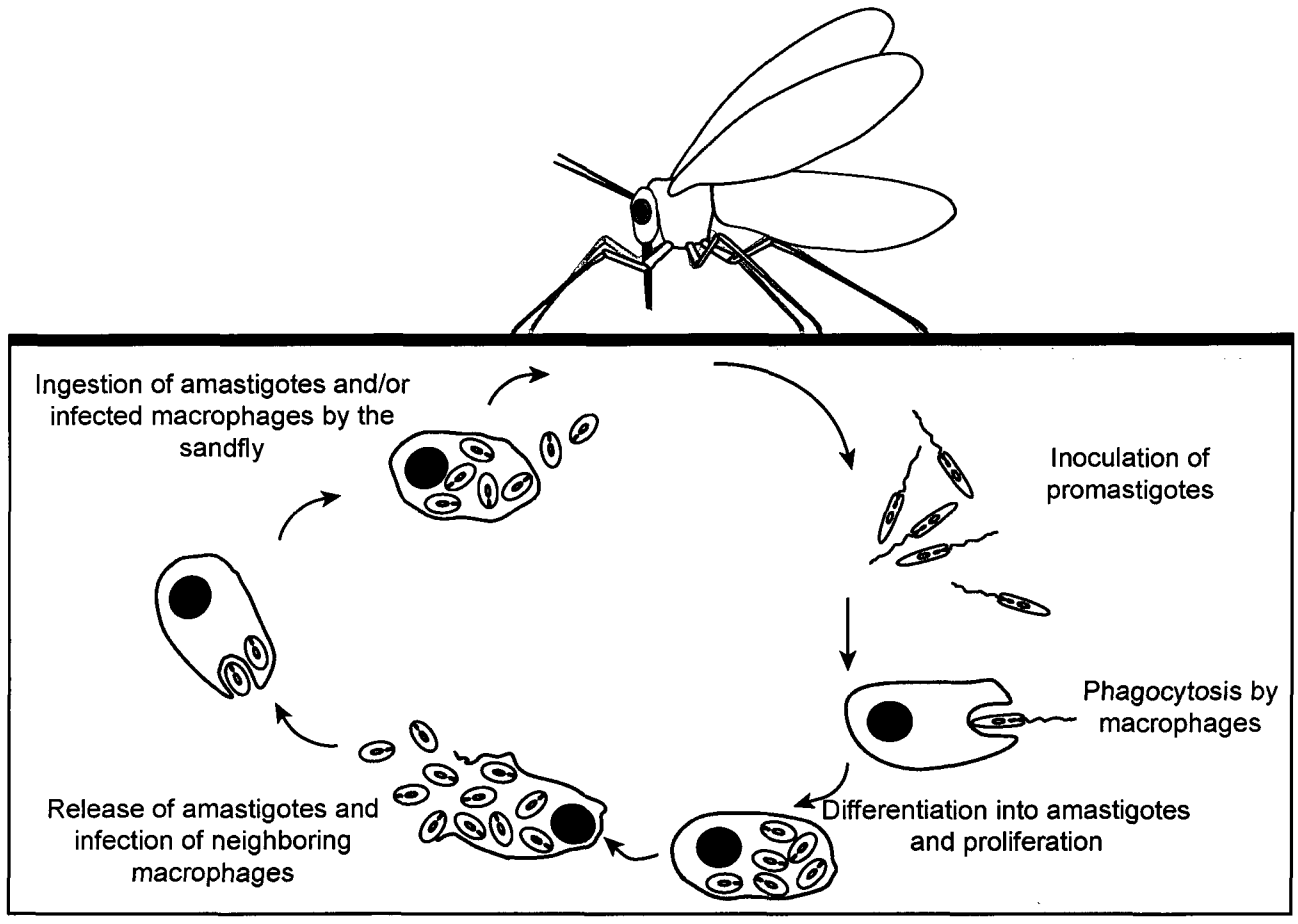
Ingestion of amastigotes and/or infected macrophages by the sandfly
Inoculation of promastigotes
Phagocytosis by macrophages
Differentiation into amastigotes and proliferation
Release of amastigotes and infection of neighboring macrophages

FIG. 5

Transmission of *Leishmania* relies on the presence a vector species, in this case the sandfly; which is found in tropical, subtropical and temperate areas within 88 countries (182). More than half of all the cutaneous leishmaniasis cases occur in eight countries: Afghanistan, Algeria, Brazil, Iran, Iraq, Saudi Arabia, Sudan and Syria (13). With respect to visceral leishmaniasis, over half of all people infected are concentrated in only two countries: India and Sudan (13). At the moment, leishmaniasis threatens approximately 350 million people across the world (359). As a result of global warming, sandflies, and therefore *Leishmania*, will likely begin to emerge in previously unaffected areas.

All *Leishmania* species display similar patterns of development and replication. Alternation between an insect vector and a vertebrate host is necessary for life cycle completion. The insect vector is required for transmission, and therefore for invection of a variety of mammalian species, including humans (182). The above described life cycle places these parasites in hostile environments: the insect digestive tract and the mammalian macrophages intracellular space, and has forced them to develop strategies for survival in these specific locations.

Leishmania parasites from the Old World (ex: *L. major* and *L. donovani*) have 36 pairs of chromosomes, while species from the New World have 34 or 35 pairs, including chromosome fusions (168, 356). Chromosomes of Kinetoplastids (including *Trypanosoma* and *Leishmania*) are arranged in directional gene clusters (168). Recently, the 32 816 678-base pair genome of *L. major* was sequenced (168). From this sequence, the presence of 911 RNA genes, 39 pesudogenes and 8272 protein-encoding genes was predicted (168). The protein-encoding genes are organised in 133 long, and are located on the same strand polycistronic clusters having tens to hundreds of protein-coding genes, which do not necessarily have related predicted functions (168). Among the above described genes, several encode virulence factors involved in host colonisation, protection, or neutralization of hosts-defence mechanisms.

Leishmania parasites take advantage of and manipulate several components of the host signalling machinery, including the mitogen-activated protein kinases (MAPKs). The infection of macrophages with opsonised *L. amazonensis* amastigotes results in ERK1/2 activation, which induces interleukin-10 (IL-10) production (367). The cytokine IL-10 has an inhibitory effect on immune function, and its synthesis was directly correlated with the severity of leishmaniasis (367). Activation of ERK1/2 by *L. amazonensis* therefore contributes to disease progression. Interestingly, in a 2007 study from Yang et al, promastigotes of *L. amazonensis* did not activate the ERK MAP kinases (367). In addition, attachment and internalization of *L. donovani* did not promote the activity of p38, JNK or ERK MAP kinases (258). Promastigote manipulation and/or circumvention of strong MAP kinase activation may represent a strategy for evasion of host cell defence mechanisms. Incubation of macrophages with a p38 inhibitor prior to exposure to *L. donovani*, increased the subsequent parasitic load (179), and attenuated anisomycin inhibited *L. donovani* survival inside macrophages (179). Moreover, *L. major* down-regulates p38 in order to impair CD40-mediated iNOS2 expression, which inhibits nitric oxide production and favours survival within macrophages (17). Through inhibition of p38, the parasite can also hijack the signal initiated by CD40 cross-linking in a fashion allowing IL-10 expression and reducing IL-12 expression (224). As IL-12 can promote the host-protective T-helper type 1 (TH1) cell response, a reduction in its expression would benefit the parasite (224). Consequently, the subversion of host-cell signalling functions, in particular the MAPK p38, could be a marker for successful and persistant infection by *Leishmania*.

Although *Leishmania* preferentially parasitizes macrophages, it is capable of infecting other cell types, including neutrophils, eosinophils, epithelial cells, dendritic cells and fibroblasts (22, 29, 247, 345, 358). Chinese hamster ovary (CHO) cells have been used as fibroblast model for the study of *Leishmania* internalization in this cell type (237). In this system, amastigote activates the re-organisation of the actin cytoskeleton

and the recruitment of vinculin to form a structure called an actin cup, which surrounds the parasite during its entry into cell (237). While parasites opsonised with IgG strongly activated Rac-1 in cells expressing the FcRII-B2 receptor, antibody-coated and non-opsonised amastigotes did not require Rac-1 for entry into CHO FcRII-B2-deficient cells, resulted in only weak activation of Rac-1 (237). It was found that, non-opsonized *L. amazonensis* amastigotes were dependent on Cdc42, and not Rac-1, for infection of CHO cells (237). In line with the above finding, increased activation of Cdc42 was seen following the exposure of CHO cells to *Leishmania* amastigotes (237). Both Cdc42 and Rac-1, however, actively participate in phagocytosis of *L. donovani* by macrophage (206, 212). In addition, Cdc42 and Rac-1 are responsible for "knitting" an actin shell at the periphery of *L. donovani* containing phagosomes (206). This layer of polymerized actin was proposed to act as a protective coat, impairing efficient maturation of the phagosome (206). These reports provide convincing evidence for initiation of signalling cascades leading to remodelling of the actin cytoskeleton during *Leishmania* infection.

1.9 GP63

Molecules found at the surface of *Leishmania* play multiple roles throughout the life cycle of the parasite, including survival in the vector, virulence, invasion and persistence in the mammalian host (103). *Leishmania* is surrounded by a glycocalyx, which is composed primarily of lipophosphoglycan (LPG), glycoinositolphospholipids and glycosylphosphatidylinositol (GPI)-anchored proteins (103). GP63, also known as major surface protease (MSP), leishmanolysin, EC3.4.24.36 or promastigote surface protease (PSP), is the most abundant protein that covers the surface of *Leishmania* promastigotes (369). This highly abundant 63-kDa protein ($5X10^5$ copies/*L. major* promastigote) represents approximately 1% of the total protein content of the organism (33). Etges et al (1986) fortuitously noted the proteolytic activity of GP63 after mixing their purified product with proteins used as molecular weight markers for SDS-PAGE (106). The

protease activity of GP63 was subsequently confirmed using casein/albumin in a zymogram assay (106). Elucidation of the GP63 structure showed that this protein consists of three domains; N-teminal, central and C-terminal (291). The N-terminal domain has several features of a zincin protease, including the concensus sequence HEXXH (291). The metzincin class of metalloendopeptidases is characterized by a signature HEXXHXXGXXH motif, in which the three histidines participate in the coordination of a zinc atom. The structure of GP63 reveals that it also possesses a third histidine that contributes to zinc binding, but the ladder is present in the central domain, and is separated from the glycine within the signature motif by 62 amino acids (291).The N-terminal and central domains are therefore both important for catalysis, and in the coordination of the zinc atom (291). In addition, the N-terminal domain bears a hydrophobic signal motif thought to target the protein to the endoplasmic reticulum (369), and a pro-peptide sequence that maintains the enzyme in an inactive state during synthesis and maturation (217, 369). The pro-peptide sequence contains a conserved cysteine that obstructs enzymatic activity through interaction with the zinc at the catalytic site (217). The above described property of GP63 is thought to protect the parasite via inhibition of uncontrolled catalytic activity. Proteolysis of the pro-peptide activates GP63 through a process called the cysteine switch mechanism; which involves release of the cysteine residue (217). The C-terminal domain contains an asparagine residue, which acts as the site of glycosylphosphatidylinositol (GPI) anchor addition, and is highly conserved but not obligatory (369). In several cases the conserved asparagine is absent and the site of GPI anchor addition is therefore not functional. In these cases, an extended hydrophobic group of amino acids found at the C-terminus likely functions as a transmembrane domain (369). The C-terminal domain is less conserved than either the N-terminal or central domains (291).

Tandem arrays of genes encoding abundant proteins are a common feature among the *Trypanosomatidae* protozoa, and multiple copies of GP63 genes, organized in tandem, have been found in various *Leishmania* species. For example, *L. mexicana*

posseses at least 10 *gp63* genes, *L. donovani* has 7 tandemly repeated *gp63* genes, as well as three additional ones in distinct regions, and the 18 *gp63* genes of *L. chagasi* lead to the expression of at least 10 different protein isoforms in stationary promastigotes (351, 369, 372). *L. major* has the lowest number (7) of *gp63* genes, and, their expression is restricted to particular stages of the parasitic life cycle (177, 347). *L. major* GP63 encoding genes 1-5 are only expressed at high levels in promastigotes, whereas a low level of gene 6 expression is found in both promastigotes and amastigotes (347). Targeted inactivation of gp63 gene 1-6 has shown that the expression of gp63 gene7 in *L. major* is developmentally regulated (177). The expression of gp63 gene 7 was seen only in metacyclic (stationary phase) promastigotes and in amastigotes (177).

1.9.1 Functions of GP63

1.9.1.1 Expression of GP63 facilitates *Leishmania* multiplication in certain species of sandfly.

Expression and secretion of GP63 by promastigotes in the sandfly gut has been proposed to facilitate nutrient acquisition and to protect the protozoan against host digestive enzymes (292, 369). Anti-sense-mediated down-regulation of GP63 in *L. amazonensis* significantly reduced early parasitic proliferation in the midgut of the fly *Lutzomia longipalpis* (135). In contrast, partial inactivation (genes 1-6) as well as complete deletion (genes 1-7) of *gp63* did not affect the multiplication and differentiation of *L. major* in *Phlebotomus* (*P. papatasi*, *P. argentipes* and *P. dubosqui*) sandflies (176, 177). It therefore seems that the importance of GP63 in protozoan colonization of the insect vector is likely dependent on the identity and combinaison of parasite and sandfly.

1.9.1.2 The expression of GP63 correlates with *Leishmania* virulence.

Both cell surface level and the proteolytic activity of GP63 is significantly higher in virulent than in avirulant promastigotes (57). Also, the specific activity of GP63 appears to be higher at 37 °C than at 27 °C; or, in other words, is more effective at the body temperature of the mammalian host than at that of the insect vector (57). In *L. chagasi*, the abundance of GP63 increases 14 fold as promastigotes progress from logarithmic to stationary phase (370). Increased diversity of GP63 isoform expression can also be correlated with the growth phase of *L. chagasi* (372). The alteration in GP63 expression pattern seen during metacyclicogenesis occurs in parallel with increased virulence; thus pointing to a putative role for this protease in the malignance of *Leishmania* parasites.

1.9.1.3 GP63 facilitates the dissemination of *Leishmania* in the mammalian host.

Dissemination of the parasite throughout the host is an obligatory phase for establishment of infection at distal target sites, and GP63 has emerged as a contributing factor in this process. In fact, both GP63 expression level and catalytic activity are important for the migration of *L. amazonensis* through a Matrigel matrix (227). In addition, surface localized as well and secreted, forms of GP63 were shown to cooperate in promotion of the passage of *Leishmania* cells across a mammalian extra-cellular matrix (ECM) (227). The ability of GP63 to enhance migration and to contribute to digest ECM constituents was confirmed by the identification of collagen type IV, fibronectin and laminin GP63 substrates (227). Interestingly, incubation of *Leishmania*-infected macrophages with GP63-processed fibronectin (or fibronectin degradation product) attenuated the production of reactive oxygen intermediates and enhanced amastigotes multiplication (194).

1.9.1.4 Functions attributed to GP63 in the *Leishmania*/macrophage interaction.

Using a virulent strain of *L. amazonensis* expressing sense or antisense *gp63* transcripts, Chen et al (2000) observed that this enzyme promotes promastigotes binding to macrophages (61). This study also provides evidence for a direct relationship between the level of GP63 expression and the survival and replication of macrophages-engulfed parasites (61). In addition, the identification of forms of GP63 expressed on amastigotes implied a potential function for this protease within the host cell (58). Interestingly, the same study exemplified that macrophages failed phagolysosomal degradation of proteins encapsulated in GP63 coated liposomes (58). In contrast, incorporation of heat-denatured GP63 on the liposomal surface failed protecting its content against the activity of macrophages, underlining the importance of GP63 proteolytic activity in this function (58). The level of GP63 activity found on phagolysosomal-residing parasites as well as the amount of the enzyme present on *L. mexicana amazonensis* parasites correlated with their ability to survive within macrophages (294). The above observations suggest that expression of active GP63 on the surface of amastigotes contributes to the preservation of their integrity within phagolysosomes. Also, the identification of the myristoylated alanine-rich C kinase substrate (MARKS)-related protein (MRP), a cytosolic protein associated with the macrophage actin network, as a substrate of GP63 provides further support for a possible role of GP63 in modulation of intracellular host machinery (82).

In addition to the macrophage response, activation of complement plays an important role in the elimination of pathogenic microorganisms. Although not strictly essential, GP63 can enhance complement fixation on *Leishmania* (37). Expression and activity of GP63 significantly reduced *Leishmania* sensitivity to complement-mediated lysis (37). In addition, the presence of active cell surface GP63 prevented the addition of the C5 and C7 terminal complement components (37). Moreover, parasites expressing wild-type GP63 showed accelerated conversion of C3b into the neoantigen form of iC3b

(37). This processing of C3b in a product similar to iC3b results in disruption of the scaffolding of the C5 convertase, leading to insertion of the membrane attack complex, and, furthermore, allows a tight interaction of the parasite with cells displaying the iC3b-receptor Mac-1 (37). In a subsequent study, the same group observed that GP63 significantly augmented complement-mediated adhesion of *Leishmania* parasites to macrophages (36), and, in parallel, GP63 was also capable of interacting with the α4/β1 fibronectin receptor (36). Although this interaction contributes only modestly to parasite attachment on the macrophages, it plays a crucial role in its internalization (36).

1.9.1.5 Deletion of specific *gp63* genes sensitises *L. major* to complement.

L. major gp63 gene1-6 deficient mutant procyclic promastigotes display increased sensitivity to complement-mediated lysis (177). This vulnerability to complement was attenuated in the metacyclic promastigotes of the same genotype (177). Correspondingly, expression of *gp63* gene 1 in the *gp63* gene 1-6 inactive mutant restored resistance to complement-mediated lysis in both procyclic and metacyclic promastigotes (177). These observations suggest that the *gp63* gene 7, which is only expressed at the metacyclic stage, can provide some protection against complement-mediated lysis, and also underscore the importance of *gp63* gene 1 expression as a promastigotic defence mechanism against the mammalian host immune system. Deletion of the first six genes encoding GP63 (genes 1-6) in *L. major* did not, however, inhibit the attachment and uptake of metacyclic promastigotes, nor did it inhibit the survival and the growth of amastigotes in macrophages (177). Also, inactivation of *gp63* genes 1-6 delayed infection establishment, but not progression of lesions subsequent to parasite implantation (177). It is possible that the expression of *gp63* gene 7 in the infectious *gp63* gene 1-6 -/- promastigotes could act to compensate for the absence of the other *gp63* genes in the pathogenic potential of this *L. major* strain. In order to investigate this possibility, Joshi et al (2002) deleted the entire segment located

between the 5' flanking region of gene 1 and the 3' flanking region of gene 7, ablating all seven genes encoding *gp63* in the genome of *L. major* (176). These mutated parasites were very sensitive to complement-mediated lysis, as compared to both *gp63-/-* gene 1 re-expressing mutant and WT protozoa (176). In addition, *gp63* deficient microorganisms displayed a significant delay in lesion formation; however, their ability to assume the progress of an established infection was maintained (176). Collectively, these findings demonstrate that GP63 is a significant *L. major* virulence factor, which allows the parasite to evade complement-mediated destruction and facilitates establishment of infection. GP63 is not, however, an essential factor for the development of *L. major* lesions stemming from an established infection. Nonetheless, these studies performed on *L. major* may not entirely represent the importance of GP63 in the virulence of *Leishmania* since there is a tremendous diversity in the sequence and quantity of *gp63* genes existing in the different species of *Leishmania*, which mediate a variety of clinical outcomes. Also, it have been proposed that the delayed infection observed with *gp63* deficient parasites may not be solely due to their increased sensitivity to the complement, but likely involves other functions of GP63 (194).

1.9.1.6 Down-regulation of *gp63* gene expression alters the cell cycle and morphology of *L. donovani*.

An independent study, also based on altered parasitic expression of GP63, indicated that the protease may have additional functions. Antisense-mediated inactivation of *gp63* genes in *L. donovani* led to significant growth retardation (249). These cells exhibited altered morphology characterized by reduced length, rounding and apparent nuclear distension (249). Interestingly, a significant proportion of the cells lacking GP63 were large, binucleated and had two flagella and kinetoplastes (249). These observations, as well as an increased proportion of G2 and M phase parasites, was interpreted to mean that *L. donovani* missing GP63 are capable of DNA and organelle replication, but failed to complete cytokinesis (249). The explanation for the divergent

phenotypes observed in various GP63 deficient *Leishmania* parasite strains is currently unknown.

1.9.2 Cellular distribution and release of GP63

Clinical isolates causing cutaneous (*L. tropica*) or visceral (*L. infantum*) leishmaniasis, as well as *L. amazonensis*, *L. major*, *L. mexicana* and *L. donovani*, were observed to release proteolytically active GP63 in cultures supernatant (103, 171, 228). *L. amazonensis* promastigotes expressing either wild type GP63 or a mutant lacking sites of N-linked glycosylation were both capable of releasing GP63 (228). The release of GP63 from *L. amazonensis* therefore does not strictly depend on glycosylation (228). Experimental approaches based on double labelling (^{35}S incorporation in total GP63 and biotinilation of surface GP63) suggested that released GP63 comes from two different cellular pools: intracellular and cell surface (228). Incubation of promastigotes with metalloprotease inhibitors or expression of mutant versions of GP63 both suggest that the release of surface GP63 is mediated by autocleavage (228). Further analysis identified two forms of secreted GP63; one with the same size as cellular GP63, and a slightly smaller one presumably generated via proteolytic cleavage (228). Yao et al (2002), however, did not observed any difference in the electrophoretic mobility of released and cellular GP63, implying a mechanism of liberation independent of proteolysis (370).

MβCD, a compound that chelates membrane cholesterol, was observed to accelerate the release of surface-anchored GP63 (368). It therefore appears that the composition of the promastigote surface lipid membrane is important for the maintenance of cell surface GP63. Upon inoculation of the mammalian host, *Leishmania* parasites transit between two different environments, which could affect the properties of their surface components. The compositions and temperatures of these two environments are different, due to the vast differentces between insect and mammalian

species. Of particular interest, incubation of stationary-phase promastigotes at 37 °C in the presence of Matrigel matrix stimulated the excretion of internal GP63, but had little effect on surface localized enzyme (368). In contrast, surface GP63 is released exclusively at room temperature (368). Yao et al proposed that the three subpopulations of GP63 (internal, surface and released) are regulated as follows (368): promastigotes undergoing logarithmic growth in the sand fly (procyclic) lose large quantities of GP63 from their surface. The release of GP63 at this stage might be related to nutrient requirements in the insect gut environment, where residual mammalian blood is a main nutrient source. Throughout the stationary phase there is reduced liberation of cell-surface GP63, along with an increased density of the protease at the external membrane, which correlates with the transformation of procyclic promastigotes into the metacyclic form (368). During metacyclogenesis, modifications to the membrane composition may occur, which would allow metacyclic promastigotes to better retain GP63 on their surface. In addition, low levels of internal GP63 are lost from metacyclic parasites residing in the insect vector, while a fraction of GP63 stably resides within the cell for at least 6 days following synthesis (371). Upon their inoculation into a mammalian host, parasites come into contact with a vastly different environment (physical and biochemical) than that found within the insect vector (368). The different properties of this new milieu have been proposed to stimulate the secretion of internal GP63 (368). It is possible that both populations of GP63 play complementary roles in infection and in evasion of the host immune response. Surface localized GP63 could provide protection against complement-mediated elimination and facilitate internalization of *Leishmania* into its target cells. Released internal GP63, on the other hand, could assist in degradation of the host's extra-cellular matrix; and hence promote promastigotes migration towards potential host cells. Recently, the release of GP63 from amastigotes was proposed to aid in their dissemination from burst-macrophages towards other mammalian host cells and organs (194). Interestingly, whereas promastigote GP63 mostly associates with membrane and microsome containing fractions, a significant proportion of amastigote GP63 is present in the cytosolic fraction

(156). Further examination of amastigotes showed that GP63 was primarily localized in the flagellar pocket, the major exocytic/endocytic site of *Leishmania* (156). Unexpectedly, analysis of supernatants from amastigote cultures failed to detect the presence of released GP63 (156). However, similarly to what was shown for promastigotes (368), it is possible that amastigotes require additional (possibly extracellular) stimuli to release GP63.

1.10 Apoptosis

As early as the mid-ninetheenth century, biologists studying the metamorphosis of amphibians and insects had noticed the occurrence of seemingly regulated cell death (211). In 1885, Walther Flemming provided early descriptions of what is defined today as an apoptotic cell (211). It is only in 1972, however, that the term "apoptosis" was proposed (184, 211). Apoptosis is an autonomous genetically programmed form of cell suicide and dismantling, which, in contrast to necrosis, avoids the induction of an inflammatory response (111). Apoptotic pathways are highly conserved among metazoan organisms, and are required for the disposal of unnecessary, infected or damaged cells (2). Regulated cell death plays a critical role in embryogenesis, tissue homeostasis and hematopoiesis (2). In addition, the apoptotic molecular machinery has been linked to numerous pathologies, clinical complications and diseases, including cancer, transplant rejection, acquired immunodeficiency syndrome (AIDS), and neurodegenerative and cardiovascular disorders (279, 384).

Figure 6. Mechanisms of caspase activation. Three principal pathways trigger the activation of the caspase cascade, and ultimately commit cells to apoptosis. Exposure to various stresses induces the intrinsic apoptotic pathway, which involves the assembly of BAX/BAK oligomers in the outer mitochondrial membrane, leading to the formation of pores, and thereby allowing the efflux of intra-mitochondrial pro-apoptotic factors. The release of mitochondrial cytochrome C plays a critical role in the formation of Apaf-1 heptamers; a complex termed the apoptosome. Recruitment of pro-caspase-9 to the apoptosome leads to its activation, which is then followed by cleavage and activation of the executioner caspases -3 and -7. Upon ligand binding, death receptors of the TNF superfamily trimerize at the plasma membrane. This stimulates the recruitment of adaptor molecules (ex: FADD) and the formation of the death-inducing signalling complex, leading to activation of the initiator caspase-8. This protease cleaves and activates caspases -3 and -7, as well as the BH3 only protein BID. Cleavage of BID results in the production of tBID, which induces BAX/BAK oligomerization. In the granzyme-B-dependent pathway, insertion of perforins in the plasma membrane of a target cell allows the delivery of granzyme-B. This proteolytic enzyme cleaves BID and caspases -3/-7; leading to their activation. All three of the above described pathways ultimately activate downstream executioner caspases, thereby leading to the cleavage of specific substrates, and to apoptotic cell death. This schematic diagram was design based on information obtained from the following references (92, 108, 267, 326).

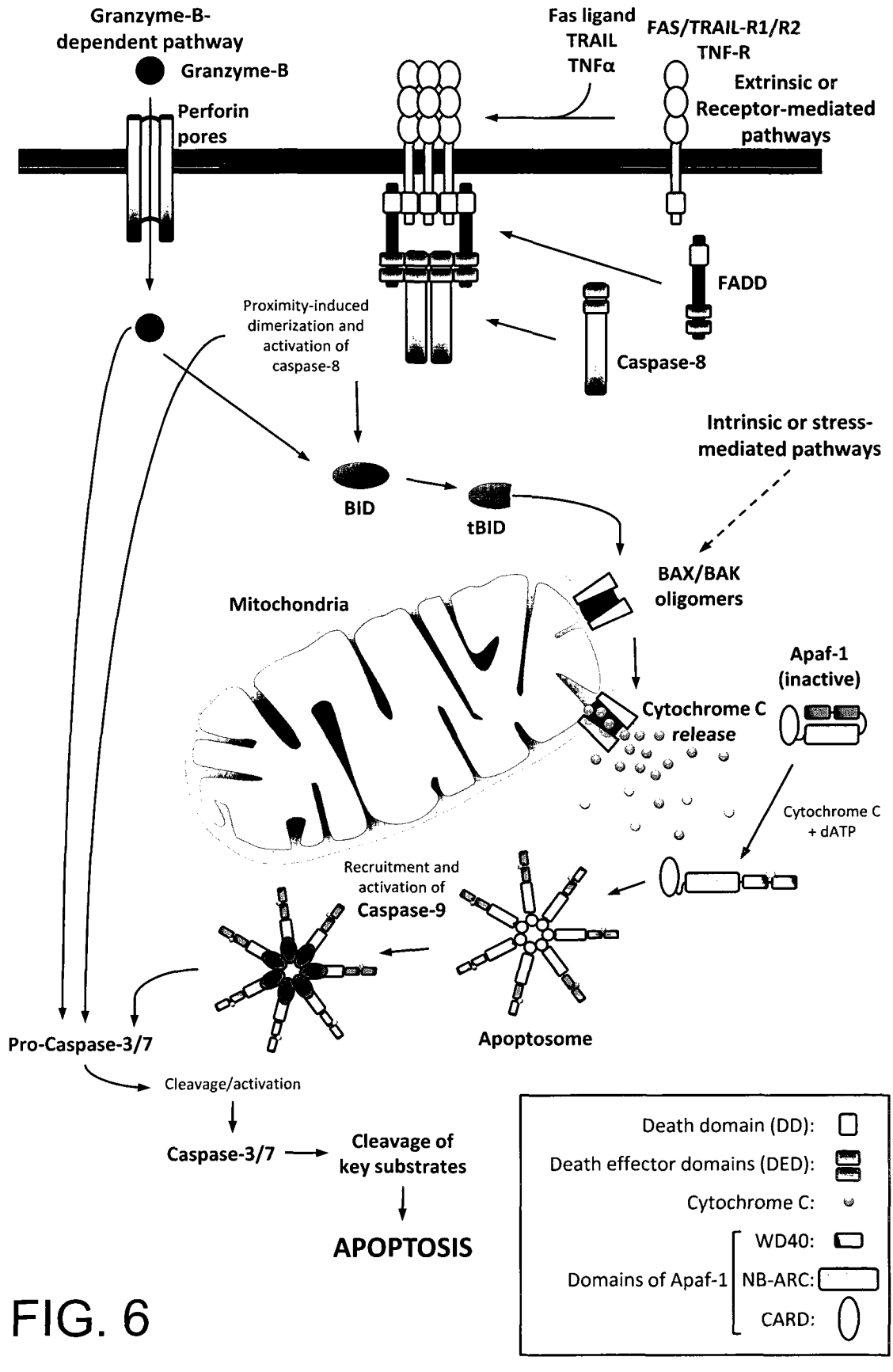
Granzyme-B-dependent pathway
Granzyme-B
Perforin pores
Fas ligand
TRAIL
TNFα
FAS/TRAIL-R1/R2
TNF-R
Extrinsic or Receptor-mediated pathways
FADD
Caspase-8
Proximity-induced dimerization and activation of caspase-8
Intrinsic or stress-mediated pathways
BID
tBID
BAX/BAK oligomers
Mitochondria
Apaf-1 (inactive)
Cytochrome C release
Cytochrome C + dATP
Recruitment and activation of Caspase-9
Apoptosome
Pro-Caspase-3/7
Cleavage/activation
Caspase-3/7
Cleavage of key substrates
APOPTOSIS
Death domain (DD):
Death effector domains (DED):
Cytochrome C:
Domains of Apaf-1
WD40:
NB-ARC:
CARD:

FIG. 6

Cells progressing through apoptosis undergo several major morphological changes, including loss of adhesion, cell rounding, membrane blebbing and cellular shrinkage, leading to the formation of apoptotic bodies (77). In addition, cells also exhibit nuclear condensation, and, fragmentation of both DNA and organelles (Golgi apparatus, endoplasmic reticulum (ER) and mitochondrial network) (326). Finally, apoptotic bodies are rapidly engulfed by phagocytes (77, 326). Rearrangements of actin filaments are tightly linked with apoptosis. Cytoskeletal disruption is a characteristic of apoptosis initiated by diverse stimuli, and, in addition, can itself initiate both anoikis and amorphosis (222). Anoikis is characterized by cell detachment, followed by cell death, while amorphosis is characterized by altered cell morphology followed by cell death (222). Finally, apoptosis induced by other stimuli involves phenotypic changes resulting from weakening of the cytoskeletal network due to caspase cleavage of actin and elements involved in its assembly (326).

Caspases play a crucial role in execution, as well as transmission and amplification, of apoptotic signals (112). These cysteine proteases cleave their substrates with remarkable specificity for a site preceded by an aspartic acid (28). Among the eleven caspases found in humans, not all are involved in apoptosis. Caspases -1, -4 and -5 play a role in proinflammatory cytokine activation, while caspase-14 is involved in keratinocyte differentiation (342). Caspases involved in apoptosis have been subdivided into two groups: the initiator caspases (caspases -2, -8, -9 and -10; with caspase-10 being absent in mice) and the executioner caspases (caspases -3, -6 and -7) (196). These enzymes are present in most healthy cells as inactive zymogens ("pro-caspases"), which, in response to a cell death signal, undergo post-translational modifications leading to their rapid activation (108). Both initiator and executioner caspases possess a large and a small subunit, the activation induced rearrangement of which is required for enzymatic activity (326). Initiator caspases are characterized by a long pro-domain, which contains interaction mediating motifs that allow their recruitment to regulatory molecules (196). The recruitment of monomeric pro-caspase (-

8 or -9) to their respective activating complexes leads to induced proximity of multiple monomeric species, and thus allows their dimerization and autoactivation (28, 267). Once activated, initiator caspases activate executioner caspases. In contrast to initiator pro-caspases, effector pro-caspases are present as dimers, and possess a short pro-domain of 20-30 amino acids (28, 268). The processing of executioner pro-caspases leads to activation via dissociation of the intersubunit linkers from the active site, providing an active conformation to the cleaved enzyme (267). The different mechanisms involved in initiator versus executioner pro-caspase processing imply that activation of initiator, but not executioner, caspases is reversible (267). Once activated, executioner caspases lead to completion of the cell death program via proteolysis of specific substrates.

There are three predominant apoptotic pathways, all of which ultimately lead to caspase activation: the intrinsic, the extrinsic and the granzyme B-dependent pathway. Members of the B-cell lymphoma-2 (BCL-2) family protein play a crucial role in regulation of the intrinsic pathway. This protein family consists of both anti- and pro-apoptotic members, which have been subdivided according to both function and their BCL-2 homology (BH) domain composition (174). The anti-apoptotic members (BCL-2, BCL-XL, BCL-W, MCL1, BCL2A1 and BCL-B) possesses four BH domains (BH4, BH3, BH1 and BH2) and (except for BCL2A1) a transmembrane domain (174, 326). The pro-apoptotic members can be further subdivided in two groups: those lacking the BH4 domain (BAX, BAK andBOK) and those containing only the BH3 domain (BIK, HRK, BIM, BAD, BID, PUMA, NOXA and BMF); termed "BH3-only" proteins (174, 326). BH3-only proteins are typically upregulated in response to various pro-apoptotic stimuli, including DNA damage, cytoskeletal alterations, and growth factor deprivation, and act to couple these signals to induce recruitment and oligomerization of BAX and BAK at the outer mitochondrial membrane (OMM) (Fig. 6) (174, 222). The assembly of BAX/BAK containing oligomers at the OMM leads to membrane permeabilization, and subsequent efflux of pro-apoptotic molecules, including cytochrome C (174). In healthy cells,

apoptotic protease-activating factor-1 (Apaf-1) is found as an inactive monomer in closed conformation (267). Following an apoptotic stimulus, cytochrome C released from the mitochondria binds to the WD40 region of Apaf-1, leading to dATP-dependent Apaf-1 opening and oligomerization (267). This cytochrome C/Apaf-1 complex is referred to as the apoptosome, and acts as a platform for the recruitment and activation of caspase-9 (267). Active caspase-9 then cleaves and activates the executioner caspases -3 and 7 (267, 271).

The extrinsic apoptotic pathway plays an important role in both embryonic development and in cytotoxic T lymphocytes (CTL) or natural killer (NK) cell-initiated death of transformed and foreign antigen presenting cells (28, 92, 108). Members of the Tumour Necrosis Factor (TNF) receptor family, including TNFR1, FAS (CD95/Apo1), TRAILR1 (DR4/Apo2), TRAILR2 (DR5/TRICK2), DR3 (TRAMP/Apo3) and DR6, act to sense and propagate death signals (92, 108). Upon ligand binding, death receptors such as FAS and TRAIL-R (1 or 2) undergo trimerization, which triggers recruitment of the adaptor molecule Fas-associated protein with death domain (FADD) via homophilic interaction between the death domains (DD) of the two proteins (Fig. 6) (92, 108). A second homophilic, this time between death effector domains (DED), leads to the recruitment of pro-caspase-8 (monomer) to FADD (92). This multimeric assembly of proteins, referred to as the death-inducing signalling complex (DISC), leads to activation of caspase-8 via induced proximity (28). Following activation, the caspase-8 N-terminal death effector domain (DED) is cleaved, which may facilitate intracellular the diffusion of active caspase-8, allowing it to reach additional substrates (28). Preferred substrates of caspase-8 include pro-caspase-3, -7 and BID (108, 326). Direct activation of caspase-3 and -7 leads to execution of the apoptotic pathway via proteolysis, while cleavage of BID (which generates truncated BID [tBID]), activates the mitochondrial apoptotic route; thereby coupling an extrinsic stimulus to the intrinsic apoptotic pathway (108, 326).

Cytotoxic T-lymphocytes (CTL) and natural killer (NK) cells function in the detection and elimination of virus infected cells. Upon recognition of a target cell, CTL and NK deliver a lethal cocktail of granules containing perforins and granzyme-B (326). Insertion and oligomerization of perforins in the plasma membrane creates pores that allow the transfer of granzyme-B (326). Granzyme-B, which is a serine protease, then proteolytically activates BID and caspase-3 and -7, leading to apoptotic elimination of virally infected cells (Fig. 6) (235, 326). In addition, CTL can also activate FAS, thus engaging both extrinsic and intrinsic apoptotic pathways (92).

The control of tyrosine phosphorylation-mediated signal transduction is an integral part of the transmission of both survival and death signals. Accordingly, numerous studies have implicated PTPs in the modulation of apoptotic cell death. An overview of the role of PTPs in apoptotic signalling is presented in the discussion of this thesis. This topic will therefore not be addressed here.

1.11 Objectives.

Although PTP-PEST interacts with several signalling modules that could target it to different subcellular compartments, it was initially observed to localize primarily in the cytosol (56). In cells stimulated with fibronectin, however, PTP-PEST was seen to relocalize at membrane ruffles at the periphery of the cell (11). PTP-PEST was also seen to co-localizes with PSTPIP in membrane ruffles of transfected COS cells stimulated with EGF (Maxime Hallé and Michel L. Tremblay, unpublished results). The above data indicates that the subcellular localization of PTP-PEST could be critical for the regulation of its function, and my doctoral research was therefore focussed, in part, on examination of this hypothesis. In addition, as PTP-PEST is an important regulator of cytoskeletal organization, it is possible that this enzyme plays a role in host-intracellular pathogen interactions and in apoptosis. The second and third objectives of my thesis were therefore to investigate the targeting and function of PTP-PEST in the context of *Leishmania* infection, and in intrinsic and extrinsic apoptotic pathways.

2 CHAPTER 2

PTP-PEST IS FOUND IN CYTOSOLIC AND MEMBRANE COMPARTMENTS, AND REGULATES LPA-MEDIATED p130CAS PHOSPHORYLATION-DEPENDENT INTERACTIONS.

Maxime Hallé[1], Christophe Blanchetot[2], Jean-Francois Théberge[1] and Michel L. Tremblay[1]

From the McGill Cancer Center and the Department of Biochemistry, McGill University, Cancer Pavilion, 1160 avenue des Pins ouest, Room 522, Montréal, Québec, Canada, H3A 1A3[1], and the department of cell biology, Utrecht University, Psadualaan 8, 3584CH, Utrecht, The Netherlands[2]

Manuscript in preparation.

2.1 SUMMARY

Localized control of tyrosine phosphorylation events is crucial for the induction of specific signalling responses. The tyrosine phosphorylation cycle of p130Cas, dependent on the intracellular protein tyrosine phosphatase (PTP)-PEST, is essential for polarized cell migration. We investigated the impact of the intracellular distribution of PTP-PEST on interactions between p130Cas and SH2 containing proteins. Examination of fibroblasts expressing PTP-PEST revealed the presence of this phosphatase in the cytosol. Intriguingly, PTP-PEST was also seen at the plasma membrane, and in structures resembling focal adhesions. Fractionation studies confirmed that the majority of both endogenous and transiently expressed PTP-PEST was cytosolic (~80%), but that there was also a significant proportion present in the membrane compartment (~20%). Although multiple proteins bound to both cytosolic and membrane-associated PTP-PEST, some interactions were found to be fraction specific. To gain a better understanding of potential PTP-PEST functions, we generated clones stably expressing either empty vector or one of the following forms of PTP-PEST: wild type, catalytic inactive (C231S or D199A), proline-rich motif 1-deleted (ΔPro1), ΔPro2, ΔPro3, ΔPro4, ΔPro5 (also termed ΔCTH), Shc binding domain-deleted (ΔSBD), or membrane-targeted (PTP-PEST-K-Ras 4B tag). In cells stimulated with lysophosphatidic acid (LPA), cytosolic PTP-PEST appeared to be the predominant form regulating the recruitment of Crk, as well as the SH2 domains of Nck and Src, to p130Cas. We propose that subcellular localization plays a significant role in the regulation of PTP-PEST functions with respect to the signal transduction machinery promoting cellular transformation.

2.2 INTRODUCTION

Uncontrolled tyrosine phosphorylation events contribute to cellular immortalization and transformation, and are therefore of significant interest with respect to cancer development. Unrestricted activity of protein tyrosine kinases (PTKs) including Src, Abl as well as the one of the numerous receptor-tyrosine kinases (RTKs), has been linked to this process (205, 255, 280, 303, 316, 379). PTK activity is counterbalanced by dephosphorylation via protein tyrosine phosphatase (PTP) activity, and disregulation of PTPs has also been linked to cancer development (178, 248). Tight regulations of these proteins, with respect to both activity and substrate specificity, is therefore of the utmost importance for maintenance of homeostasis.

Several structural and sequence similarities exist among the catalytic domains of PTPs (10). Substrate specificity is conferred by variation among the less conserved residues of the phosphatase domain. Specificity can also be conferred by a subcellular targeting/substrate interaction motif following the catalytic domain (330). Although PTP-1B and T-cell PTP (TC-PTP) display significant homology in their catalytic domains, the majority of their cellular functions as well as the phenotypes of their respective null mice are divergent (102, 313). This characteristic can, in part, be attributed to their distinct subcellular localization: PTP-1B is anchored on the endoplasmic reticulum, while TC-PTP localizes in the nucleus (115, 313). The importance of proper subcellular targeting is further illustrated by the fact that membrane associated PTPε and PTPα were more efficient in the regulation of insulin signalling than were their cytosolic counterparts (9).

Like its homologues PTP-PEP and PTP-HSCF, PTP-PEST is an intracellular enzyme with an amino terminal catalytic domain (5, 56). The carboxy-terminal non-catalytic segment of PTP-PEST contains a domain responsible for binding to Shc (Shc binding domain [SBD]), as well as five proline-rich motifs involved in the recruitment of various

partners (53). The first proline-rich motif interacts with the SH3 domain of Crk-associated substrate (p130Cas) (117), the second binds the LIM domains of paxillin and Hic-5 (86, 243), the fourth associates with CSK and filamin-A (94, 257), and the fifth, termed CTH binds to PSTPIP (85). Cell culture studies involving the manipulation of PTP-PEST levels effectively illustrated the role of this enzyme in the regulation of cell migration (11, 120). Notably, p130Cas failed to translocate to the leading edge of cells over-expressing PTP-PEST following a migration-initiating signal (120). Moreover, the recruitment of paxillin to PTP-PEST is critical for the regulation of cell adhesion and membrane protrusion formation; two key processes in adherent cell translocation (172). In addition, the dephosphorylation of Shc by PTP-PEST may play a role in regulation of the Ras-mitogen activated protein kinase (MAPK) pathway (53, 95). Interestingly, PTP-PEST was seen to redistribute from a diffuse cytosolic location to membrane ruffles following fibronectin initiated spreading (11, 56). However, the functional role of subcellular localization in the interaction of PTP-PEST with its binding partners remains to be determined.

The expression and phosphorylation of p130Cas contributes to cellular transformation. p130Cas phosphorylation is enhanced in fibroblasts expressing either ornithine decarboxylase (ODC) or Ras, as well as in invasive carcinoma cells, and its expression is required to maintain the transformed phenotype (15, 188). Additionally, increased expression of the p130Cas human homologue breast cancer antiestrogen resistance 1 (BCAR1) correlated with enhanced cell proliferation, breast cancer progression and tamoxifen resistance (35, 344). Moreover, Src-mediated transformation was impaired in p130Cas deficient cells (153). In recent studies performed on trangenic mice overexpressing p130Cas in the mammary gland, extensive epithelial hyperplasia and delayed involution were reported (46). Although enhanced p130Cas synthesis was not sufficient for tumor formation, its increased expression accelerated HER2-Neu-mediated tumor development (46). In both of the above mouse models, up-regulation of p130Cas was associated with increased Erk1/2 MAPK, Akt and Src (Y416 - activating site)

phosphorylation, which paralleled sustained proliferation and decreased apoptosis (46). Although a cooperative mechanism involving focal adhesion kinase (FAK) and Src is required for maximal p130Cas phosphorylation, Src alone can interact with and phosphorylate p130Cas (277). The phosphorylation of p130Cas acts as an apical event in signal transduction, through recruitment of the adaptor proteins Crk and Nck via their SH2 domains (188, 290). Of note, assembly of p130Cas/Crk complexes stimulates cell migration, protects cells against apoptosis, and activates the small GTPase Rac (69, 187).

A possible route by which p130Cas may contribute to cellular transformation is that of the lysophosphatidic acid (LPA) activated signalling pathway. LPA, a simple soluble phospholipid, is able to stimulate multiple pathways, including the Ras-MAPK cascade, and promotes cell proliferation, migration and survival, which are hallmarks of cancer (191, 234). LPA has, in fact, been implicated in the initiation, promotion and pathophysiology of multiple cancers, including, among others, ovarian, prostate, breast, melanoma, head, neck, intestine and thyroid cancer (234). At a molecular level, cell migration up an LPA gradient requires the p130Cas/Crk association mediated relocalization and activation of Rac, followed by the formation of pseudopodia (70). Interestingly, reduced expression of the p130Cas modulator FAK inhibited the LPA-mediated morphological changes required for cell motility (170). As the expression of PTP-PEST is necessary for the controlled phosphorylation of p130Cas (11, 305), it is possible that this PTP plays a role in LPA associated signalling.

The interplay between subcellular localization and the activity of PTP-PEST likely contributes to its integration in the signal transduction machinery. In the present study, we have investigated the cellular distribution of PTP-PEST, and the impact of this distribution on interaction with various binding partners. Using immunofluorescence and fractionation techniques, we observed that PTP-PEST was primarily localized to the cytosol and plasma membrane. Both cytosolic and membrane associated PTP-PEST was capable of interaction with Shc, paxillin and a number of additional candidate proteins.

We also generated clones, derived from *PTP-PEST* null cells, into which different forms of PTP-PEST had been introduced. This system allowed us to further investigate the role of cytosolic PTP-PEST in the regulation of LPA stimulated recruitment of SH2-containing molecules by p130Cas. This study provides evidence that subcellular localization modulates the functions of PTP-PEST.

2.3 MATERIALS AND METHODS

2.3.1 Reagents and antibodies.

Chemicals used in this study were purchased at BioShop Canada Inc., Fisher Scientific and Sigma. The PTP-PEST polyclonal antibodies (2530) and pre-immune serum were previously described (85). Monoclonal antibodies specific for Crk, p130Cas, Shc, and paxillin were from BD Transduction Laboratories. Polyclonal rabbit antibodies against PTP-1B and monoclonal anti-phosphotyrosine antibodies (4G10) were from Upstate. Antibodies specific for phospho-thr202/tyr204 p44/42 MAPKs were from Cell Signaling Technology.

2.3.2 Plasmids, cDNAs and transfection.

Murine PTP-PEST expression vectors, pcDNA3.1/Zeo-PTP-PEST (wild type [WT], C231S, Pro1 deletion mutant [ΔPro1], ΔPro2 and ΔCTH) were described previously (85, 86). The pcDNA3.1/Zeo-PTP-PEST D199A, PTP-PEST ΔP3 (^{520}PPRPDCLP^{527}), PTP-PEST ΔP4 (^{673}SPPPLPER^{680}) and PTP-PEST ΔShc binding domain (SBD, ^{599}NPLH^{602}) constructs were generated by site-directed mutagenesis (Quick Change site-directed mutagenesis kit; Stratagene). To generate pcDNA3.1/Zeo-PTP-PEST-K-Ras 4B tag, PTP-PEST cDNA was amplified by PCR using a sense oligo containing a *BamHI* site and an antisense oligo

containing the K-Ras 4B palmitoylation sequence as previously described, and followed by an *XhoI* site (265). PCR products were cloned into a pGEMT Vector, which was then digested with *BamHI/NotI*. The appropriate digestion product was then inserted in pcDNA3.1/Zeo. All cDNAs were verified by sequencing (Genome Québec). All transfections were performed using Lipofectamin 2000 (Invitrogen) according to the instructions of the manufacturer's instructions.

2.3.3 Cell lines.

All cell lines were maintained in Dulbecco modified Eagle medium (DMEM) supplemented with 10 % fetal bovine serum (FBS) and 50 μg/ml gentamicin (Gibco) at 37 °C in a 5 % CO_2 humid atmosphere. Swiss 3T3 cells were obtained from Dr. Nathalie Lamarche-Vane (McGill University) and were grown in a 10 % CO_2 humid atmosphere. Primary mouse embryonic fibroblasts (P-MEFs) from BALB/c mice (Jackson) were generated as described (67). *PTP-PEST* -/- parental cells have been previously described (84). Stable re-expression of PTP-PEST in the PTP-PEST null cells was obtained as follows: subconfluent PTP-PEST -/- fibroblasts were transfected with one of the following: linearized (*Sca*1) pcDNA3.1/Zeo (empty vector, EV), pcDNA3.1/Zeo-PTP-PEST (wild type, WT), pcDNA3.1/Zeo-PTP-PEST D199A, pcDNA3.1/Zeo-PTP-PEST C231S, pcDNA3.1/Zeo-PTP-PEST Pro1 deletion mutant (ΔPro1), pcDNA3.1/Zeo-PTP-PEST ΔPro2, pcDNA3.1/Zeo-PTP-PEST ΔPro3, pcDNA3.1/Zeo-PTP-PEST Shc binding domain deletion mutant (ΔSBD), pcDNA3.1/Zeo-PTP-PEST ΔPro4, pcDNA3.1/Zeo-PTP-PEST ΔCTH or pcDNA3.1/Zeo-PTP-PEST-K-Ras 4B tag. Cells were reseeded at reduced confluency 48h after transfection, and positive clones were selected using 100 μg/ml of Zeocin (Invitrogen). The media was changed every two days for 10 days and isolated colonies were expanded in selection media. Clones expressing PTP-PEST were identified by immunoblot analysis. Clones were grown in media supplemented with 50 μg/ml Zeocin during routine culture and were maintained in absence of Zeocin during experimental manipulation.

2.3.4 Microinjection and immunofluorescence.

Microinjection of Swiss 3T3 nuclei with filtered (0.22 µm cellulose acetate filter, Spin-x, Corning, costar) pcDNA3.1/Zeo-PTP-PEST (WT) (0,1 µg/µl) mixed with Texas red-couple dextran (5 mg/ml) was conducted as previously described (161, 202). Cells were incubated (37 °C, 10 % CO_2, humid atmosphere) for four hours to allow protein expression, and then rinsed with PBS, fixed in 4% paraformaldehyde (PFA) (w/v) in PBS for 18 min, permeabilized with 0.1% (v/v) Triton X-100 in 4% PFA for 18 min, incubated in blocking solution (2% BSA, 1% goat serum) for 45 min, incubated in presence of primary PTP-PEST antibody (2530, 1/1000, in 2% BSA, 1% goat serum), rinsed three times with PBS, incubated in blocking solution for 10 min and rinsed again with PBS. Cells were then incubated for 45 min with a mixture of Alexa 488 conjugated anti-rabbit antibody (Molecular Probes) and 4',6-diamidino-2-phenylindole (DAPI) (Roche). Cells were rinsed three times, incubated in blocking solution for 10 min, rinsed and mounted using Vectashield mounting medium (Vector Laboratories, Inc.). Random field images were captured using a confocal microscope (Zeiss LSM 510 - NLO).

PTP-PEST -/- cells were transfected with pcDNA3.1ZeoPTP-PEST (WT) as previously described (138). Fixation, permeabilization and processing for indirect immunofluorescence was conducted as described above. Random field images were acquired by confocal microscopy (Zeiss LSM 510 - NLO).

2.3.5 Fractionation, protein complexes analysis and immunoblotting

Adherent cells were washed twice with ice cold PBS, gently collected in PBS using a rubber policeman, and centrifuged at 1500 × rpm for 5 min at 4 °C (5810R, A-4-62, Eppendorf centrifuge). Cells were then resuspended in homogenisation buffer (HB) (4mM imidazole [pH 7.4], 8.5% sucrose) and, using a 1 ml syringe and a 22G needle, fragmented by passaging several times through the needle. An aliquot of the

homogenate was stained with trypan blue and inspected under a microscope to ensure that nuclei were intact. Nuclei and intact cells were removed by centrifugation at 2500 × rpm (5810R, A-4-62, Eppendorf centrifuge) for 10 min at 4 °C, and the supernatant was further fractionated by centrifugation at 100 000 × g for 15 min at 4 °C. This procedure generated in two fractions: the supernatant (S100), corresponding to the cytosolic fraction (C), and the pellet (P100), consisting of membrane-derived particules including plasma membrane and endoplasmic reticulum, and considered to represent crude membrane (M). The membrane pellet was washed once with HB and centrifuged at 100 000 × g for 15 min at 4 °C. The washed resulting membrane pellet was resuspended in 1X lysis buffer (50mM Tris [pH 7.4], 150mM NaCl, 1% NP-40, 1% Triton X-100 and complete protease inhibitor), the cytosolic fraction was diluted in 2X lysis buffer (100mM Tris [pH 7.4], 300mM NaCl, 2% NP-40, 2% Triton X-100 and complete protease inhibitor), and both fractions were incubated on ice for 15 min. 10% of each fraction was denatured in SDS-sample buffer and analysed by immunoblotting as previously described (138).

To analyse the interactions mediated by endogenous PTP-PEST, fourteen 10 cm dishes of P-MEFs were rinsed with PBS and incubated in methionine/cysteine free eagle's minimum essential medium (Sigma, M2289) for one hour. Dialyzed FBS (10% final), L-glutamine and [^{35}S] protein labelling mix (PerkinElmer) were then added and cells were incubated for an additional 16 hours. Cells were fractionated as described above. The cytosolic fraction was diluted in 2X lysis buffer (300 mM NaCl, 100 mM Tris [pH 7.4], 2% NP-40 and complete protease inhibitor), the washed membrane pellet was resuspended in 1X lysis buffer (150 mM NaCl, 50 mM Tris [pH 7.4], 1% NP-40 and complete protease inhibitor), and extracts were pre-cleared using protein A agarose beads (Invitrogen). Pre-cleared extracts were incubated with control (3.5 µl pre-immune serum in presence of protein A agarose beads) or PTP-PEST (3.5 µl 2530 immune serum in presence of protein A agarose beads) antibodies for two hours at 4 °C. Resulting immunocomplexes were washed five times with 1X lysis buffer, resuspended in SDS sample buffer, boiled for 4 min and analysed by SDS-PAGE. The interaction of PTP-PEST

with paxillin and Shc was analysed as described above, except that cells were not radio-labelled and the immunocomplexes were detected by immunoblot analysis.

To analyse the interaction between Crk and p130Cas, serum starved (0.05% FBS in DMEM, 16 hours) *PTP-PEST -/-* derived clones were incubated without or with 1 μM LPA for 5 min, rinsed with ice-cold PBS and resuspended in lysis buffer (100mM Tris [pH 7,4], 5mM EDTA, 150mM NaCl, 1% TritonX-100, 10 mM NaF, 1 mM Na_3VO_4 and Complete protease inhibitor [Roche]). Cell extracts were centrifuged at 16000 × g for 10 min at 4 °C, and the protein concentration of each sample was measured by Bradford assay (Bio-Rad protein assay). Cleared protein lysates (2.6 mg) were incubated at 4 °C for 3h with 1.25 μg of anti-Crk monoclonal antibody (mAB) (Transduction Laboratory) and protein G agarose beads (Invitrogen). Beads were then washed three times with lysis buffer, boiled in SDS-sample buffer and subjected to immunoblot analysis.

The affinity of p130Cas for various SH2 domains was assessed in vitro as follows. Vectors encoding various GST fusion proteins (GST, GST-Src-SH2 and GST-Nck-SH2) were obtained from Dr. Morag Park (McGill University). GST fusion proteins were bound to glutathione Sepharose beads as previously described (84, 86). *PTP-PEST -/-* derived clones were serum-starved (0.05% FBS in DMEM, 16 hours), stimulated with LPA (1 μM, 5 min) and lysed in modified RIPA buffer (50mM Tris [pH 7.4], 150 mM NaCl, 0.1% sodium dodecyl sulphate [SDS], 0.5% sodium deoxycholate, 1% NP-40, 10 mM NaF, 1 mM Na_3VO_4 and Complete protease inhibitor [Roche]). Cell extracts were centrifuged at 16000 × g for 10 min at 4 °C, and the protein concentration of each sample was measured by Bradford assay. Cleared protein lysates (1.3 mg) were incubated at 4 °C for 2h with GST-proteins conjugated beads. Beads were then washed three times with modified RIPA buffer, resuspended in SDS sample buffer, and the resulting complexes subjected to immunoblot analysis.

2.4 RESULTS

2.4.1 PTP-PEST is present in a diffused cytosolic pattern and at the plasma membrane of fibroblasts cells.

The targeting of PTPs to different cellular compartments plays a key role in delivering their activity to the appropriate substrate. The PTP-PEST amino acids sequence has neither a trans-membrane domain nor an organelle targeting motif (56). In order to gain additional insight into the localization of PTP-PEST, immunofluorescence conditions were first tested on *PTP-PEST* null cells. Only *PTP-PEST* -/- cells transiently expressing PTP-PEST (transfected cells) displayed a significant signal following immunofluorescence analysis using a PTP-PEST antibody (Fig. 1A) confirming the specificity of the PTP-PEST antibody. Swiss 3T3 cells were subsequently microinjected with cDNA encoding wild type (WT) PTP-PEST, incubated for four hours, fixed and subjected to immunofluorescence analysis. This method, unlike transient transfection, allowed for evaluation of the initial localization of PTP-PEST, shortly following translation. Confocal analysis demonstrated that the majority of PTP-PEST was present in the cytosol (Fig. 1B). Interestingly, PTP-PEST-associated immunostaining was concentrated in triangular structures at the cell-substratum interface, which were morphologicaly similar to focal adhesions (Fig. 1B, 0.00 and 0.40 μm). Moreover, images acquired across the cell body revealed an intense signal corresponding to PTP-PEST in membrane ruffle-like structures at the periphery of the cell (Fig. 1B, 1.20 and 1.60 μm). The distribution of PTP-PEST was distinct from that of microinjected Texas Red dye, which was diffusely distributed throughout the nucleus and the cytoplasm, and weakly present in membrane ruffles (Fig. 1C). Additional three dimensional analysis of PTP-PEST localization in microinjected Swiss 3T3 cells and transiently transfected *PTP-PEST* -/- fibroblasts showed increased PTP-PEST-signal intensity on the cell surface and at the cell

periphery (data not shown). PTP-PEST was absent from the nucleus. These results suggest that PTP-PEST is present in the cytosol and likely at the plasma membrane.

Figure 1. PTP-PEST is present in the cytosol and is initially localized at focal adhesions-like structures at the cell-substratum interface and at the edge of membrane ruffles. (A) *PTP-PEST* -/- fibroblasts transiently expressing PTP-PEST were fixed, permeabilized, immunostained and examined by confocal microscopy as described in the materials and methods. Cells expressing PTP-PEST (solid arrowheads) showed an intense fluorescence signal (green), while negative cells displayed a very low background signal (open arrowheads). Non-transfected cells were detected by nuclear staining (DAPI, blue). (B) Swiss 3T3 cells were microinjected with vector encoding PTP-PEST cDNA in the presence of Texas red dye and incubated for 4 h. Expression of PTP-PEST was visualized by immunofluorescence. Confocal images illustrating the signal corresponding to PTP-PEST (white) and DAPI (blue) were acquired from the cell-substratum interface (0.00 μm) through to the dorsal cellular surface (2.00 μm). PTP-PEST present in pointed structures of the ventral surface, as well as at the plasma membrane, are indicated (arrowheads). (C) 20 sections of the area shown in (B) (from the cell substratum interface to the surface of the cell) were acquired by confocal microscopy and three dimensional projection of the assemble sections was generated by computerized imaging. Signal in blue (top left) correspond to the nucleus (DAPI staining), green signal displays the localization of PTP-PEST (top right) and the red signal represents the Texas red co-injected dye (bottom left). Merged images are shown (bottom right). Although Texas red coupled dextran could freely diffuse everywhere in the cell, three dimensional reconstitution images illustrate that PTP-PEST signal is predominant in structures resembling to focal adhesions and at the periphery of the cell, likely in membrane ruffles (white arrowheads). Green arrowheads indicate examples of area where the intensity of PTP-PEST corresponding signal was increased as compared to that of the Texas red. Pictures are representative of three independent experiments, in which 50 to 100 cells per coverslip were microinjected. Scale bar, 10 μm.

A.

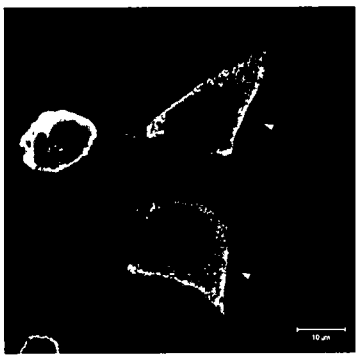

B.

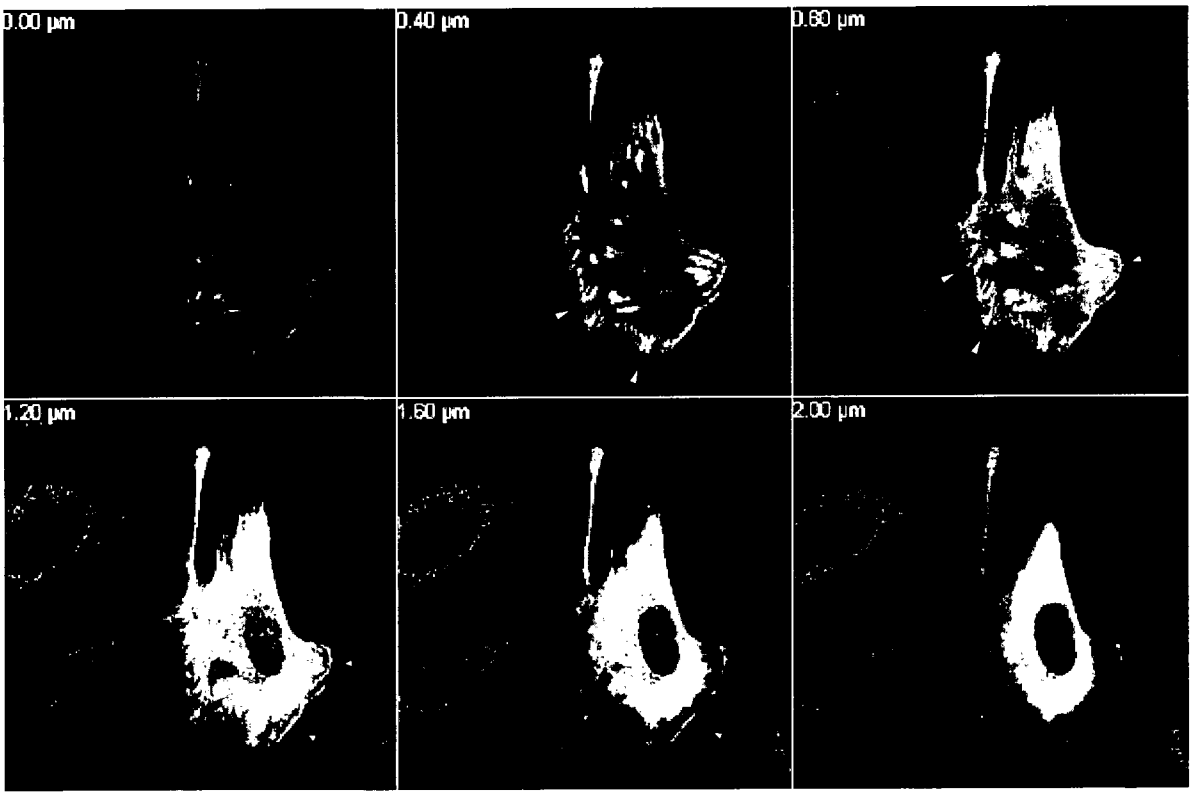

FIG. 1 A, B

C.

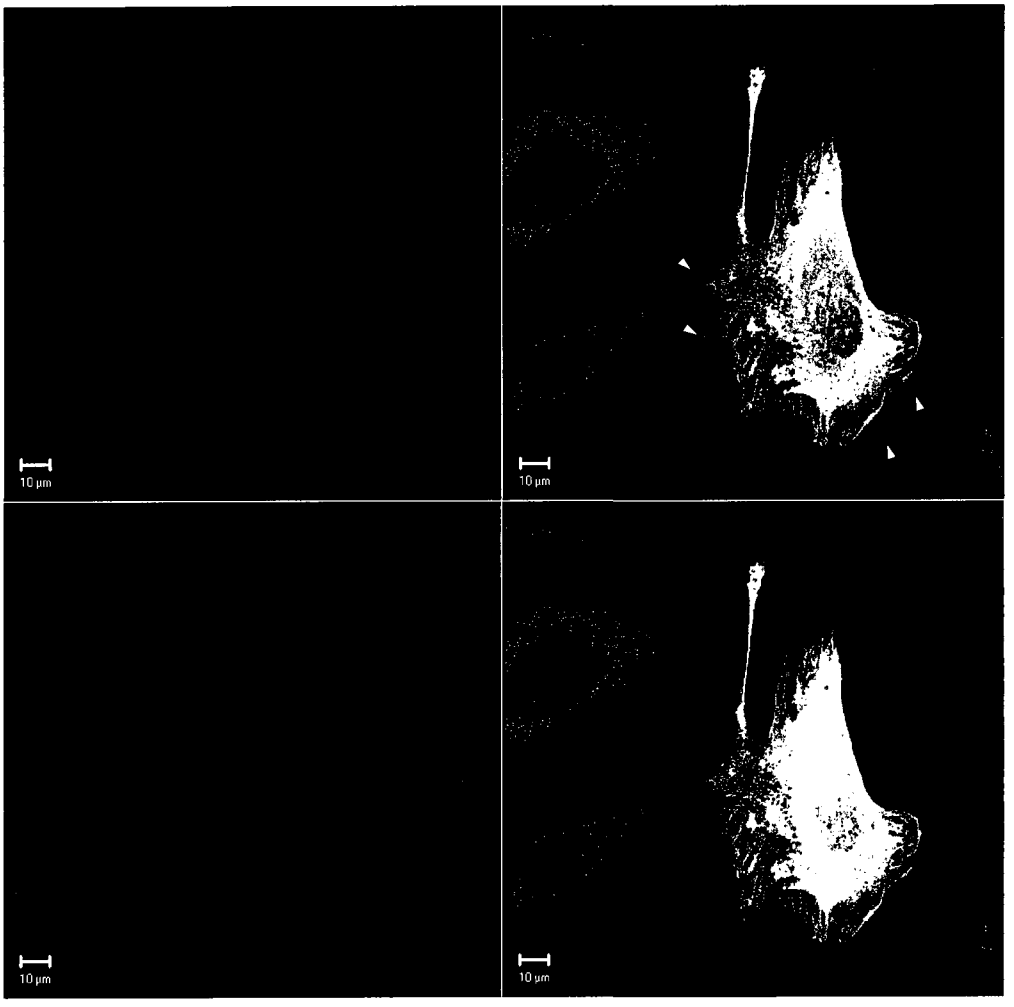

FIG. 1 C

To obtain further information about the cellular distribution PTP-PEST, *PTP-PEST* null cells and *PTP-PEST* null cells transiently expressing WT PTP-PEST were fractionated and analysed by immunoblot. Examination of PTP-PEST content in crude cytosolic and membrane fractions revealed there is a high abundance of this enzyme in the cytosol (Fig. 2A). In fact, we observed that approximately 80% of the total cellular content of PTP-PEST was cytosolic. Paxillin, a PTP-PEST interacting partner (86), was also enriched in the cytosol (>90%), with a small percentage present in the total membrane fraction (<10%) (Fig. 2A). A significant and reproducible PTP-PEST signal was seen in the membrane fraction, representing approximately 20 % of the total cellular content of this protein. To confirm the purity of the fractions, the localization of PTP-1B, a PTP that bears an endoplasmic-reticulum targeting motif (115), was analyzed. As expected, PTP-1B was exclusively associated with the membrane fraction. Similar results to those described above were obtained when the distribution of endogenous PTP-PEST in P-MEFs was analysed (Fig. 2B). The aforementioned data confirms the primarily cytosolic localization of PTP-PEST, and also suggests that a significant fraction of this enzyme is associated with the plasma membranes.

Figure 2. PTP-PEST is present at high levels in the cytosol and significant amounts in the membrane fraction. Crude cytosolic and membranes fractions were obtained from *PTP-PEST* -/- cells transfected with either an empty vector or with a vector encoding PTP-PEST (A), as well as from P-MEFs (B), and were processed as described in materials and methods. Levels of PTP-PEST and paxillin in each fraction were quantified. Values correspond to the mean ± standard error and are representative of at least five independent experiments (A) or of three independent experiments (B). In every experiment, PTP-1B was exclusively present in the membrane fraction. C, cytosol; M, membrane.

A.

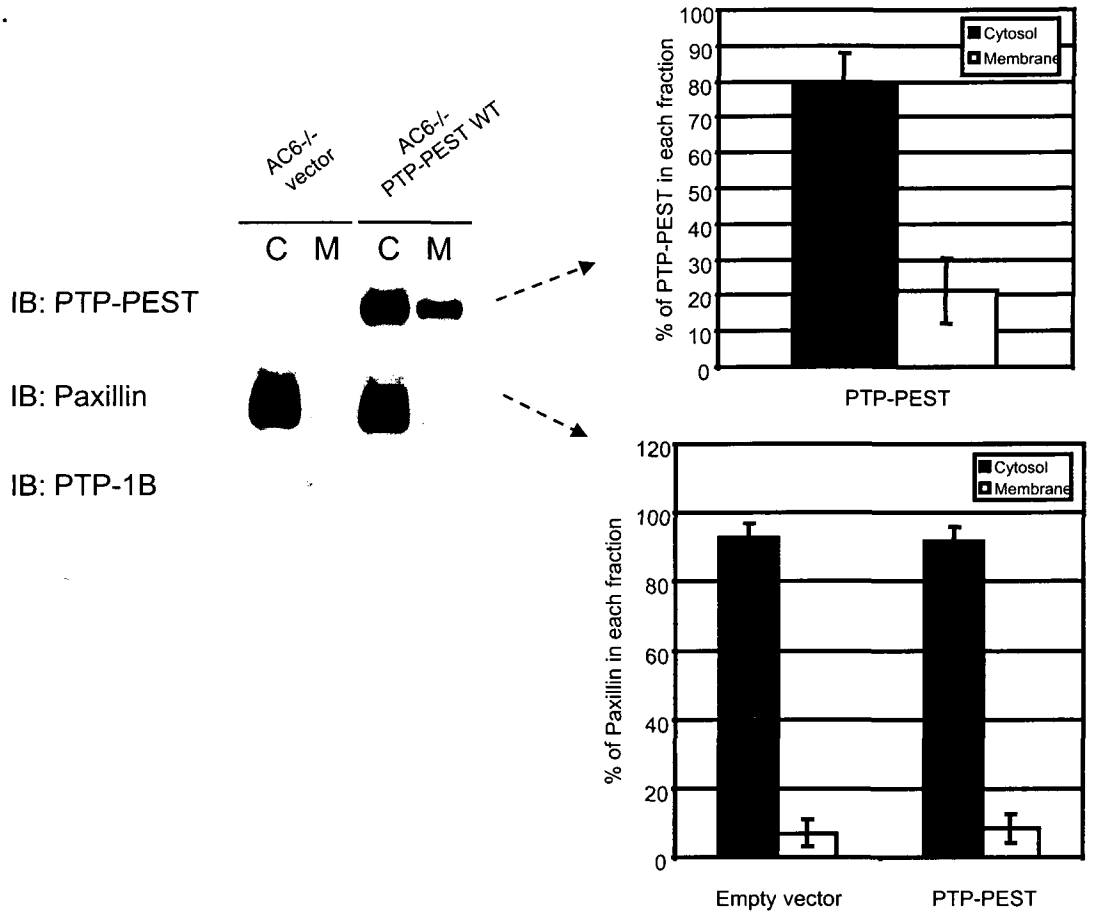
AC6-/- vector
AC6-/- PTP-PEST WT
C M C M
IB: PTP-PEST
IB: Paxillin
IB: PTP-1B
Cytosol
Membrane
% of PTP-PEST in each fraction
PTP-PEST
% of Paxillin in each fraction
Empty vector
PTP-PEST

B.

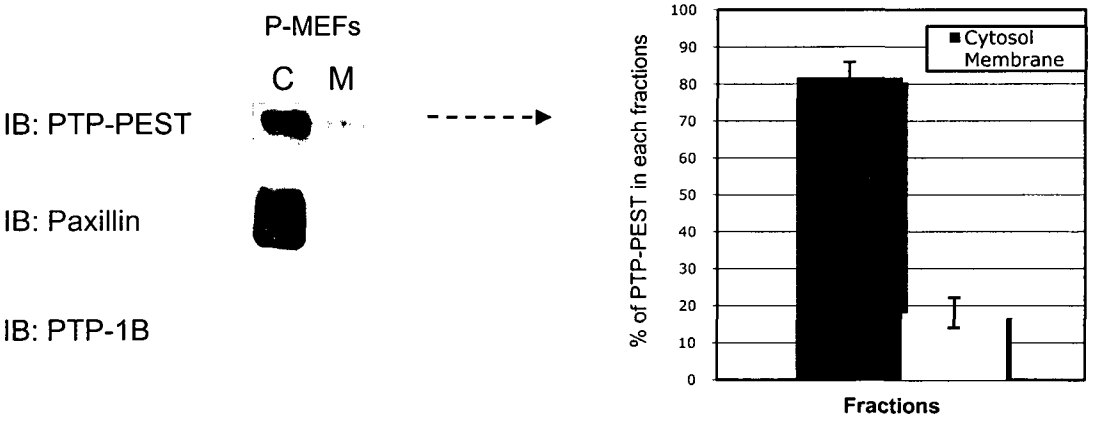
P-MEFs
C M
IB: PTP-PEST
IB: Paxillin
IB: PTP-1B
Cytosol
Membrane
% of PTP-PEST in each fractions
Fractions

FIG. 2

2.4.2 Analysis of protein interactions mediated by different subpopulations of PTP-PEST.

PTP-PEST associates with several signalling molecules, including paxillin and Shc via its non-catalytic segment (53, 86, 300). It is possible that the subcellular localization of PTP-PEST influences its interactions with various binding partners. In order to investigate this possibility, we examined endogenous PTP-PEST in ^{35}S-methionine/cysteine labelled P-MEFs, using an approach combining fractionation and immunoprecipitation techniques. PTP-PEST was found to associate with several molecules in both cytocolic and membrane fractions (Fig. 3A arrow and arrowheads). Interestingly, some of these interactions were enriched in a fraction specific manner (Fig. 3A red arrow and arrowheads). Paxillin and Shc have been described as important mediators of PTP-PEST activity (53, 172). In order to determine the influence of PTP-PEST localization on the recruitment of these two proteins, we looked at their association with both cytosolic and membrane localized PTP-PEST. As expected, PTP-PEST interacted with both proteins (Fig. 3B), and, in both cases, the association was enriched in the cytosolic fraction. However, a significant fraction of Shc, but not of paxillin, was associated with membrane localized PTP-PEST (Fig. 3B). The above results suggest that the intra-cellular localization of PTP-PEST influences the composition of its associated protein complexes.

Figure 3. Cytosolic and membrane associated PTP-PEST containing protein complexes. (A) Endogenous P-MEFs proteins were radio-labelled through incorporation of [^{35}S]-cysteine and [^{35}S]-methionine, harvested, fractionated and subjected to immunoprecipitation analysis, in order to determine the cellular distribution PTP-PEST protein complexes. Arrows indicate bands co-precipitating with cytosolic PTP-PEST, and arrowheads indicate those associated with plasma membrane localized PTP-PEST. Red arrows or arrowheads identify bands specifically enriched in a definite fraction, while the blue ones indicate PTP-PEST. (B) Immunoprecipitation of PTP-PEST from non-radiolabelled P-MEFs subcellular fractions, analysed by immunoblot for PTP-PEST, paxillin and Shc.

A.

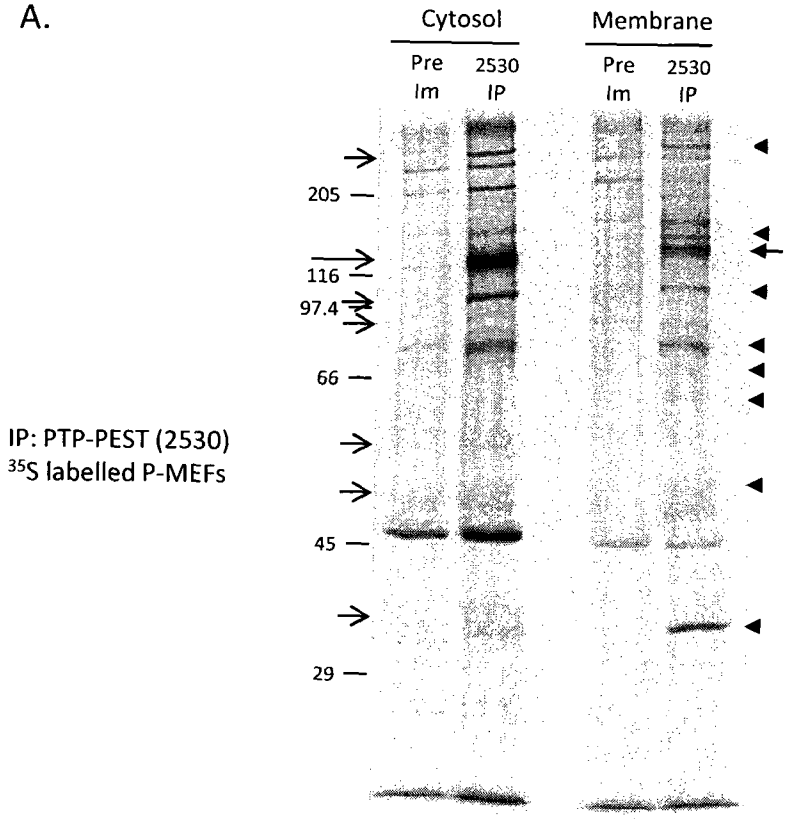
Cytosol
Membrane
Pre Im
2530 IP
Pre Im
2530 IP
205
116
97.4
66
45
29
IP: PTP-PEST (2530)
35S labelled P-MEFs

B.

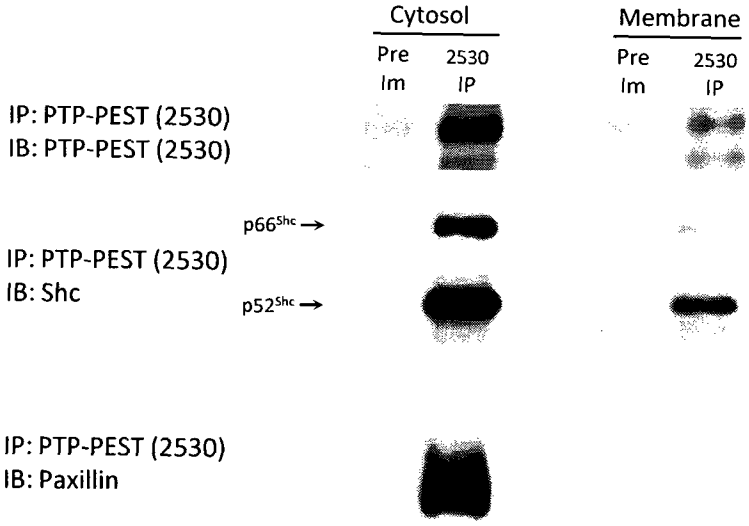
Cytosol
Membrane
Pre Im
2530 IP
Pre Im
2530 IP
IP: PTP-PEST (2530)
IB: PTP-PEST (2530)
p66Shc
IP: PTP-PEST (2530)
IB: Shc
p52Shc
IP: PTP-PEST (2530)
IB: Paxillin

FIG. 3

2.4.3 Generation of PTP-PEST -/- rescued cell lines.

The amino terminal catalytic domain of PTP-PEST, is followed by a carboxy-terminal tail containing a Shc-binding-domain (SBD) as well as five proline-rich motifs, some of which have been implicated in association with various interactors and substrates (53, 84-86, 94, 95, 117, 300). The addition of targeting sequences to molecules of interest facilitates the understanding of their role in a particular cellular compartment. K-Ras 4B is exclusively found at the plasma membrane due to the presence of a prenylation motif (73). Consequently, this motif is frequently employed to create chimeric proteins targeted to the plasma membrane (265). In order to further investigate the relevance of PTP-PEST subcellular localization, we generated a vector encoding PTP-PEST fused to the K-Ras 4B prenylation signal sequence (PTP-PEST-K-Ras 4B tag). This form of PTP-PEST was primarily localized at the plasma membrane (Maxime Hallé and Michel L. Tremblay, un-published data and Fig. 4B). We also engineered a form of PTP-PEST fused to a Gag-derived myristoylation signal sequence. However, addition of this peptide did not lead to efficient membrane targeting (Maxime Hallé and Michel L. Tremblay, un-published results). The PTP-PEST-K-Ras 4B tag construct was therefore used in future studies.

To further characterize the functions of PTP-PEST, we re-introduced PTP-PEST, as well as several mutant versions of the enzyme, into *PTP-PEST* -/- cells. To this end, *PTP-PEST* null cells were transfected with an empty vector (pcDNA3.1/Zeo) or with a vector encoding one of the following PTP-PEST cDNAs: pcDNA3.1/Zeo-PTP-PEST wild type (WT), pcDNA3.1/Zeo-PTP-PEST D199A, pcDNA3.1/Zeo-PTP-PEST C231S, pcDNA3.1/Zeo-PTP-PEST ΔPro1, pcDNA3.1/Zeo-PTP-PEST ΔPro2, pcDNA3.1/Zeo-PTP-PEST ΔPro3, pcDNA3.1/Zeo-PTP-PEST ΔSBD, pcDNA3.1/Zeo-PTP-PEST ΔPro4, pcDNA3.1/Zeo-PTP-PEST ΔCTH, or pcDNA3.1/Zeo-PTP-PEST-K-Ras 4B-tag. Cells were then selected with Zeocin and over 500 resistant colonies expanded and analyzed. Clones growing in presence of

the selection agent were examined for PTP-PEST expression by immunoblot analysis (Fig. 4A). Multiple clones expressing varying levels of WT PTP-PEST were generated, all of which had Shc levels similar to those of the parental cells (Fig. 4B). Several clones expressing various, yet stable, levels of the mutant PTP-PEST constructs were also obtained (Fig. 4B, inserted table). As expected, addition of a K-Ras 4B prenylation signal resulted in membrane targeting (Fig. 4C). In summary, PTP-PEST was efficiently re-introduced in the *PTP-PEST* -/- cells.

Figure 4. Stable expression of different forms of PTP-PEST in *PTP-PEST* null cells. (A) Schematic representation of the approach used to generate clones stably expressing different forms of PTP-PEST. (B) Immunoblot analysis of PTP-PEST and Shc expression in lysates from 11 different PTP-PEST WT clones and from 2 PTP-PEST C231S clones. The inserted table provides the number of positive clones obtained for each construct. For each form of PTP-PEST, expression levels for two clones are shown. Cells expressing PTP-PEST-K-Ras 4B tag (clone 146) were subjected to fractionation and immunoblot analysis. C, cytosol fraction; M, membrane fraction.

PTP-PEST -/- cells

↓

Cells were transfected with different constructs of PTP-PEST [vector, WT, D199A, C231S, ΔPro1, ΔPro2, ΔPro3, ΔShc binding domain (ΔSBD), ΔPro4, ΔCTH(Pro5), K-Ras 4B tag]

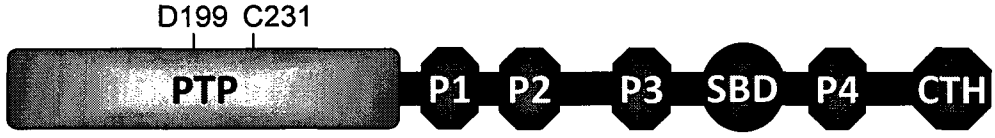

↓

Selection with 100μg/ml of Zeocin

↓

Pick clones, expand them and look for PTP-PEST expression.

FIG. 4 A

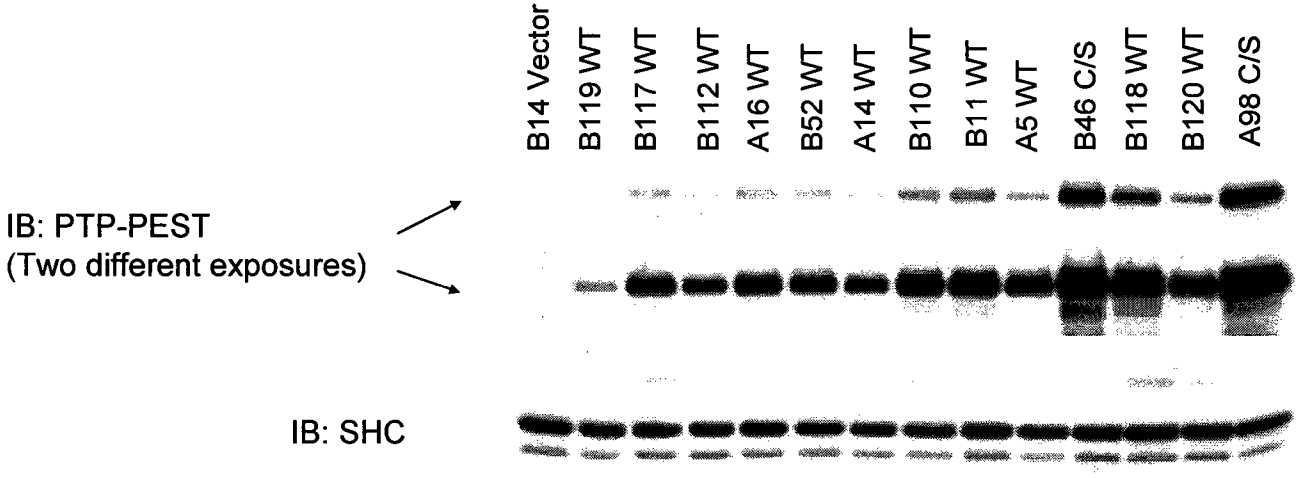
B14 Vector
B119 WT
B117 WT
B112 WT
A16 WT
B52 WT
A14 WT
B110 WT
B11 WT
A5 WT
B46 C/S
B118 WT
B120 WT
A98 C/S
IB: PTP-PEST
(Two different exposures)
IB: SHC

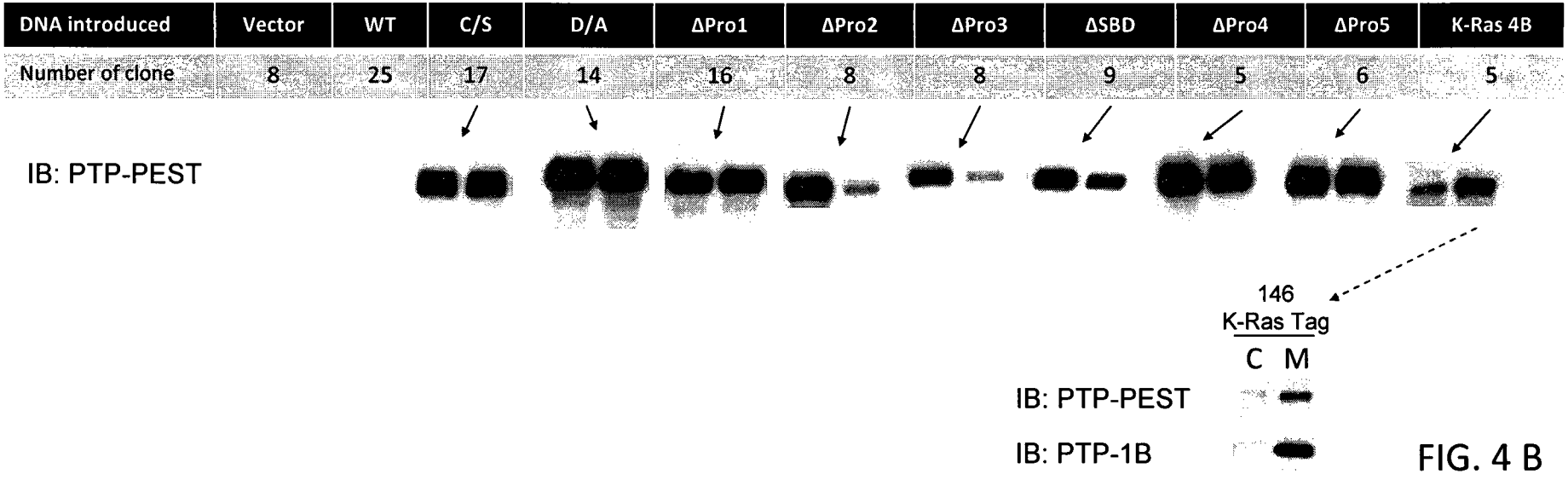
DNA introduced
Vector
WT
C/S
D/A
ΔPro1
ΔPro2
ΔPro3
ΔSBD
ΔPro4
ΔPro5
K-Ras 4B
Number of clone
8
25
17
14
16
8
8
9
5
6
5
IB: PTP-PEST
146
K-Ras Tag
C M
IB: PTP-PEST
IB: PTP-1B

FIG. 4 B

2.4.4 PTP-PEST regulates LPA-induced p130Cas interactions.

The role of PTP-PEST could be affected by subcellular localization. The phosphorylation of p130Cas can be induced by a variety of stimuli, including lysophosphatidic acid (LPA), and plays a central role in signal transduction by triggering interaction with Crk, and can be regulated by PTP-PEST (70, 117, 118). To evaluate the effect of PTP-PEST expression and localization on the interaction between p130Cas and Crk, various *PTP-PEST* -/- rescued clones were stimulated with LPA, processed, and subjected to immunoprecipitation with an anti-Crk antibody. The stimulation of PTP-PEST negative clones (B14V and B15V) with LPA increased the affinity of p130Cas for Crk (Fig. 5A). In contrast, PTP-PEST expressing clones (A5WT, B11WT and B118WT) showed significantly lower levels of p130Cas/Crk complex formation following addition of LPA (Fig. 5A). This effect appeared to be dependent on the level of PTP-PEST expression; clones expressing lower levels of PTP-PEST (A5WT) had less inhibitory effect on p130Cas/Crk complex formation than did clones expressing higher levels (B11WT, B118WT) (Fig. 5A). In addition, the amount of p130Cas associated with Crk in serum-starved cells was significantly lower in cells expressing WT PTP-PEST than in those stably transfected with an empty vector (Fig. 5A). This effect of PTP-PEST was dependent on its catalytic activity as well as on its cytosolic localization, as re-introduction of either an inactive mutant (A98C/S) or a membrane targeted construct (146K-RasTag) was significantly less effective in reduction of p130Cas/Crk association. Increased general tyrosine phosphorylation, as well as MAPK specific phosphorylation, was observed in lysates from all LPA-treated clones suggesting that they were all responsive to this stimulus (Fig. 5B). The above results indicate that PTP-PEST regulates the LPA-mediated interaction between p130Cas and Crk.

The phosphorylation of p130Cas facilitates its recognition by interacting partners such as Src and Nck (240, 290). To extend our investigation of the PTP-PEST contribution

to p130Cas-phosphorylation-dependent interactions, in vitro binding assays using GST fusion proteins were performed using cellular extracts derived from PTP-PEST clones, with or without LPA stimulation. The SH2 domains of Nck and Src displayed increased affinity for p130Cas when expressed in PTP-PEST null cells stimulated with LPA (Fig. 6A). LPA stimulation of cells expressing WT PTP-PEST also led to an increased association between p130Cas and Nck/Src SH2 domains, but to a lesser extent than that seen in the null cells transfected with an empty vector. Interestingly, in lysates from PTP-PEST null cells, Src-SH2 also associated with a slower migrating form of p130Cas. This presumably hyperphosphorylated form of p130Cas was not seen in analysis of cells expressing WT PTP-PEST. Neither the C231S mutant of PTP-PEST nor the membrane targeted form of the enzyme was as effective in inhibition of the p130Cas-Nck/Src SH2 domain interaction as was WT PTP-PEST. In every tested condition, the GST tag was not able to precipitate p130Cas. All clones expressed similar levels of p130Cas, and displayed increased MAPK phosphorylation following LPA treatment (Fig. 6B). Together, these data support the hypothesis that the activity as well as the localization of PTP-PEST plays a role in p130Cas recruitment of SH2-domain containing molecules.

Figure 5. PTP-PEST catalytic activity and cytosolic localization are required for inhibition of the LPA induced interaction between p130Cas and Crk. *PTP-PEST* -/- derived clones were serum starved for 16 hours, and treated with (+) or without (-) 1 μM LPA for 5 min. (A) Cells were solubilised in lysis buffer, Crk was immunoprecipitated from protein extracts, and the co-precipitation of p130Cas was determined by immunoblotting. The precipitation of Crk in each samples was verified by reprobing the membrane with an antibody against Crk. (B) Total cell extracts were subjected to immunoblotting with anti phosphotyrosine (4G10) and anti-phospho p44/42 MAK. TCL, total cell lysate; IB, immunoblot. Arrowheads indicate examples of bands increasing in a LPA-dependent manner. Values on the left correspond to molecular sizes in kDa.

Figure 6. PTP-PEST catalytic activity and cytosolic localization are required to prevent p130Cas recruitment of SH2 containing molecules in vitro. *PTP-PEST* -/- derived clones were serum starved for 16 hours, treated with (+) or without (-) 1 μM LPA for 5 min, lysed and extracts were subjected to a GST fusion protein based in vitro binding assay using GST, GST-SH2 [Nck] or GST-SH2 [Src]. Samples were resolved by SDS-PAGE and bound p130Cas was detected by immunoblotting. (B) Total cell lysates (TCL) were analysed for their p130Cas content and for the activation of p44/42 MAPK via immunoblot analysis using the appropriate antibody. IB, immunoblot; IVBA, in vitro binding assay; Ctl, control lysate. Values on the left correspond to molecular sizes in kDa.

A.

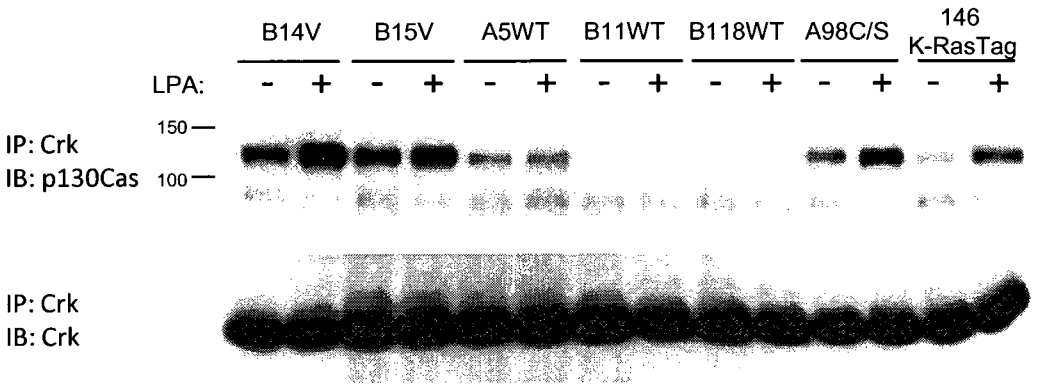
B14V
B15V
A5WT
B11WT
B118WT
A98C/S
146
K-RasTag
LPA:
- + - + - + - + - + - + - +
150
100
IP: Crk
IB: p130Cas
IP: Crk
IB: Crk

B.

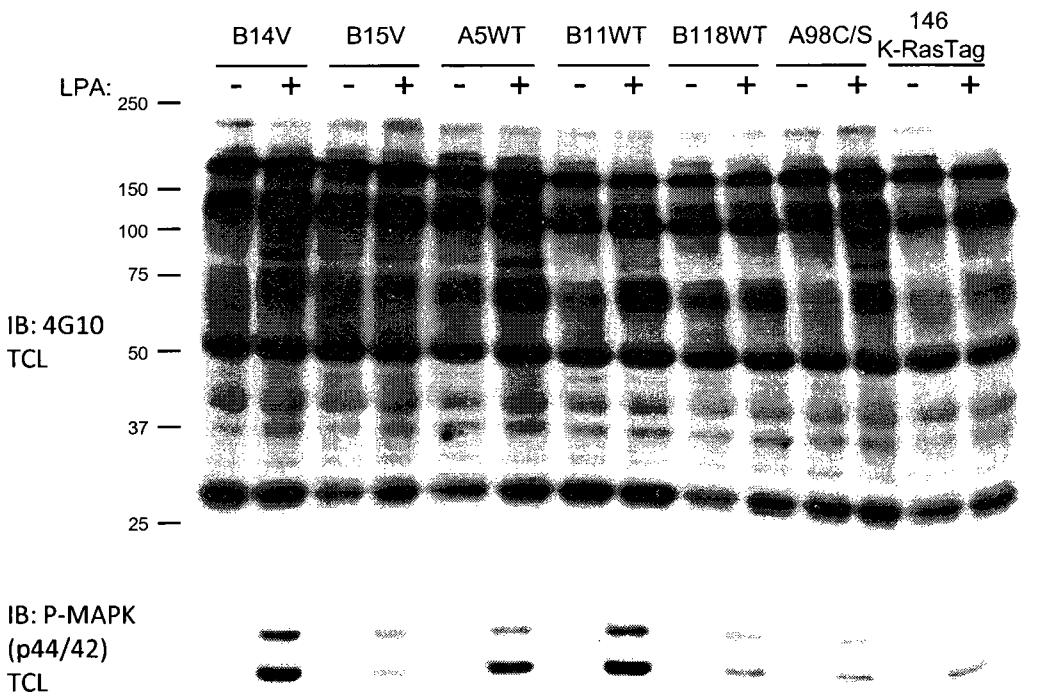
B14V
B15V
A5WT
B11WT
B118WT
A98C/S
146
K-RasTag
LPA:
- + - + - + - + - + - + - +
250
150
100
75
50
37
25
IB: 4G10
TCL
IB: P-MAPK
(p44/42)
TCL

FIG. 5

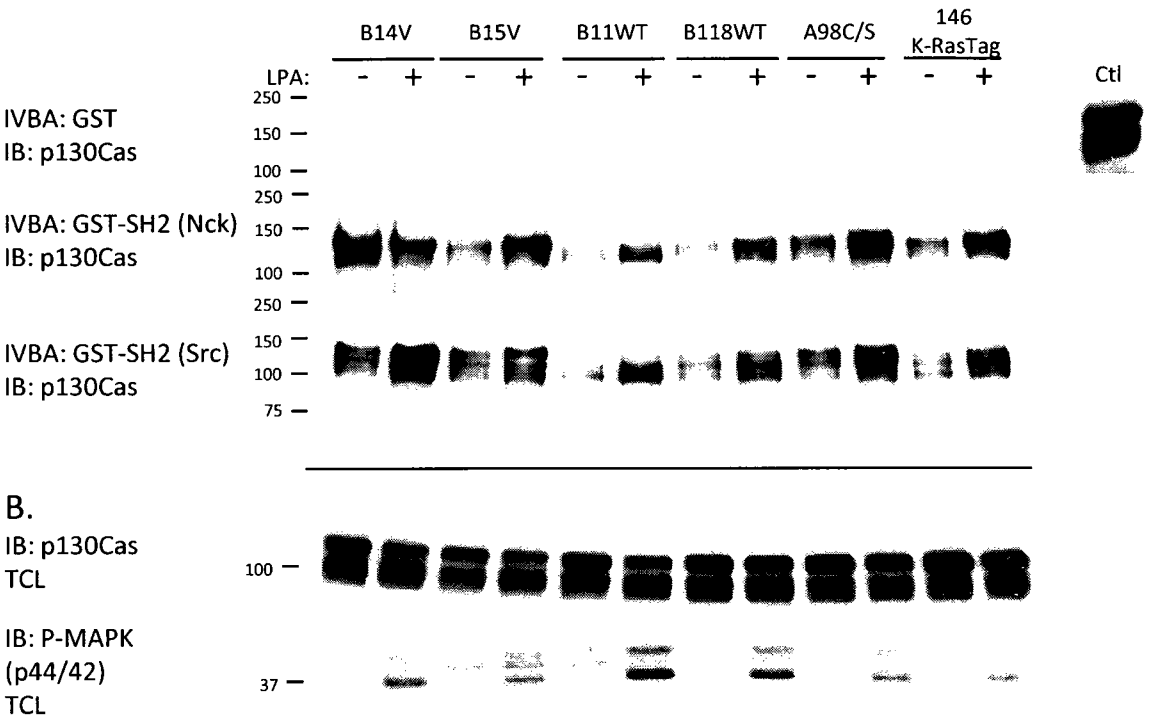
A.
B14V
B15V
B11WT
B118WT
A98C/S
146
K-RasTag
LPA:
- + - + - + - + - + - +
Ctl
IVBA: GST
IB: p130Cas
IVBA: GST-SH2 (Nck)
IB: p130Cas
IVBA: GST-SH2 (Src)
IB: p130Cas
250
150
100
250
150
100
250
150
100
75
B.
IB: p130Cas
TCL
IB: P-MAPK
(p44/42)
TCL
100
37

FIG. 6

2.5 Discussion

The ubiquitous expression of PTP-PEST and its essential role in embryonic development imply that regulatory functions attributed to this enzyme are of fundamental importance (88, 305). The partitioning of PTPs in defined subcellular locales is crucial for restriction of their activity to specific substrates and cell signalling events. Herein, we demonstrate that PTP-PEST is distributed throughout the cytosol and also accumulates at the cell membrane. The discrete localization of PTP-PEST appears to be a relevant element in the regulation of LPA-induced p130Cas-phospho-dependent associations.

The absence of hydrophobic segments or membrane targeting motifs in the PTP-PEST sequence indicated an intracellular localization but failed to predict its targeting to specific compartments (321, 365). Early immunofluorescence investigations illustrated the cytosolic distribution of PTP-PEST (56). However, fibronectin-mediated adhesion and spreading stimulated the accumulation of PTP-PEST in membrane ruffles, at the periphery of COS cells (11). In the same cell line, treatment with EGF induced PTP-PEST and PSTPIP to co-localize at the plasma membrane (Maxime Hallé and Michel L. Tremblay, un-published results). In addition, the perfect co-localization of these two proteins at this site was dependent on the integrity of the PTP-PEST CTH domain, a motif necessary to stabilize the PTP-PEST/PSTPIP complex (Maxime Hallé and Michel L. Tremblay, un-published results) (85). In Swiss 3T3 cells plated on fibronectin, PTP-PEST transiently localized at the tip of membrane protrusions, in focal adhesion like structures (286). Microinjection is a powerful approach for examination of the cellular distribution of a protein, because it allows precise timing of cDNA delivery to the target nucleus. This facilitates the prediction of the time window during which protein expression begins, and, therefore, the observation of immediate intracellular localization following synthesis. Confocal analyses performed on Swiss 3T3 cells microinjected with a vector

encoding PTP-PEST protein revealed that the PTP is mostly localized in the cytosol. Interestingly, PTP-PEST was present in focal adhesion-like structures, present at the cell-substratum interface. In addition, an intense signal corresponding to PTP-PEST was observed at the edge of cellular periphery, likely at the plasma membrane. Importantly, fractionation experiments confirmed that while the majority of PTP-PEST was cytosolic, a significant proportion of the enzyme was associated with the membrane fraction. The presence of PTP-PEST in adhesion-like structures and membrane ruffles could be relevant to its previously characterized roles in focal adhesion turn-over and lamellipodia formation (11, 286, 287).

Fibronectin stimulated cell adhesion also promoted PTP-PEST catalytic activity (286). This phenomenon occurred in parallel with the translocation of PTP-PEST to the extremity of membrane protrusions (286). Our findings indicate that both cytosolic and membrane associated PTP-PEST interact with multiple candidate proteins. Interestingly, some of these interactions were particularly enriched in the membrane fraction, whereas others were more restricted to the cytosolic fraction. It therefore appears that the intracellular location of PTP-PEST may influence its preference for specific binding partners as well as its enzymatic activity.

The carboxy-terminal tail of PTP-PEST is characterized by the presence of a number of motifs mediating its recruitment to several signalling and cytoskeletal proteins, including p130Cas, paxillin, Shc, Grb-2 and PSTPIP (53, 54, 84-86, 117). Herein, we observed that PTP-PEST is capable of interacting with Shc and paxillin in the cytosol. Through binding to paxillin, PTP-PEST was previously proposed to be targeted to focal adhesion structures, which link the extra-cellular matrix with the actin cytoskeleton, and are in close proximity to the plasma membrane (86). However, only a minute percentage of paxillin was seen to interact with PTP-PEST in the membrane fraction, implying that this interacting partner may not be essential for recruitment of PTP-PEST to the plasma membrane. Conversely, membrane fractions from cells expressing PTP-PEST-K-Ras 4B

tag had increased levels of paxillin, suggesting that PTP-PEST translocation to this site may lead to co-transport of paxillin (Maxime Hallé and Michel L. Tremblay, un-published results). Similarly, PSTPIP, a protein normally co-localized with actin-containing structures (307), adopts the localization pattern of PTP-PEST when co-expressed with this enzyme (85). Thus, it appears that neither paxillin nor PSTPIP are key components in mediating targeting of PTP-PEST to the plasma membrane.

Another PTP-PEST binding partner shown to interact with transmembrane proteins is Shc (53). We observed that the association between PTP-PEST and Shc, which was enriched in the cytosol, was present in the membrane fraction and proportionally more abundant than PTP-PEST-paxillin in this fraction. Although Shc can interact with multiple receptors at the plasma membrane, its contribution to the transport of PTP-PEST in this micro-environment remains elusive because Shc binds PTP-PEST and RTKs via the same domain: the phosphoryrosine binding (PTB) domain (53). Interestingly, binding of PTP-PEST to the adaptor Grb-2 mediates the coupling of this PTP to the epidermal growth factor receptor (EGF-R) (54). Additionally, PTP-PEST was found in a complex with the platelet-derived growth factor receptor (PDGF-R) (220), an association that could involve a similar mode of assembly. Nevertheless, the exact mechanism underlying the translocation of PTP-PEST between different subcellular compartments remains unclear. Further studies using cell lines expressing different mutants of PTP-PEST may contribute to our understanding of this phenomenon.

In cells stimulated with LPA, we observed that a variety of proteins became tyrosine phosphorylated (Fig. 5B); which implicating PTPs as potential antagonists of LPA induced signalling. A number of mechanisms are involved in LPA-induced tyrosine phosphorylation: LPA indirectly transactivates members of the EGF-R family, promotes phosphorylation of the focal adhesion component TRIP6 in a Src-dependent manner, as well as FAK and paxillin independently of EGF-R activity (200, 234, 283). Recently, Fas-associated phosphatase-1 (FAP1) was demonstrated to attenuate LPA-mediated cell

migration by dephosphorylating TRIP6 (201). Also, the association of the PTP SHP-2 with the receptor-like protein SHPS-1 was proposed to play a role in LPA-driven MAPK activation (319). To our knowledge, little else is known regarding the implication of PTPs in the control of tyrosine phosphorylation arising from LPA stimulus. In this report, we present data indicating that recruitment of SH2 containing molecules to p130Cas is regulated by PTP-PEST, implicating this PTP as a novel regulator of LPA signalling.

Efficient tyrosine phosphorylation of p130Cas is achieved by the synergistic action of FAK and Src (277). The phosphorylation of the p130Cas substrate domain (SD) triggers the recruitment of adaptor molecules such as Crk and Nck, whereas binding to Src is favoured by the phosphorylation of a carboxy-terminal site termed the Src-binding domain (SBD) (188, 240, 290). LPA stimulates tyrosine phosphorylation of p130Cas (298) and its interaction with Crk, which results in growth of pseudopodia, thereby promoting cell motility (70). The regulation of p130Cas by PTP-PEST in the context of LPA could occur at two levels: up-stream, via the inactivation of molecules inducing its phosphorylation, or through direct dephosphorylation.

In support of the first hypothesis, PTP-PEST was found to form a complex with FAK and with the EGF-R (54, 300), and to inhibit Src-dependent villin phosphorylation (223). However, several lines of evidence do not support this model. Although FAK is hyperphosphorylated in *PTP-PEST* null cells (11), this kinase was proposed to be a poor substrate for PTP-PEST (216). Also, even though it would be expected to have access to the EGF-R and to Src (which is also anchored at the membrane by myristoylation), our results show that the membrane targeted PTP-PEST-K-Ras 4B only weakly regulated the recognition of p130Cas by SH2 containing proteins as compared to the WT enzyme. In addition, Crk interacted poorly with p130Cas in the membrane fraction of fibronectin stimulated cells (Supplementary Figure 1), a well documented stimulus inducing their association (120, 348). Moreover, we observed that the majority of Crk/p130Cas interaction occurred in the cytosol, and that this interaction was amplified in the

absence of PTP-PEST (Supplemental Figure 1). We therefore concluded that PTP-PEST directly regulates the interaction between p130Cas and Crk in the cytosol. Compared to the vector control and PTP-PEST C231S cells, total cellular p130Cas from clones expressing the WT enzyme had less affinity for Crk and for the SH2 domains of Nck and Src, which implies that PTP-PEST regulates the phosphorylation of both the SD and SBD sites of p130Cas. Further investigations will be necessary to determine whether PTP-PEST dephosphorylates p130Cas in a precise sequence or if it acts on all sites simultaneously. In summary, we believe that the direct action of PTP-PEST on its previously established substrate p130Cas (118), predominantly takes place in the cytosol.

Herein, we have presented a series of clones expressing various mutated forms of PTP-PEST. Our group actively uses them, as well as a breast cancer cell model infected with adenovirus encoding various forms of PTP-PEST, to clarify the role of PTP-PEST in the regulation of oncogenic transformation (Hidehisa Shimizu, Maxime Hallé and Michel L. Tremblay). The data obtained, which correlate with those presented here, underscore the critical importance of PTP-PEST Pro1 integrity for the regulation of p130Cas tyrosine phosphorylation, cell proliferation, migration and invasion (Hidehisa Shimizu, Maxime Hallé and Michel L. Tremblay, unpublished results).

Tyrosine phosphorylation events are critical for a wide array of physiologic phenomena including cell growth, proliferation and migration. Aberrant signals, which can arise from the loss of spaciotemporal control, contribute to cellular transformation. Herein, we observed that PTP-PEST localizes in the cytosol and at the plasma membrane, which influences its interactions and presumably affects its functions. Both LPA and p130Cas have been implicated in promoting cellular survival, proliferation and motility, which contribute to cancer progression (46, 153, 234, 344). Our findings provide additional insight into the control of LPA-promoted p130Cas signalling complex assembly. The possible involvement of PTP-PEST in modulating the oncogenic activity of

LPA remains to be established. Notably, mutated variants of PTP-PEST displaying modified catalytic activity were recently discovered in human breast cancer cell lines and tumor samples (310). Our data illustrates the importance of PTP-PEST in some critical events promoting cellular transformation and metastasis.

2.6 Acknowledgments

We thank Dr. Feng Gu for providing expert advice on cellular fractionation. We are grateful to Dr. Nathalie Lamarche-Vane for generously providing access to her microinjection system and for her helpful discussions, and to Ibtissem Triki for her help with the culture of Swiss 3T3 cells. We thank Hannah Heath-Engel and Matthew Stuible for critical reviews of the manuscript. M.H. is a recipient of a Fonds pour la Formation de Chercheurs et l'Aide à la Recherche (FCAR) studentship. M.L.T. is a recipient of the Jeanne et Jean-Louis Lévesque Chair in Cancer Research. This work was supported by the Canadian Institutes of Health Research (CIHR) (MOP-12466).

2.7 Supplementary data.

Supplementary figure 1. Crk/p130Cas complexes are present in cytosolic fractions, and are regulated by PTP-PEST. PTP-PEST negative (B14V) and positive (B118WT) clones were serum-starved for 16 h in 0.1% FBS DMEM, held in suspension for 30 min, and then seeded on fibronectin coated dishes for 45 min. Cells were collected and fractionated, and the interaction between Crk and p130Cas was analysed by immunoprecipitation and immunoblotting as described in materials and methods. IP, immunoprecipitation; IB, immunoblot; C, cytosolic fraction; M, membrane fraction; S, cells held in suspension; FN, fibronectin stimulated cells.

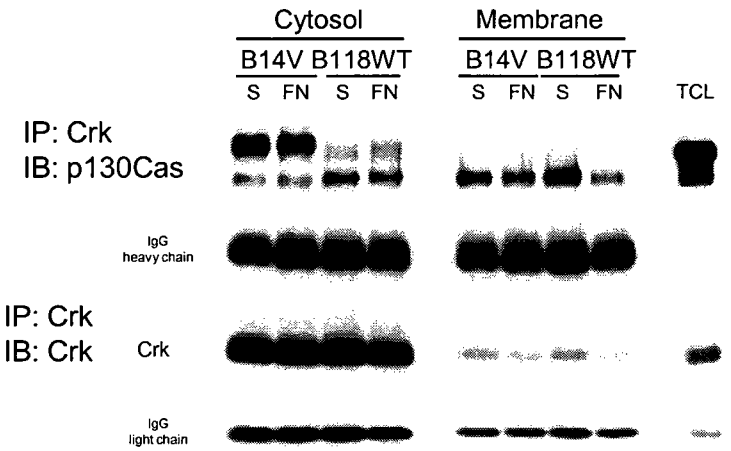
Cytosol
Membrane
B14V B118WT
B14V B118WT
S FN S FN
S FN S FN
TCL
IP: Crk
IB: p130Cas
IgG
heavy chain
IP: Crk
IB: Crk
Crk
IgG
light chain

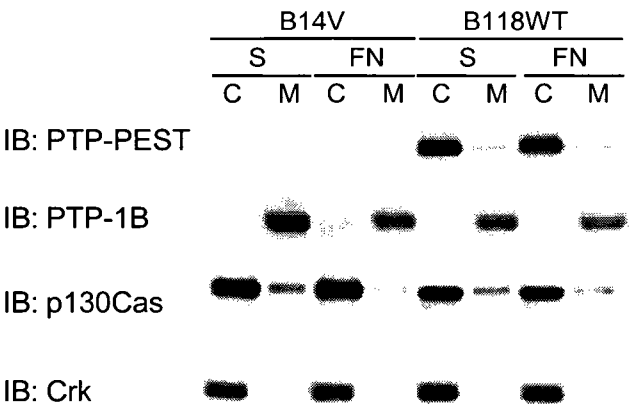
B14V
B118WT
S
FN
S
FN
C M C M C M C M
IB: PTP-PEST
IB: PTP-1B
IB: p130Cas
IB: Crk

SUPP. FIG. 1

3 CHAPTER 3

THE *LEISHMANIA* SURFACE PROTEASE GP63 CLEAVES MULTIPLE INTRACELLULAR PROTEINS AND ACTIVELY PARTICIPATES IN p38 MITOGEN ACTIVATED PROTEIN KINASE INACTIVATION

Maxime Hallé[1], Maria Adelaida Gomez[2], Matthew Stuible[1], Hidehisa Shimizu[1], W. Robert McMaster[3], Martin Olivier[2*] and Michel L. Tremblay[1*]

J. Biol. Chem.

Manuscript accepted for publication.

From the Rosalind and Morris Goodman Cancer Centre and the Department of Biochemistry, McGill University, Cancer Pavilion, 1160 avenue des Pins ouest, Room 508, Montréal, Québec, Canada, H3A 1A3[1], the Department of Microbiology and Immunology, McGill University, Duff Medical Building, 3775 University Street, Montréal, Québec, Canada, H3A 2B4[2], and the Department of Medical Genetics, Jack Bell Research Centre, University of British Columbia and Immunity and Infection Research Centre, Vancouver Hospital, 2660 Oak Street, Vancouver, BC, Canada V6H 3Z6. [3]

Running title: *Leishmania* GP63 targets host-cell signalling components

Address correspondence to: Martin Olivier, Department of Microbiology and Immunology, McGill University, Duff Medical Building, 3775 University Street, Room 600, Montréal, Québec, Canada, H3A 2B4. Tel: (514) 398-5592; Fax: (514) 398-7052; martin.olivier@mcgill.ca. Michel L. Tremblay, Rosalind and Morris Goodman Cancer Centre, McGill University, Cancer Pavilion, 1160 avenue des Pins ouest, Room 617, Montréal, Québec, Canada, H3A 1A3. Phone: (514) 398-7290; Fax: (514) 398-6769; E-mail: michel.tremblay@mcgill.ca. *

3.1 Abstract

The *Leishmania* parasite is a widespread disease threat in tropical areas, causing symptoms ranging from skin lesions to death. *Leishmania* (*L.*) typically invade macrophages but are also capable of infecting fibroblasts, which may serve as a reservoir for recurrent infection. Invasion by intracellular pathogens often involves exploitation of the host cell cytoskeletal and signalling machinery. Here, we have observed a dramatic rearrangement of the actin cytoskeleton and marked modifications in the profile of protein tyrosine phosphorylation in fibroblasts infected with *Leishmania major*. Correspondingly, exposure to *L. major* resulted in degradation of the phosphorylated adaptor protein p130Cas and the protein tyrosine phosphatase (PTP)-PEST. Cellular and in vitro assays using pharmacological protease inhibitors, recombinant enzyme, and genetically modified strains of *L. major* identified the parasite protease GP63 as the principle catalyst of proteolysis during infection. A number of additional signalling proteins were screened for degradation during *L. major* infection: a small subset including cortactin, TC-PTP and caspase-3 were cleaved, but the majority remained unaffected. Protein degradation occurred in cells incubated with *Leishmania* extracts in the absence of intact parasites, suggesting a mechanism permitting transfer of functional GP63 into the intracellular space. Finally, we evaluated the impact of *Leishmania* on MAPK signaling: unlike p44/42 and JNK, p38 was inactivated upon infection in a GP63- and protein degradation-dependent manner, which likely involves cleavage of the upstream adapter TAB1. Our results establish that GP63 plays a central role in a number of host-cell molecular events that likely contribute to the infectivity of *Leishmania*.

3.2 Introduction

Protozoans of the genus *Leishmania* cause a complex disease called leishmaniasis, whose clinical manifestations have been divided into three principal types – cutaneous, mucocutaneous and visceral – exhibiting different degrees of severity and mortality (90, 270). This disease threatens over 350 million people in 88 countries in tropical, subtropical and temperate regions (182, 359). The development, multiplication and transmission of *Leishmania* in the form of promastigotes between mammalian hosts are achieved by the sandfly insect vector (182).

Following inoculation into a vertebrate host, promastigotes are typically phagocytosed by macrophages where they differentiate into and multiply as amastigotes (90, 147). Heavily infected macrophages lyse and liberate amastigotes that will colonise other cells. In addition, both promastigotes and amastigotes of *L. major* can be internalized by fibroblast cells (29). Despite their capability to synthesise nitric oxide, fibroblasts produce a much lower quantity of this microbicidal compound than macrophages (29). The limited capacity of fibroblast to eliminate parasites implies that these cells could act as a reservoir for long-term infection (29). Nevertheless, little is known regarding the molecular events occurring in fibroblasts cells upon contact with *Leishmania* parasites.

Several intracellular parasites hijack the actin cytoskeletal machinery in order to infiltrate and traffic inside their host cells (276, 309). Cellular proteins such as cortactin, Wiskott-Aldrich syndrome protein (WASP), Crk and Crk-associated substrate (p130Cas) have been identified as targets of intracellular bacteria (125, 297, 308, 353). *Leishmania* amastigotes induce activation of Cdc42 in order to re-organize the actin network and enter into Chinese hamster ovary (CHO) fibroblasts (237). Additionally, the activity of Cdc42 is involved in knitting a shell of actin around the internalized *Leishmania* parasite,

a site at which other cytoskeletal regulators such as vinculin and WASP are also recruited (212, 237). Numerous biological processes, including those modulating the dynamics of actin cytoskeleton assembly, are controlled by the dual effects of protein tyrosine kinases (PTKs) and protein tyrosine phosphatases (PTPs). *Leishmania* can affect the state of tyrosine phosphorylation in macrophage cells by activating SHP-1 (Src homology-2 (SH2) domain-containing phosphatase-1) (27, 241). However, the specific roles of other PTPs in this pathogenic process remain unclear. Interestingly, another non-receptor PTP, PTP-PEST, has been extensively implicated in the regulation of WASP and p130Cas phosphorylation as well as in the modulation of vinculin-containing adhesion structure formation (11, 85, 118, 120). These studies have established PTP-PEST as a critical regulator of actin remodelling and present this enzyme as a particularly interesting candidate target of *Leishmania*.

Downstream elements of cellular signal transduction such as members of the Mitogen-Activated Protein Kinases (MAPKs) have also been linked to the pathogenic outcome of *Leishmania* infection. The ability of promastigotes to manipulate and circumvent MAPK activation may represent a strategy to evade the macrophage-host cell defence mechanism. Incubation of macrophages with a p38 inhibitor prior to exposure to *L. donovani* augmented their subsequent invasion by the parasite (179). Similarly, the anisomycin-mediated inhibition of *L. donovani* survival inside macrophages was dependent on p38 (179). Moreover, *L. major* down-regulates p38 in order to impair CD40-induced iNOS2 expression, inhibiting nitric oxide production and favouring survival within macrophages (17). By inhibiting p38, the parasite can also hijack another signal initiated by CD40 cross-linking, altering cytokine expression to its advantage: interleukin-12 (IL-12), a promoter of the host-protective T-helper type 1 (T_H1) cells response, is reduced while IL-10, an inhibitor of T_H1 cell and of NO production, is increased (186, 224). Although the interplay between p38 activity and *Leishmania* persistence is accepted, little is known regarding the parasitic elements involved in regulation of this MAPK.

Leishmania is coated by a characteristic glycocalyx, whose molecular components play a critical role in the initial contact between the parasite and its host environment. GP63, also referred to as major surface protease (MSP), leishmanolysin, or promastigote surface protease (PSP), is the most abundant protein covering *Leishmania* promastigotes (33, 369). Studies performed using different parasitic models demonstrated that GP63 plays a crucial role in complement fixation and processing, which protects *Leishmania* during its sojourn into mammalian hosts (37, 176, 177). Similarly, GP63 was recently shown to defend the parasite against antimicrobial peptides such as defensins and pexiganan (195). The abundance and diversity as well as the high catalytic activity at mammalian body temperature of this virulence factor (57, 370, 372) favour the dissemination of the parasite as it digests constituents of the host's extracellular matrix such as collagen type IV, fibronectin and laminin (227). Several species of *Leishmania* release proteolytically active GP63 in the surrounding milieu (103, 171, 228, 368) presumably facilitating the propagation of the parasite. In addition, fragments from GP63-processed fibronectin can protect parasites within macrophages, as they attenuate production of reactive oxygen intermediates and favour amastigote proliferation (194). Furthermore, GP63 maximizes promastigote binding to and internalization in macrophages through its ability to interact with the α4/β1 integrin and to promote complement-dependent adhesion (36, 61). Moreover, similar to fibronectin, coating polystyrene surfaces with GP63 enhances in vitro spreading of fibroblasts (269). The expression of specific *gp63* genes in the intracellular amastigote form (156, 177, 347), implies an intra-host-cell function for this parasitic protease. Interestingly, the activity of GP63 was implicated in the protection of encapsulated proteins against phagolysosomal degradation as well as intra-macrophage survival of *L. mexicana amazonensis* (58, 294). The identification of the myristoylated alanine-rich C kinase substrate (MARKS)-related protein (MRP), a cytosolic protein associated with the actin network of macrophages, as a substrate of GP63 reinforces the potential of this enzyme to modulate host cell activities within the intracellular space (82). Nonetheless, little else

is known concerning its impact on host-cell signal transduction or the existence of additional intracellular substrates for this parasitic protease.

Subverting normal cellular functions is a widespread strategy among intracellular parasites to take advantage of mammalian hosts. In the present study, we describe distinctive effects of *Leishmania* infection on cell signalling in fibroblasts. During *L. major* infection, we found that the parasite manipulates cellular components, in part by altering the tyrosine phosphorylation state of several proteins. Upon contact with *L. major*, the adaptor Crk interacts with a truncated form of p130Cas, which further correlates with cleavage of two novel substrates, p130Cas and PTP-PEST, by GP63. Moreover, through GP63, *L. major* impacted the stability of additional proteins including cortactin, TC-PTP (T-cell PTP) and caspase-3. Additionally, *L. major* was found to down-regulate p38 in a GP63-dependent manner. Direct activators of p38 include the MAPK kinase MKK3, MKK6 and the adaptor molecule TAB1 (TAK-1-binding protein-1) which interacts directly with p38 (121, 380). Interestingly, the inhibition of p38 occurred in concert with the GP63-mediated proteolysis of TAB1. This report reveals diverse and novel mechanisms by which *Leishmania* can monopolize different constituents of the fibroblast signal transduction machinery.

3.3 EXPERIMENTAL PROCEDURES

3.3.1 Reagents, antibodies and plasmids.

Chemicals were purchased at BioShop Canada Inc., Fisher Scientific and Sigma. The PTP-PEST polyclonal antibodies (2528 and 2530) were previously described (85). Monoclonal antibodies specific for Crk, p130Cas, Integrin-β1, Shc, and paxillin were from BD Transduction Laboratories. Antibodies against IκBα, STAT5 (C17) and JNK1 were from Santa Cruz Biotechnology. TC-PTP monoclonal antibodies (3E2) were described

previously (162). Polyclonal rabbit antibodies against PTP-1B and FAK as well as monoclonal anti-cortactin (4F11) and phosphotyrosine (4G10) were from Upstate. Antibodies specific for AKT, caspase-3, phospho-thr202/tyr204 p44/42 MAPKs, p44/42 MAPKs, phospho-thr183/tyr185 JNK, phospho-thr180/tyr182 p38 MAPK, p38 MAPK, TAB1, MKK3 and MKK6 were from Cell Signaling Technology. The vector encoding GST-PTP-PEST (pEBG-PTP-PEST) has been described (138). cDNAs encoding p38 (image ID: 4195842) and TAB1 (image ID: 5356886) were obtained from American Type and Culture Collection (ATCC). pET-28(c+)TAB1 was generated by PCR cloning of the TAB1 cDNA between *EcoR1* and *Not1* sites. Flag-TAB1-myc-myc WT and 1-418 (amino acid numbering) were made by inserting TAB1 cDNA amplified by PCR into pcDNA4/Myc-HisA between the *EcoR1* and *Not1* restriction sites. The sense oligonucleotide sequence contains the Flag epitope, whereas the antisense oligonucleotides for both full length and truncated TAB1 encodes an additional myc epitope. The mammalian expression vector encoding GST-p38 was obtained by successively cloning p38 PCR product into pDONR221 and pDEST27 using Gateway technology according to the manufacturer's instructions (Invitrogen). The integrity of the inserted DNA in each vector was verified by sequencing (Genome Quebec).

3.3.2 Cells and parasites.

Transient transfections were performed and PTP-PEST clones (B14V, B15V, B11WT (wild-type) and B118WT) were generated and maintained as described previously (138). Primary mouse embryonic fibroblasts (P-MEFs) were isolated from BALB/c embryos (Jackson Laboratories) and grown as described (138). *L. major* A2 and *gp63*-null (*L. major*$^{gp63-/-}$) and rescued strains (in which *gp63 gene 1* was re-introduced, *L. major*$^{gp63-/-rescued}$) (176) as well as *L. donovani* strain 2211, *L. mexicana*, *L. tarentolae* and *L. braziliensis* 2249 promastigotes were all maintained at 25 °C in SDM-79 medium supplemented with 10% heat-inactivated FBS (Wisent) as described (127).

3.3.3 Cellular treatment, infection and immunoblotting.

Stationary-phase *Leishmania* promastigotes were centrifuged at 2500 × rpm (Allegra 6R Centrifuge, Beckman Coulter) for 5 min. Supernatant was removed, pellets of parasites were washed with phosphate-buffered saline (PBS) and centrifuged at 2500 × rpm for 5 min (Allegra 6R Centrifuge, Beckman Coulter). Parasites were resuspended in DMEM (containing the indicated concentration of heat-inactivated FBS) and added onto cells at the specified parasite:cell ratio and for the indicated duration. Cells were then rinsed on ice with PBS and lysed (100mM Tris (pH 7.4), 5 mM EDTA, 150 mM NaCl, 1 % Triton X-100, 0.1 % sodium dodecyl sulphate (SDS), 50 mM NaF, 1 mM Na_3VO_4, Complete protease inhibitor (Roche)). Cell extracts were cleared by centrifugation at 16000 × g for 10 min at 4 °C, and the protein concentration of each sample was measured by Bradford assay (Bio-Rad protein assay). Proteins were separated by SDS-polyacrylamide gel electrophoresis (PAGE), transferred to polyvinylidene difluoride membranes (Immobilon-P; Millipore) and immunoblotted as described (138).

The effect of pharmacological protease inhibitors on cellular protein degradation induced by *L. major* infection was determined as follows: caspase inhibitor (Z-VAD-FMK; Cedarlane), calpain inhibitor (PD150606; Calbiochem), proteasome inhibitor (lactacystin; Sigma) as well as calpain inhibitor and proteasome inhibitor combined together were added to cells 2h prior to addition of parasites and co-incubated for an additional 15 min. Cells that were not exposed to any of the inhibitors were incubated with media containing DMSO as a vehicle control. Cells were harvested, lysed and analyzed by immunoblotting as described above.

The effect on mammalian cells of parasite-conditioned-medium and protein lysates prepared from cultured *L. major* was evaluated as follows: *L. major* cultures were centrifuged 5 min at 2500 × rpm (Allegra 6R Centrifuge, Beckman Coulter). Supernatants were carefully harvested, avoiding contact with the pellet and the wall of the tube.

Conditioned-SDM was centrifuged a second time for 10 min at 3500 × rpm (Allegra 6R Centrifuge, Beckman Coulter) to remove any potentially residual parasites. Supernatant from cultured-parasites was then diluted in normal parasite growth media to normalize the volume according to the parasite concentration in the original culture. Conditioned or fresh growth media was deposited on P-MEFs for 1h, and cell lysates were prepared and analysed as described above.

To prepare parasite lysates, *L. major* parasites were washed three times with PBS, resuspended in serum-free DMEM, sonicated (Ultrasonic Processor, Sonics & Materials Inc.) two times for 10 seconds at an intensity of 50 % at 4 °C with a 30 seconds incubation on ice between sonication steps. Lysates were then cleared by centrifugation for 2 min at 16000 × g at 4 °C, and protein concentration was determined by Bradford assay. P-MEFs were then incubated with serum-free DMEM supplemented with 333 µg/ml of *L. major* protein extract for 1h. The absence of parasites in both the conditioned media and *L. major* lysates was confirmed by microscopic examination (data not shown). Following the incubation, protein lysates were prepared from treated cells and analysed by immunoblotting according to the procedures described above.

3.3.4 Incubation of cellular extracts and recombinant proteins with parasite lystate.

The procedure for preparation of parasite extracts from *L. major* promastigotes (WT and *gp63*$^{-/-}$) was based on a previously published protocol (82). *L. major* stationary phase promastigotes were washed with PBS and with TNB (10 mM Tris-HCl (pH 7.4), 100 mM NaCl, 0.4 mg/ml bovine serum albumin (BSA, Gibco), 5 µg/ml pepstatin, 1 mM phenylmethylsulfonyl fluoride (PMSF), 10 µg/ml leupeptin, 10 µg/ml aprotinin) before being resuspended in TNB. Parasites were then sonicated (Ultrasonic Processor, Sonics & Materials Inc.) two times at 4 °C for 5 seconds at an intensity of 50 % with a 5-second incubation on ice between each sonication step. Samples were then centrifuged for 2 min at 16000 × g at 4 °C and supernatants were kept to perform the cleavage assay. *PTP-*

PEST$^{-/-}$-WT expressing cells (clone B11WT) were rinsed with ice-cold PBS, collected in TNB and lysed by three sonication steps of 15 seconds at an intensity of 50 % at 4 °C, which were separated by 15 second incubations on ice. Samples were then centrifuged for 5 min at 16000 × g at 4 °C, supernatants were collected and protein concentrations were determined by Bradford assay. Next, 200 µg of protein lysates from *PTP-PEST*$^{-/-}$-WT expressing cells was incubated with lystates made from 20 × 10^6 promastigotes (either from WT or *gp63*$^{-/-}$ *L. major*) or with TNB (control) at 37 °C for the indicated time. Samples were immediately placed on ice and SDS sample buffer was added. Samples were boiled for 4 min, separated by SDS-PAGE and analysed by immunoblotting.

To obtain purified GST-PTP-PEST, protein extracts from transfected fibroblasts (138) were prepared in lysis buffer (100mM Tris (pH 7,4), 5mM EDTA, 150mM NaCl, 1% TritonX-100, Complete protease inhibitor (Roche)). Cell lysates were cleared by centrifugation for 10 min at 16000 × g at 4 °C and then incubated for 1 h at 4 °C with glutathione Sepharose beads (Amersham Biosciences). The beads were then washed three times with lysis buffer and two times with TNB. Next, beads were resuspended in TNB, incubated with the indicated quantity of *L. major* lysates, prepared as described above, for 15 min at 37 °C. Samples were immediately placed on ice, rinsed twice with ice-cold lysis buffer and resuspended in SDS-sample buffer. Samples were boiled for 4 min, separated by SDS-PAGE and analysed by immunoblotting.

3.3.5 Incubation of recombinant proteins with recombinant GP63.

GST-PTP-PEST was purified as described above. To produce His-TAB1, *Escherichia coli* transformed with pET-28(c+)TAB1 were induced for 2h at 37 °C with 1 mM isopropyl-β-D-1-thiogalactopyranoside and harvested by centrifugation. Bacterial cells were lysed (50 mM Tris (pH 7.5), 500 mM NaCl, 40 mM imidazole, 1% TritonX-100 and EDTA-free complete protease inhibitor) and recombinant proteins were isolated on nickel sepharose beads (Ni Sepharose 6 Fast Flow, GE Healthcare) according to the

manufacturer's instructions. Immobilized His-TAB1 was eluted in elution buffer (1 M imidazole, 500 mM NaCl, 50 mM Tris (pH 7.5), 1% TritonX-100, complete protease inhibitor) for 1h at 4 °C, concentrated in storage buffer (50 mM Tris (pH 7.5), 150 mM NaCl, 0.1 mM EGTA, 0.1 mM EDTA, 25 % glycerol, 0.25 mM DTT, complete protease inhibitor) using Microcon filters (Millipore), and stored at -80 °C. Purified GST-PTP-PEST or His-TAB1 were incubated with recombinant GP63 (rGP63) (44) in TNB at 37 °C for 30 min. Samples were immediately placed on ice and resuspended in SDS-sample buffer. Samples were boiled for 4 min, separated by SDS-PAGE and analysed by immunoblotting.

3.3.6 Immunofluorescence.

Glass microscope coverslips were coated with 0.2% gelatin at 37 °C for 30 min and rinsed with PBS prior to seeding with primary mouse embryonic fibroblasts (PMEFs). Infected PMEFs were rinsed three times with PBS, fixed in 4 % PFA (diluted in PBS) for 20 min, treated with permeabilizing solution (4 % PFA, 0.1 % Triton X-100 in PBS) for 20 min at 4 °C and incubated for 45 min with 2 % BSA/PBS. Cells were washed with PBS and stained with a mixture of rhodamine-conjugated phalloidin (Molecular Probes) and 4',6-diamidino-2-phenylindole (DAPI) (Roche). Cells were washed three times with PBS, rinsed once with water and coverslips were deposited on slides using Vectashield mounting medium (Vector Laboratories, Inc.). Random field images were acquired by confocal microscopy (Zeiss LSM 510 - NLO).

3.3.7 Immunoprecipitation and protein complex analysis.

To analyse Crk interactions, serum-starved- and *L. major*-infected-cells were rinsed with ice-cold PBS and lysed (100mM Tris (pH 7,4), 5mM EDTA, 150mM NaCl, 1% TritonX-100, 10 mM NaF, 1 mM Na_3VO_4 and Complete protease inhibitor (Roche)). Cell

extracts were centrifuged at 16000 × g for 10 min at 4 °C, and the protein concentration of each sample was measured by Bradford assay. Cleared protein lysates (2.4 mg) were then incubated at 4 °C for 2h in presence of 1.25 µg of anti-Crk monoclonal antibody (mAB) (Transduction Laboratory) 25 µl of protein G agarose beads (Invitrogen). Beads were then washed three times with lysis buffer, boiled in SDS-sample buffer and analyzed by immunoblotting.

To analyse the interaction between p38 and TAB1, control and *L. major*-infected cells expressing Flag-TAB1-myc-myc were rinsed with ice-cold PBS and lysed in interaction buffer (20 mM Tris (pH 7.5), 120 mM NaCl, 10 % glycerol, 2 mM EDTA, 1 % TritonX-100, 1 mM Na_3VO_4, 10 mM NaF and Complete protease inhibitor (Roche)). Cell extracts were centrifuged at 16000 × g for 10 min at 4 °C, and the protein concentration of each sample was measured by Bradford assay. Cleared protein lysates (2.4 mg) were then incubated at 4 °C for 2h in presence of GST or GST-p38 immobilised on glutathione sepharose beads prepared as described below. Beads were then washed three times with interaction buffer, resuspended in SDS-sample buffer, boiled and analyzed by immunoblotting. To isolate GST fusion proteins (GST and GST-p38), transiently transfected HeLa cells (138) were rinsed with ice-cold PBS, lysed in interaction buffer and protein extracts were cleared by centrifugation (10 min, 16000 × g, 4 °C). Protein lysates were then incubated with glutathione sepharose beads for 1 h at 4 °C, then washed three times with interaction buffer, washed for 10 min in interaction buffer and resuspended in interaction buffer.

3.4 Results

3.4.1 Leishmania major is capable of infecting primary embryonic fibroblasts in culture.

Fibroblasts have been observed to be an alternative cell type to macrophages as hosts for the parasite *Leishmania* in animal models (29). Additionally, genetically

manipulated fibroblasts generated by our laboratory have proved to be valuable models to investigate molecular mechanisms of signal transduction (11, 84, 138). In order to observe the infection of cultured fibroblasts, primary mouse embryonic fibroblast cells (P-MEFs) were incubated with *L. major*, fixed and stained, and examined for the presence of parasites by confocal microscopy. Under these experimental conditions, actin staining illustrated cellular morphology whereas DAPI allowed the detection of both mammalian and parasitic nuclei as well as the kinetoplast of the parasite. Following 12h00 of incubation in the presence of parasites, most cells became infected. In several cases, we observed that spread cells became rounded and exclusively exhibited F-actin cortically as well as in retracting filipodia at the cell-substratum interface (Fig. 1A basal section and middle section, Fig. 1B). These detaching cells contained numerous parasites as seen by three dimensional reconstitution of the DAPI signal (Fig. 1A). Fig. 1B illustrates another sample treated under similar conditions. Intriguingly, nuclear condensation, which is characteristic of apoptosis, was not observed in the infected cells, even those harbouring a heavy load of parasites. In addition, we failed to detect increased caspase activity in cells exposed to *L. major*, even following a 24h00 incubation (Supp. Fig. 1). This indicates that despite the magnitude of the stress induced by the parasite in its host cell, it does not activate apoptosis. Interestingly, we noticed the presence of parasites that appear to be surrounded by actin-rich structures similar to the previously described actin cup (Fig. 1B, arrowheads) (237). These observations imply communication between *L. major* and cytoskeletal regulators that could influence the infection process in fibroblasts.

Figure 1. *L. major* parasites accumulate in P-MEFs and cause actin cytoskeleton rearrangements. P-MEFs were infected with *L. major* parasite at a ratio of 1:20 (cells:parasite) for 12 h. Cells were then fixed, permeabilized, stained and observed by confocal microscopy as described in materials and methods. (A) Uninfected control cells show normal cytoskeletal organization. Basal section illustrates the cell-substratum interface. Detection of actin reveals the presence of numerous retracting filipodia in a *L. major*-infected cell. Section acquired across the infected cell shows the presence of several parasite nuclei (small blue dots) throughout the intracellular space delimited by the cortical actin cytoskeleton. Three-dimensional reconstitution of the detected DAPI signal illustrates the high number of parasites within the infected cell. (B) *L. major* accumulate and form actin cups inside fibroblasts. Arrowheads point to examples of actin cups. Experiment was performed as described for (A). Scale bar, 10 μm.

A.

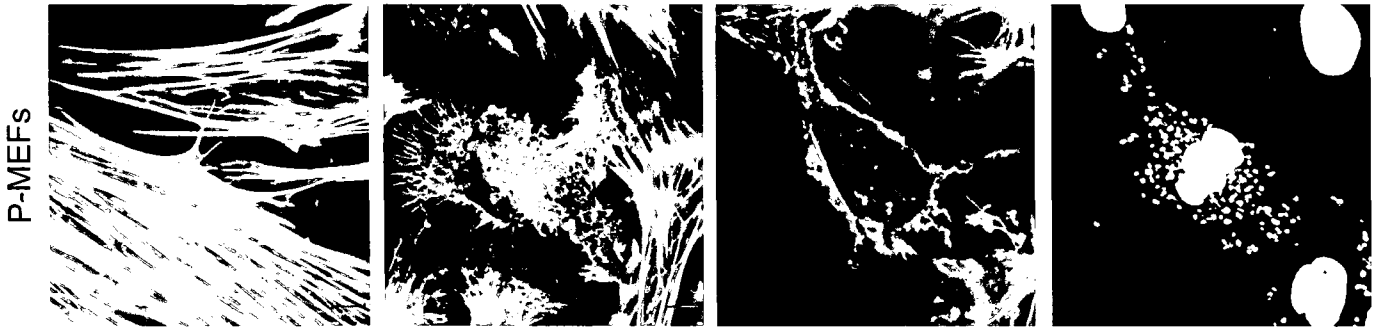
P-MEFs
Uninfected cells
Basal section
Middle section
3D reconstitution
12h00 post infection

B.

FIG. 1

3.4.2 Cellular profile of tyrosine phosphorylation as well as p130Cas/Crk complexes are modulated during L. major infection.

Functional modulation of numerous cytoskeletal proteins depends on their tyrosine phosphorylation. PTP-PEST has been recognized as an important phosphatase for the balanced activities of several of these molecules (172, 287). We used our PTP-PEST rescued fibroblast lines (138) to investigate the possible modulation of phospho-tyrosine proteins in response to parasitic infection. In *PTP-PEST*$^{-/-}$ fibroblasts, re-expression of PTP-PEST correlates with a reduction of the phosphorylation level of some proteins (one near 250 kDa, another near 130 kDa and one just less than 75 kDa) under serum starved control conditions (Fig. 2A). Incubation of both cell lines (B14V$^{PTP\text{-}PEST\text{-}}$, B11WT$^{PTP\text{-}PEST+}$) with *L. major* parasites leads to dramatic changes in the phosphorylation state of numerous proteins. During the course of the infection, the phosphorylation content of proteins of approximately 167, 128, 54 and 29 kDa decreased (Fig. 2A, black arrowheads) whereas those of approximately 153, 89, 63, 49 and 33 kDa were augmented (Fig. 2A, white arrowheads). These results suggest that upon contact with the target cell, *L. major* can induce rapid modification of the tyrosine-phosphorylation profile of cellular proteins, which undoubtedly impacts cellular signal transmission.

Interestingly, the phosphorylation of a prominent band between 100 and 150 kDa significantly decreases during infection. An abundant phosphoprotein of this size, p130Cas, is a substrate of PTP-PEST (Supp. Fig. 2) (84, 118) that plays a role in the invasion of host cells by other microorganisms such as *Salmonella typhimurium* (301). To gain insight into the possible regulation of p130Cas signalling during infection with *L. major*, we investigated its interaction with Crk, an important signalling adapter that binds to tyrosine-phosphorylated p130Cas (96). It was previously observed that expression of PTP-PEST decreased the formation of the p130Cas/Crk complex (120). In our cell system, we observed the assembly of this complex only in the absence of PTP-PEST (Fig. 2B, *PTP-PEST* -/- cells, B14V non-infected). Exposure of these cells (B14V) to *L.*

major resulted in the interaction of Crk with a smaller form of p130Cas as demonstrated by co-immunoprecipitation (Fig. 2B) as well as in vitro binding to purified Crk SH2 domain (Supp. Fig. 3). Also, in both cell lines (B14V and B11WT), we observed that the total amount of full length p130Cas was diminished while a smaller form appeared during the infection with *Leishmania* (Fig. 2B, bottom). The cellular content of Crk remained unchanged. These results suggest that p130Cas/Crk-mediated signalling events are modulated during infection by *L. major*.

Figure 2. *L. major* modulates fibroblast tyrosine phosphorylation profile and alters the interaction of p130Cas with Crk. (A) *PTP-PEST-/-* EV (B14V) and *PTP-PEST*$^{-/-}$-expressing WT (B11WT) cells were serum-starved (SS) (0.05 % heat-inactivated FBS DMEM) for 16h and incubated in the absence or presence of *L. major* for the indicated time. Protein extracts were resolved by SDS-PAGE and analyzed by immunoblotting for protein tyrosine phosphorylation using an anti-phospho-tyrosine antibody (4G10). (B) B14V and B11WT were serum-starved and incubated for 15 min with or without *L. major*. Crk was immunoprecipitated from protein lysates. Immuno-isolated Crk and co-precipitated p130Cas were separated by SDS-PAGE and analysed by immunoblotting. Filled arrowheads correspond to decreasing signals whereas empty arrowheads point to increasing signals corresponding to tyrosine phosphorylated candidates detected under the different conditions. SS, serum-starved. The values on the right correspond to molecular weights in kDa.

A.

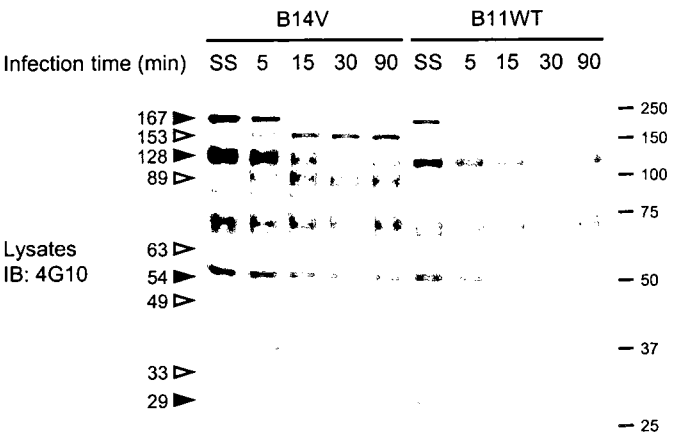
B14V
B11WT
Infection time (min)
SS 5 15 30 90 SS 5 15 30 90
167
153
128
89
63
54
49
33
29
Lysates
IB: 4G10
250
150
100
75
50
37
25

B.

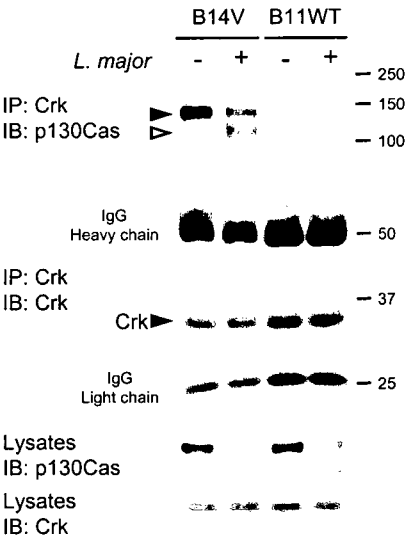
B14V B11WT
L. major - + - +
IP: Crk
IB: p130Cas
250
150
100
IgG
Heavy chain
50
IP: Crk
IB: Crk
Crk
37
IgG
Light chain
25
Lysates
IB: p130Cas
Lysates
IB: Crk

FIG. 2

3.4.3 Cellular exposure to Leishmania leads to proteolysis of p130Cas and PTP-PEST.

The diminished amount of p130Cas and the binding of Crk to a smaller protein recognized by a p130Cas antibody were indicative of potential proteolysis of p130Cas in cells exposed to *L. major*. Therefore, we examined the consequence of incubating our PTP-PEST cell lines with *L. major* on p130Cas stability. Infection with *L. major* leads to cleavage of p130Cas in a time- and parasite concentration-dependent manner (Fig. 3A, B). As infection progresses, p130Cas cleavage products accumulate at ~82, ~70, ~50 and ~29 kDa. To our surprise, we also found that PTP-PEST was cleaved during the infection, which yielded fragments of ~81, ~62 and ~40 kDa. However, *L. major* does not require PTP-PEST expression to promote the proteolysis of p130Cas since it occurs in both *PTP-PEST* null and rescued clones (Fig. 3A, C). Interestingly, in both primary and B11WT fibroblasts, p130Cas and PTP-PEST were degraded when cells were incubated with *L. major*, *L. donovani* and *L. mexicana* but not with *L. tarentolae* nor *L. braziliensis* (Fig 4 and data not shown). The absence of cleavage induced by *L. tarentolae* and *L. braziliensis* is not simply due to delayed kinetics, since extended incubation of fibroblasts with these species did not increase p130Cas or PTP-PEST proteolysis (Supp. Fig. 4). These data identify p130Cas and PTP-PEST as novel signalling targets of specific *Leishmania* species. To our knowledge, these observations comprise the first example of p130Cas and PTP-PEST cleavage occurring during parasitic infection.

Figure 3. *L. major* infection induces proteolysis of p130Cas and PTP-PEST. (A) Fibroblasts positive and negative for PTP-PEST expression were starved for 16h in 0.05 % heat-inactivated FBS DMEM and incubated in starvation medium without or with *L. major* at a ratio of 1:20 (cells:parasites) for the indicated duration. (B) *PTP-PEST*$^{-/-}$-cells expressing WT PTP-PEST (clone B11WT) were exposed to different ratios (cells:parasites) of *L. major* for 10 min. (C) *PTP-PEST*$^{-/-}$-cells rescued with either empty vector (clones B14V, B15V) or with the WT enzyme (clones B11WT, B118WT) were maintained in starvation or regular media (non-starved) 16h prior to treatment. Indicated clones were incubated with or without *L. major* in the absence of serum or with media supplemented with 10 % heat-inactivated-FBS. Cell lysates were prepared and analyzed by immunoblotting for p130Cas and PTP-PEST. Filled arrowheads identify intact proteins, and empty arrowheads point to cleavage products. *L.m*, *L. major*; SS, serum-starved; NS, non-starved or in presence of serum. The values on the right correspond to molecular weights in kDa.

Figure 4. *L. major*, *L. donovani* and *L. mexicana*, but neither *L. tarentolae* nor *L. braziliensis* infections result in degradation of p130Cas and PTP-PEST. P-MEFs were exposed to the indicated species of *Leishmania* for 1h00 at a ratio of 1:20. Protein lysates were harvested and analysed by immunoblotting for p130Cas and PTP-PEST. Filled arrowheads identify intact proteins, and empty arrowheads point to cleavage products. The values on the right correspond to molecular weights in kDa.

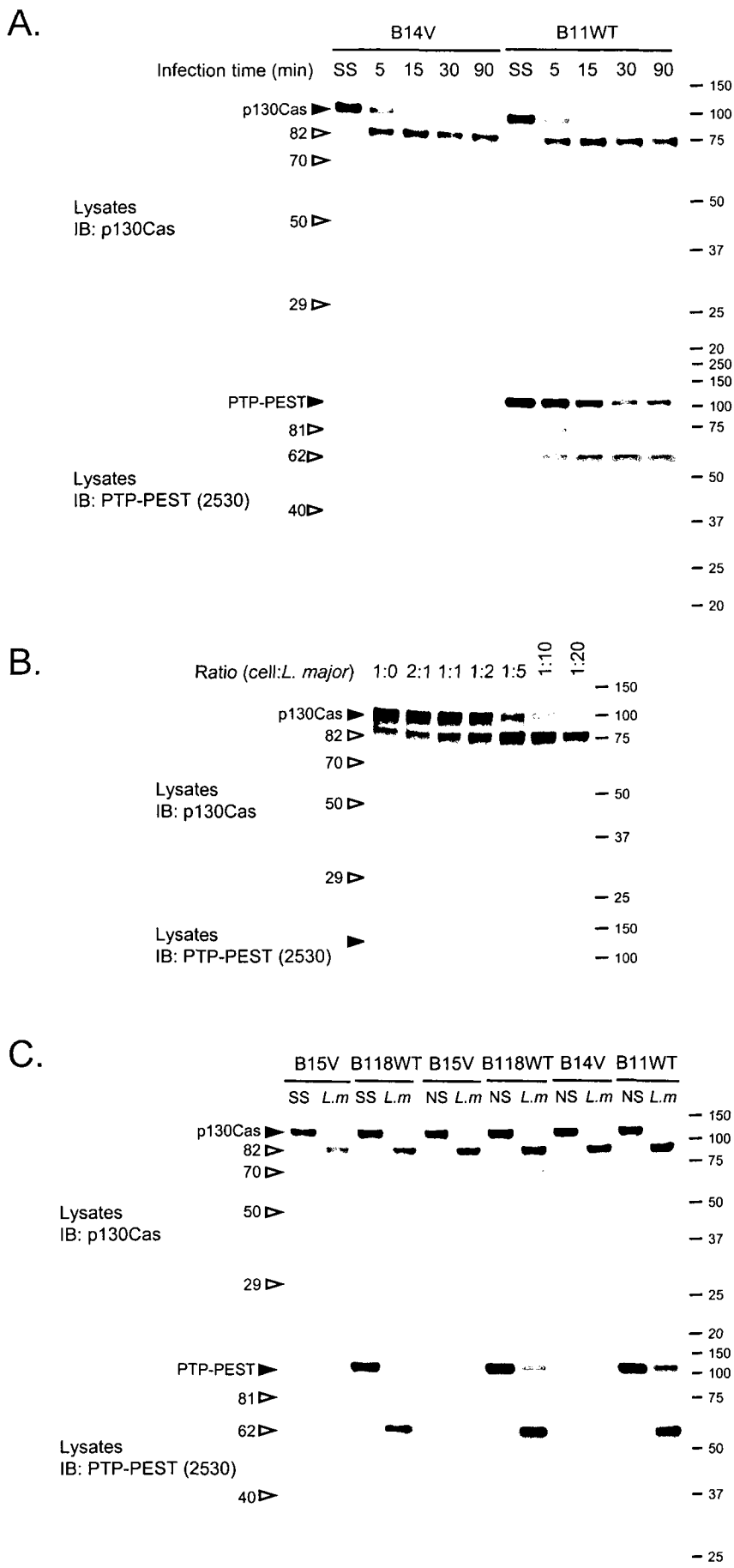
A.
B14V
B11WT
Infection time (min) SS 5 15 30 90 SS 5 15 30 90
p130Cas
82
70
Lysates
IB: p130Cas
50
29
PTP-PEST
81
62
Lysates
IB: PTP-PEST (2530)
40
150
100
75
50
37
25
20
250
B.
Ratio (cell:L. major) 1:0 2:1 1:1 1:2 1:5 1:10 1:20
p130Cas
82
70
Lysates
IB: p130Cas
50
29
Lysates
IB: PTP-PEST (2530)
C.
B15V B118WT B15V B118WT B14V B11WT
SS L.m SS L.m NS L.m NS L.m NS L.m NS L.m
p130Cas
82
70
Lysates
IB: p130Cas
50
29
PTP-PEST
81
62
Lysates
IB: PTP-PEST (2530)
40

FIG. 3

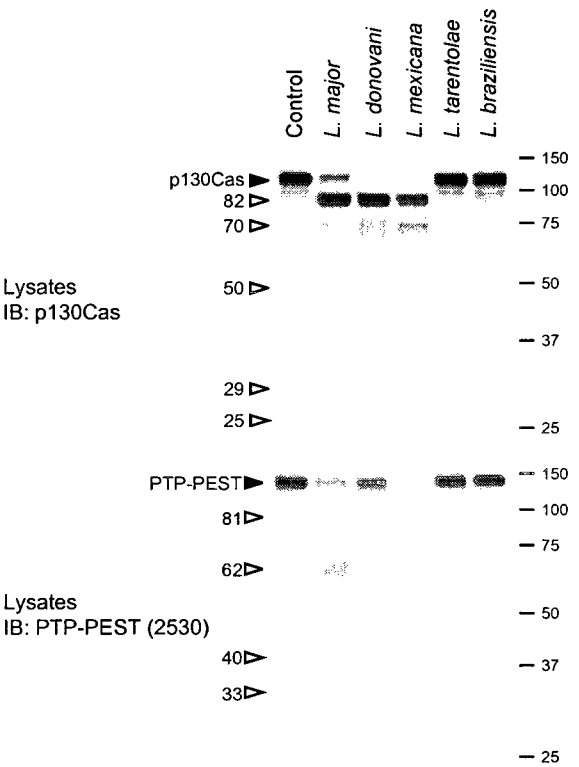
Control
L. major
L. donovani
L. mexicana
L. tarentolae
L. braziliensis
p130Cas
82
70
50
Lysates
IB: p130Cas
29
25
PTP-PEST
81
62
Lysates
IB: PTP-PEST (2530)
40
33
150
100
75
50
37
25
150
100
75
50
37
25

FIG. 4

3.4.4 Leishmania surface metalloprotease GP63 cleaves p130Cas and PTP-PEST.

We next investigated whether factors including host physiologic state as well as endogenous proteases influence p130Cas and PTP-PEST proteolytic processing. The conditions under which cells are maintained contribute to signalling responses and may affect the activity of cellular proteases. To explore the possible impact of the cellular physiologic state on p130Cas and PTP-PEST stability, we compared the consequence of *L. major* infection among various clonal fibroblast lines (B14V, B15V, B11WT and B118WT) as well as between serum-starved (SS) and growing cells (non-starved (NS)). p130Cas and PTP-PEST from either SS or NS cells were both cleaved at a similar rate following incubation with *L. major* (Fig. 3C). In addition, the proteolysis of p130Cas and PTP-PEST occurred similarly in all clones tested. p130Cas was previously identified as a substrate of both the calpain and caspase-3 proteases while PTP-PEST was demonstrated to be cleaved by caspase-3 during apoptosis (138, 189, 302). We found that incubation of cells with protease inhibitors such as caspase inhibitor (Z-VAD-FMK), calpain inhibitor (PD150606) and proteasome inhibitor (lactacystin) failed to block p130Cas and PTP-PEST cleavage induced by *L. major* infection (Fig. 5A). Moreover, the pattern of cleavage products for p130Cas and PTP-PEST present following infection differs from the typical caspase-mediated profile observed during apoptosis (induced by TNF-α, Fig. 5B). Correlating with this observation, the characteristic cleavage of caspase-3, which activates this enzyme during apoptosis, was not induced by *L. major* infection. Instead, upon exposure to *L. major*, cellular caspase-3 undergoes distinct proteolytic processing leading to the emergence of a slightly smaller form detected by immunoblot (Fig. 5B). Also, it appears that some p130Cas fragments were targeted to the proteasome during the infection since an additional product was detected in cells treated with lactacystin (Fig. 5A, grey arrow). These results suggest that *L. major*-induced p130Cas and PTP-PEST cleavage occurs independently of host-cell factors, including three important classes of proteases.

The inability of these protease inhibitors to block *L. major*-induced protein cleavage suggests that an enzyme of parasitic origin performs this proteolysis. The major surface metalloprotease, GP63, is the most abundant protein at the surface of the *Leishmania* parasite (33, 369). To determine whether GP63 plays a role in the degradation of p130Cas and PTP-PEST, we examined the consequence of incubating cells with parasites in which the genes encoding GP63 were ablated (176). In contrast to *L. major*^{WT}, *L. major*$^{gp63-/-}$ parasites do not induce the cleavage of p130Cas and PTP-PEST (Fig. 5C). Importantly, re-introduction of *gp63* into the -/- parasite (*L. major*$^{gp63-/-rescued}$) rescued this phenomenon. Similar observations were also obtained from primary embryonic fibroblasts placed in the presence of these different genotypes of *L. major* (data not shown).

Part of the infection processes of several intracellular parasites, including *Leishmania*, consists of taking control of specific cytoskeletal, tyrosine phosphorylation and apoptotic modulators (27, 49, 206, 212, 237, 241). Interestingly, we found that another cytoskeletal regulator, cortactin, and classical PTP, TC-PTP, as well as the apoptotic executioner caspase-3 were all degraded as a result of *L. major* infection, in a GP63-dependent manner (Fig. 5D). In contrast, Crk, Integrinβ1, STAT5, the MAP kinases (ERK1/ERK2, JNK and p38), Shc, FAK, Paxillin, IκB, AKT and PTP1B remained stable in cells incubated with *L. major* (Fig. 2, Fig. 8, Supp. Fig. 5). This underscores that the action of GP63 is specific to a subset of substrates. Together, these results identify GP63 as a novel regulator of p130Cas, PTP-PEST, cortactin, TC-PTP and caspase-3 integrity.

Figure 5. The parasitic protease GP63 is essential for *L. major*-induced degradation of p130Cas and PTP-PEST. (A) To inhibit various endogenous cellular proteases, B11WT fibroblasts were preincubated with 100 μM ZVAD-FMK, 100 μM PD150606, 10 μM Lactacystin, or 100 μM PD150606 with 10 μM Lactacystin for 2h and subsequently exposed to *L. major* stationary promastigotes at a ratio of 1:20 (cells:parasites) in the presence of the same compounds for an additional 15 min. Lysates were then analyzed by immunoblotting for p130Cas and for PTP-PEST. (B) B11WT cells were either treated with 10 ηg/ml TNFα in presence of 10 μg/ml of cycloheximide or with *L. major* at a ratio of 1:20 (cells:parasites) for the indicated times. Control cells for the TNFα treatment were incubated with media supplemented with 10 μg/ml of cycloheximide only. (C, D) B11WT cells were infected for the indicated times (C) or for 1h30 (D) with *L. major*$^{\text{wild type (WT)}}$, *L. major*$^{gp63\text{-}/\text{-}}$ or *L. major*$^{gp63\text{-}/\text{-}}$-rescue at a cell:parasite ratio of 1:20. Protein extracts were analyzed by immunoblotting for PTP-PEST (using 2530 or 2528 antibodies, as indicated), p130Cas, caspase-3, cortactin, TC-PTP and integrin-β1. C, control. Filled arrowheads identify intact proteins, the grey arrowhead points to a cleavage product specific to the Lactacystin conditions and empty arrowheads point to other cleavage products. The values on the right correspond to molecular weights in kDa.

A.

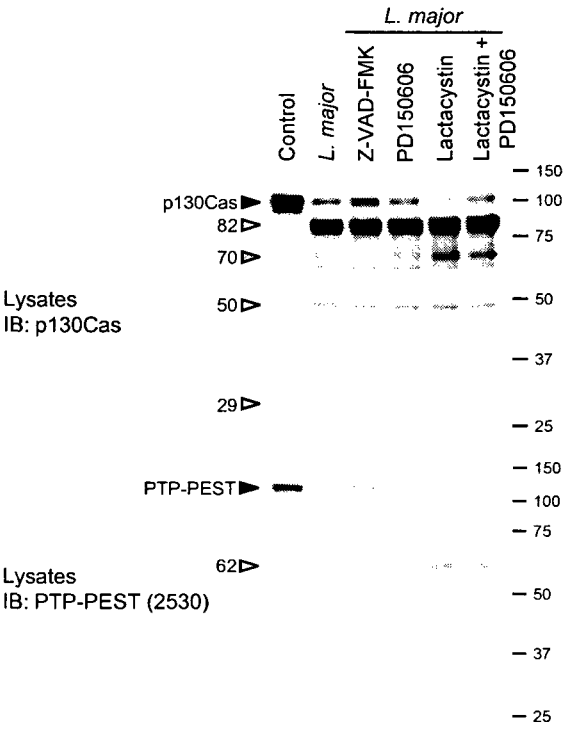
L. major
Control
L. major
Z-VAD-FMK
PD150606
Lactacystin
Lactacystin + PD150606
p130Cas
82
70
50
Lysates
IB: p130Cas
29
PTP-PEST
62
Lysates
IB: PTP-PEST (2530)
150
100
75
50
37
25
150
100
75
50
37
25

B.

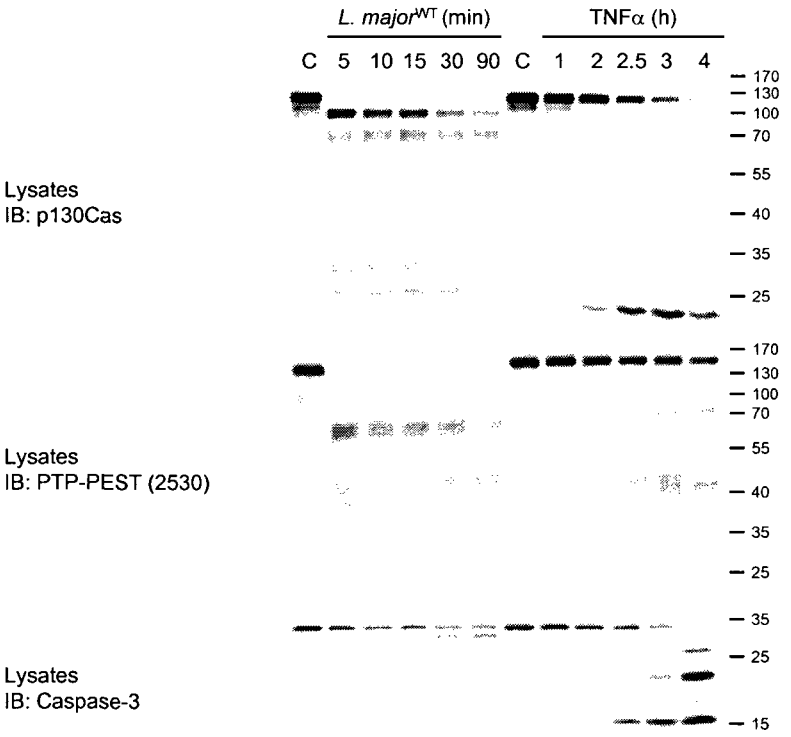
L. major^WT (min)
TNFα (h)
C 5 10 15 30 90 C 1 2 2.5 3 4
Lysates
IB: p130Cas
Lysates
IB: PTP-PEST (2530)
Lysates
IB: Caspase-3
170
130
100
70
55
40
35
25
170
130
100
70
55
40
35
25
35
25
15

FIG. 5 A, B

C.

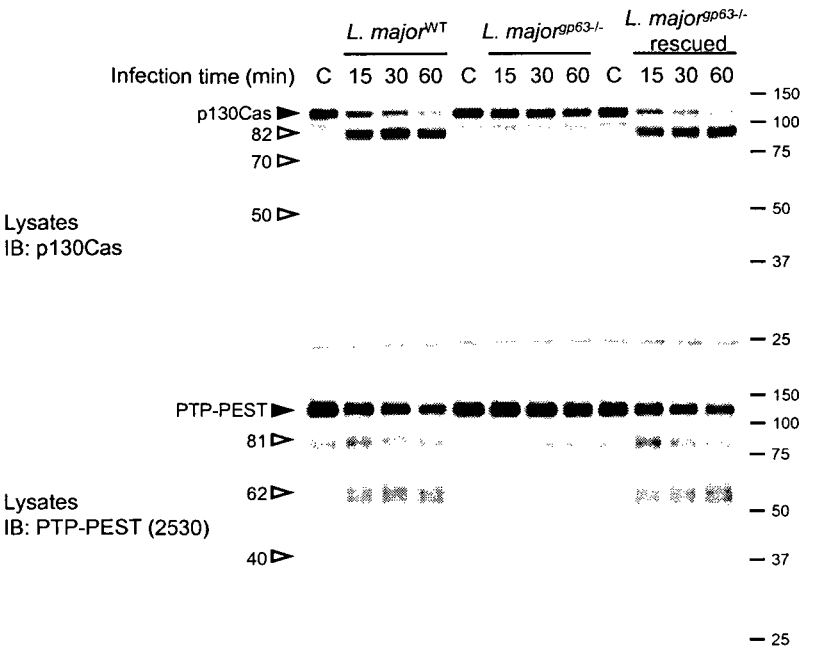
L. major^WT
L. major^gp63-/-
L. major^gp63-/- rescued
Infection time (min) C 15 30 60 C 15 30 60 C 15 30 60
p130Cas
82
70
50
Lysates
IB: p130Cas
PTP-PEST
81
62
40
Lysates
IB: PTP-PEST (2530)
150
100
75
50
37
25

D.

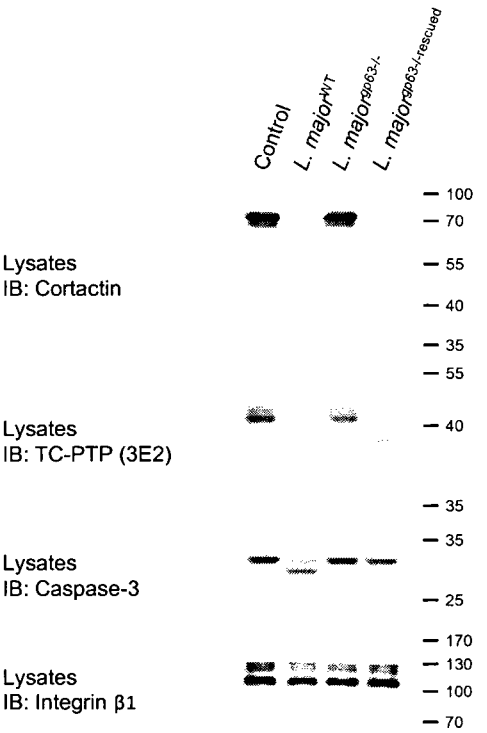
Control
L. major^WT
L. major^gp63-/-
L. major^gp63-/-rescued
Lysates
IB: Cortactin
Lysates
IB: TC-PTP (3E2)
Lysates
IB: Caspase-3
Lysates
IB: Integrin β1
100
70
55
40
35
25
170
130

FIG. 5 C, D

To obtain further insight into the regulation of p130Cas and PTP-PEST protein stability by GP63, we incubated fibroblast lysates or purified GST-PTP-PEST with protein extracts prepared from different *L. major* genotypes. As shown in Fig. 6A, the addition of extracts from WT *L. major* parasites to a total cell lysate induced the degradation of p130Cas and PTP-PEST following 5 and 20 min of incubation. The profile of bands observed in this *in vitro* assay was quite similar to that obtained when fibroblast cells were exposed to live parasites (Fig. 3). In contrast, no significant cleavage was detected, neither after 5 or 20 min of incubation, when proteins extracted from *gp63 -/- L. major* were added to the total cell lysate. These observations imply that the integrity of both parasitic and host cells is not essential for the cleavage reaction to occur. Importantly, purified PTP-PEST incubated with *L. major* lysates was also degraded when GP63 was present (Fig. 6B), confirming that cellular proteins are dispensable for the cleavage of PTP-PEST triggered by the parasite. Finally, recombinant GP63 efficiently cleaved purified GST-PTP-PEST (Supp. Fig. 6). These experiments point to GP63 as a prerequisite for p130Cas and PTP-PEST degradation and strongly suggest that these cellular signalling proteins are genuine substrates of GP63.

Figure 6. *L. major* lysates depend on parasite expression of GP63 to induce the proteolysis of p130Cas and PTP-PEST in vitro. (A) Extracts from B11WT cells were incubated with lysates from stationary phase wild type (WT) or *gp63-/-* (KO) *L. major* promastigotes or with lysis buffer (control, C) for the indicated times. (B) GST-PTP-PEST was isolated from transfected *PTP-PEST*$^{-/-}$ cells, incubated under control conditions, or with either 5 µg or 20 µg of parasite-lysates prepared from the identified *L. major* genotypes for 15 min. Samples were analysed by immunoblotting for p130Cas (A) and PTP-PEST (2530 antibody) (A, B). Filled arrowheads point to intact proteins, and empty arrowheads identify cleavage products. The values on the right correspond to molecular weights in kDa.

A.

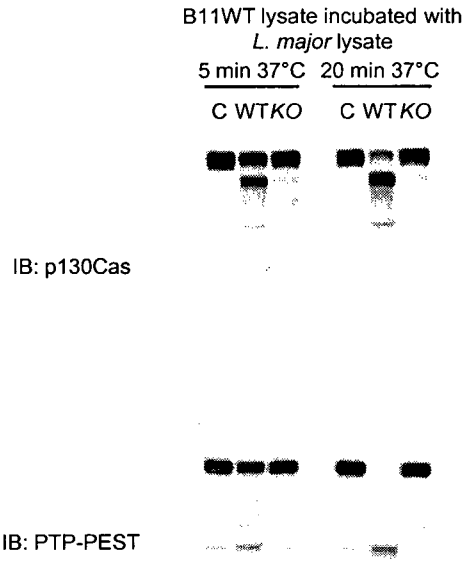
B11WT lysate incubated with
L. major lysate
5 min 37°C
20 min 37°C
C WT KO
C WT KO
IB: p130Cas
IB: PTP-PEST

B.

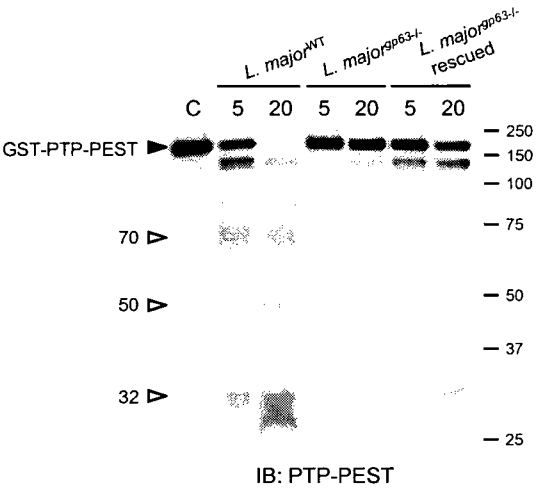
L. major^WT
L. major^gp63-/-
L. major^gp63-/- rescued
C
5
20
5
20
5
20
GST-PTP-PEST
70
50
32
250
150
100
75
50
37
25
IB: PTP-PEST

FIG. 6

The cleavage of p130Cas and PTP-PEST occurs rapidly following the cellular exposure to the parasite. This suggests the existence of a mechanism facilitating entry of GP63 into target cells, before internalization of the protozoan commences. To test this hypothesis, we examined the impact of challenging P-MEFs with either live parasite, supernatant from promastigote cultures or parasite lysates. As expected, incubation of P-MEFs with live parasites leads to the cleavage of both p130Cas and PTP-PEST. Interestingly, detectable levels of p130Cas cleavage products were present following exposure of the cells to media in which *L. major* was growing (Fig. 7, SDM supernatant). Importantly, incubation of cells with *Leishmania*-lysates that do not contain intact parasites induced pronounced cellular p130Cas and PTP-PEST cleavage. Under all these conditions, the occurrence of cellular protein degradation was strictly dependent on the capacity of the protozoan to synthesize GP63. These findings imply a process that promotes the transfer of GP63 from the parasite to its target cells.

Figure 7. Exposure of P-MEFs to *L. major*-conditioned medium and to parasite lysates induces protein fragmentation in a GP63-dependent manner. P-MEFs were exposed to live parasites, centrifuged culture supernatant or lysates of *L. major* for 1h. Control cells for the live parasite and parasite lysate groups were incubated with serum-free DMEM during the course of the experiment, while the supernatant control was incubated in fresh SDM. Fibroblast protein integrity was analyzed by immunoblotting using antibodies specific for p130Cas and PTP-PEST (2530). Filled arrowheads point to intact proteins whereas empty arrowheads identify cleavage products. The values on the right correspond to molecular weights in kDa.

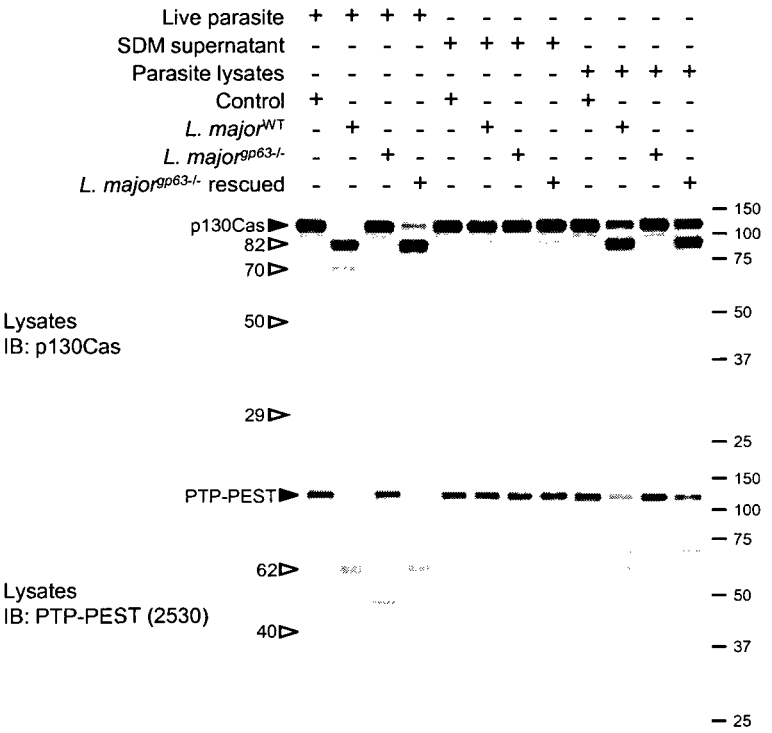
Live parasite + + + + - - - - - - - -
SDM supernatant - - - - + + + + - - - -
Parasite lysates - - - - - - - - + + + +
Control + - - - + - - - + - - -
L. major^WT - + - - - + - - - + - -
L. major^gp63-/- - - + - - - + - - - + -
L. major^gp63-/- rescued - - - + - - - + - - - +
p130Cas
82
70
50
Lysates
IB: p130Cas
29
PTP-PEST
62
Lysates
IB: PTP-PEST (2530)
40
150
100
75
50
37
25
150
100
75
50
37
25

FIG. 7

3.4.5 L. major infection modulates MAP kinases and causes GP63-dependent inactivation of p38.

The phosphorylation of p130Cas favors JNK (198) and p44/42 MAPK activation (312) whereas the expression of PTP-PEST in B cells interferes with Ras-mediated p44/42 phosphorylation (95), and promotes the activation of p38 in fibroblasts stimulated with anisomycin (Supp. Fig 7). To evaluate the impact of GP63 on the activity of host MAPKs, we measured the phosphorylation levels of three members of the MAPKs (p44/42, JNK and p38) in P-MEFs exposed to different strains of *L. major*. Immunoblotting using a phospho-specific antibody shows an increase in p44/42 MAPK phosphorylation in cells incubated with *L. major* for 5 min, which is followed by a gradual decrease as the infection progressed (Fig. 8A). This transient ERK activation occurred similarly in cells infected with parasites both positive and negative for GP63 (WT, *gp63*$^{-/-}$ or *gp63*$^{-/-\ rescued}$). Likewise, JNK was up- and down-regulated independently of *gp63* genotype. In contrast, a dramatic dephosphorylation of p38 occurred following *L. major* infection (Fig. 8B). Interestingly, parasites lacking GP63 induced only a partial dephosphorylation of p38 (Fig. 8B). Noteworthy, re-introduction of *gp63* in the *L. major*$^{gp63\ -/-}$ strain (rescued) was sufficient to restore its capacity to inactivate p38 (Fig. 8B). Since our results, presented on Fig. 4, revealed that the ability to provoke p130Cas and PTP-PEST cleavage is species-specific, we sought to verify the possible correlation between the proteolytic capacity of certain species and the modulation of p38 phosphorylation. Treatment of P-MEFs with *L. major*, *L. donovani* and *L. mexicana* but not with *L. tarentolae* nor *L. braziliensis* caused the disappearance of the phosphorylated form of p38 (Fig. 8C). This inactivation of p38 correlated with the ability of the parasite to induce protein cleavage as detected by p130Cas degradation. The reduced level of phosphorylated p38 was not due to its degradation because the total amount of p38 remained constant throughout all tested infections (Fig. 8B, C). Altogether, these results reveal a novel mechanism of p38 regulation dependent on protein cleavage in which GP63 appears to play a key role.

Figure 8. *Leishmania* infection modulates MAPKs and depends on GP63 activity to downregulate p38. P-MEFs were left uninfected or incubated with *L. major*^{WT} (A, B, C), with strains in which the *GP63* gene was excised or re-introduced (*L. major*$^{gp63-/-}$ or *L. major*$^{gp63-/-}$rescued) (A, B), or with *L. donovani*, *L. mexicana*, *L. tarentolae* or *L. braziliensis* (C) for the indicated times. The activity of p44/42 (A), JNK (A) and p38 (B, C) MAPKs was measured by immunoblotting using phospho-specific antibodies for each protein. Total input of p44/42 (A), JNK (A) and p38 (B, C) as well as stability of p130Cas (C) was also measured. (B, right panel) Phosphorylated-p38 levels were quantified and normalized to the total amount of p38 by densitometry. Values correspond to the mean ± standard error of three independent experiments.

A.

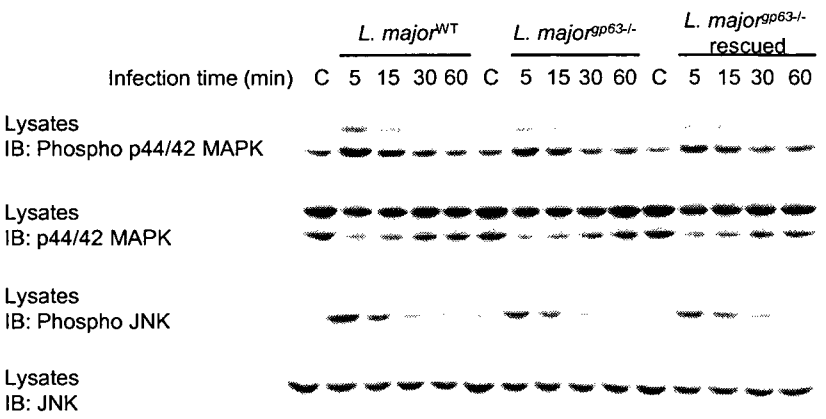
L. major^WT
L. major^gp63-/-
L. major^gp63-/- rescued
Infection time (min) C 5 15 30 60 C 5 15 30 60 C 5 15 30 60
Lysates
IB: Phospho p44/42 MAPK
Lysates
IB: p44/42 MAPK
Lysates
IB: Phospho JNK
Lysates
IB: JNK

B.

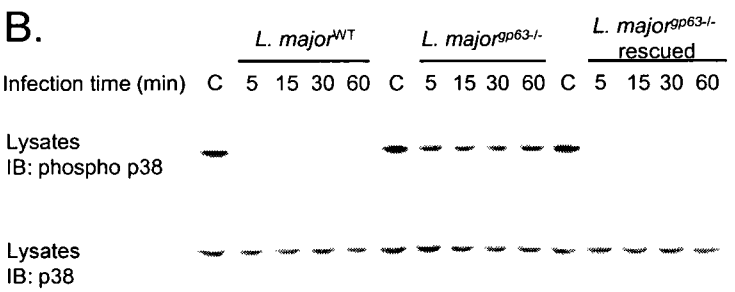
L. major^WT
L. major^gp63-/-
L. major^gp63-/- rescued
Infection time (min) C 5 15 30 60 C 5 15 30 60 C 5 15 30 60
Lysates
IB: phospho p38
Lysates
IB: p38

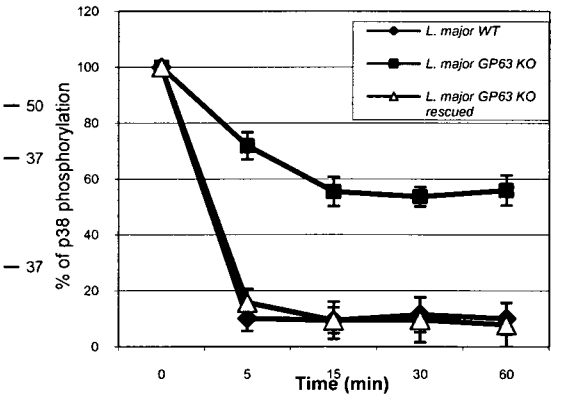
L. major WT
L. major GP63 KO
L. major GP63 KO rescued
% of p38 phosphorylation
Time (min)
120
100
80
60
40
20
0
50
37
37
0
5
15
30
60

C.

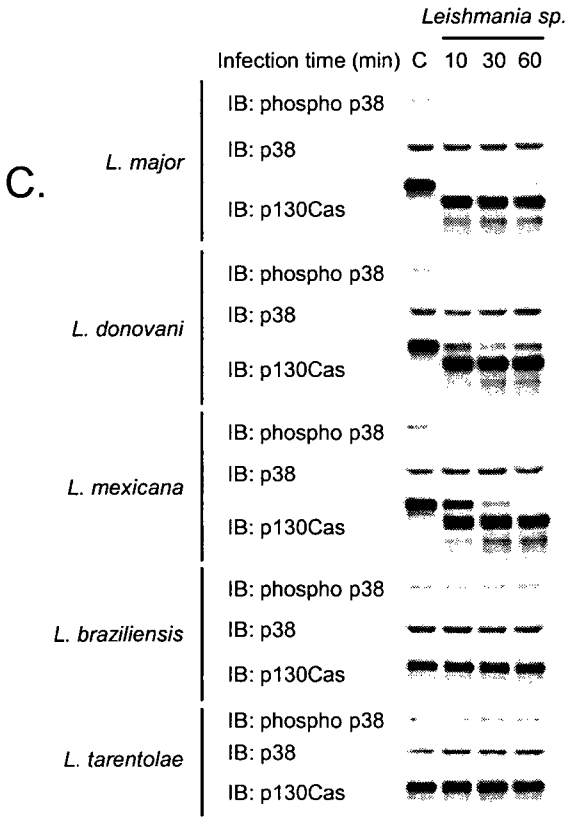
Leishmania sp.
Infection time (min) C 10 30 60
L. major
IB: phospho p38
IB: p38
IB: p130Cas
L. donovani
IB: phospho p38
IB: p38
IB: p130Cas
L. mexicana
IB: phospho p38
IB: p38
IB: p130Cas
L. braziliensis
IB: phospho p38
IB: p38
IB: p130Cas
L. tarentolae
IB: phospho p38
IB: p38
IB: p130Cas

FIG. 8

3.4.6 GP63 cleaves the p38 regulator TAB1 during L. major infection, generating products unable to bind p38.

The modulation of MAPKs observed during the infection with *L.* major prompted us to analyze molecules that lie upstream of p38. Even though PTP-PEST expression regulates p38 in certain contexts, we did not observe differences in p38 modulation between *PTP-PEST*$^{-/-}$ and re-expressing fibroblasts treated with *L. major* (data not shown). As direct regulators of p38, the MAPK kinase (MKK) MKK3 and MKK6 can phosphorylate its activation loop whereas binding of the scaffolding protein TAB1 induces its autophosphorylation (121, 380). *L. major* infection induced a marked disappearance of cellular TAB1 while MKK3 and MKK6 levels remained constant (Fig. 9A). The diminished TAB1 levels correlated with the presence of GP63 on *L. major* and paralleled p130Cas degradation. Moreover, recombinant his-TAB1 is degraded by purified GP63 (Fig. 9B). These data identify TAB1 as a novel substrate of GP63.

To examine further the mode of TAB1 proteolysis, we exposed cells expressing different forms of TAB1 (WT or 1-418), flanked by Flag (N-terminus) and myc (C-terminus) epitopes, to *L. major*. Truncation of the C-terminal portion of TAB1 was previously found to generate a form of the protein (TAB1 1-418) that displays increased affinity for p38 and contains the residues essential for their interaction (121). Both versions of TAB1 were degraded in infected cells and produced the same N-terminal fragment (46 kDa) detected by antibodies against Flag (Fig. 9C). The C-terminal cleavage products detected via the myc tag were substantially less abundant and therefore appear only upon longer exposure (Fig. 9C, IB: myc). In addition, profile of these C-terminal fragments differed according to the version of TAB1 expressed (WT or 1-418) (Fig. 9C, IB: myc, bottom). In all cases, the efficient generation of cleavage products depended on the parasitic expression of GP63 (Fig. 9D). Thus, GP63-mediated TAB1 proteolysis generates a stable N-terminal fragment and other smaller C-terminal products, suggesting that GP63 cleaves TAB1 at multiple sites. Importantly, *L. major*

infection impaired p38 binding to TAB1 (both WT and 1-418) (Fig. 9E). Specifically, none of the TAB1 cleavage products (Flag or myc tagged) generated during *L. major* infection were able to interact with GST-p38. Together, these results show that GP63 processes TAB1, which alters the formation of TAB1-p38 complexes and could thereby modulate p38-signaling.

Figure 9. *L. major* regulates p38/TAB1 binding via GP63-mediated proteolysis of TAB1. (A) P-MEFs were incubated with *L. major*^{WT}, *L. major*$^{gp63-/-}$ or *L. major*$^{gp63-/-}$rescued for the indicated duration. Protein lysates were collected and the stability of the p38 regulators TAB1, MKK3 and MKK6 was verified by immunoblotting. (B) His-TAB1 purified from expressing bacteria was incubated under control conditions (C) or with 0.2 µg or 1 µg of reGP63 for 30 min. The stability of TAB1 was then analyzed by immunoblotting using anti-TAB1 antibodies. (C) *PTP-PEST*$^{-/-}$ cells transfected with an empty vector or with vectors encoding either Flag-TAB1 (WT)-myc-myc or Flag-TAB1 (1-418)-myc-myc were incubated under control conditions (C) or with *L. major*^{WT} at a ratio of 1:20 (cells:parasites) for the indicated time. Protein lysates were harvested and analyzed by immunoblotting using the indicated antibodies. (D) *PTP-PEST*$^{-/-}$ cells transfected with an empty control vector or with vectors encoding Flag-TAB1 (WT)-myc-myc or Flag-TAB1 (1-418)-myc-myc were incubated under control conditions (C) or with *L. major*^{WT}, or *L. major*$^{gp63-/-}$ (KO), or *L. major*$^{gp63-/-}$-rescue(RSC) at a ratio of 1:20 (cells:parasites) for 15 min. Protein lysates were harvested and analyzed by immunoblotting using the indicated antibodies. (E) *PTP-PEST*$^{-/-}$ cells expressing either Flag-TAB1 (WT)-myc-myc or Flag-TAB1 (1-418)-myc-myc were incubated under control conditions (C) or with *L. major*^{WT} at a ratio of 1:20 (cells:parasites) for the indicated time. Lysates extracted from infected and non-infected cells were incubated with either GST or GST-p38 immobilized on glutathione sepharose beads, and the ability of the GST fusion proteins to interact with various forms of TAB1 was investigated by immunoblotting for the Flag and myc epitopes. The quantity of GST fusion proteins used in each assay was assessed by immunoblot against GST. The presence of TAB1 proteins in each extracts was also verified by immunoblotting with the indicated antibody (E, right panel). The values on the right correspond to molecular weights in kDa.

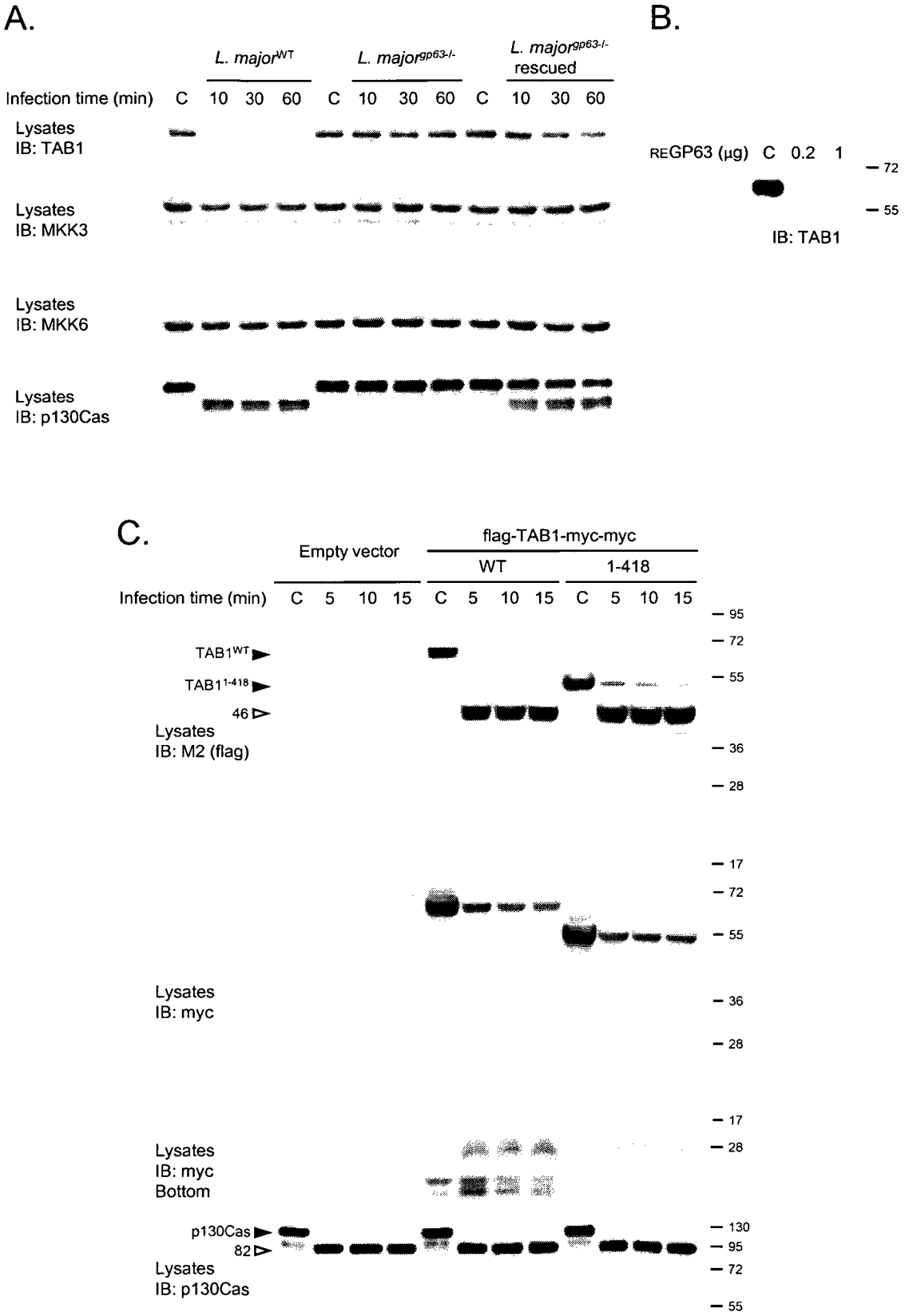
A.
L. major^WT
L. major^gp63-/-
L. major^gp63-/- rescued
Infection time (min)
C 10 30 60 C 10 30 60 C 10 30 60
Lysates IB: TAB1
Lysates IB: MKK3
Lysates IB: MKK6
Lysates IB: p130Cas
B.
REGP63 (μg) C 0.2 1
72
55
IB: TAB1
C.
Empty vector
flag-TAB1-myc-myc
WT
1-418
Infection time (min)
C 5 10 15 C 5 10 15 C 5 10 15
95
72
55
36
28
17
TAB1^WT
TAB1^1-418
46
Lysates IB: M2 (flag)
Lysates IB: myc
Lysates IB: myc Bottom
p130Cas
82
Lysates IB: p130Cas
130

FIG. 9 A, B, C

D.

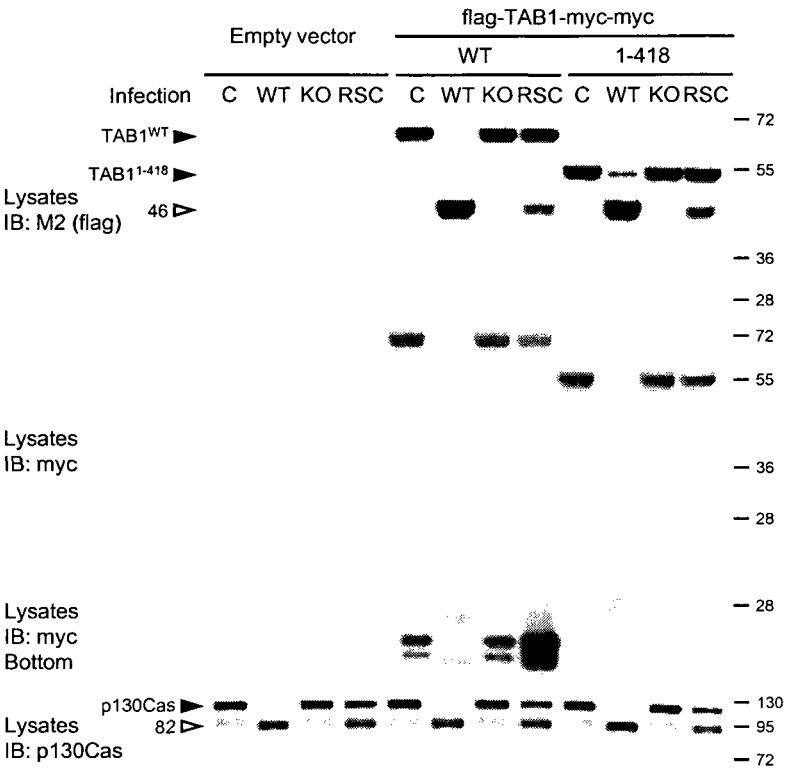
Empty vector
flag-TAB1-myc-myc
WT
1-418
Infection
C WT KO RSC C WT KO RSC C WT KO RSC
TAB1WT
TAB1 1-418
Lysates
IB: M2 (flag)
46
72
55
36
28
72
55
Lysates
IB: myc
36
28
Lysates
IB: myc
Bottom
28
p130Cas
82
Lysates
IB: p130Cas
130
95
72

E.

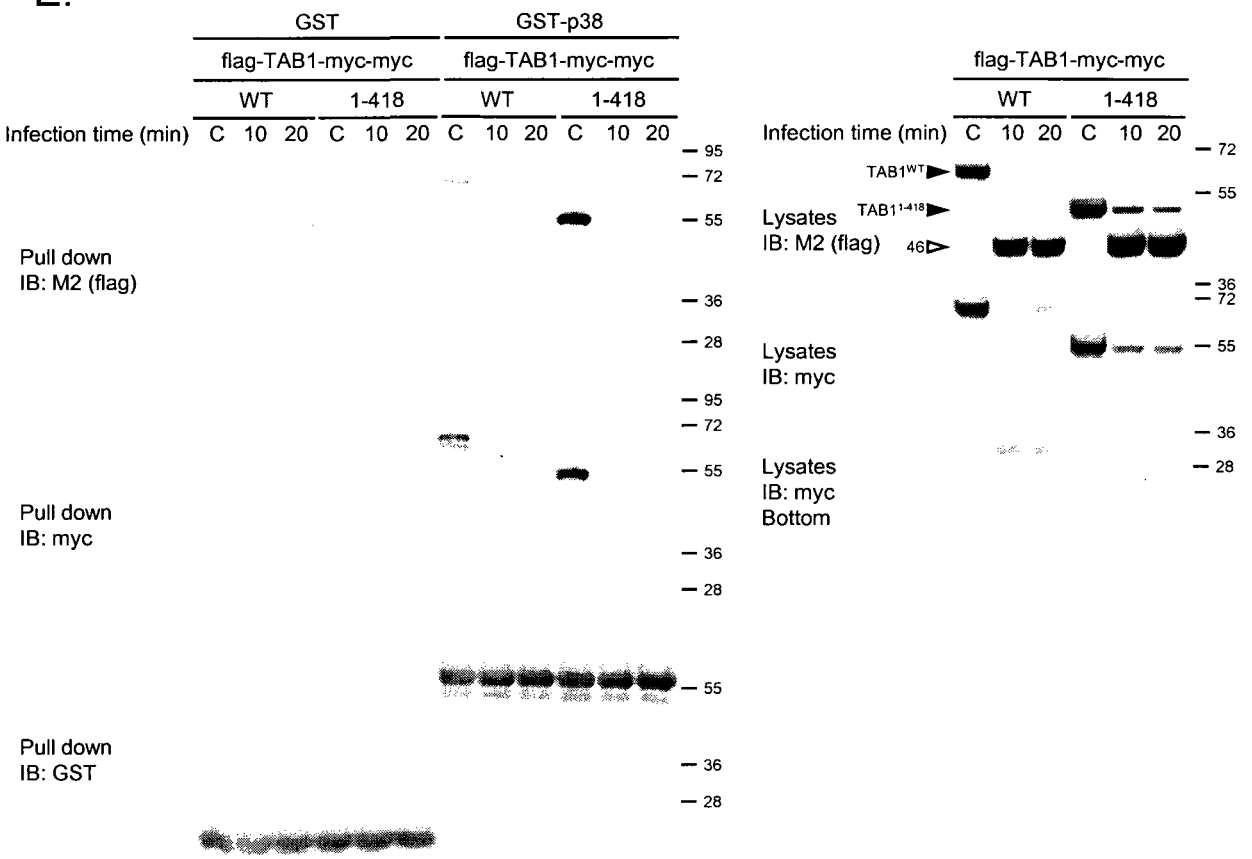
GST
GST-p38
flag-TAB1-myc-myc
flag-TAB1-myc-myc
WT
1-418
WT
1-418
Infection time (min)
C 10 20 C 10 20 C 10 20 C 10 20
95
72
55
Pull down
IB: M2 (flag)
36
28
95
72
55
Pull down
IB: myc
36
28
55
Pull down
IB: GST
36
28
flag-TAB1-myc-myc
WT
1-418
Infection time (min)
C 10 20 C 10 20
72
TAB1WT
55
Lysates
IB: M2 (flag)
TAB1 1-418
46
36
72
Lysates
IB: myc
55
36
Lysates
IB: myc
Bottom
28

FIG. 9 D, E

3.5 Discussion

Upon inoculation into a mammalian organism, *Leishmania* parasites must adapt to this foreign environment and take advantage of their immediate surrounding components and cells. During this process, molecules covering the parasite undoubtedly play a critical role as they are directly in contact with their extra-cellular milieu. Herein, we demonstrate that the modulation of multiple mammalian signalling molecules occurs early during infection by *Leishmania*. Importantly, GP63 appears to be a critical player in disrupting the state of several signalling proteins.

Even though macrophages are believed to be the primary target of *Leishmania*, this parasite is capable of colonizing other cell types (22, 29, 247, 345, 358). Fibroblasts are abundant in the immediate environment where promastigotes are inoculated, can harbour parasites in animal models and were proposed to play an important role for long term infection (29). Our data confirm that *L. major* is capable of infecting cultured fibroblasts isolated from mouse embryos. The accumulation of parasites within them gave rise to heavily infected spheroids similar to those typically observed in spleen biopsies from infected individuals (270). Interestingly, no nuclear condensation or caspase activation characteristic of apoptotic cells was detected in highly infected fibroblasts despite the intense stress undoubtedly induced by the presence of parasites. Correspondingly, *Leishmania* mediates a delay in programmed cell death induction in neutrophils and macrophages (3, 236). This implies that the parasite induces modifications in the cellular signalling machinery early during the infectious process to avoid activation of the apoptotic program. Besides the involvement of the mannose receptors in the attachment of *Leishmania* to fibroblasts and the implication of Cdc42 in parasitic internalization (149, 237), little else is known about the molecular events occurring within fibroblasts during *Leishmania* infection. Here, we have shown that the

interaction between *Leishmania* and fibroblasts induces several additional modifications of host signalling proteins.

Leishmania provoked important changes in the tyrosine-phosphorylation level of several proteins (Fig. 2). The effect of inhibition of protein tyrosine kinases (PTKs) illustrates their requirement for the internalization of *L. donovani* by macrophages (122). On the other hand, the modulation of tyrosine-phosphorylation content in macrophages infected with *L. donovani* was associated with general activation of PTPs, including SHP-1 (27). Our results identify another PTP, PTP-PEST that is proteolysed in cells that encounter *Leishmania*. This post-translational modification of PTP-PEST could modulate its enzymatic properties, as the cleavage of PTP-PEST was shown to augment its catalytic activity (138). Additionally, *Leishmania* induced GP63-dependent cleavage of TC-PTP likely near its C-terminal nuclear localization signal (NLS) (Supp. Fig. 8). Removal of the NLS could allow the phosphatase to access additional substrates and also enhance its catalytic activity (80, 140, 382). The altered tyrosine phosphorylation profile found in cells infected with *Leishmania* may also be due to the cleavage of highly phosphorylated proteins such as p130Cas. The phosphorylation of p130Cas fragments was likely maintained since they remained capable of binding Crk. Thus, the combined regulation of PTKs, PTPs and protein stability is likely responsible for the dramatic changes in phospho-protein levels in *Leishmania*-infected cells.

Proteolysis of cellular proteins including p130Cas and PTP-PEST during the *Leishmania* infective process could be a manoeuvre used by the parasite to take control of the cellular machinery. PTP-PEST and p130Cas cleavage occurred independently of growth conditions or the presence of various cellular-protease inhibitors, which implies that the host-cell proteolytic apparatus is not activated during *L. major* infection. In contrast, in vivo and in vitro analysis, taking advantage of *L. major* strains positive or negative for *gp63* gene expression, supports the identification of p130Cas and PTP-PEST as novel, genuine substrates of the parasite protease GP63. Additionally, the in vitro

cleavage of PTP-PEST by reGP63 indicates that it is directly responsible for this proteolytic event. Interestingly, cells exposed to *L. major*, *L. mexicana* or *L. donovani* all exhibited p130Cas and PTP-PEST proteolysis whereas those incubated with *L. braziliensis* or *L. tarentolae* did not. Genetic analysis based on *gp63* gene organization and sequences has grouped members of the *Viannia* subgenus (which includes *L. braziliensis*) in a separate cluster from other *Leishmania* species (346). Divergence in the composition of *L. braziliensis gp63* genes could limit their access to intracellular substrates or modify their specificity, thereby explaining the limited cleavage observed in our experiments. On the other hand, the lizard parasite *L. tarentolae* possesses a variant GP63 lacking enzymatic activity (48). Experiments using genetically modified strains of *L. major* led to the identification of additional substrates of GP63: cortactin, TC-PTP, caspase-3 and TAB1. Even though GP63 is targeting several substrates, we believe that this enzyme does not cause general protein degradation since the majority of signalling proteins tested were resistant to its presence. The specific contributions of each of these individual cleavage events to *Leishmania* pathology remain unresolved. Nonetheless, the GP63 substrates we have identified are implicated in multiple physiologic functions including cytoskeletal rearrangement, cell proliferation and apoptosis, pointing to several potential avenues by which the parasite may take advantage of its host.

The secretion and transfer of virulence factors into host cells is of paramount importance for the pathogenic processes of several microorganisms (75). Here, we have provided evidence for the rapid cleavage of p130Cas and PTP-PEST upon initial contact between *L. major* and fibroblast cells, presumably before internalization of the parasite. The previously reported cleavage of the intracellular protein MRP (82), as well as the activity of GP63 found on amastigotes (194) are also indicative of an important role for GP63 inside mammalian cells. The capability of the parasite to induce protein degradation before it enters into its host cells implies a mechanism allowing the transfer of GP63 to the intracellular space of its host. Clinical isolates causing cutaneous (*L. tropica*) or visceral (*L. infantum*) leishmaniasis as well as *L. amazonensis*, *L. major*, *L.*

mexicana and *L. donovani* were observed to release proteolytically active GP63 in culture supernatants (103, 171, 228). Recent investigations performed with *L. chagasi*, indicated that incubation of stationary-phase promastigotes under parameters reproducing the extra-cellular-mammalian host environment (37 °C and Matrigel) stimulated the secretion of internal GP63 (368). Furthermore, in amastigotes, the majority of GP63 is localized in the flagellar pocket of the parasite, which is the principal site of exocytosis (156), indicating a role for the liberation of GP63 inside the host cell. During the course of our experiments, we noticed that throughout the initial contact between the protozoan and the fibroblasts, a large proportion of the microorganisms presented their flagellum (and flagellar pocket) toward the mammalian cells (M. Hallé, M. Olivier and M. L. Tremblay, unpublished observations). This behaviour could allow parasites to concentrate their secretion products, including GP63, in the direction of their targeted cell. Remarkably, incubation of fibroblasts with *L. major* culture supernatant and even parasite lysates led to the appearance of degradation products, which correlated with GP63 protein expression. These observations reveal that *L. major* secretes or contains all the components necessary for GP63 entry, and that this phenomenon does not require parasitic integrity. Interestingly, a recent study on *L. donovani* reported the presence of microvesicles budding from the flagellar pocket and identified a set of 151 distinct proteins secreted by the parasite (304). We postulate that during the *Leishmania*-mammalian cell initial interaction, release of GP63 in close vicinity to the host cell surface, possibly with other secreted transport effectors, facilitates its entry into the cytosolic space, allowing it to reach additional substrates.

Reorganisation of the actin cytoskeleton plays a central role in the internalization of many intracellular parasites. Interestingly, heat killing of *L. amazonensis* amastigotes, a process that also abrogates GP63 activity (58), prevent their internalization in CHO cells, supporting a unique property of live amastigotes to accomplish entry into cells (237). The small Rho-GTPase Cdc42 is also necessary for *Leishmania* entry into CHO cells (237). Cdc42 was previously shown to signal towards WASP and N-WASP in order to

stimulate actin nucleation (150). During intracellular trafficking of *Leishmania*, WASP, vinculin, Arp2/3 and other cytoskeletal regulators gather with actin filaments around engulfed parasites to form an actin cup structure thought to protect the foreign parasite from phagolysosomal digestion (206, 212, 237). Cortactin, another actin regulator that interacts with Arp2/3 and N-WASP, is similarly recruited to actin-rich structures exploited by other intracellular microbes (297). The assembly of the PTP-PEST-PSTPIP-WASP complexes was previously shown to allow PTP-PEST to dephosphorylate WASP (85) and to inhibit WASP-induced actin polymerization (18). It was recently demonstrated that caspase-3-mediated cleavage of PTP-PEST dissociates its phosphatase domain from PSTPIP and was expected to prevent it from dephosphorylating and inhibiting WASP (138, 139). Importantly, we show that GP63 mediates the degradation of PTP-PEST during *Leishmania* infection, which could function to affect parasite-induced actin cytoskeleton remodelling. Moreover, we observed that p130Cas and cortactin were cleaved in cells exposed to parasites expressing GP63. MRP, another identified substrate of GP63, is associated with actin filaments in macrophages cells (82). GP63 was also shown to interact with fibronectin receptor (integrin) and to stimulate the internalization of *Leishmania* parasites (36). Thus, we propose that GP63 will act from both outside and inside the cell to alter the activity of host cell signalling molecules. This modulation may assist parasite engulfment through the formation of actin fibres and membrane protrusions. Future investigations will attempt to decipher the precise role of GP63 in modulating the dynamic remodelling of the cytoskeleton.

Some inconsistencies are present in the literature regarding the response of the p38 MAPK to *Leishmania* infection. Several reports suggest that the parasite either actively inhibits or avoids activating p38 (17, 224, 258), while others indicate that p38 is induced during infection (19, 179, 210, 278). Despite the discrepancy, most reports affirm that activation of p38 is detrimental to parasite survival. Here, we report that activating phosphorylation of p38 is diminished following exposure of fibroblasts to *L. major* and correlates with the capability of GP63 to cleave intracellular substrates.

Moreover, the ability to down-regulate p38 was specific to certain *Leishmania* species: *L. major*, *L. mexicana* and *L. donovani* caused complete inactivation of p38, a task which *L. tarentolae* and *L. brasiliensis* failed to perform. These results underscore that *Leishmania* requires functional GP63 to achieve inactivation of p38. Importantly, this GP63-dependent cellular response was unique to p38. In contrast, the p44/42 and JNK MAPKs reacted similarly in response to infection, regardless of *gp63* genotype. *Leishmania* did not entirely monopolise the host signalling machinery since infected cells maintained the ability to activate MAPKs (p44/42) and STAT-5 following growth hormone stimulation as well as MAPKs (p44/42) and AKT downstream of lysophosphatidic acid (LPA) stimulation (data not shown). Interestingly, another pathogenic microorganism, *Bacillus anthracis*, also secretes a metalloproteinase termed lethal factor (LF) in order to inhibit MAPK signalling (343). In this case, LF cleaves the MKKs, preventing efficient MAPKs activation (343). Thus, we verified the integrity of p38-upstream-regulators in cells submitted to *L. major*. While we did not notice any effect on MKK3 nor MKK6, the adaptor molecule TAB1 was depleted upon infection. We then showed that TAB1 is cleaved in a GP63-dependent manner, generating fragments unable to interact with p38. As the p38/TAB1 interaction was previously shown to modulate p38 activity (121), we believe that alterations in the stability of this complex caused by GP63 could contribute to the decreased p38 phosphorylation occurring during *Leishmania* infection.

As the most abundant protein covering the surface of *Leishmania* (33, 369), GP63 undoubtedly plays fundamental roles in signals initiated upon contact with host cells. In the extracellular milieu within mammalian host, parasites are significantly protected from complement-mediated lysis by GP63 (37, 177, 329). Nevertheless, the vulnerability of GP63-deficient *L. major* to the effect of complement may not be solely responsible for their reduced infectivity in an animal model (176). Indeed, additional functions including the promotion of host-cell attachment and internalization have been attributed to GP63 (36, 61). In addition, the GP63-mediated degradation of extracellular matrix components

such as fibronectin facilitates parasite dissemination and inhibits the activation of protective response of infected macrophages (194, 227). A limited number of intracellular functions have also been ascribed to GP63. For example, two intracellular substrates of GP63, MRP and NF-κB $p65^{RelA}$, have been identified (82, 127). Also, expression and activity of GP63 are important to protect engulfed parasites during phagolysosomal transition (58, 294). Our results expand significantly the number of known targets of GP63 and emphasize its importance in the parasitic program that remodels intracellular signalling networks of host cells in its proximity.

The intrusion of virulence factors and the exploitation of cellular components are crucial strategies for host invasion by a wide array of pathogenic microorganisms. In this study, we have uncovered a series of intracellular effects of *Leishmania* in fibroblasts, a potentially important target cell of this parasite. Our results point to the importance of the metalloprotease GP63 in regulating several important signaling proteins, contributing to downstream changes in global protein tyrosine phosphorylation levels as well as a specific effect on p38 MAPK activation. In addition, proteins modulating apoptosis and the actin cytoskeleton are overrepresented among the identified GP63 targets. Thus, our results suggest novel mechanisms by which GP63 could actively participate in the conditioning of host cells through the modulation of both signaling and structural regulators. If these changes are prerequisite for efficient infection by *Leishmania*, our results could contribute to the development of drugs that would impair host cell invasion by this virulent parasite.

3.6 FOOTNOTES

We would like to thank Dr. Greg Matlashewski, Dr. Laurent Lessard and Karen Doody for their critical reviews of the manuscript. We thank Jacynthe Laliberté for her advice on confocal microscopy and Dr. Serge Hardy for his help with apoptosis assays. M.L.T. is a recipient of the Jeanne et Jean-Louis Lévesque Chair in Cancer Research. M.S. is a recipient of a Fonds de la recherche en santé du Québec doctoral award. This work was supported by Canadian Institutes of Health Research (CIHR) (MOP-12466) and National Cancer Institute of Canada (NCIC) (015200) operating grants to M.L.T.. The laboratory of M.O. is supported by the CIHR (MOP-12671).

The abbreviations used are: CHO, Chinese hamster ovary; IB, immunoblot; IP, immunoprecipitation; *L.*, *Leishmania*; p130Cas, Crk-associated substrate; P-MEFs, primary mouse embryonic fibroblast cells; PTP, protein tyrosine phosphatase; PTK, protein tyrosine kinase; TC-PTP, T-cell PTP; WASP, Wiskott-Aldrich syndrome protein; WT, wild-type

3.7 SUPPLEMENTARY DATA.

Supplementary figure 1. Infection with *L. major* does not induce apoptosis. P-MEFs were incubated under control conditions or treated with *L. major* or 10 ηg/ml tumour necrosis factor-α (TNFα) in presence of 10 μg/ml cycloheximide (TNFα treatment only) for the indicated duration. Caspase activity was measured by DEVDase as described previously (138). Values correspond to the rate of Ac-DEVD-7-amino-4-trifluoromethyl coumarin (AFC) peptide substrate hydrolysis and represent means ± standard deviation of two independent experiments performed in triplicate. Increased apoptotic caspase activation was not detected in cells incubated for either 12 or 24 hours with *L. major*. As expected, treatment with TNFα induced a dramatic increase in caspase activity leading to apoptosis. These data provide strong evidence that prolonged exposure to *L. major* does not significantly induce apoptosis.

Supplementary figure 2. The phosphorylation of p130Cas is increased in the B14V cells. p130Cas expressed in PTP-PEST cells (B14V and B11WT) was immunoprecipitated, separated by SDS-PAGE and its level of tyrosine phosphorylation was revealed by immunoblotting using an anti-phosphotyrosine antibody (4G10). Cells expressing PTP-PEST (B11WT) showed decreased levels of phosphorylation of p130Cas as compared to cells lacking PTP-PEST (B14V).

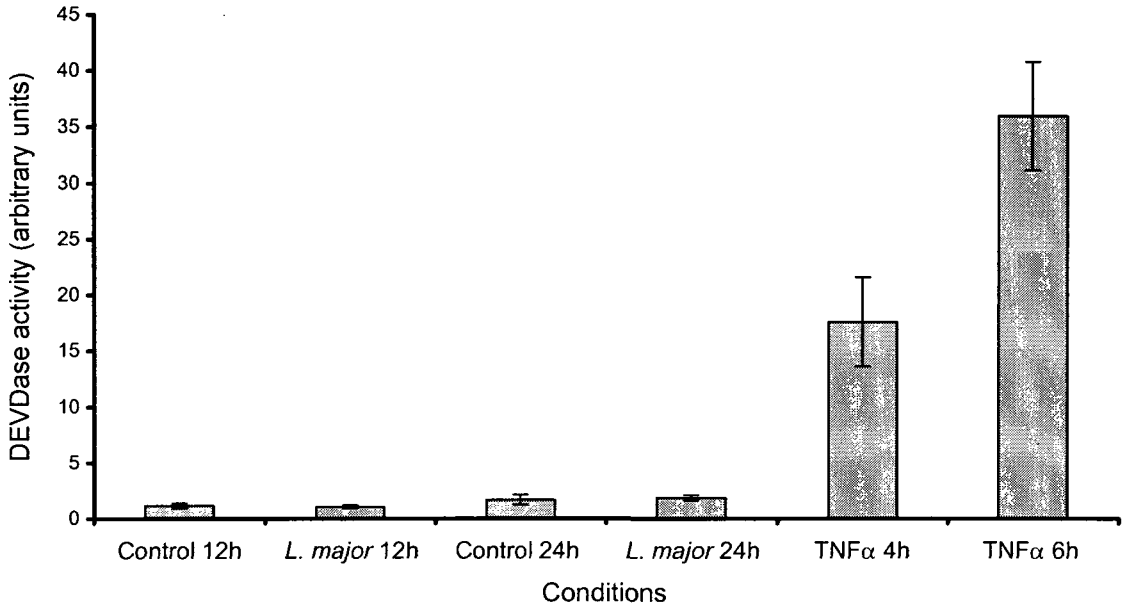
DEVDase activity (arbitrary units)
45
40
35
30
25
20
15
10
5
0
Control 12h
L. major 12h
Control 24h
L. major 24h
TNFα 4h
TNFα 6h
Conditions

Supp. Fig. 1

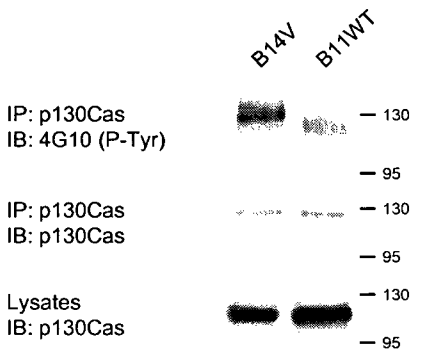
B14V
B11WT
IP: p130Cas
IB: 4G10 (P-Tyr)
130
95
IP: p130Cas
IB: p130Cas
130
95
Lysates
IB: p130Cas
130
95

Supp. Fig. 2

Supplementary figure 3. Forms of p130Cas found in control and *L. major*-infected B14V fibroblasts interact with the SH2 domain of Crk in vitro. Serum-starved B14V and B11WT cells were incubated with or without *L. major* for 15 min, rinsed with ice-cold PBS and lysed in mRIPA (50mM Tris pH 7.4, 150 mM NaCl, 0.1% SDS, 0.5% sodium deoxycholate, 1% NP40, 10 mM NaF, 1 mM Na_3VO_4, Complete protease inhibitor). Cell extracts were centrifuged at 16000 × g for 10 min at 4 °C, and the protein concentration was determined by Bradford assay. Cleared protein lysates (1 mg) were incubated for 2h at 4 °C with GST fusion proteins (GST or GST fused to the SH2 domain of Crk (GST-$SH2^{[Crk]}$), purified as described (85)) immobilized on glutathione sepharose beads (GE Healthcare). Beads were then washed three times with mRIPA, boiled in SDS-sample buffer and analyzed by immunoblotting. p130Cas is expressed similarly in B14V and B11WT cells, and *L. major* infection induces the appearance of a smaller form of p130Cas in both cell lines (right panel). The two forms of p130Cas protein interact with Crk SH2 exclusively in the absence of PTP-PEST (left panel). Filled arrowheads correspond to the long form of p130Cas and empty arrowheads point to the smaller form. The values on the right correspond to molecular weights in kDa.

Supplementary figure 4. *L. major*, but neither *L. tarentolae* nor *L. braziliensis* infection leads to rapid degradation of p130Cas and PTP-PEST. B11WT fibroblasts were incubated for the indicated time with the indicated *Leishmania* species at a ratio of 1:20. Protein lysates were harvested and analyzed by immunoblotting for p130Cas and PTP-PEST. Cellular p130Cas and PTP-PEST proteins were degraded within 15 min of incubation with *L. major*, whereas both proteins remained intact in cells incubated with *L. tarentolae* or *L. braziliensis* for 1h and 2h. Filled arrowheads identify intact proteins, and empty arrowheads point to cleavage products. The values on the right correspond to molecular weights in kDa.

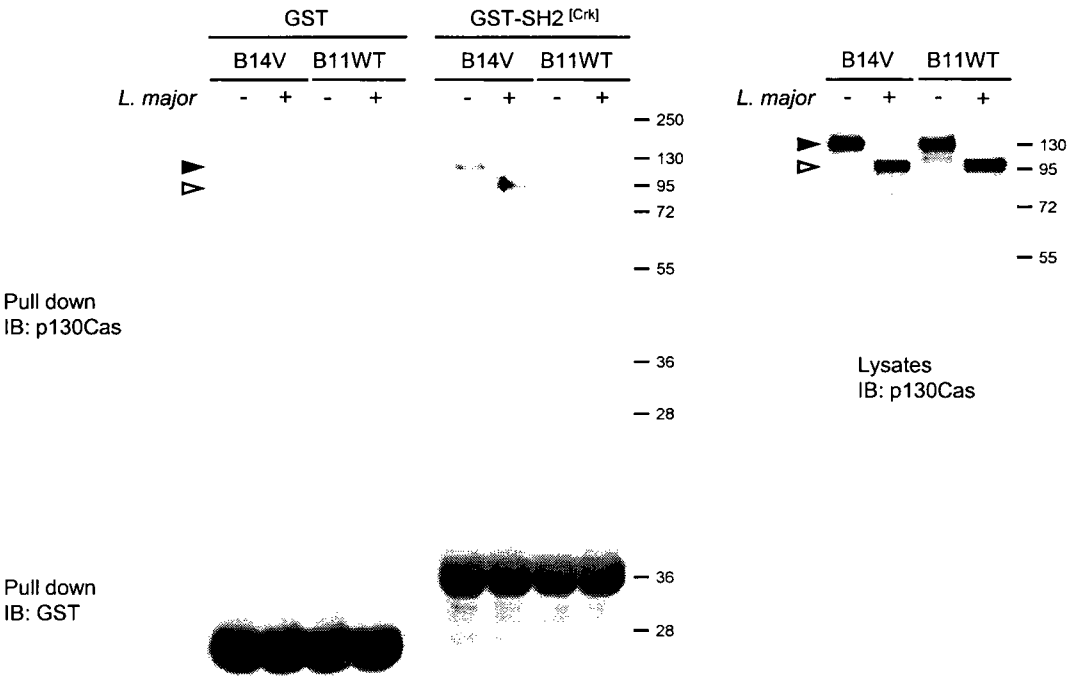
GST
GST-SH2 [Crk]
B14V
B11WT
B14V
B11WT
L. major
- + - + - + - +
250
130
95
72
55
36
28
Pull down
IB: p130Cas
Pull down
IB: GST
B14V
B11WT
L. major
- + - +
130
95
72
55
Lysates
IB: p130Cas

Supp. Fig. 3

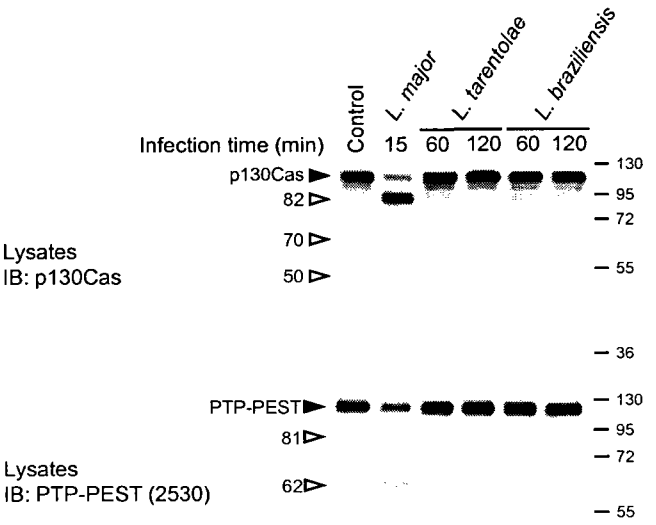
Control
L. major
L. tarentolae
L. braziliensis
Infection time (min)
15
60
120
60
120
p130Cas
82
70
50
Lysates
IB: p130Cas
130
95
72
55
36
PTP-PEST
81
62
Lysates
IB: PTP-PEST (2530)
130
95
72
55

Supp. Fig. 4

Supplementary figure 5. Infection with *L. major* does not induce the degradation of several proteins expressed in fibroblast-cells. P-MEFs were incubated with either *L. major*^{WT} or *L. major*$^{gp63-/-}$ for 30 min at a ratio of 1:20 (cells:parasites). Protein extracts were analysed by immunoblotting for p130Cas, TC-PTP, integrin-β1, STAT5, Shc, focal adhesion kinase (FAK), paxillin, IκBα, AKT and PTP-1B. IB, immunoblot.

Supplementary figure 6. Recombinant GP63 cleaves GST-PTP-PEST. GST-PTP-PEST was isolated from transfected *PTP-PEST*$^{-/-}$ cells and incubated under control conditions or with 0.2 μg or 1 μg of purified recombinant GP63 (REGP63) for 30 min. Samples were analysed by immunoblotting for PTP-PEST (2530 antibody). The values on the right correspond to molecular weights in kDa.

Supplementary figure 7. Expression of PTP-PEST promotes anisomycin-induced p38 MAP kinase phosphorylation. PTP-PEST$^{-/-}$ parental cells and rescued clones were serum-starved (0.05% FBS DMEM, 16h) and stimulated with 50 ηg/ml anisomycin in serum-free DMEM for the indicated time. Protein lysates were harvested and the level of phosphorylation of p38 was measured by immunoblotting using phospho-specific antibodies against phospho-thr180/tyr182 p38 MAP kinase. Total input of p38 as well as the expression level of PTP-PEST in each clone was also verified. Following treatment with anisomycin, *PTP-PEST* deficient cells displayed increased p38 phosphorylation. p38 was also activated in response to anisomycin in cells in which the empty vector was re-introduced (B14V). Importantly, all clones expressing PTP-PEST (B11WT, B118WT and B119WT) displayed increased phosphorylation of p38 following 15 min and 30 min treatment with anisomycin as compared to cells lacking *PTP-PEST*. These results strongly suggest that expression of PTP-PEST enhances the activation of p38 in anisomycin-treated cells.

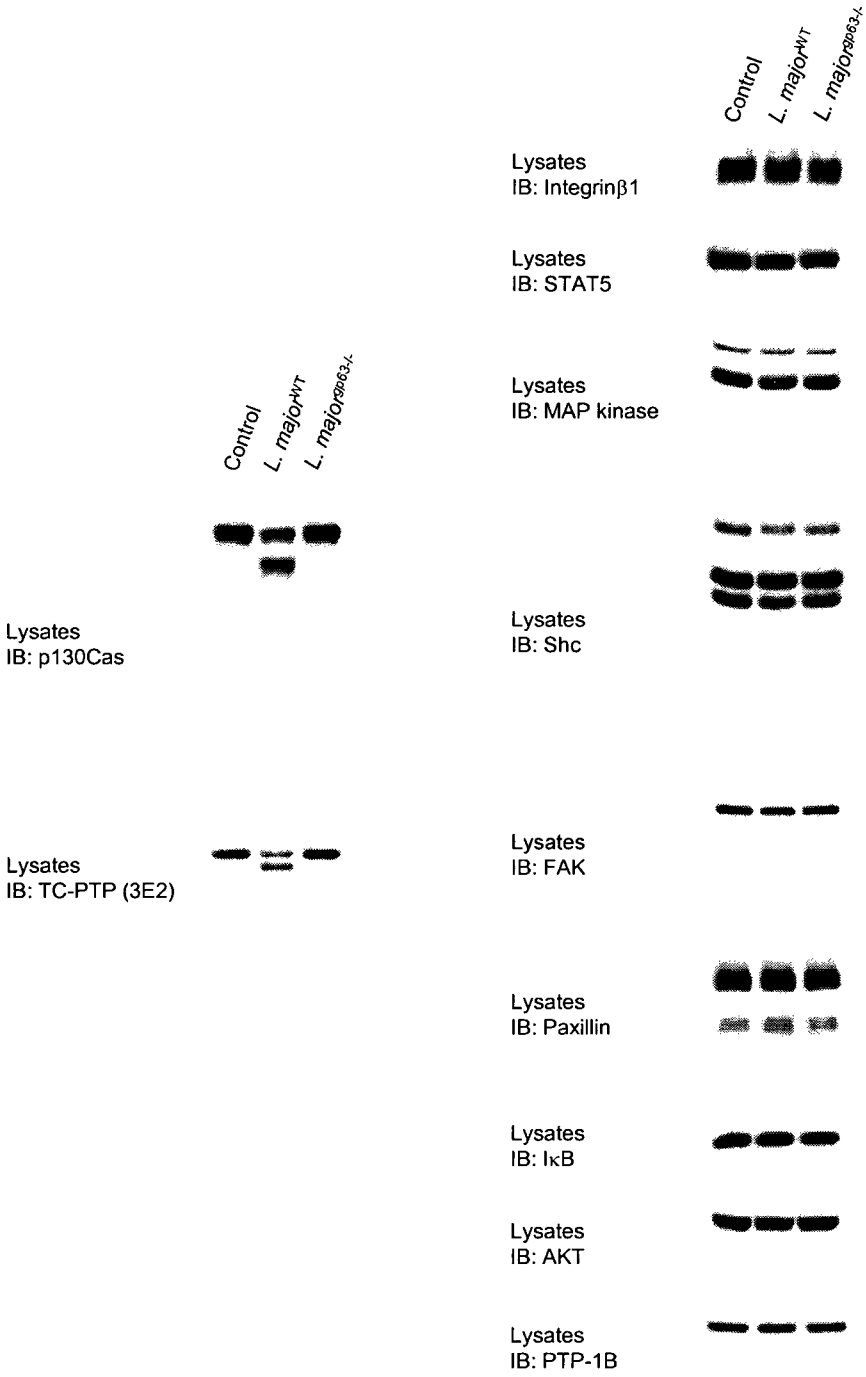
Control
L. major WT
L. major gp63-/-
Lysates
IB: Integrinβ1
Lysates
IB: STAT5
Lysates
IB: MAP kinase
Lysates
IB: Shc
Lysates
IB: p130Cas
Lysates
IB: FAK
Lysates
IB: Paxillin
Lysates
IB: TC-PTP (3E2)
Lysates
IB: IκB
Lysates
IB: AKT
Lysates
IB: PTP-1B

Supp. Fig. 5

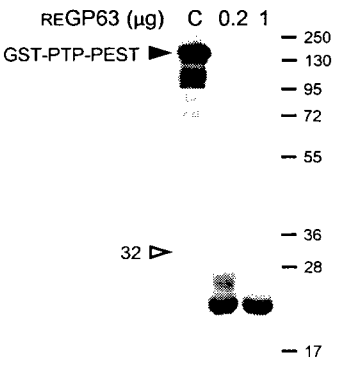

Supp. Fig. 6

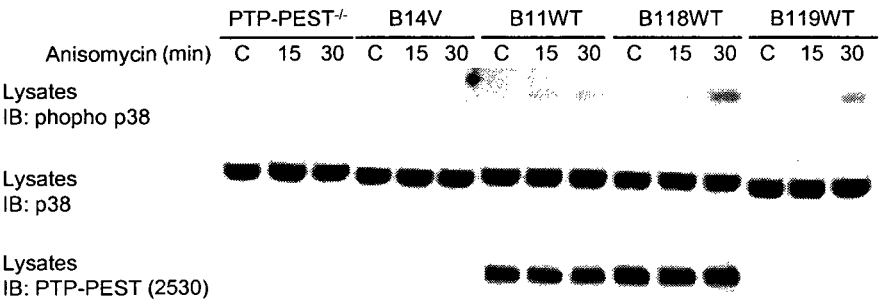
PTP-PEST-/-
B14V
B11WT
B118WT
B119WT
Anisomycin (min)
C 15 30 C 15 30 C 15 30 C 15 30 C 15 30
Lysates
IB: phopho p38
Lysates
IB: p38
Lysates
IB: PTP-PEST (2530)

Supp. Fig. 7

Supplementary figure 8. Infection with *L. major* induces cleavage of TC-PTP near its C-terminus. (A) Schema illustrating the structural organisation of TC-PTP (TC45). The N-terminal catalytic domain (phosphatase) is followed by a nuclear localization signal (NLS). Localization of epitopes recognized by various antibodies (12A3, 6F7, 3E2 and 10B4) is shown. (B) P-MEFs were incubated with either *L. major*^{WT} or *L. major*$^{gp63-/-}$ for 30 min at a ratio of 1:20 (cells:parasites). The stability of TC-PTP was evaluated by immunoblotting of cellular lysates using different monoclonal antibodies specific for TC-PTP (12A3, 6F7, 10B4) (B). Although TC-PTP of P-MEFs infected with *L. major*^{WT} was cleaved, this PTP remained intact in cells exposed to *L. major*$^{gp63-/-}$. These results imply that GP63 is necessary for parasite-mediated TC-PTP cleavage. Antibodies that are directed against the N-terminus segment of TC-PTP (12A3, 6F7, 3E2) all recognized a degradation product slightly smaller than the intact form (Fig. 5 D, Supplementary Fig. 1 and 2 B). In contrast, even following a long exposure, antibodies recognizing the C-terminus of TC-PTP (10B4) were not able to detect the same cleavage product (B). Together, these results suggest that the parasitic protease GP63 actively participates in the targeted cleavage of TC-PTP, a process that likely occurs within the C-terminal half of the enzyme. IB, immunoblot.

A.

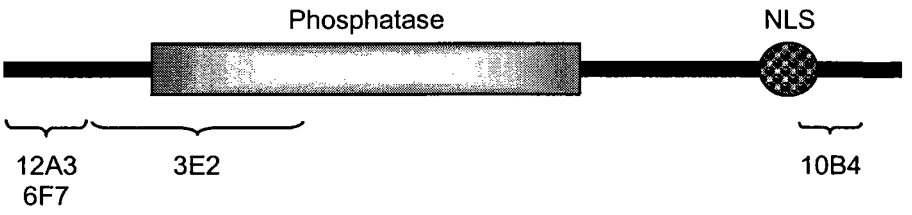

B.

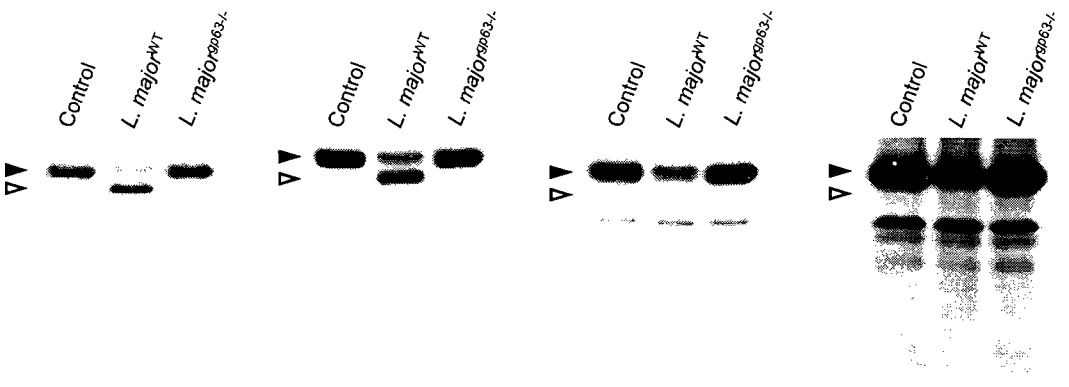

Lysates
IB: TC-PTP (12A3)

Lysates
IB: TC-PTP (6F7)

Lysates
IB: TC-PTP (10B4)

Lysates
IB: TC-PTP (10B4)
(long exposure)

Supp. Fig. 8

4 CHAPTER 4

CASPASE-3 REGULATES CATALYTIC ACTIVITY AND SCAFFOLDING FUNCTIONS OF THE PROTEIN TYROSINE PHOSPHATASE-PEST, A NOVEL MODULATOR OF THE APOPTOTIC RESPONSE

Maxime Hallé[1], Ying-Chih Liu[2], Serge Hardy[1], Jean-François Théberge[1], Christophe Blanchetot[3], Annie Bourdeau[1], Tzu-Ching Meng[2]* and Michel L. Tremblay[1]*

Mol. Cell. Biol., 2007, 27 (3): 1172-1190.

The Department of Biochemistry and McGill Cancer Center, McGill University, McIntyre Medical Sciences Building, 3655 Promenade Sir-William-Osler, Montréal, Québec, Canada, H3G 1Y6, [1] Institute of Biological Chemistry, Academia Sinica, 128 Academia Road, Section 2, Nankang, 105 Taipei, Taiwan, ROC, [2] The department of cell biology, Utrecht University, Psadualaan 8, 3584CH, Utrecht, The Netherlands[3]

* Co-corresponding authors. Mailing address for T.-C. Meng: Institute of Biological Chemistry, Academia Sinica, 128 Academia Road, Section 2, Nankang 115, Taipei, Taiwan, Tel: +886-2-27855696 ext 6140, Fax: +886-2-27889759, Email: tcmeng@gate.sinica.edu.tw Mailing address for M. L. Tremblay: McGill Cancer Center, McGill University, 3655 Promenade Sir-William-Osler, Room 701, Montréal, Québec H3G 1Y6, Canada. Phone: (514) 398-8480. Fax: (514) 398-6769. E-mail: michel.tremblay@mcgill.ca.

4.1 Abstract

The protein tyrosine phosphatase PEST (PTP-PEST) is involved in the regulation of the actin cytoskeleton. Despite the emerging functions attributed to both PTPs and actin cytoskeleton in apoptosis, the involvement of PTP-PEST in apoptotic cell death remains to be established. Using several cell-based assays, we show that PTP-PEST participates in the regulation of apoptosis. As apoptosis progresses, a pool of PTP-PEST localized to the edge of retracting lamellipodia. Expression of PTP-PEST also sensitized cells to receptor-mediated apoptosis. Concertedly, specific degradation of PTP-PEST was observed during apoptosis. Pharmacological inhibitors, immunodepletion experiments and *in vitro* cleavage assays identified caspase-3 as the primary regulator of PTP-PEST processing during apoptosis. Caspase-3 specifically cleaved PTP-PEST at the ^{549}DSPD motif and generated fragments, some of which displayed increased catalytic activity. Moreover, caspase-3 regulated PTP-PEST interactions with paxillin, leupaxin, Shc and PSTPIP. PTP-PEST acted as a scaffolding molecule connecting PSTPIP to additional partners: paxillin, Shc and Csk, and activation of caspase-3 correlated with the modulation of PTP-PEST adaptor function. In addition, cleavage of PTP-PEST facilitates cellular detachment during apoptosis. Together, our data demonstrate that PTP-PEST actively contributes to the cellular apoptotic response and reveal the importance of caspases as regulators of PTPs in apoptosis.

4.2 Introduction

Tyrosine phosphorylation is involved in signal transduction pathways that are necessary for multiple cellular phenomena such as growth and proliferation, differentiation, locomotion and apoptosis. The protein tyrosine phosphatases (PTPs) are the predominant enzymes that mediate the removal of the phosphate moiety from tyrosine residues, and therefore, are indispensable regulators of proper development and homeostasis of a wide variety of living organisms.

PTP-PEST is classified as a cytosolic PTP whose closest homologues are PTP-PEP and PTP-HSCF (5). Although PTP-PEST contains PEST regions previously proposed to stimulate protein degradation (272), pulse-chase analysis demonstrated that PTP-PEST is a stable protein with a half-life of more than four hours (56). PTP-PEST is ubiquitously expressed, although it is found at higher levels in hemopoietic tissues (85, 94). Inactivation of the PTP-PEST gene results in an early embryonic lethality and establishes PTP-PEST as an essential gene for mouse development (84, 305). Studies performed in fibroblast cells link PTP-PEST expression with the regulation of cell migration and adhesion (11, 120). Indeed, Sastry et al. have shown that PTP-PEST inhibits Rac1-induced cytoskeletal changes thereby preventing membrane ruffles formation (286). Furthermore, in aortic smooth muscle cells, nitric oxide inhibits cell migration by activating PTP-PEST (208). In *Xenopus* blastomeres, forced over-expression of PTP-PEST interferes with cell motility and results in a gastrulation defect (88). Concomitant with these reported phenotypes, PTP-PEST was found to directly interact or to be associated in complexes with several signaling and cytoskeleton-associated molecules including p130Cas, Sin, Hef-1, leupaxin, Hic-5, paxillin, FAK, Pyk2, Grb-2, Shc, Csk, PSTPIP, WASP, Abl and gelsolin (53, 54, 60, 79, 85, 86, 94, 118, 131, 216, 243). Interestingly, PTP-PEST decreased WASP-promoted immunological synapse formation and actin polymerization in T-cells (18). PTP-PEST reduces lymphocyte activation by inhibiting the Ras-MAP-kinase

pathway (95). Finally, altered PTP-PEST interactions were associated with the human auto-inflammatory disorders: PAPA syndrome (357).

Apoptosis-mediated cell death is necessary for proper development, efficient immune function and maintenance of tissue homeostasis (2). Two primary pathways activate apoptosis: the extrinsic pathway and the intrinsic pathway (28). The extrinsic pathway depends on the activation of the death receptor members of the TNF receptor family (92), whereas proteins sensing the diverse cellular stress trigger the intrinsic pathway (2). To amplify the apoptotic signal, these two pathways lead to the activation of the caspase cascade (28). Once activated, the executioner caspases commit cells to apoptosis by cleavage and alteration of function of their substrates (112).

Proper cellular adhesion is essential to mediate anchorage-dependent cell survival signals (314). In addition, to maintain physiological equilibrium, cells need to adopt a specific morphology. Apoptosis can results from the loss of cellular attachment, termed anoikis, or from a disturbance of the cytoskeleton leading to improper cellular morphology known as amorphosis cell death (222). Importantly, cleavage of cytoskeletal proteins by caspases correlates with morphological changes and cellular detachment that characterize apoptosis (77, 112). Interestingly, the caspase-mediated cleavage of p130Cas, a PTP-PEST-targeted protein, contributes to the dismantling of adhesion structures, whereas the cleavage of ROCK I induces formation of membrane blebbing (78, 189, 295).

Cumulative evidence recognizes phosphatases as critical regulators of apoptosis. For example, LAR-PTP (331), SHP-1 (377), YopH (40), PTP-1B (129), SAP-1 (318), TC-PTP (132) and PTP-PEP (143) were reported to promote apoptosis whereas SHP-2 (169), FAP-1 (166) and MKP (361) attenuate the apoptotic response. Reactive oxygen species (ROS), which inhibit PTP activity (230), contribute to the induction of apoptosis (181). In addition, several kinases and phosphatases have been identified as important

modulators of the apoptotic response by siRNA screening (218). Some protein serine/threonine phosphatases are substrates of caspases as exemplified by calcineurin and PP2A (112). Furthermore, caspase-3 regulates the protein stability of the dual specific phosphatase PTEN (338). Nevertheless, as of yet there are no reports of tyrosine-specific PTPs cleaved by caspases during apoptosis.

Through its numerous protein-protein interactions, PTP-PEST contributes to cytoskeletal organization, regulates immune cell activation and plays a pivotal role in embryonic development. The function and regulation of PTP-PEST in apoptosis, however, have not yet been explored. Herein, we show that expression of PTP-PEST sensitizes cells to receptor-mediated apoptosis. In cells undergoing apoptosis, we observed a consistent correlation between the presence of PTP-PEST in membrane ruffles and lamellipodia retraction. We demonstrated that PTP-PEST integrity, activity and adaptor function were all modulated specifically by caspase-3. Furthermore, the cleavage of PTP-PEST contributes to cellular detachment during apoptosis. This study links PTP-PEST to the regulation of apoptosis and implicates caspases in the regulation of PTPs.

4.3 MATERIALS AND METHODS

4.3.1 Reagents and antibodies used in this study.

Chemicals were from BioShop Canada Inc., Fisher Scientific and Sigma. Recombinant active caspase-3 was from Upstate®. The PTP-PEST polyclonal antibodies (2528 and 2530) and monoclonal (AG25) were previously described (85, 118). Monoclonal antibodies specific for Shc, p130Cas and paxillin were from BD Transduction Laboratory. Antibodies against Csk, GST and SHP-2 were from Santa Cruz Biotechnology. TC-PTP monoclonal antibodies (3E2) kindly provided by Daniel Brunet were described previously (162) and CF4-1D antibodies were from Calbiochem. Polyclonal rabbit antibodies against PTP-1B and monoclonal anti-myc (9E10) were from Upstate®. Antibodies specific for caspase-3, caspase-8 and caspase-9 were from Cell Signaling Technology. Antibodies against GFP, PTP-1B (FG6), caspase-6 and caspase-7 were respectively from Clonetech, Calbiochem, Upstate® and BD Biosciences.

4.3.2 Plasmids, cDNAs and transfections.

Murine PTP-PEST expression vectors, pcDNA3.1/Zeo-PTP-PEST (WT and C231S) and pEGFP-C2-PTP-PEST (WT), were described previously (85). PSTPIP cDNA described in (85) was subcloned into pEBG using *Bam*H1 and *Not*1 restriction sites. The pcDNA3.1/Zeo-PTP-PEST ^{549}ASP^{552}A, ^{604}ADS^{607}A, ^{740}AKK^{743}A and ^{549}ASPA/^{604}ADSA constructs were generated by site-directed mutagenesis (QuikChange site-directed mutagenesis kit, Stratagene). pEGFP-C2-PTP-PEST WT and ^{549}ASP^{552}A were generated by PCR cloning of the appropriate cDNA using oligonucleotides containing *Bam*H1 and *Xho*1 and were respectively inserted between *Bgl*II and *Sal*1 restriction sites. pEBG-PTP-PEST

WT and ^{549}ASP^{552}A were generated by PCR cloning of the appropriate cDNA using oligonucleotides containing *Bam*H1 and *Not*1 restriction sites. pCS2mycECFP-PTP-PEST-EYFP (WT or ^{549}ASP^{552}A or ^{604}ADS^{607}A or ^{740}AKK^{743}A or ^{549}ASPA/^{604}ADSA) were obtained by replacing PTPαSpD2 by PTP-PEST in pCS2mycECFP-PTPαSpD2-EYFP (26) using *Nco*1/*Bgl*II with the corresponding PTP-PEST cDNA amplified by PCR. Human PTP-PEST (hPTP-PEST) cDNA (Open Biosystems) amplified by PCR was subcloned into pGEX-6P1 (Pharmacia) using *Bam*H1 and *Sal*1 restriction sites. GST-hPTP-PEST cDNA was further amplified by PCR and subcloned into pRK5 using *Xba*1 and *Sal*1 restriction sites. All cDNAs were verified by sequencing. All transfections were performed using Lipofectamine™ 2000 (Invitrogen) according to the manufacturer's instructions.

4.3.3 Cell lines.

All cell lines were maintained in DMEM supplemented with 10% fetal bovine serum (FBS) and 50 μg/ml gentamicin (Gibco) at 37°C in a 5% CO_2 humid atmosphere. For 293T cells, media was also supplemented with 1% L-glutamine. Primary mouse embryonic fibroblasts (P-MEFs) from BALB/c mice (Jackson) were generated as described (67). Mouse spontaneously immortalized fibroblasts (MEFs) were previously described (128). HeLa299 cells were a generous gift of N. Sonenberg (McGill University). PTP-PEST -/- parental cells were described by Côté et al. (84). Stable re-expression of PTP-PEST in the PTP-PEST null cells was obtained as follows: subconfluent PTP-PEST -/- fibroblasts were transfected with linearized (*Sca*1) pcDNA3.1/Zeo (empty vector, EV) or with pcDNA3.1/Zeo-PTP-PEST (wild type, WT). After 48h, the cells were split and positive clones were selected using 100 μg/ml of Zeocin (Invitrogen). The media was changed every two days for 10 days and isolated colonies were picked and expanded in selection media. Clones expressing PTP-PEST were identified by immunoblot. Clones were grown in media supplemented with 50 μg/ml Zeocin during routine culture and were maintained in absence of Zeocin during the course of each experiment.

4.3.4 Induction of apoptosis and immunoblots.

Cells were stimulated with 60 μM cisplatin (Calbiochem), 1 μM staurosporine (Sigma) or 10 ng/ml tumor necrosis factor-α (TNF-α) (Sigma) in the presence of 10 μg/ml cycloheximide (Sigma) for the indicated time, adherent and detached cells were rinsed on ice with PBS and lysed (1% NP-40, 150 mM NaCl, 50 mM Tris pH 7.4, 0.1% SDS, 50 mM NaF, 1 mM Na_3VO_4, Complete protease inhibitors (Roche)). Cell extracts were centrifuged at 16000 × g for 10 min at 4°C, and the protein concentration of each sample was calculated by a Bradford assay (Bio-Rad Protein Assay). Equal amounts (20 μg) of denatured protein were separated by SDS-PAGE and transferred to polyvinylidene difluoride (PVDF) membranes (Immobilon-P, Millipore). Commercial antibodies were used accordingly to the manufacturer's instructions and non-commercial TC-PTP and PTP-PEST antibodies were used as described previously (85, 162). Blots were stripped using Re-Blot Plus Strong (Chemicon International) and re-probed accordingly to the instructions from the manufacturer.

The effect of pharmacological protease inhibitors on PTP-PEST degradation during apoptosis was determined as follows: caspase inhibitor (Z-VAD-FMK, Cedarlane) and calpain inhibitor (PD150606, Calbiochem) were added to cells 2 h prior to addition of 1 μM staurosporine and co-incubation was continued for an additional 6 h. Adherent and floating cells were harvested, lysed and analyzed as described above.

4.3.5 Analysis of PTP-PEST localization.

HeLa299 were transfected for 6 h with 6 μg of pEGFP-C2-PTP-PEST in 10 cm dishes. Cells were then re-plated at 2.2×10^5 cells per 35 mm fibronectin coated (10 μg/ml fibronectin/PBS (Sigma), 2 h, 37°C) glass bottom dish (Mat Tek Corporation) and incubated for 16 h. HeLa299 cells expressing EGFP-PTP-PEST were treated with 50 ng/ml

anti-Fas (human activating, Upstate®) and 10 μg/ml cycloheximide for the indicated period of time. Cells were maintained at 37°C in 5% CO_2 humid atmosphere using a digital temperature controller 37-2 (Zeiss) and a digital CTI-controller 3700 (Zeiss) connected to an Inkubator S (Zeiss) installed on an Axiovert 200M (Zeiss) confocal microscope. Random field images were acquired at the indicated times using the LSM510 Meta confocal system and software. Profile analysis was performed using the same software. For the time-lapse video confocal microscopy, images were acquired at 15 seconds intervals.

4.3.6 Measurement of apoptosis.

PTP-PEST -/- parental cells and re-expressing clones were seeded at 1.7×10^6 cells/60mm dish. Eight hours following their adhesion, cells were rinsed with PBS and starved in 0.1% FBS DMEM for 16 h. Cells were treated with 10 μg/ml cycloheximide in the presence or absence of 10 ng/ml TNFα in 10% FBS DMEM for 2.5 h. Adherent and floating cells were rinsed with ice-cold PBS, lysed (20 mM Hepes pH 7.4; 2 mM EDTA; 1% NP-40, 10 μg/mL aprotinin, 10 μM leupeptin and 2 mM dithiothreitol (DTT)) and samples were centrifuged at 4°C for 10 minutes at 16000 × g. Protein content was normalized using the Bradford method and caspase activation was quantified by DEVDase assay as described in (141). HeLa299 cells were transfected with 6 μg DNA for 6 h in 10 cm dishes, trypsinized, harvested and seeded at 5×10^5 cells/60mm dishes for 18 h. After 24 h of serum starvation (0.1% FBS DMEM), cells were treated for 6 h with or without 50 ng/ml human anti-Fas (Upstate®) in presence of 10 μg/ml cycloheximide in 10% FBS DMEM. Cells were lysed and caspase activity was measured as described above.

4.3.7 Measurement of cellular attachment by flow cytometry.

HeLa299 cells were transfected with 13μg of either pEGFP-PTP-PEST WT or pEGFP-PTP-PEST ^{549}ASPA for 6 h in 10 cm dishes, trypsinized, harvested and seeded at 310 000 cells/well (6 wells plate) in 1% FBS DMEM for 16 h. Cells were treated for the indicated time with or without 50 ng/ml human anti-Fas (Upstate®) in presence of 10 μg/ml cycloheximide in 10% FBS DMEM. Following incubation, media was removed, cells were rinsed two times with PBS and attached cells were gently detached using TrypLE™Express (Gibco) and harvested in PBS (supplemented with 2% FBS, 10 mM EDTA). Cells were transferred to polystyrene round-bottom tube (BD Falcon) and centrifuged at 1550 rpm at 4°C for 5 min (Eppendorf centrifuge 5810R). Cell pellets were resuspended in 500 μl PBS (supplemented with 2 % FBS and 10 mM EDTA) and samples were kept on ice. Tubes were vortexed for 3 sec and read using FACScan (BD Bioscience) leaving 10 sec for flow stabilization followed by a 30 sec acquisition time for each reading. Each sample was analyzed three times using this method and vortexed for 3 sec between each analysis. Results are representative of two independent experiments in which each condition was performed in triplicate. Cells were analyzed with Cell Quest Pro software (BD Bioscience) based on forward and side scatter (eliminating doublets) and EGFP positive cells were read in FL1 channel.

4.3.8 In vitro caspase-3 cleavage assay.

To monitor the cleavage of protein *in vitro*, clones from PTP-PEST -/- cells were rinsed with ice-cold PBS and lysed in cleavage assay buffer (20 mM Hepes pH 7.4, 1% NP-40, 2 mM EDTA, 5 mM DTT, 10 μM leupeptin, 10 μg/ml aprotinin) as described in (189). Following determination of protein concentration, 65 μg of protein lysate was incubated with 25 ng of recombinant caspase-3 (Upstate®) for the indicated time period at 30°C.

Control samples were incubated under the same conditions in the absence of caspase-3. Samples were immediately placed on ice, SDS sample buffer was added, samples were boiled for 4 min and proteins were separated and detected using immunoblot. To identify caspase-3 cleavage site in PTP-PEST, HeLa299 cells transiently expressing either EGFP or different version myc-ECFP-PTP-PEST-EYFP (WT, ^{549}ASPA, ^{604}ADSA, ^{740}AKKA, ^{549}ASPA/^{604}ADSA) were lysed, incubated with recombinant active caspase-3 and processed as described above. When isolated GST-PTP-PEST was used as a substrate, PTP-PEST -/- cells expressing GST-PTP-PEST were lysed in HMNETG (50 mM Hepes pH 7.5, 1% Triton X-100, 150 mM NaCl, 1.5 mM $MgCl_2$, 1 mM EGTA, 10% glycerol, Complete protease inhibitors), as described above, and the lysate was incubated for 1 h at 4°C with glutathione sepharose beads (Amersham Biosciences). Beads were then rinsed three times with HMNETG and two times with cleavage assay buffer. Samples were resuspended in cleavage assay buffer in the presence or absence of 50 ng of recombinant caspase-3, incubated at 30°C for the indicated time period, chilled on ice, rinsed once with lysis buffer (1% NP-40, 150 mM NaCl, 50 mM Tris pH7.4), resuspended in SDS-sample buffer and analyzed by immunoblot.

4.3.9 Analysis of PTP-PEST and PSTPIP protein complexes.

PTP-PEST -/- cells transiently expressing GST or GST-PTP-PEST were rinsed with ice-cold PBS, lysed in HMNETG and protein extracts were centrifuged 10 min at 16000 × g at 4°C. GST proteins were extracted on glutathione sepharose beads at 4°C for 80 min. Beads were washed once with HMNETG, two times by inversion for five minutes at room temperatures in HMN^{300}ETG (containing 300 mM NaCl) and washed twice with cleavage assay buffer. Beads bearing GST proteins were incubated for 30 min in caspase assay buffer with (sample number 2) or without (samples 1, 3, 4 and 5) 50 ng recombinant caspase-3 (Upstate®) at 30°C (see Fig. 8B). Samples were chilled on ice and washed once with HMN^{300}ETG and twice with the interaction buffer (1% NP-40, 150 mM NaCl, 50 mM

Tris pH 7.4, Complete protease inhibitor). At this step, PTP-PEST association with paxillin and Shc could not be detected (data not shown). Each sample was then incubated at 4°C for 2.5 h with P-MEF cell extract (2.5 mg of protein in 1 ml of interaction buffer) to recreate PTP-PEST interactions *in vitro*. Then, beads were washed three times with the interaction buffer and once with modified cleavage assay buffer (without DTT). Samples 3, 4 and 5 were then incubated in modified cleavage assay buffer with or without 250 ng caspase-3 for 30 min at 30°C (Fig. 8B). Then, interaction buffer was added to samples 4 and 5, incubated for 10 min on ice and washed twice with interaction buffer. All samples were resuspended in SDS-sample buffer and protein content was analyzed by immunoblotting as described above.

To evaluate the importance of the ^{549}DSPD site of PTP-PEST in the effect of caspase-3 on its interactions, GST proteins expressed in PTP-PEST -/- cells were isolated, washed and incubated with or without recombinant caspase-3. After additional washes, they were incubated with P-MEF cell extract, washed again and analyzed as described above for samples 1 and 2. To assess the ability of caspase-3 to regulate PSTPIP/PTP-PEST association, PTP-PEST -/- cells transiently expressing either EGFP or myc-ECFP-PTP-PEST (WT or ^{549}ASPA)-EYFP with GST-PSTPIP were rinsed with PBS and lysed in modified cleavage assay buffer as described above. Aliquots of 1 mg of protein were incubated for 60 min at 30°C with or without 0.3 µg of recombinant caspase-3. Following the incubation, samples were centrifuged at 16000 × g for 2 min, chilled on ice and diluted 10 times with interaction buffer. Proteins were recovered following incubation with glutathione sepharose beads as described above. Beads were washed three times with interaction buffer, boiled in SDS-sample buffer and analyzed by immunoblot.

To analyze the PSTPIP protein complexes *in vivo*, HeLa299 cells transiently expressing either GST, GST-PSTPIP (WT or W232A) with myc-ECFP-PTP-PEST (WT or ^{549}ASPA)-EYFP were treated with cycloheximide with or without anti-Fas for the indicated time. Both floating and adherent cells were colleted and lysed in interaction buffer for 10 min on ice and samples were then centrifugated at 16000 × g for 10 min.

Cleared lysates (2.5 mg) were then incubated at 4°C for 2.5 h with glutathione sepharose beads as described above. Beads were washed three times with interaction buffer, boiled in SDS-sample buffer and analyzed by immunoblot.

4.3.10 In vitro caspases activation assay.

293T cells were trypsinized and collected by centrifugation. Cell pellets were washed with an equal volume of ice-cold NPM buffer (50 mM PIPES, 50 mM NaCl, 5 mM EGTA, 1 mM MgCl2, 5 mM DTT, 1 mM PMSF, 50 μg/ml pepstatin, 50 μg/ml leupeptin, 100 μg/ml aprotinin) and subsequently washed with five volumes of NPM buffer. The 293T cells were lysed with 3 cycles of snap freeze-and-thaw, and cell lysates were cleared by centrifugation at 16000 × g for 5 min. Aliquots of the 293T lysates were stored in liquid nitrogen. The 293T cell lysates were stimulated with 2 mM dATP (Roche) at 37°C for the indicated time points. The reaction was terminated by mixing lysates with SDS-sample buffer and boiled for 3 min prior to analysis.

4.3.11 In-gel phosphatase assay.

^{32}P-ATP labeled polypeptide (1×10^6 CPM) was incorporated into a 10% SDS-polyacrylamide gel prior to polymerization (231). Following electrophoresis, the gel was incubated for 1 h and then for 16 h in fixing buffer (20% isopropanol, 50 mM Tris pH 8.0). The gel was incubated in denaturation buffer (6 M Guanidine-HCl, 50 mM Tris pH 8.0, 0.3% β-mercaptoethanol) for 1.5 h, and twice in renaturation buffer (50 mM Tris pH 8.0, 1 mM EDTA, 0.04% Tween-40, 0.3% β-mercaptoethanol) for 1 h. The gel was subsequently incubated within the PTP reaction buffer (50 mM Tris pH8.0, 1 mM EDTA, 0.04% Tween-40, 0.3% β-mercaptoethanol, 3 mM DTT) for 1 h, followed by incubation

with fresh reaction buffer for 16 h. Following Coomassie blue staining, the gel was dried and subjected to autoradiography for visualization of PTP activity.

4.3.12 Immunodepletion.

The dATP-treated 293T cell lysate (240 μg) was diluted to 0.8 μg/μl with lysis buffer (20 mM Hepes pH 7.5, 50 mM NaCl, 1 % NP-40, 10 mM NaF, 10 mM $Na_4P_2O_7$, 10% glycerol, 100 μM PMSF, 5 μg/ml Pepstatin, 5 μg/ml Leupeptin, 10 μg/ml Aprotinin). Followed by pre-cleaning with 50 μl protein-G Sepharose beads (Amersham), the lysate was then incubated with 25 μg PTP-PEST antibody (AG25), which has been conjugated with protein-G Sepharose, at 4°C for 2.5 h. Samples were analyzed by immunoblot and in-gel PTP assay. For immunodepletion of capase-9, caspase-3 and caspase-7, 1400 μg of 293T lysates were incubated with 12.5 μg of the appropriate antibody conjugated with protein-A/G Sepharose beads (Amersham), at 4°C for 2.5 h. Samples were then centrifugated and the supernatants were collected and subjected to an additional round of immunodepletion in order to completely remove the specific caspases. Subsequently, each caspase-deprived lysate was subjected to treatment with 2mM dATP, and then examined by immunoblotting or in-gel PTP assay.

4.3.13 In-solution phosphatase activity assay.

520 ng of GST-hPTP-PEST bound to glutathione sepharose beads was incubated for 20 h at 37°C in the presence or absence of active caspase-3. Treated and control beads coupled with GST-hPTP-PEST were mixed with 3 μM ^{32}P labeled PTP substrates (polypeptide $(Glu:Tyr)_{4:1}$) in 60 μl reaction buffer (25 mM Hepes pH 7.5, 1mM EDTA, 1mM DTT) and then incubated at 30°C for 10 min with vigorous shaking. The reaction was terminated by addition of 180 μl 20% TCA. 20 μl of BSA (25 mg/ml) was added into

the solution as a carrier protein to facilitate substrate precipitation. Following centrifugation (16000 × g, 5 min), the supernatant was collected and counted using a Multi-Purpose Scintillation Counter (LS6500, Beckman) to detect the amount of released ^{32}P. The catalytic activity of PTP was expressed as pmol of ^{32}P released per minute.

4.4 RESULTS

4.4.1 PTP-PEST localizes to retracting membrane ruffles of apoptotic cells.

Progression of apoptosis is characterized by important changes in cellular morphology such as membrane blebbing, cell rounding and detachment that are intimately associated with modifications of the actin cytoskeleton (77). Several reports link PTP-PEST to the regulation of the architecture of the actin cytoskeleton (11, 12, 18, 203, 286). To explore whether PTP-PEST physiologically contributes to apoptosis, we first examined its cellular localization during this phenomenon. HeLa299 cells expressing EGFP-PTP-PEST were incubated with anti-Fas and observed live using confocal microscopy. Prior to cellular detachment, PTP-PEST was localized predominantly in the cytosol. Interestingly, there was also a pronounced signal at the periphery of the cell (Fig. 1A). Profile analysis showed that the signal corresponding to PTP-PEST detected in membrane ruffles on the cell periphery was at least as intense as that present in the cytosol (Fig. 1B). This suggests substantial localization of PTP-PEST to the cytosol and likely the plasma membrane. To obtain more insight into the dynamic localization of PTP-PEST during apoptosis, time-lapse confocal video microscopy analysis was performed on anti-Fas-treated cells. Figure 1C illustrates that incubation with anti-Fas induced an apoptotic cell phenotype. In lamellipodia that either expanded or remained static, a low amount of PTP-PEST was observed (Fig. 1D, empty arrowheads). Preceding apoptotic cell death, PTP-PEST appeared at the edge of the lamellipodias (filled white arrowheads) that immediately retracted (filled white double arrowheads, Fig. 1D and

Supplementary Data, movies 1 and 2). Moreover, PTP-PEST was maintained at the edge of the contracting membrane ruffles during their movement inward (filled white double arrowheads, Fig. 1D and Supplementary Data, movies 1 and 2). The presence of PTP-PEST in the retracting lamellipodia was observed in 91% of the cells analyzed (55 cells). Similar results were obtained when caspase-3 was microinjected in COS-7 cell expressing EGFP-PTP-PEST (data not shown). PTP-PEST was also concentrated at the base of membrane blebs in some cells (data not shown). Two other non-receptor PTPs, PTP-1B and TC-PTP, as well as the adaptor protein Nck did not significantly localize to the retracting membrane ruffle of anti-Fas treated cells (data not shown). The presence of PTP-PEST in retracting lamellipodia implies that this enzyme could participate in the morphological changes and membrane detachment of cells undergoing apoptosis.

Figure 1. Localization of EGFP-PTP-PEST in live cells during apoptosis. HeLa299 cells expressing EGFP-PTP-PEST were stimulated with 50 ng/ml anti-Fas in presence of 10 μg/ml cycloheximide and analyzed using confocal microscopy. (A) Cellular distribution of EGFP-PTP-PEST following 5 h 50 min of treatment. (B) Profile of intensity (arbitrary unit) of the fluorescence against the distance (μm) traversed by the arrow (drawn on A) representing the quantity of signal detected in different area of the cell. (C) Pictures taken at the indicated time of incubation. Scale bar: 10 μm. (D) Time lapses analysis of the area delimited by the squares drawn on panel C (see Supplemental Movies 1 and 2). Images captured between 5:05:29 and 5:10:71 were acquired inside the white square whereas those from 5:42:00 to 5:49:15 correspond to the gray square. Scale bar: 5 μm. Empty arrowheads point to sites where low amounts of EGFP-PTP-PEST are detected, filled arrow heads denote the accumulation of signal and double filled arrow heads identify site of inward movement on the cell periphery.

A.

B.

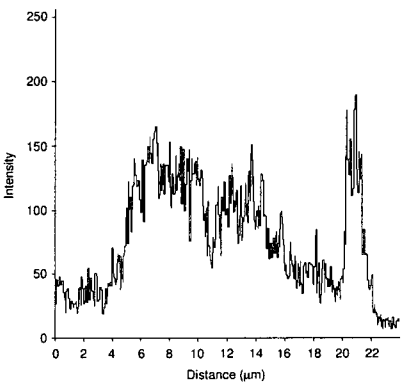

FIG. 1A and B

C.

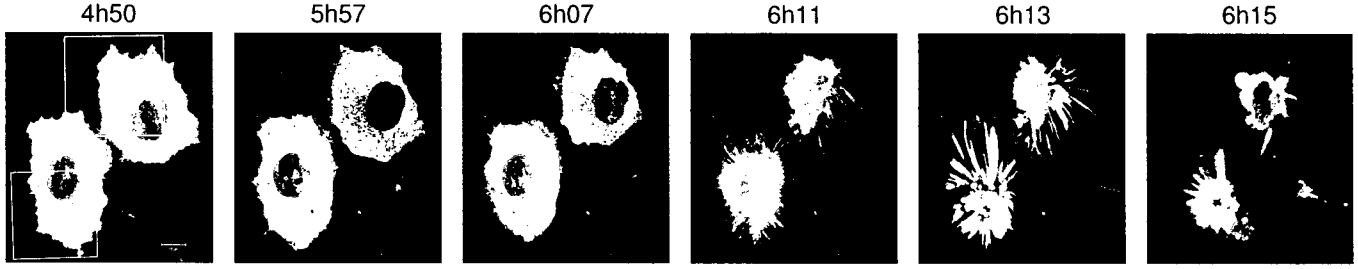

D.

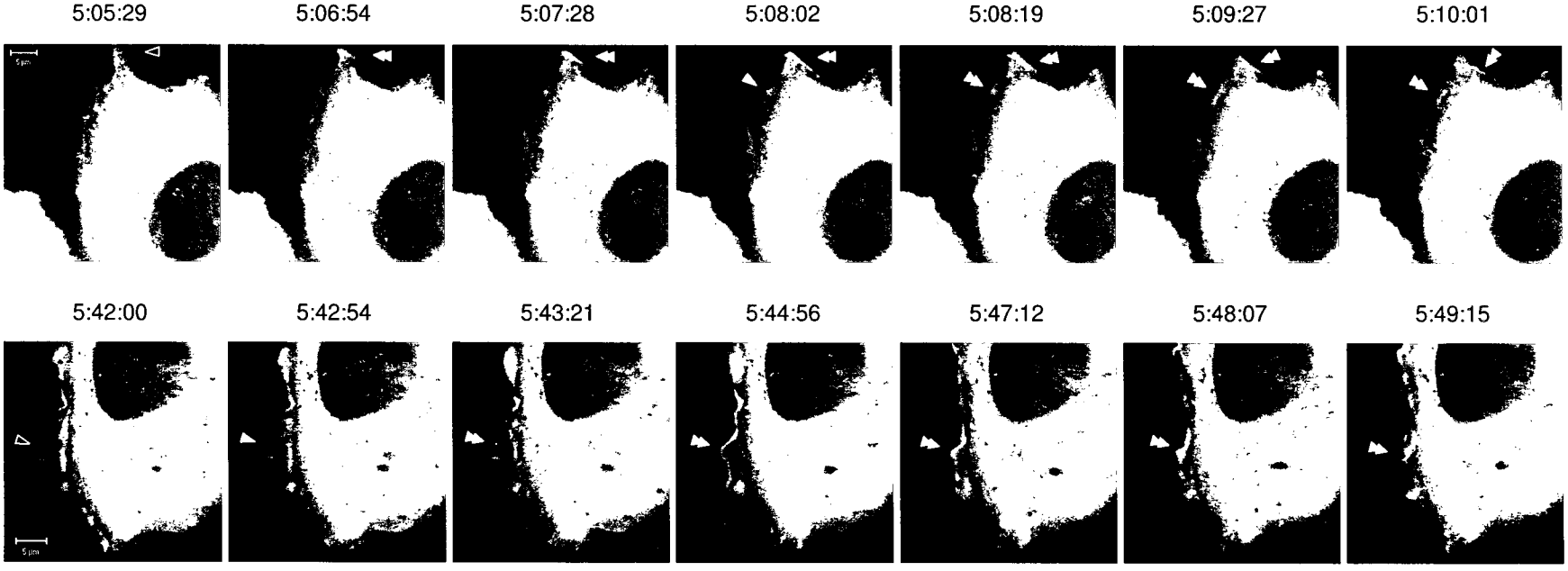

FIG. 1C and D

4.4.2 Expression of PTP-PEST sensitizes cells to receptor-mediated apoptosis.

The specific presence of PTP-PEST in retracting membrane ruffles of apoptotic cells suggests that this enzyme potentially plays important functions in this type of cell death. Consequently, we evaluated the possibility that PTP-PEST influences the cellular response to apoptotic stimuli. For this purpose, PTP-PEST cDNA was reintroduced in PTP-PEST -/- parental cells and single clones were isolated. Each clone expressed a different yet stable level of PTP-PEST (Fig. 2B). Clones expressing PTP-PEST that were treated with TNFα exhibited enhanced induction of apoptosis compared to PTP-PEST -/- parental cells and PTP-PEST -/- EV control clones (Fig. 2A). In addition, the level of DEVDase induction appeared to correlate with the level of PTP-PEST expression: clones expressing higher levels of PTP-PEST exhibited greater sensitivity to TNFα than the clones with lower PTP-PEST expression.

These results were also validated in transient expression experiments using a different cell line (HeLa299) and a different apoptotic stimulus (anti-Fas, Fig. 2C). Cells expressing PTP-PEST displayed a greater increase in apoptosis than the empty vector transfected controls. In contrast, the catalytically dead PTP-PEST mutant (C231S) failed to induce a significant increase in apoptosis as compared to the empty vector control, indicating that the catalytic activity of PTP-PEST is essential for its effect on the Fas-mediated apoptotic response. Efficiency of the transfection is shown in figure 2D. In both the rescued fibroblast and HeLa models, PTP-PEST expression did not spontaneously induce apoptosis in cells growing under control condition (Fig. 2A, C). Together, these results suggest that expression and catalytic activity of PTP-PEST increase sensitivity to receptor-mediated apoptosis.

Figure 2. Expression of PTP-PEST sensitizes cells to receptor-mediated apoptosis. (A) PTP-PEST -/- parental cells and rescued clones were treated with 10 μg/ml cycloheximide in absence (control) or in presence of 10 ng/ml TNFα for 2.5 h and apoptosis was measured by DEVDase assay as described in materials and methods. Values are fold increases over control PTP-PEST -/- parental cells (-/-) and represent means ± S.E. of three independent experiments. Asterisks denote values significantly different from -/- cells (*, $p < 0.05$). (C). DEVDase activity measure in cell lysates obtained from HeLa299 cells transfected with either pcDNA3 (EV), pcDNA3-PTP-PEST-WT (WT), pcDNA3-PTP-PEST-C231S (C/S) incubated for 6 h with 10 μg/ml cycloheximide in absence (control) or in presence of 50 ng/ml anti-Fas. Values are fold increases over control EV and represent means ± S.E. of three independent experiments performed in duplicate. Asterisks denote values significantly different from control EV cell lysates (*, $p < 0.01$). Expression of PTP-PEST in the -/- and in the various clones (B) and in transfected HeLa299 cells (D) was measured by SDS-PAGE and immunoblot for PTP-PEST (2528 rabbit antibody). Clones derived from -/- cells, which harbor the empty vector (B14), do not express PTP-PEST whereas clones, in which PTP-PEST wild type was reintroduced (B11WT, B112WT, B117WT, B118WT, B119WT) express different levels of PTP-PEST. The amount of protein on the immunoblot was normalized with the expression of Shc and values on the right correspond to the molecular size in kilodaltons (kD). EV, empty vector, WT, wild type, IB, immunoblot.

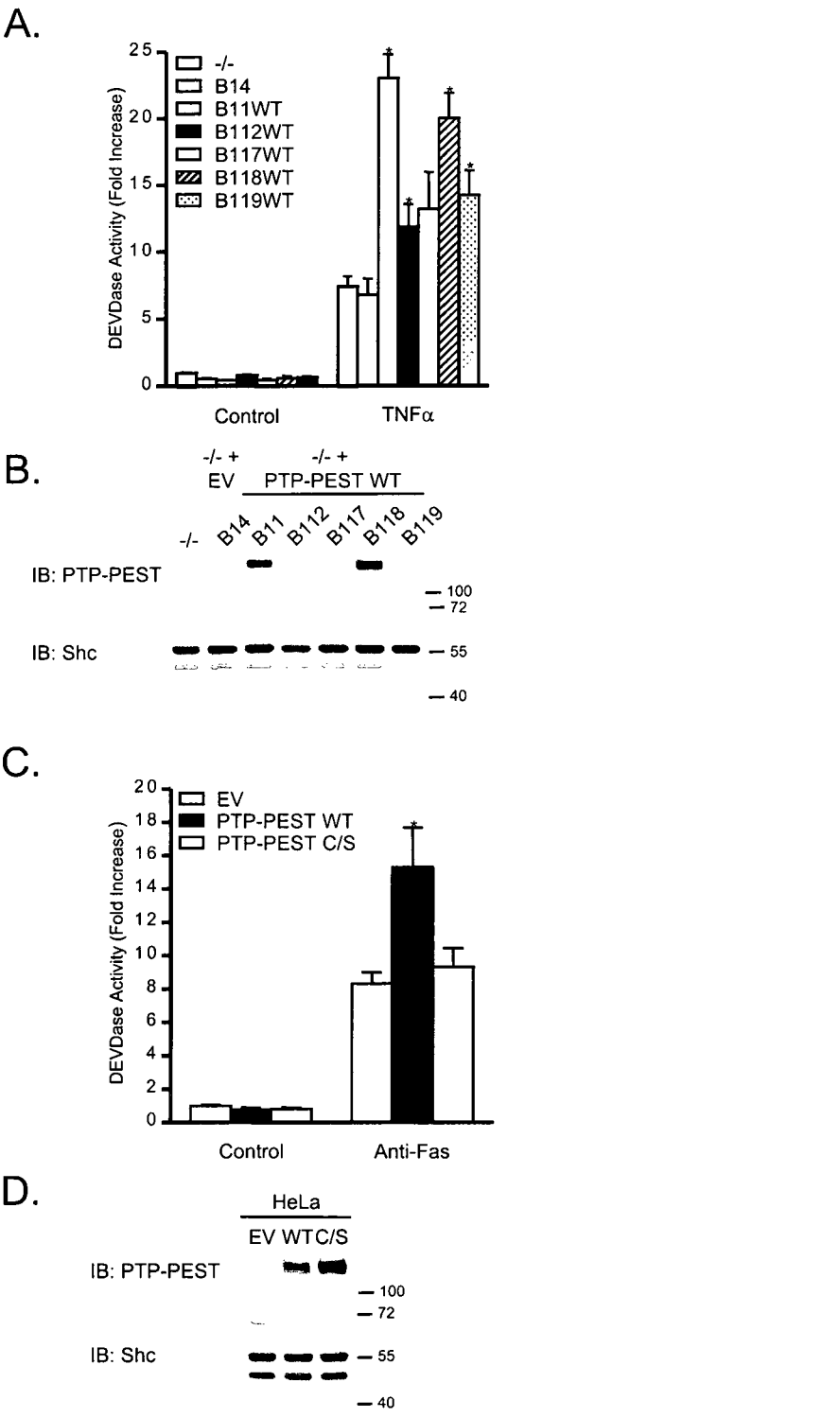
A.
DEVDase Activity (Fold Increase)
25
20
15
10
5
0
-/-
B14
B11WT
B112WT
B117WT
B118WT
B119WT
*
Control
TNFα
B.
-/- +
EV
-/- +
PTP-PEST WT
-/-
B14
B11
B112
B117
B118
B119
IB: PTP-PEST
IB: Shc
100
72
55
40
C.
DEVDase Activity (Fold Increase)
20
18
16
14
12
10
8
6
4
2
0
EV
PTP-PEST WT
PTP-PEST C/S
*
Control
Anti-Fas
D.
HeLa
EV WTC/S
IB: PTP-PEST
IB: Shc
100
72
55
40

FIG. 2

4.4.3 PTP-PEST is cleaved during apoptosis.

Several cytoskeletal proteins are degraded during apoptosis (112). Since PTP-PEST seems to play an important role in programmed cell death, we sought more insight into its regulation during apoptosis. We examined the consequences of activating the intrinsic or extrinsic apoptotic pathways on the integrity of PTP-PEST. Following stimulation of PTP-PEST -/- + WT clone with staurosporine or TNFα and treatment of transfected HeLa299 cells with cisplatin, the amount of full length PTP-PEST decreased in a time dependent fashion (Fig. 3A, C, E). PTP-PEST antibodies detected a protein fragment of approximately 60 kilodaltons (kD). Also, PTP-PEST degradation induced by staurosporine and cisplatin treatment resulted in diffuse bands detectable by SDS-PAGE at ~38 and ~30 kD (Fig. 3A, E). Treatment with tunicamycin induced similar PTP-PEST degradation (data not shown). Interestingly, under the same apoptotic conditions, p130Cas was also degraded and gave the typical band pattern described previously ((189) and Fig. 3B, D, F). We observed that PTP-PEST expression accelerated TNFα- and cisplatin-induced p130Cas degradation in rescued PTP-PEST -/- cells and in transfected HeLa cells (Fig. 3D, F). The enhanced p130Cas cleavage correlated with the increased DEVDase activity in PTP-PEST-WT-expressing cells (Fig. 2). Taken together, these results show that PTP-PEST is cleaved in a time-dependent manner during apoptosis triggered by the intrinsic cellular stress, DNA damage and the extrinsic pathways.

Figure 3. PTP-PEST is cleaved during apoptosis. PTP-PEST -/- EV and PTP-PEST -/- + WT cells (clones B14 and B11WT), described in figure 2, were treated with 1 μM staurosporine (A, B), with 10 μg/ml cycloheximide (control, C) or with 10 ng/ml TNFα in presence of 10 μg/ml cycloheximide for the indicated times (C, D). HeLa299 trasfected with either empty vector or with PTP-PEST WT cDNA were treated under control conditions (DMSO) or with 60 μM cisplatin for different periods of time (E, F). Longer exposure of the anti-PTP-PEST immunoblot is shown (E, bottom). Protein extracts were analyzed by immunoblot for PTP-PEST using 2530 rabbit antibody (A) or 2528 rabbit antibody (C, E) as well as for p130Cas (B, D, F). Filled arrowhead point to intact proteins and empty arrowheads identify degradation products. EV, empty vector, WT, wild type, IB, immunoblot. Values on the right correspond to the molecular sizes in kD.

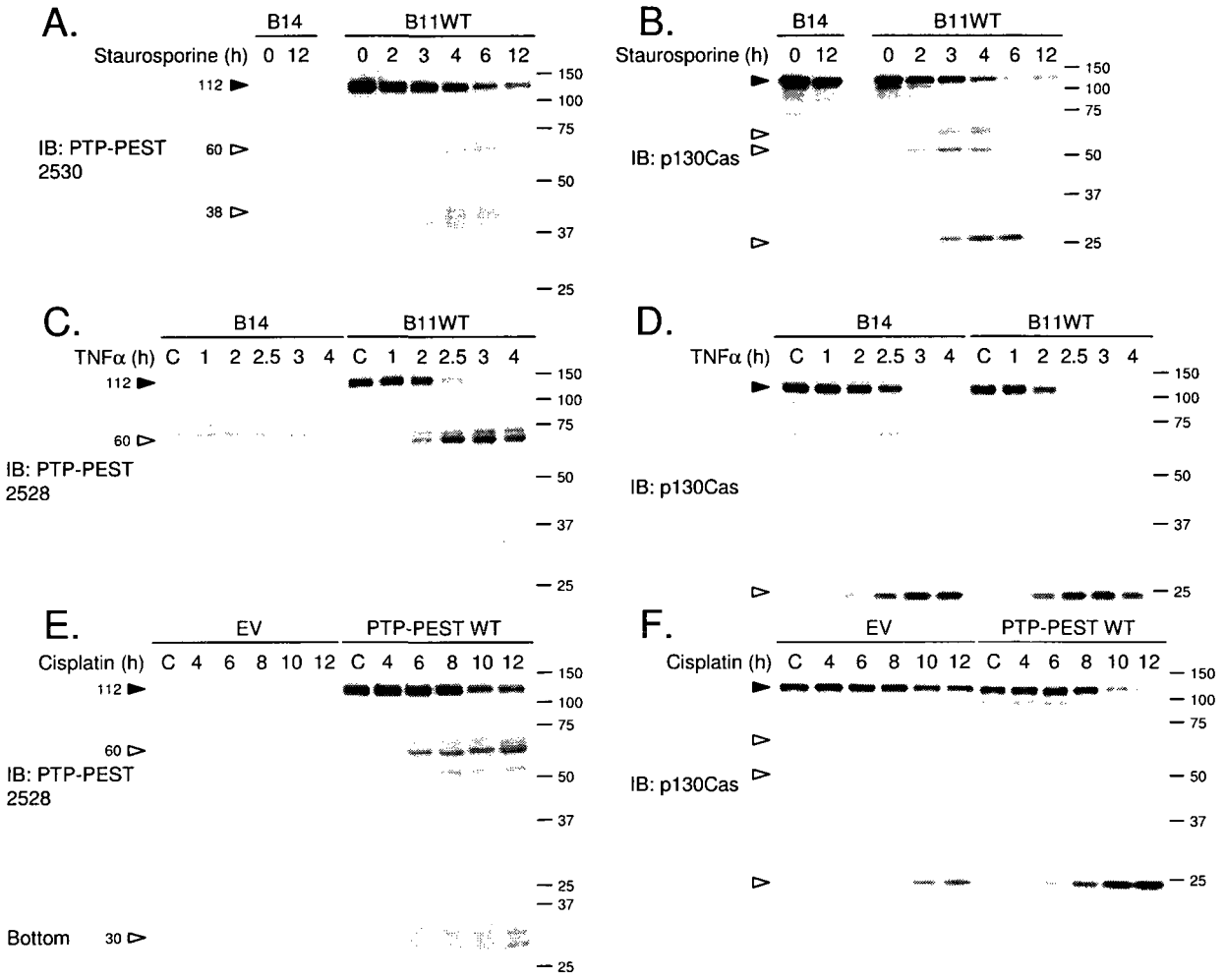
A.
B14
B11WT
Staurosporine (h) 0 12 0 2 3 4 6 12
112
60
38
IB: PTP-PEST 2530
150
100
75
50
37
25
B.
B14
B11WT
Staurosporine (h) 0 12 0 2 3 4 6 12
IB: p130Cas
150
100
75
50
37
25
C.
B14
B11WT
TNFα (h) C 1 2 2.5 3 4 C 1 2 2.5 3 4
112
60
IB: PTP-PEST 2528
150
100
75
50
37
25
D.
B14
B11WT
TNFα (h) C 1 2 2.5 3 4 C 1 2 2.5 3 4
IB: p130Cas
150
100
75
50
37
25
E.
EV
PTP-PEST WT
Cisplatin (h) C 4 6 8 10 12 C 4 6 8 10 12
112
60
IB: PTP-PEST 2528
Bottom 30
150
100
75
50
37
25
37
25
F.
EV
PTP-PEST WT
Cisplatin (h) C 4 6 8 10 12 C 4 6 8 10 12
IB: p130Cas
150
100
75
50
37
25

FIG. 3

4.4.4 Degradation of PTP-PEST during apoptosis is specific.

Increasing evidence in the literature implicates PTPs in the regulation of apoptotic signal transduction, but the mechanism of PTPs regulation is not largely understood and none of the classical PTPs have been reported to be cleaved during apoptosis. Therefore, we examined whether the cleavage of PTP-PEST during apoptosis was specific or reflected general processing of PTP family members. For this purpose, we employed a cell-free system in which dATP stimulates caspase activity (271). Control- and dATP-treated 293T cell extracts were analyzed by in-gel PTP assay in order to visualize the population of active PTPs (Fig. 4A). Following *in vitro* caspase activation, a PTP of approximately 115 kD became less abundant and the phosphatase activity of proteins migrating at ~78 and ~58 kD increased. Furthermore, the effect of dATP-mediated caspase activation seemed to be specific for these three bands since the signal corresponding to PTPs at other molecular weights remained unchanged. Under these conditions, we observed that the initiator caspases -8 and -9, as well as the effector caspases -3, and -7 were activated (Fig. 4B). To confirm the identity of the modulated PTPs (Fig. 4A), dATP-stimulated 293T cell extracts were subjected to immunodepletion with anti-PTP-PEST antibody prior to in-gel PTP assay. The efficiency of the immunodepletion was assessed by immunoblot (Fig. 4C, bottom). Our results suggest that the ~115 kD band corresponds to the non-cleaved form of PTP-PEST, while both the ~78 and ~58 kD signals represent truncated forms of the protein (Fig. 4C). To confirm these data *in vivo*, we took advantage of our PTP-PEST -/- cells in which either an empty vector or PTP-PEST were reintroduced and expressed in a stable manner. Following staurosporine stimulation, no significant changes could be observed in tyrosine phosphatase activity patterns among PTP-PEST -/- EV (B14, B15) clones analyzed (Fig. 4D and data not shown). In contrast, treatment of cells expressing PTP-PEST WT (B11) (as well as B118 clone, data not shown) led to a decrease of the 120 kD band and an increased activity detected near the 70 and 40 kD markers. PTP-PEST expression and

modulation were confirmed by immunoblot (data not shown). As expected, PTP-PEST catalytic activity is not required for its cleavage since PTP-PEST C231S mutant was also efficiently degraded during staurosporine treatment (data not shown). Among the enzymes detected by in-gel PTP assay, PTP-PEST is the predominant phosphatase showing variation during apoptosis. The generation of smaller bands with phosphatase activity, seen with expression of an active form of PTP-PEST, suggests that some cleaved products of this enzyme are potentially catalytically active.

We then investigated the integrity of particular members of the PTPs family during apoptosis. Following *in vitro* treatment with dATP, immunoblot analysis showed that only PTP-PEST signal, but not that of SHP-2, PTP-1B or TC-PTP was reduced (Fig. 5A). The stability of endogenous phosphatases was then confirmed in cell culture using spontaneously immortalized mouse embryonic fibroblast (MEFs). In cells exposed to TNFα, PTP-1B and TC-PTP remained intact whereas PTP-PEST was degraded as activation of caspase-3 occurred (Fig. 5B). Together, these results demonstrate that the cleavage of PTPs during apoptosis is not a general phenomenon among the family but is likely limited to specific members including PTP-PEST.

Figure 4. PTP-PEST is specifically cleaved during apoptosis. (A) Proteins were extracted from 293T cells, treated with or without 2 mM dATP for various times and subjected to in-gel PTP assay. (B) Activation of caspases in dATP-treated 293T cell extracts was confirmed by immunoblot with anti caspase-8, -9, -3 and -7. (C) 293T cell lysates treated with or without dATP were incubated with beads in presence or in absence of AG25 PTP-PEST antibody. Supernatants from bead control and PTP-PEST immunodepleted (ID) samples as well as PTP-PEST immunoprecipitate (IP) samples were subjected to in-gel PTP assay analysis. Control lysate, beads, immunodepleted and immunoprecipitated protein samples were analyzed for their content in actin and in PTP-PEST by immunoblot (bottom). (D) PTP-PEST -/- EV and PTP-PEST -/- + WT cells (clones B14 and B11WT), described in figure 2, were treated with 1 μM staurosporine for different periods of time, lysed and subjected to in gel-PTP assay. PTP-PEST expression in these samples was also confirmed by immunoblot (data not shown). Filled arrowheads indicate decreasing signals whereas empty arrowheads point increasing signals observed during the different treatments. IB, immunoblot, WT, wild type. Values on the right correspond to the molecular sizes in kD.

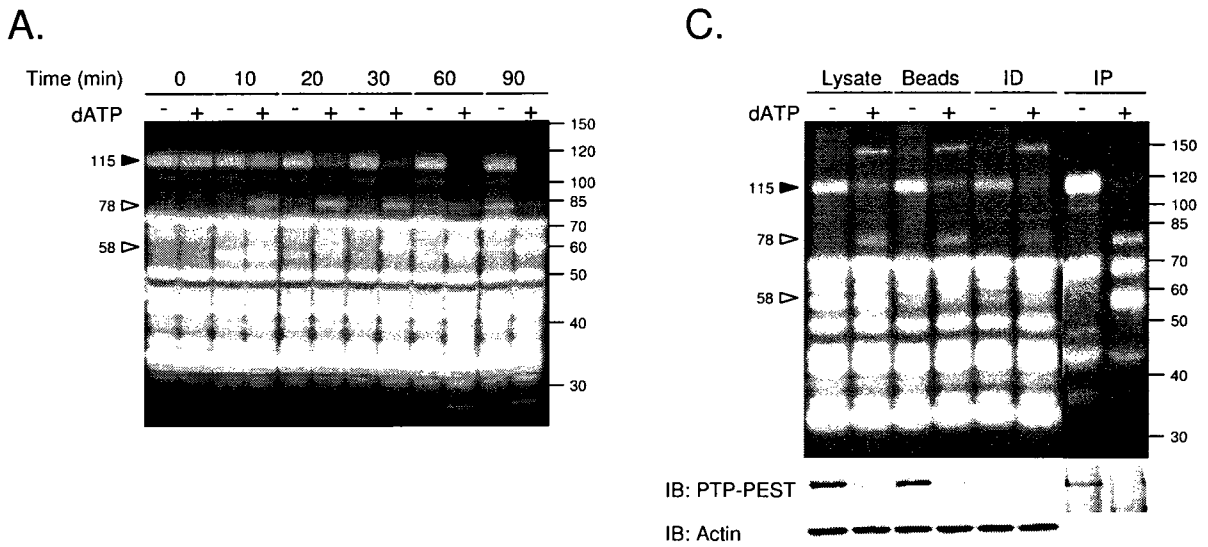
A.
Time (min)
0
10
20
30
60
90
dATP
115
78
58
150
120
100
85
70
60
50
40
30
C.
Lysate
Beads
ID
IP
dATP
115
78
58
150
120
100
85
70
60
50
40
30
IB: PTP-PEST
IB: Actin
B.
Time (min)
0
10
20
30
60
90
dATP
IB: Caspase-8
IB: Caspase-9
IB: Caspase-3
IB: Caspase-7
50
30
50
30
30
20
15
40
30
20
D.
B14
B11WT
Staurosporine (h)
0
4
6
8
150
120
100
85
70
60
50
40
30

FIG. 4

Figure 5. PTP-PEST, but not SHP-2, PTP-1B and TC-PTP is cleaved during apoptosis. (A) Caspases were activated *in vitro* in 293T cell lysates and the stability of different phosphatases was investigated by immunoblot using antibodies specific for SHP-2, PTP-1B (FG6), TC-PTP (CF4-1D) and PTP-PEST (AG25). (B) Spontaneously immortalized mouse embryonic fibroblast (MEFs) were incubated with 10 μg/ml cycloheximide in absence (control, C) or in presence of 10 ng/ml TNFα for the indicated times. Samples were analyzed by immunoblot for PTP-PEST (2528 rabbit antibody), TC-PTP (3E2), PTP-1B (rabbit polyclonal) and caspase-3. IB, immunoblot. Filled arrowhead point intact proteins and empty arrowheads identify cleavage products. Values on the right correspond to the molecular sizes in kD.

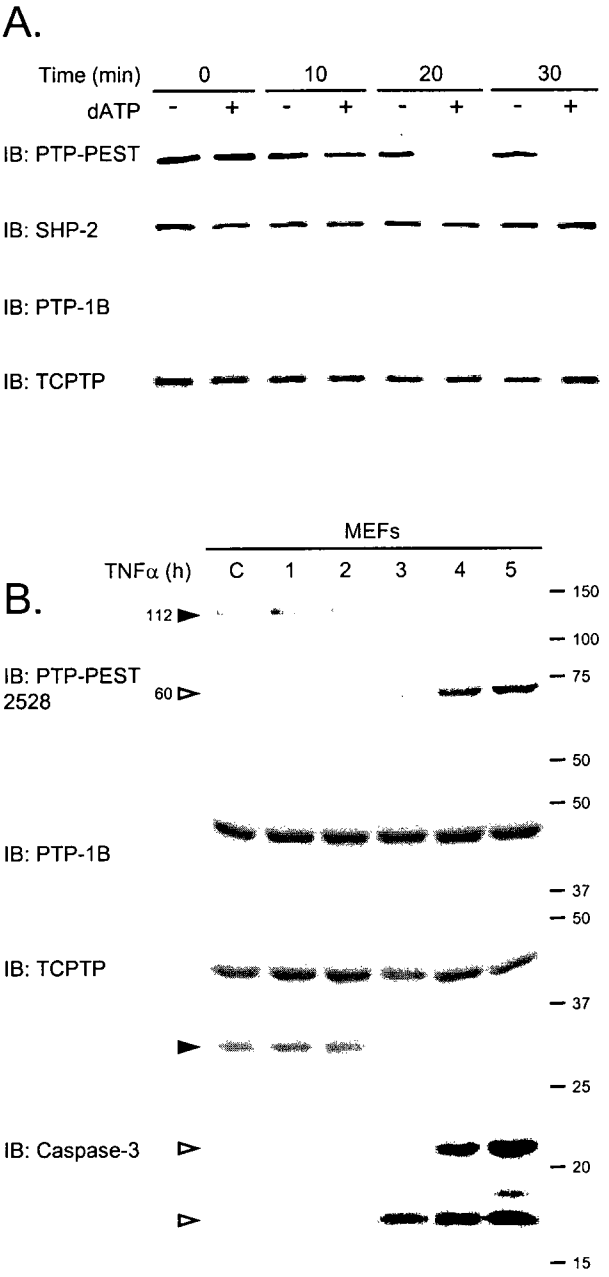
A.
Time (min)
0
10
20
30
dATP
- + - + - + - +
IB: PTP-PEST
IB: SHP-2
IB: PTP-1B
IB: TCPTP
B.
MEFs
TNFα (h)
C 1 2 3 4 5
112
60
150
100
75
50
50
37
50
37
25
20
15
IB: PTP-PEST 2528
IB: PTP-1B
IB: TCPTP
IB: Caspase-3

FIG. 5

4.4.5 PTP-PEST is a substrate of caspase-3.

Degradation of PTPs caused by UV irradiation was recently shown to be dependent on activation of calpain, a group of proteases activated during apoptosis (130, 302). In addition, in apoptotic cells, several proteins, including molecules involved in cell adhesion and cytoskeletal network organization, are substrate of caspases (112). In order to identify whether calpain or caspase are responsible for PTP-PEST degradation *in vivo*, apoptosis was induced in cells expressing PTP-PEST (clone B11) in the presence of specific pharmacological inhibitors. Degradation of PTP-PEST induced by staurosporine was prevented by the caspase inhibitor Z-VAD, but not by the calpain inhibitor PD150606 (Fig. 6A). In Rat-1 cells, inhibition of caspase by Z-VAD also blocked degradation of endogenous PTP-PEST (data not shown). The proteasome inhibitor lactacystin did not impair efficient PTP-PEST proteolysis during apoptosis (data not shown). The cleavage of PTP-PEST occurred in parallel with that of p130Cas and with the activation of caspase-3 (Fig. 6A). This experiment reveals that caspases are the proteases responsible for PTP-PEST cleavage during apoptosis.

To determine which caspase cleaves PTP-PEST, caspase-3, -7 and -9 were individually immunodepleted from 293T lysates prior addition of dATP. Samples were then subjected to in-gel PTP assay. Immunodepletion of caspase-7 did not interfere with the cleavage of PTP-PEST (Fig. 6B). Conversely, immunodepletions of either caspase-3 or caspase-9 could block the cleavage of PTP-PEST. Under these conditions, caspase-3 requires active caspase-9 for its induction (109). Since caspase-9 was still present following caspase-3 immunodepletion, these results suggest that only caspase-3 was responsible for this cleavage. Immunoblot analysis performed on supernatant demonstrated that specific immunodepletion of caspase-3, -7 and -9 was obtained (Fig. 6B, bottom). Caspase-8 was excluded from the immunodepletion analysis, since its activation occurred following the rapid cleavage of PTP-PEST (Fig. 4A, B). In contrast, the

activation of caspase-3 *in vitro* and *in vivo* (see Fig. 4, 5 and 6) was concomitant with the proteolysis of PTP-PEST. In order to verify that active caspase-3 could directly cleave PTP-PEST, we incubated cell extracts (Fig. 6C) and purified GST-PTP-PEST (Fig. 6D) with the recombinant active caspase-3. As depicted in figure 6C, addition of active purified caspase-3 to lysates from PTP-PEST-expressing cells led to a similar degradation pattern as previously observed *in vivo* (Fig. 3 and 6C). p130Cas was also cleaved under these conditions, and the cleavage products typically generated during apoptosis were obtained (Fig. 6C and (189). Importantly, caspase-3 could cleave purified GST-PTP-PEST, suggesting that other proteins were not required for the proteolysis (Fig. 6D). Together, these observations indicate that caspase-3 cleaves PTP-PEST during apoptosis. To our knowledge, this is the first example of a classical PTP directly cleaved by a caspase.

Figure. 6. Caspase-3 cleaves PTP-PEST. (A) To inhibit caspases or calpain proteases, PTP-PEST -/- + WT cells (clones B11WT) were pre-incubated with either 100 μM Z-VAD-FMK or 100 μM PD150606 for 2 h and subsequently treated with 1 μM staurosporine in presence of the indicated inhibitor for an additional 6 h. Protein lysates were then subjected to immunoblot analysis for PTP-PEST (2528 and 2530 rabbit polyclonal), p130Cas and caspase-3. (B) 293T cell extracts were immunodepleted (ID) for either caspase-3, caspase-9 or caspase-7, treated with dATP for the indicated time and subjected to in-gel PTP assay. Presence of caspase-9, -3 and -7 in the immunodepleted samples was verified by immunoblot (bottom). (C) Protein lysates from PTP-PEST -/- EV (B14) and WT rescued (B11WT) cells were incubated with active recombinant caspase-3 or under control conditions (C) for the indicated times. Samples were further analyzed by immunoblot for PTP-PEST (2528 rabbit polyclonal) and p130Cas. (D) GST or GST-PTP-PEST were isolated from transfected PTP-PEST -/- cells, incubated with active recombinant caspase-3 or under control conditions (C) and analyzed by immunoblot using anti-GST antibody. Filled arrowheads point intact proteins and empty arrowheads identify cleavage products. Values on the right correspond to the molecular sizes in kD. IB, immunoblot.

A.

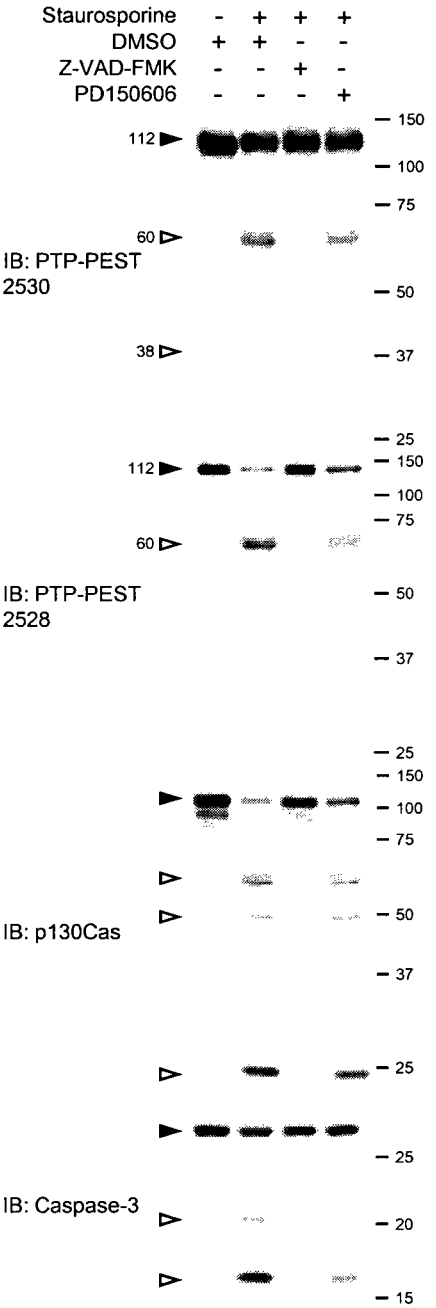
Staurosporine - + + +
DMSO + + - -
Z-VAD-FMK - - + -
PD150606 - - - +
112
60
IB: PTP-PEST 2530
38
112
60
IB: PTP-PEST 2528
IB: p130Cas
IB: Caspase-3
150
100
75
50
37
25
20
15

FIG. 6A

B.

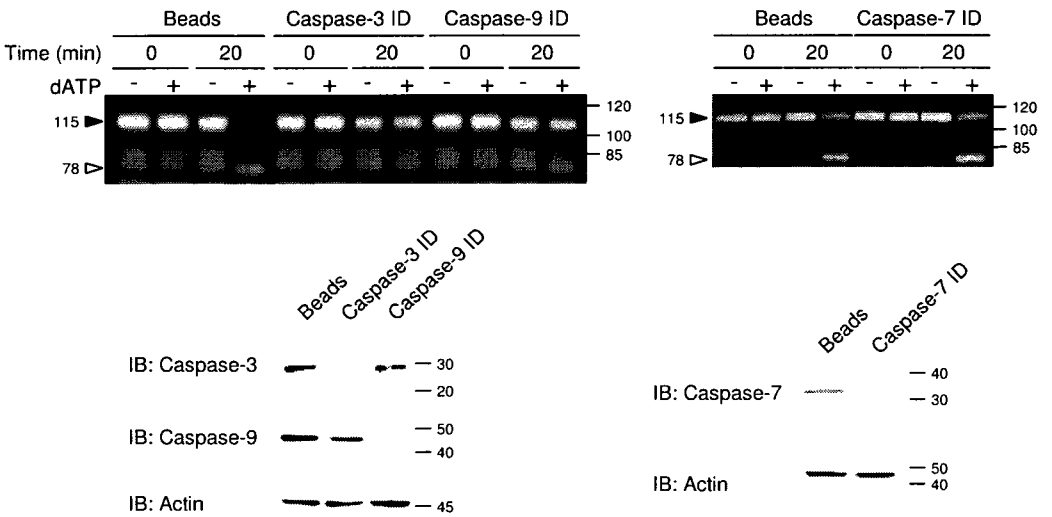

C.

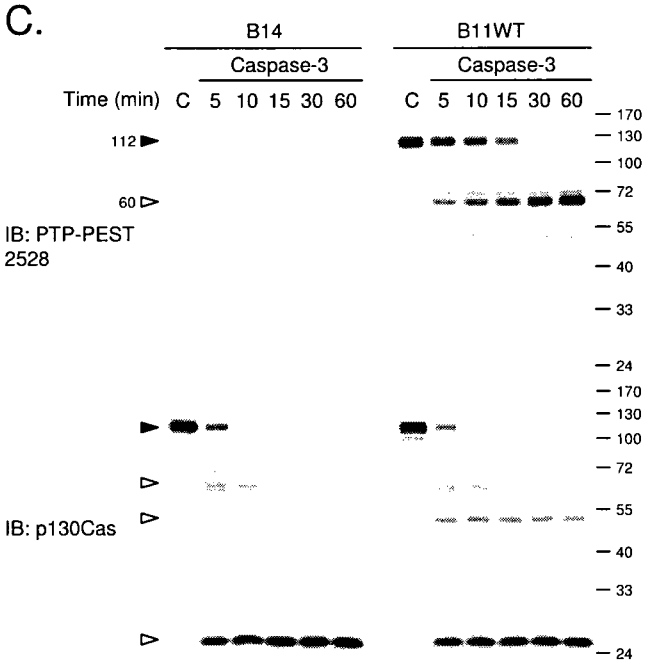

D.

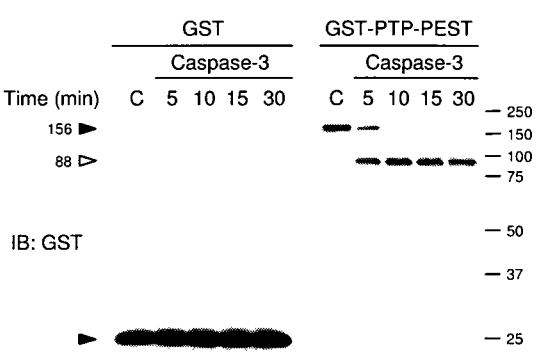

FIG. 6B, C and D

4.4.6 Caspase-3 cleaves PTP-PEST on its ^{549}DSPD site.

The analysis of the murine PTP-PEST sequence revealed the presence of several potential caspase cleavage sites (Fig. 7A). We mutated each DXXD motif individually in PTP-PEST cDNA (^{549}DSPD to ^{549}ASPA, ^{604}DDSD to ^{604}ADSA, ^{740}DKKD to ^{740}AKKA) and inserted it between sequences corresponding to myc-ECFP and EYFP tags.

Protein extracts from HeLa299 cells expressing the different mutants of PTP-PEST were incubated with or without caspase-3 and subjected to immunoblot analysis. An anti-GFP antibody, which recognizes both ECFP and EYFP, revealed that following incubation with caspase-3, two fragments of approximately 110 kD and 63 kD appeared when WT, ^{604}ADSA and ^{740}AKKA forms of PTP-PEST were expressed (Fig. 7B). The ^{549}ASPA mutation was sufficient to completely prevent cleavage of PTP-PEST by caspase-3. These observations establish that caspase-3 cleaves PTP-PEST into two main fragments by targeting its ^{549}DSPD motif. Detection of the myc-epitope tag identified the 110 kD cleavage product as the N-terminal portion of PTP-PEST that contains its catalytic domain whereas the 63 kD fragment revealed by anti-GFP immuno blot corresponded to the C-terminal segment. With regards to the *in vivo* situation, PTP-PEST was cleaved during cisplatin-induced apoptosis of HeLa cells. Efficient proteolysis of PTP-PEST depended on the ^{549}DSPD site since its mutation to ^{549}ASPA significantly reduced its degradation *in vivo* (Fig. 7C). Importantly, this mutation abolished the generation of the ~60 kD product and of the smaller fragments near 30 kD. The degradation of p130Cas occurred in a similar fashion in both WT and ^{549}ASPA PTP-PEST expressing cells (Fig. 7C). Moreover, as previously observed in figure 3, the rate of p130Cas degradation was more apparent in PTP-PEST-expressing cells than in vector controls. This demonstrates that caspase-3 cleaves PTP-PEST at ^{549}DSPD while apoptotic cell death progresses.

Figure 7. Caspase-3 cleaves PTP-PEST on its ^{549}DSPD site. (A) Schematic views of murine PTP-PEST showing the catalytic domain (PTP), the five regions rich in proline (Pro1, Pro2, Pro3, Pro4 and CTH) and the Shc binding domain (SBD). Four potential caspase cleavage sites (^{423}EHID, ^{549}DSPD, ^{604}DDSD, ^{740}DKKD) are indicated. Stars (*) identify the amino acids targeted by mutagenesis. (B) Lysates from HeLa299 expressing EGFP or different version of myc-ECFP-PTP-PEST-EYFP were prepared, incubated with or without active recombinant caspase-3 and analyzed by immunoblot using antibodies directed against GFP and myc (9E10). (C) HeLa299 cells transfected with a non-tagged version of PTP-PEST in pcDNA3 (EV, WT, ^{549}ASPA) were incubated with 60 μM cisplatin for the indicated times and lysed as described in materials and methods. Protein lysates were resolved by SDS-PAGE and analyzed by immunoblot for PTP-PEST (2528 rabbit polyclonal) and p130Cas. (C, bottom) Longer exposure of the anti-PTP-PEST immunoblot is shown. Filled arrowheads point intact proteins and empty arrowheads identify cleavage products. EV, empty vector, WT, wild type, IB, immunoblot. Values on the right correspond to the molecular sizes in kD.

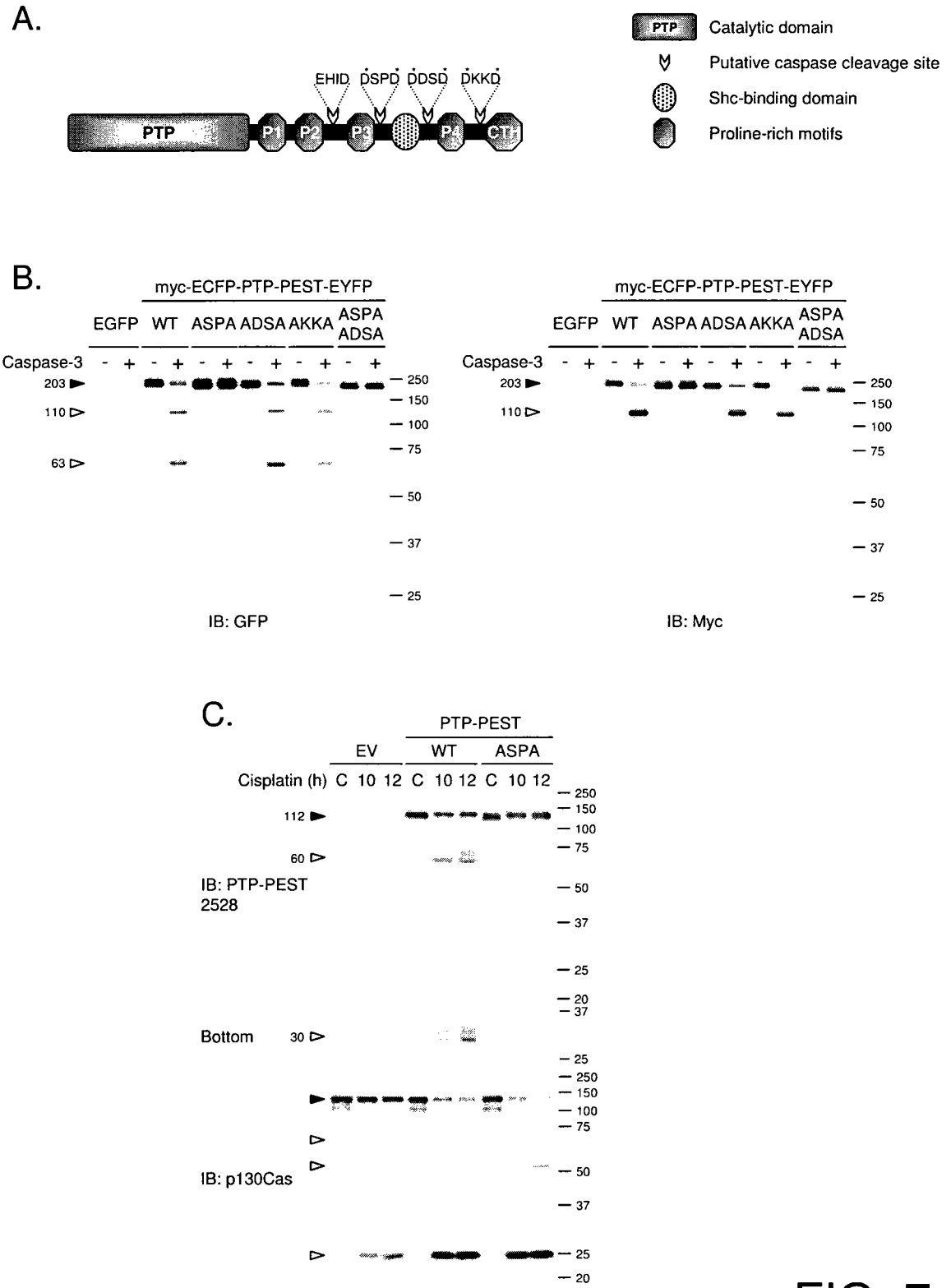
A.
PTP
Catalytic domain
Putative caspase cleavage site
Shc-binding domain
Proline-rich motifs
EHID
DSPD
DDSD
DKKD
PTP
P1
P2
P3
P4
CTH
B.
myc-ECFP-PTP-PEST-EYFP
EGFP
WT
ASPA
ADSA
AKKA
ASPA ADSA
Caspase-3
203
110
63
250
150
100
75
50
37
25
IB: GFP
IB: Myc
C.
PTP-PEST
EV
WT
ASPA
Cisplatin (h) C 10 12 C 10 12 C 10 12
112
60
IB: PTP-PEST 2528
Bottom
30
IB: p130Cas
20

FIG. 7

4.4.7 Caspase-3 regulates PTP-PEST activity, interactions and adaptor function.

Cleavage of proteins involved in organizing the actin cytoskeleton affects their properties, redistributes them to different protein complexes and modifies their functions (112, 185). We observed that the catalytic activity of PTP-PEST was important for its ability to increase sensitivity to receptor-mediated apoptosis. To evaluate the effect of caspase-3 on PTP-PEST catalytic activity, purified GST-hPTP-PEST from 293T transfected cells was incubated in the presence or absence of caspase-3 followed by an in-solution phosphatase assay. Figure 8A shows that after caspase-3 proteolysis, PTP-PEST exhibited an approximately two fold increase in catalytic activity. Immunoblot with anti-GST showed the efficiency of the treatment with caspase-3. These observations indicate that caspase-3 regulates PTP-PEST catalytic activity in a cleavage-dependent manner.

To understand how caspase-3 could affect PTP-PEST function, we investigated whether the cleavage of PTP-PEST could regulate its ability to interact with signaling molecules. Located at the amino terminus, the catalytic domain of PTP-PEST is followed by a carboxy-terminal (C-terminal) tail. This segment contains a Shc binding domain (SBD) and five proline-rich segments among which the second (P2) interacts with paxillin family members (paxillin, Hic-5 and leupaxin), the fourth (P4) recruits Csk and the fifth, termed CTH, associates with PSTPIP (53, 85, 86, 94, 131, 243). We used an *in vitro* approach to characterize the effect of caspase-3 on PTP-PEST interactions as described in figure 8B. GST-PTP-PEST was purified from PTP-PEST -/- transfected cells and incubated with primary MEF (P-MEF) cell lysate in order to reconstitute PTP-PEST protein complexes. As expected, intact PTP-PEST can interact with Shc (p52 and p66), paxillin and leupaxin (Fig. 8C, GST-PTP-PEST lanes 1, 4). When PTP-PEST was cleaved before incubation with lysates, the N-terminal fragment failed to bind Shc, whereas paxillin and leupaxin interactions were maintained (Fig. 8C, GST-PTP-PEST lane 2). We

also investigated the effect of caspase-3 cleavage on PTP-PEST protein complexes following *in vitro* reconstitution (Fig. 8C, GST-PTP-PEST lanes 3, 5). Under these conditions, caspase-3 drastically decreased the association of PTP-PEST with Shc and leupaxin but only slightly affected recruitment of paxillin (Fig. 8C, GST-PTP-PEST compare lane 4 with 5). Paxillin and leupaxin have been previously identified as caspase-3 substrate, which explains their reduced affinity for PTP-PEST following treatment with active caspase-3 *in vitro* (59). The interactions observed in that experiment were specific to PTP-PEST as they were not detected with the GST tag alone (Fig. 8C, GST). The impact of active caspase-3 on PTP-PEST interactions was then measured using the ^{549}ASPA mutant. Samples were processed as condition 1 and 2 depicted in figure 8B. Prior incubation with caspase-3 was sufficient to abolish the interaction between the PTP-PEST (WT) N-terminal fragment and Shc without affecting the interaction with paxillin and leupaxin (Fig. 8D). The ^{549}ASPA mutations of PTP-PEST efficiently reverted the caspase-3 mediated dissociation of Shc. Finally, we examined the effect of caspase-3 on the C-terminal region of PTP-PEST (Fig. 8E) using lysates of cells co-expressing myc-ECFP-PTP-PEST-EYFP (WT or ^{549}ASPA) with GST-PSTPIP. Whole cell extracts were incubated with or without active caspase-3, and PSTPIP was pulled down using glutathione sepharose beads. We noticed that following incubation with caspase-3, PSTPIP could interact with a shorter form of PTP-PEST-WT (Fig. 8E, immunoblot anti-GFP, top panel). This fragment was identified as the PTP-PEST C-terminal cleavage product because it could not be detected by anti-myc antibody (Fig. 8E). Caspase-3 cleavage of PTP-PEST did not inhibit the interaction with PSTPIP, as binding was seen to both the intact protein and the C-terminal fragment (Fig. 8E). In addition, no detectable caspase-3 cleavage of PSTPIP was observed under these conditions. These results support the model that the action of caspase-3 on PTP-PEST prevents its catalytic domain from associating with leupaxin, Shc (p52 and p66), PSTPIP and to a lesser extent with paxillin. This is due to the action of caspase-3 on both PTP-PEST, at the ^{549}DSPD site, and leupaxin/paxillin. In addition, caspase-3 cleavage of PTP-PEST liberated a C-terminal fragment that was still able to interact with PSTPIP. Together, these results implicate

active caspase-3 in the modulation of both the catalytic activity and the interactions of PTP-PEST.

Figure 8. Caspase-3 regulates PTP-PEST activity and interactions of protein complexes. (A) GST-hPTP-PEST was isolated from transfected 293T cells, incubated with or without caspase-3 and subjected to in-solution phosphatase assays as described in materials and methods section. GST, GST-PTP-PEST (C, D) and GST-PTP-PEST ^{549}ASPA (D) were isolated from transfected PTP-PEST -/- cells. (B) Schematic representation of the approach used to investigate the effect of caspase-3 on the different protein-protein interactions. (C) Samples were processed (see numbers 1 to 5 outlined in B and materials and methods) and subjected to immunoblot analysis with antibody directed against Shc, paxillin and GST. (D) Samples were processed as number 1 and 2 described in B then examined by immunoblot with anti-Shc, anti-paxillin and anti-GST antibodies. (E) PTP-PEST -/- cells transiently co-expressing GST-PSTPIP with either EGFP, myc-ECFP-PTP-PEST (WT)-EYFP or myc-ECFP-PTP-PEST (^{549}ASPA)-EYFP were lysed, treated with or without active recombinant caspase-3 and GST-PSTPIP was isolated using glutathione sepharose beads. Isolated GST-PSTPIP and bound PTP-PEST were detected by immunoblot using antibodies directed against GFP, GST and myc. The expression of EGFP and PTP-PEST fusion proteins was also verified by immunoblotting the cell lysates. Filled arrowheads point intact proteins and empty arrowheads identify cleavage products. IB, immunoblot, WT, wild type, TCL, total cell lysate. Values on the right correspond to the molecular sizes in kD.

A.

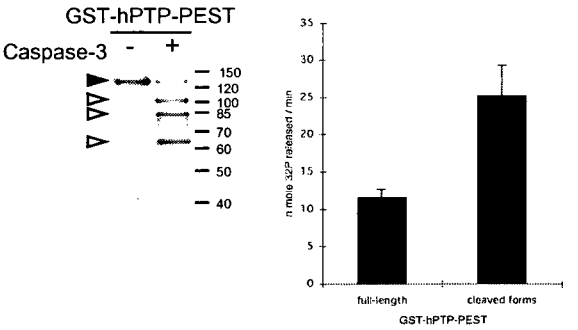

B.

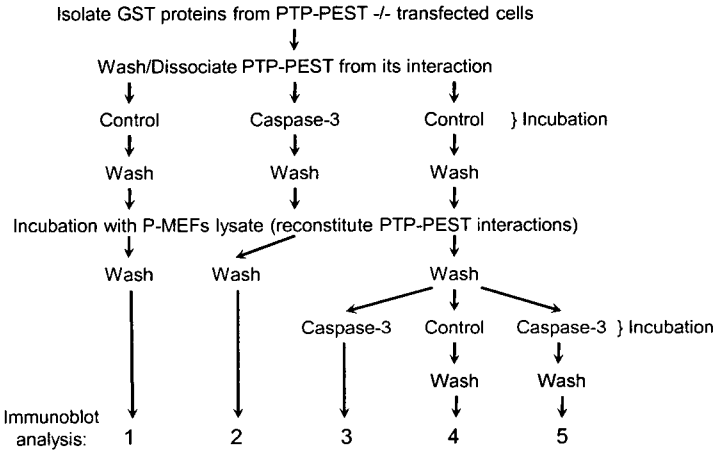

C.

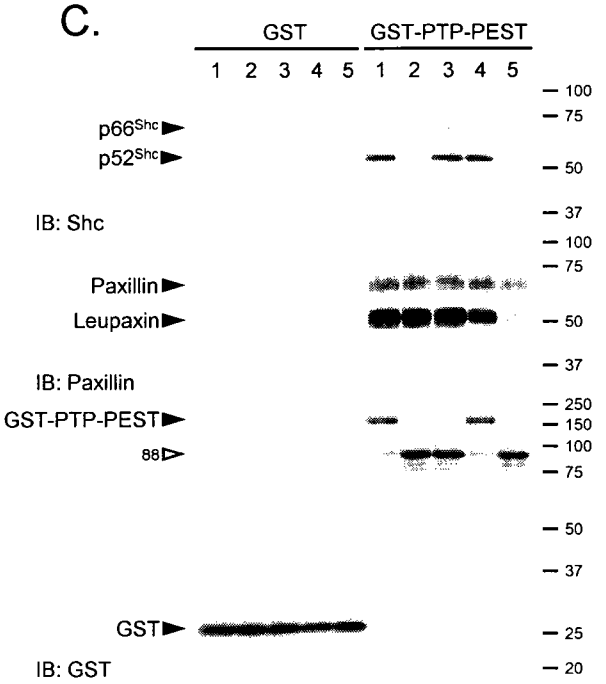

D.

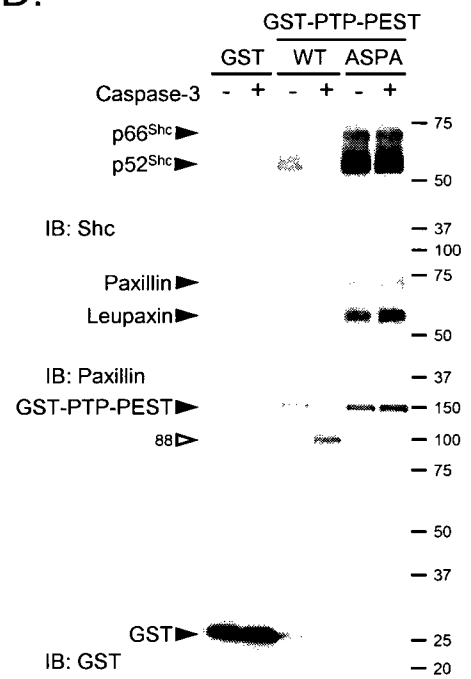

FIG. 8A, B, C and D

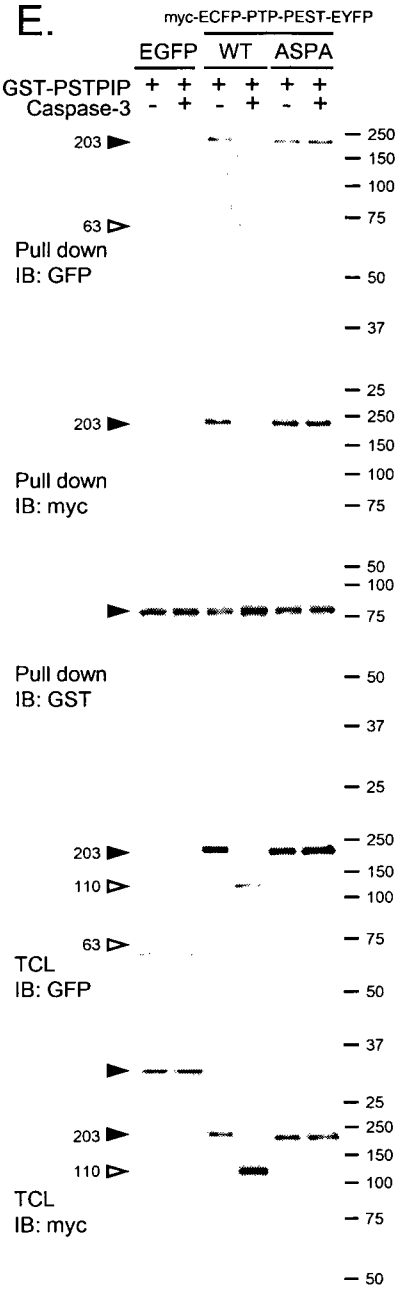
E.
myc-ECFP-PTP-PEST-EYFP
EGFP
WT
ASPA
GST-PSTPIP + + + + + +
Caspase-3 - + - + - +
203
63
Pull down
IB: GFP
250
150
100
75
50
37
25
Pull down
IB: myc
Pull down
IB: GST
110
TCL
IB: GFP
TCL
IB: myc

FIG. 8E

The numerous partners reported to interact with the carboxy-terminal end of PTP-PEST are indicative of an adaptor function. To support this premise, we investigated the capability of PTP-PEST to bridge PSTPIP to new interacting partner. As observed in figure 9, PSTPIP associated with PTP-PEST was also recruited to paxillin, Shc and Csk. In contrast, a mutant version of PSTPIP (W232A), which is unable to bind PTP-PEST (85), failed to associate with paxillin, Shc and Csk (Fig. 9A). These complexes were also specifically observed when the WT but not the W232A form of PSTPIP was expressed in the PTP-PEST -/- + WT cells (clone B11) (data not shown). These results suggest that PTP-PEST has the ability to perform adaptor functions that link PSTPIP toward paxillin, Shc or Csk. To define the consequence of caspase activation on PTP-PEST scaffolding functions, we examined the proteins associated with PSTPIP in cells co-expressing GST-PSTPIP with either WT or ^{549}ASPA mutant of myc-ECFP-PTP-PEST-EYFP during treatment with anti-Fas. As apoptosis progressed, the association of PSTPIP with the intact form of PTP-PEST WT was diminished, while the interaction with the PTP-PEST C-terminal fragment increased (Fig. 9A). This paralleled a decreased association of PSTPIP with paxillin. In contrast, the associations of PSTPIP with Shc and Csk were maintained during apoptosis. This modulation did not occur when PTP-PEST ^{549}ASPA was expressed since paxillin, Shc, Csk and intact PTP-PEST co-precipitated with PSTPIP during apoptotic progression. The isolation of each GST fusion proteins was confirmed by immunoblot. Figure 9B shows the expression of PTP-PEST in the different conditions, and the activation of caspase-3 following treatment with anti-Fas. The reduction of paxillin interacting with PSTPIP indicates that the scaffolding function of PTP-PEST is modulated by caspase cleavage on its ^{549}DSPD site during apoptosis. In addition, the preserved association of PSTPIP with Shc and Csk suggests that the PTP-PEST C-terminal cleavage product is competent to perform these associations. Together, these data support that PTP-PEST adaptor functions are modulated in cells undergoing apoptosis.

Figure 9. Scaffolding function of PTP-PEST is modulated during apoptosis. (A) HeLa299 cells co-transfected with cDNA encoding for either GST or GST-PSTPIP (WT or W232A) with myc-ECFP-PTP-PEST (WT or ^{549}ASPA)-EYFP were treated with 10 μg/ml cycloheximide in absence (control, C, 6 h) or in presence of 50 ng/ml anti-Fas for the indicated times. Lysates extracted from cells were incubated with glutathione sepharose beads and the ability of the expressed GST fusion protein to interact with other partners was determined by immunoblotting. The co-precipitated paxillin, Shc, Csk and PTP-PEST were analyzed by immunoblotting for the indicated proteins and epitopes. Filled arrowheads point intact PTP-PEST and empty arrowheads indicate cleavage products. (B) Total cell extracts were subjected to immunoblotting with anti-GFP, 9E10 (anti-myc) and anti-caspase-3. Filled arrowheads point to intact PTP-PEST or caspase-3 and empty arrowheads indicate cleavage products. IB, immunoblot, WT, wild type, TCL, total cell lysate. Values on the right correspond to the molecular sizes in kD.

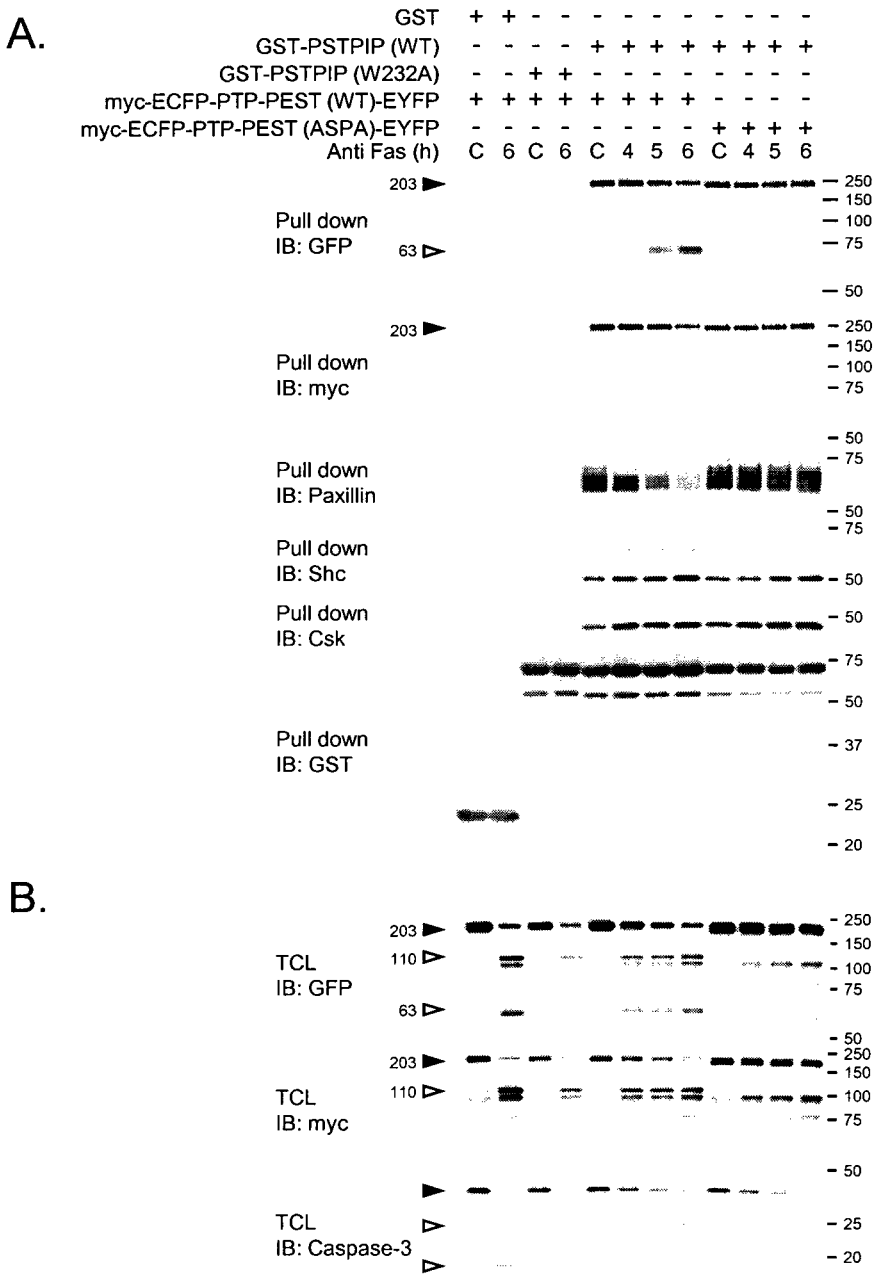
A.
GST
GST-PSTPIP (WT)
GST-PSTPIP (W232A)
myc-ECFP-PTP-PEST (WT)-EYFP
myc-ECFP-PTP-PEST (ASPA)-EYFP
Anti Fas (h)
C 6 C 6 C 4 5 6 C 4 5 6
Pull down
IB: GFP
Pull down
IB: myc
Pull down
IB: Paxillin
Pull down
IB: Shc
Pull down
IB: Csk
Pull down
IB: GST
B.
TCL
IB: GFP
TCL
IB: myc
TCL
IB: Caspase-3

FIG. 9

4.4.8 Caspase cleavage of PTP-PEST facilitates cellular detachment during apoptosis.

Caspase-mediated proteolysis of cytoskeletal protein causes membrane blebbing, cell rounding and adhesion lost as apoptosis progress (77, 112). The localization of PTP-PEST to the retracting membrane ruffles and its caspase-3-dependent modulation infers that the regulation of this enzyme could participate in cellular detachment during apoptosis. To determine whether the cleavage of PTP-PEST during apoptosis plays a role in loss of adhesion, we used flow cytometry to count the number of cells remaining attached to the culture dish following treatment with anti-Fas. Incubation of HeLa299 cells expressing EGFP-PTP-PEST (WT or ^{549}ASPA) with anti-Fas decreased the number of cells attached to the culture dish (Fig. 10A). Interestingly, the proportion of cells that have detached during the progression of apoptosis was significantly diminished in ^{549}ASPA mutant as compared to WT PTP-PEST expressing cells (Fig. 10B). Two hours following anti-Fas treatment, ^{549}ASPA PTP-PEST mutant expressing cells exhibited a two-fold decrease in the loss of adhesion versus those expressing WT PTP-PEST. Moreover, at 4 h, detachment of cells harboring the ^{549}ASPA mutant was delayed compared to PTP-PEST WT expressing cells as revealed by a three-fold decrease in adhesion lost. These results identify that cleavage of PTP-PEST by caspase-3 contributes to cellular detachment during apoptosis.

Figure 10. Caspase cleavage of PTP-PEST facilitates cellular detachment during apoptosis. (A) HeLa299 cells expressing either EGFP-PTP-PEST WT or EGFP-PTP-PEST ^{549}ASPA were incubated with 10 μg/ml cycloheximide in absence (control) or in presence of 50 ng/ml anti-Fas. Following treatment, adherent cells were harvested and counted using flow cytometry as described in materials and methods. Cells expressing EGFP-PTP-PEST (WT or ^{549}ASPA) were selected based on fluorescence intensity (inset). The area between the control curve and the anti-Fas stimulated curve correspond to the number of cells that have detached during the treatment. (B) Values are the percentage of cellular detachment over control and represent means ± S.E. of two independent experiments in which each condition was performed in triplicate and each sample was analyzed three times by flow cytometry. Asterisks denote values significantly different from EGFP-PTP-PEST WT expressing cells (*, $p < 0.05$; **, $p < 0.01$).

A.

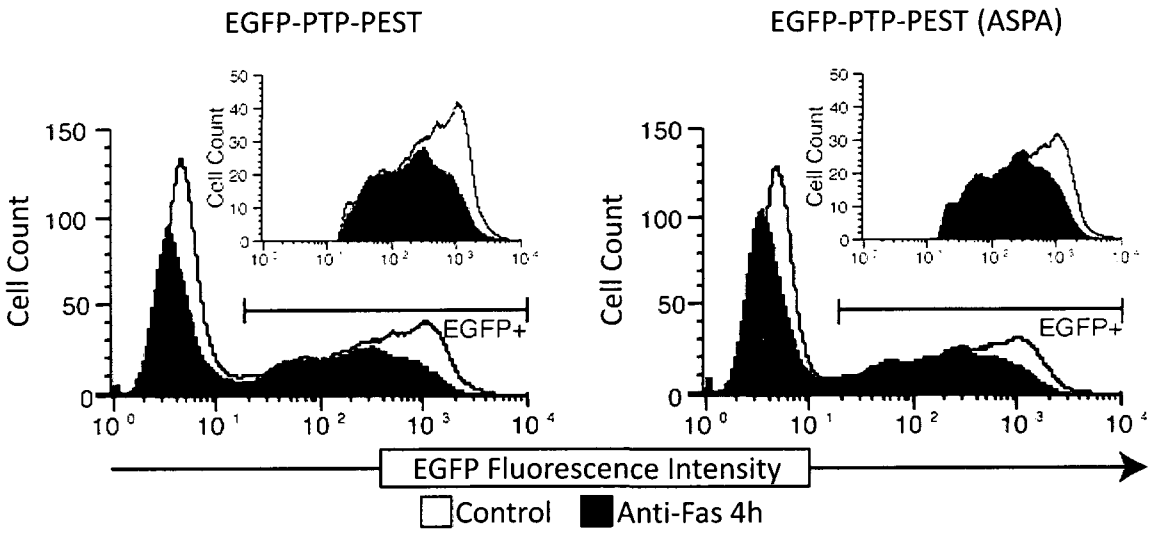
EGFP-PTP-PEST
EGFP-PTP-PEST (ASPA)
Cell Count
EGFP+
EGFP Fluorescence Intensity
Control
Anti-Fas 4h

B.

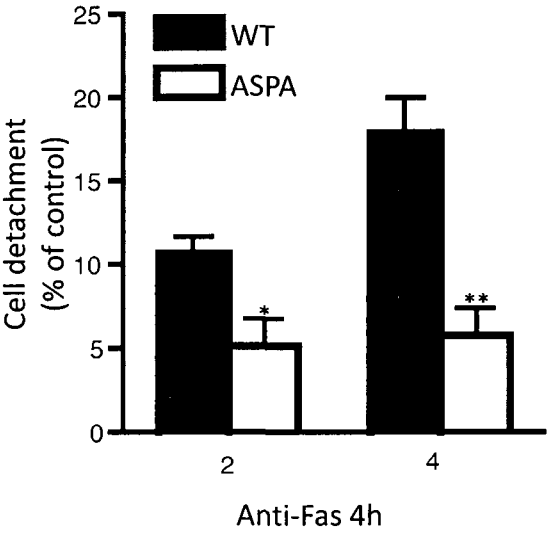
WT
ASPA
Cell detachment (% of control)
Anti-Fas 4h

FIG. 10

4.5 Discussion

Ubiquitous expression of PTP-PEST maintained throughout development and in adult animals points towards a fundamental biologic role for this enzyme (56). Indeed, mice lacking the PTP-PEST gene exhibit severe developmental defects leading to embryonic lethality (84, 305). PTP-PEST accomplishes several of its functions through the regulation of the actin cytoskeleton (12, 203). Nevertheless, the contribution and the regulation of PTP-PEST have not been investigated in apoptosis, a physiological phenomenon essential for proper development involving major cytoskeletal rearrangement. Here, we provide the first evidence that PTP-PEST plays a role in the progression of apoptotic cell death. Importantly, we have identified PTP-PEST as a new caspase substrate and linked its caspase-mediated cleavage and modulation to the process of cell detachment during apoptosis.

PTP-PEST was previously reported to regulate membrane ruffling, cell adhesion and spreading; proper balance of these physiological processes is crucial for cell migration (11, 120, 286). Functions involving p130Cas, Rac, WASP, paxillin, PKL and VAV2 are suggested to couple PTP-PEST to the modulation of the cytoskeleton organization in migrating cells (11, 18, 85, 86, 120, 172, 286, 287). Interestingly, several proteins that govern cell migration are modulated during apoptosis in order to remodel cell shape (77). The effects of PTP-PEST on signaling cascades that orchestrate actin dynamics led us to explore its possible modulation in apoptotic cell death. In growing cells, PTP-PEST is reported to be primarily localized in the cytosol (11, 85). However, in cells undergoing apoptosis, we observed concurrent localization of PTP-PEST to retracting lamellipodia as well as the cytosol. The exact mechanism by which PTP-PEST is specifically targeted to the edge of retracting lamellipodia is still unknown, but it is possible that some of the mechanisms involved in detachment of apoptotic cells are conserved with those controlling tail retraction in cells undergoing polarized migration. Indeed, in cells

stimulated with fibronectin, PTP-PEST is recruited to the plasma membrane and has been detected in adhesion structures (11, 286). Moreover, PTP-PEST promotes tail retraction by regulating p190RhoGAP (287). Numerous regulators of actin cytoskeleton organization are also associated with the morphological conversion occurring during apoptosis (77, 78, 89, 295). The presence of PTP-PEST in retracting lamellipodia during apoptosis indicates a novel function for this enzyme in the progression of cell death and potentially in cellular detachment.

Since PTP-PEST sensitizes cells to both anti-Fas and TNFα-induced cell death, our results identify PTP-PEST as a modulator of receptor-mediated apoptosis. Observations showing that orthovanadate, a general PTPs inhibitor, could protect cells against the cytotoxic effect of TNFα provided the first evidence for a function of these enzymes in receptor-mediated programmed cell death (339). In hematopoietic cells, SHP-1 is required for efficient Fas-induced apoptosis (315, 377). On the other hand, FAP-1 associates with and attenuates Fas (Apo-1) trafficking to the cell surface, thereby inhibiting Fas-induced apoptosis (166). Recently, PTP-PEST was shown to be involved in the trafficking of the Fas-Ligand (21). ROS inhibition of MAP kinase phosphatase (MKP) induced by TNFα increases JNK-mediated cell death (181), whereas PTP1B null mice exhibited an increased resistance to Fas-dependent hepatic apoptosis (284). Together, these reports underline the importance of PTPs regulation in receptor-mediated apoptosis. Of interest, the effect of PTP-PEST is dependent on its catalytic activity, which suggests that an unidentified substrate is targeted in this phenomenon. In addition, PTP-PEST expressing-cells display accelerated cleavage of p130Cas, suggesting that PTP-PEST can act as a regulator of the apoptotic response. Interestingly, the proteolysis of p130Cas, a substrate of PTP-PEST, has been proposed to be highly dependent on its phosphorylation status and contributes to the morphological characteristics of apoptotic cells (118, 154, 189). FAK, a reported substrate of PTP-PEST (11, 95, 300), was recently proposed to bind RIP and suppress its pro-apoptotic signal in death receptor-induced apoptosis (197).

Post-translational modifications of PTPs such as nitrosylation (20), ubiquitination (175, 263), phosphorylation (119), calpain degradation (130) and oxidation (334) are important for their regulation. Here, we report the caspase-mediated cleavage of a classical PTP, PTP-PEST, during apoptosis. *In vitro* and *in vivo* experiments identified caspase-3 as the protease executing PTP-PEST cleavage during apoptosis. Despite the presence of four putative caspase cleavage sites, mutation of the ^{549}DSPD site was sufficient to block caspase-3 cleavage of PTP-PEST *in vitro* and precluded its degradation *in vivo*. The DSPD sequence is processed by caspases in other proteins including p130Cas and RAD21 (62, 189), and its corresponding site (^{580}DLVD) found in the human PTP-PEST has been described as a caspase cleavage site in Hef1 (245). In addition, our observations indicate that the cleavage of PTP-PEST during apoptosis is conserved between different cell types in several mammalian species and is a common characteristic of different apoptotic pathways. This degradation of PTPs appears to be specific to PTP-PEST since TC-PTP, PTP-1B, SHP-2 and most candidates highlighted by in-gel PTP assays were resistant to caspase activity.

The non-cleavable mutant of PTP-PEST contributed to caspase activation to the same extent as the WT form (data not shown). Consequently, we also observed equivalent, accelerated p130Cas cleavage in both WT and ^{549}ASPA PTP-PEST expressing cells (Fig. 7C). This implies that the cleavage of PTP-PEST is not involved in amplifying the caspase cascade. As caspase activation precedes PTP-PEST cleavage, the cleaved products may have an impact on the apoptotic process downstream of caspase induction. Interestingly, *in vitro* analysis indicates that caspase cleavage of PTP-PEST liberates fragments that display increased catalytic activity compared to the intact form. Furthermore, proteolysis of PTP-PEST would prevent its catalytic domain from being associated with its targets, Shc and PSTPIP (85, 95), and therefore, would change its substrate specificity. Intramolecular interaction has been characterized as an autoinhibition mechanism for other PTPs (242). Thus, in addition to its adaptor function,

the C-terminus of PTP-PEST could inhibit its catalytic domain, or may bind a protein that modulates PTP-PEST enzymatic activity. As the process of apoptotic cell death involves tightly regulated molecular mechanisms, the caspase-dependent modulation of the interactions and catalytic activity of PTP-PEST suggests that it participates in the progression of apoptosis.

Cellular detachment is a major feature of the execution phase of apoptosis. The detailed mechanisms that coordinate this complex event remain unclear. In this study, we show that the cleavage of PTP-PEST during apoptotic cell death promotes cellular detachment. Our experiments indicate that cleavage of PTP-PEST produces an N-terminal fragment that maintains the ability to recruit the multidomain focal adhesion adaptor protein paxillin. Paxillin plays a central role in regulating cell attachment and migration (38). The association of PTP-PEST with paxillin was reported to target the enzyme to its substrate PKL and is essential for inhibition of cell adhesion and membrane protrusion (172). Therefore, the recognition of an altered subset of substrates, such as paxillin-linked focal adhesion proteins, by the active PTP-PEST fragment might stimulate cellular detachment during apoptosis. Another binding partner of PTP-PEST is PSTPIP, through which PTP-PEST regulates the phosphorylation status and actin polymerization activity of WASP (18, 85). Mutations in the gene encoding WASP were reported to accelerate lymphocyte apoptotic cell death (264). Importantly, we observed that active caspase-3 uncouples PSTPIP from PTP-PEST catalytic domain. Because modifications to the structure of the actin network cause the morphological conversions associated with apoptosis (77, 222), deregulation of WASP activity during programmed cell death may also contribute to this phenomenon. We demonstrate that PTP-PEST is additionally able to act as a scaffolding molecule bridging PSTPIP to paxillin, providing a link between adhesion signaling and actin polymerization. During apoptosis, caspase cleavage of PTP-PEST uncouples PSTPIP from the PTP-PEST catalytic domain and from paxillin, consequently interrupting their potential communication. In addition, we observed that proteolysis of PTP-PEST in cells

undergoing apoptosis generates a fragment still competent to couple PSTPIP to Shc or Csk. Notably, Shc and Csk have both been implicated in cell adhesion (225, 226). Through these multiple protein interactions, PTP-PEST may also function as a platform, bringing together different signaling modules in close proximity to control cellular adhesion and migration. Caspase-dependent cleavage of PTP-PEST rearranges these complexes, which would result in unstable cytoskeletal architecture and reduced cell adhesion. In summary, we propose that the cleavage of PTP-PEST during apoptosis enhances its catalytic activity, alters its substrate specificity, and disrupts its scaffolding properties, thereby facilitating cellular detachment (Fig. 11).

PTPs are major modulators of signal transduction and also function as integral regulators of the apoptotic response. Cellular progression through apoptosis correlates with the redistribution of PTP-PEST toward the site of cellular detachment suggesting an active participation of PTP-PEST in the apoptotic process. PTP-PEST expression results in enhanced caspase activity and an accelerated cleavage of p130Cas subsequent to induction of apoptosis. This indicates that PTP-PEST operates upstream of the initiation of the caspase cascade. Interestingly, caspase-3 cleavage of PTP-PEST, which modulates its catalytic activity and scaffolding properties, facilitates cellular detachment, a hallmark of programmed cell death. In this manner, proteolysis would permit a functional transition of PTP-PEST during apoptosis. Apoptosis plays an important role in embryonic development and in lymphocyte selection during their maturation. Since PTP-PEST is essential for proper embryonic development and is highly expressed in T- and B-lymphocytes (84, 95, 305), our current characterization of its function during caspase-mediated cell death could contribute to a better understanding of these phenomena. Finally, our data reveal the importance of caspases in the regulation of PTPs during apoptosis.

Figure 11. Proposed functions of PTP-PEST in apoptosis. By bridging PSTPIP to additional partners (paxillin, Shc or Csk), PTP-PEST acts as a scaffold involved in regulating cell adhesion and migration. During initiation of apoptosis, PTP-PEST expression enhances caspase activation in cells exposed to TNFα and anti-Fas. The extrinsic and the intrinsic apoptotic pathways both lead to the activation of the executioner caspase-3, which cleaves PTP-PEST on its ^{549}DSPD motif. This produces an N-terminal fragment that displays increased catalytic activity and retains the ability to bind paxillin. The C-terminal fragment remains competent to link PSTPIP exclusively to Shc or Csk. The targeting of active PTP-PEST fragments to paxillin-associated focal adhesion proteins as well as the remodeling of PTP-PEST protein complexes following caspase activation may destabilize the actin network and stimulate cellular loss of adhesion. Therefore, cleavage of PTP-PEST facilitates cellular detachment during the execution phase of apoptosis.

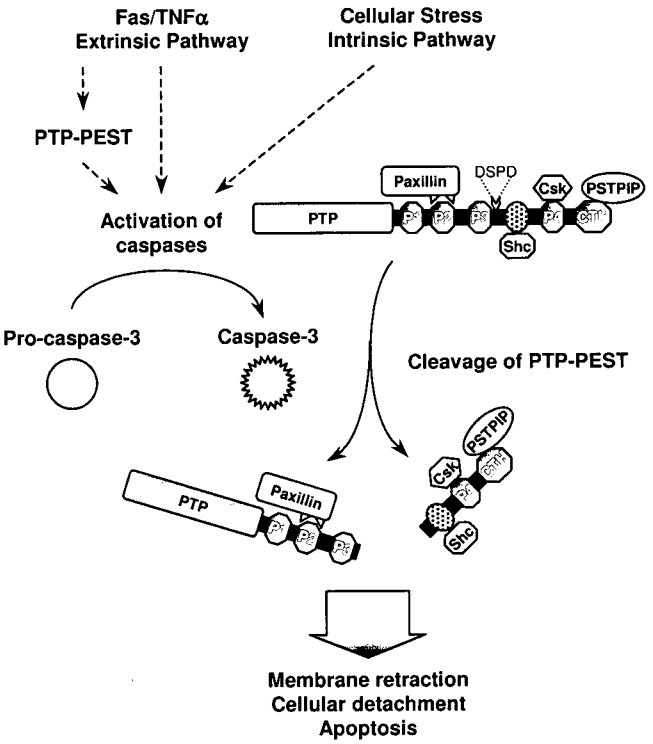
Fas/TNFα
Extrinsic Pathway
Cellular Stress
Intrinsic Pathway
PTP-PEST
Activation of
caspases
Paxillin
DSPD
Csk
PSTPIP
PTP
Shc
Pro-caspase-3
Caspase-3
Cleavage of PTP-PEST
PSTPIP
Csk
PTP
Paxillin
Shc
Membrane retraction
Cellular detachment
Apoptosis

FIG. 11

4.6 Acknowledgements

We are grateful for the support from National Science Council of Taiwan (grant number NSC 94-2311-B-011-032 and NSC 94-2311-B-001-020 to T.C.M.). M.H. is recipient of a Rolande and Marcel Gosselin Graduate Studentship, S.H. was supported by a postdoctoral fellowship from the Canadian Institute of Health Research (CIHR), C.B. is the recipient of a Human Frontier Science Program postdoctoral fellowship, A.B. is a recipient of a fellowship from the Lymphoma Research Foundation. M.L.T. is recipient of the Jeanne et Jean-Louis Lévesque Chair in Cancer Research, is a chercheur-Nationaux of the Fonds de Rercherche en Santé du Québec and recipient of a James McGill Professor Fellowship. This work was supported by a CIHR operating grant (MT-12466) to MLT.

We thank Ryan Petrie and Jacynthe Laliberté for their advice on live imaging as well as Dr. John W. Hanrahan for access to the confocal microscope. PTP-PEST polyclonal antibodies were provided by Dr. Jean-François Côté. We are grateful to Serge Morin and Martin Calille for their assistance with computer software. We thank Dr. Yves Boiclair and Matthew Stuible for critical review of the manuscript.

4.7 Supplementary data

Supplementary Movies can be visualized at:

http://mcb.asm.org/cgi/content/full/27/3/1172/DC1

http://mcb.asm.org/cgi/content/full/27/3/1172?view=long&pmid=17130234

5 CHAPTER 5

GENERAL DISCUSSION

As critical regulators of numerous signalling cascades, PTPs are involved in a wide array of cellular processes, including cell growth, proliferation, motility, transformation, and, death, as well as events modulating the organisation of the cytoskeleton (5, 41). The molecular machinery responsible for the assembly and arrangement of actin filaments is a central player in diverse physiological processes, including cell migration, transformation, cytokinesis, infection by intracellular pathogens, and apoptosis (77, 137, 309, 322). PTP-PEST was previously identified as an important regulator of the cytoskeleton and of cell migration (11, 18, 120, 172, 287). Correpondingly, the principal objectives of my thesis were: 1- to determine and evaluate the functional importance of PTP-PEST subcellular localization; 2- to investigate the possibility that PTP-PEST regulates or is regulated during *Leishmania*-host cell interaction; and 3- to study the role of PTP-PEST in apoptosis and caspase-mediated cleavage on its functions.

Examination of PTP-PEST distribution by confocal microscopy and cell fractionation revealed the presence of the enzyme in the cytosol and in association with the plasma membrane. Accordingly, some PTP-PEST interactions were unique to the cytosol or to the membrane, and others were common to both compartments. In clones stably expressing different versions of PTP-PEST, p130Cas tyrosine phosphorylation-dependent interactions were found to be regulated by the cytosolic enzyme. These data imply that the subcellular localization of PTP-PEST affects its role in intracellular signalling events, and they are summarized on figure 1.

Figure 1. Proposed model for PTP-PEST-mediated regulation of phosphorylation-dependent p130Cas interactions during LPA signalling. Treatment of cells with LPA induces the tyrosine phosphorylation of p130Cas, which leads the recruitment of Crk, and also allows the recruitment of other SH2-containing proteins, including Nck and Src. PTP-PEST appears to regulate the formation of these complexes via the maintenance of low p130Cas phosphorylation levels; thereby reducing the interaction with Crk, as well as recognition by the SH2 domains of Nck and Src. Since LPA and p130Cas phosphorylation both play a role in cell proliferation, migration and transformation (70, 71, 151, 188, 234), the regulation of p130Cas signalling by PTP-PEST could be involved in these processes.

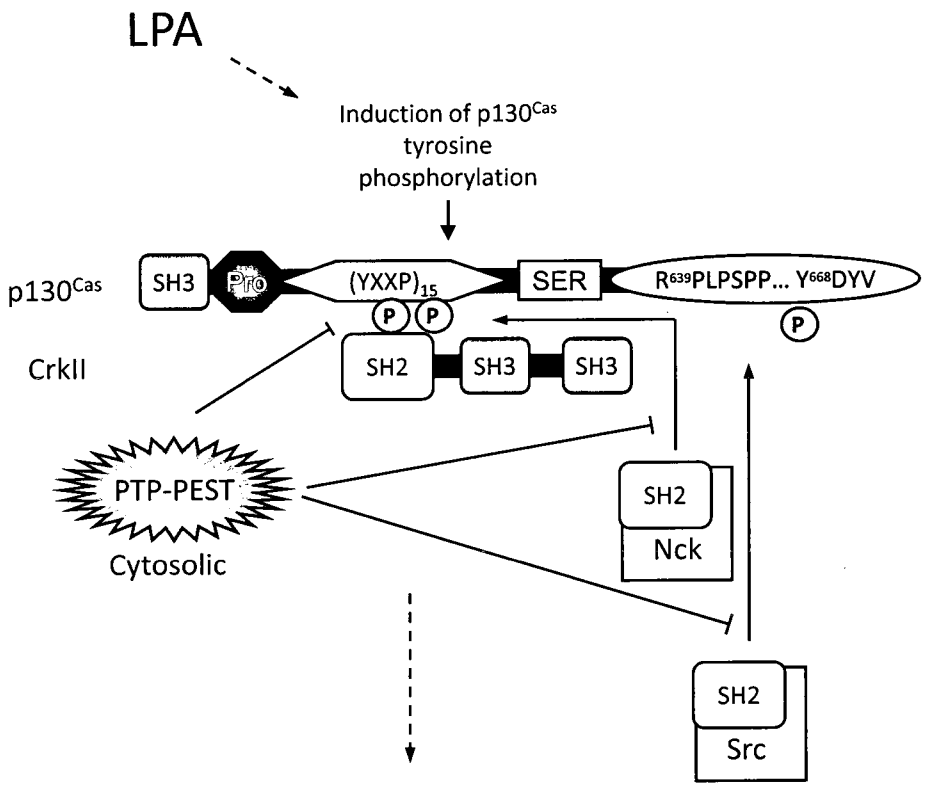
LPA
Induction of p130Cas tyrosine phosphorylation
p130Cas
SH3
Pro
(YXXP)15
SER
R639PLPSPP... Y668DYV
P
P
P
CrkII
SH2
SH3
SH3
PTP-PEST
Cytosolic
SH2
Nck
SH2
Src
Effects on cell proliferation, migration and transformation?

FIG. 1

The infection of fibroblasts by *Leishmania* parasites led to dramatic modifications of the actin cytoskeleton and tyrosine phosphorylation profile. Exposure of fibroblast cells to *Leishmania* also resulted in alterations in the p130Cas/Crk interaction, with Crk recognizing a smaller form of p130Cas. In addition, p130Cas and PTP-PEST, as well as cortactin, caspase-3 and TC-PTP were all cleaved during *L. major* infection. Further analysis pointed to the parasitic protease GP63 as being responsible for these cleavage events. Interestingly, a mechanism allowing the transfer of GP63 to the host cell presumably leads to these proteolytic events, and inactivates the MAPK p38; likely via the cleavage of TAB1. Even though the precise function of PTP-PEST in the regulation of the *Leishmania*-host cell interaction remains unclear, the above data firmly establishes that PTP-PEST is targeted during infection.

Figure 2. Proposed model for GP63-mediated molecular events in *Leishmania* infected host cells. Prior to the entry of the parasite, *Leishmania* may secrete the protease GP63, which would then be internalized by the target cell via a yet unknown mechanism. GP63 proteolyses several host cell proteins, including TC-PTP, caspase-3, cortactin, p130Cas and PTP-PEST. GP63 also mediates the inactivation of p38, which correlates with the cleavage of the adaptor protein TAB1. Although the precise function of these biochemical events remains un-clear, it could be speculated that the cleavage of TC-PTP, as well as the inactivation of p38, could modulate gene expression and impair host cell apoptosis. The cleavage of caspase-3, which does not result in its activation, could also play a role in parasite-mediated inhibition of apoptosis. Finally, the cleavage of cortactin, p130Cas and PTP-PEST likely plays a role in the dramatic cytoskeletal rearrangement seen during *Leishmania* infection. Interestingly, Crk can interact with cleaved, phosphorylated, p130Cas. As fibroblasts act to harbour the parasite during long term infection (29), it is possible that some of the above described molecular events participate in this process.

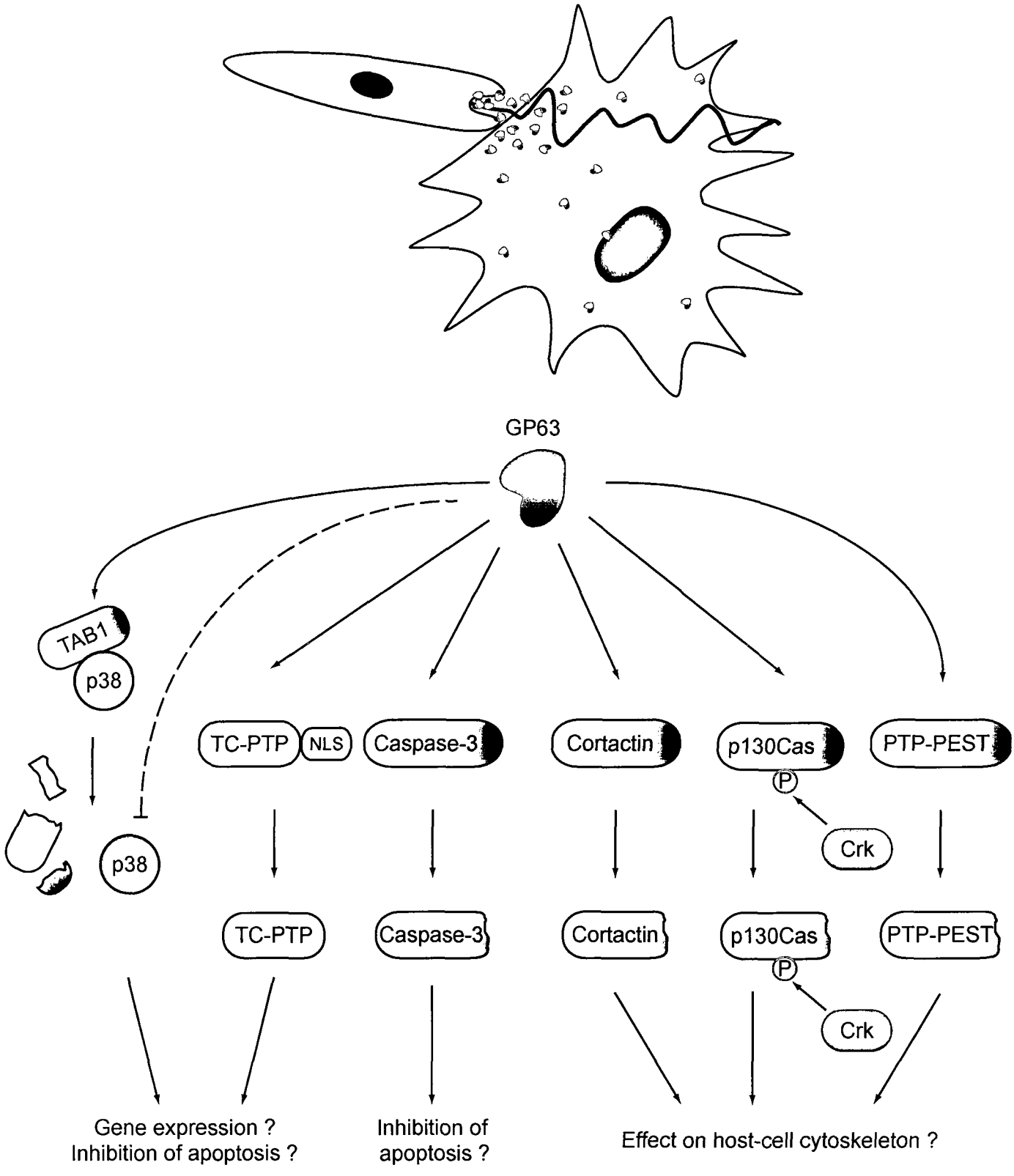
GP63
TAB1
p38
p38
TC-PTP
NLS
Caspase-3
Cortactin
p130Cas
P
PTP-PEST
Crk
TC-PTP
Caspase-3
Cortactin
p130Cas
P
PTP-PEST
Crk
Gene expression ?
Inhibition of apoptosis ?
Inhibition of apoptosis ?
Effect on host-cell cytoskeleton ?
Effect on long term parasites survival?

FIG. 2

In correlation with observations obtained from localization studies, PTP-PEST was found to accumulate at the edge of retracting membrane ruffles of cells undergoing apoptosis. Interestingly, expression of PTP-PEST increases cellular sensitivity to receptor-mediated apoptosis. Importantly, caspase-3 cleaves PTP-PEST at the ^{549}DSPD sequence, which increases the phosphatase activity and modulates the scaffolding properties of this enzyme. Moreover, the cleavage of PTP-PEST was shown to facilitate the detachment of cells undergoing apoptosis.

Prior to the studies described herein, little was known about the cleavage of PTPs during apoptosis. The data and conclusions presented in chapter 4 indicate that caspase-mediated proteolysis of PTPs could be an important and underestimated mechanism by which these enzymes are regulated. Moreover, they underscore the possible role of multiple PTPs in the modulation of apoptotic signal transduction. Accordingly, I present an analysis of how PTPs function during apoptosis, as well as an evaluation of the presence and distribution of putative caspase-cleavage sites in the "PTPome". In the subsequent sections, I then focus on the cellular role and regulation of PTP-PEST.

5.1

PROTEIN TYROSINE PHOSPHATASES: EMERGING REGULATORS OF APOPTOSIS

Maxime Hallé[1], Michel L. Tremblay[1*] and Tzu-Ching Meng[2*]

Cell Cycle, 2007, 6 (22): 2773-2781.

The McGill Cancer Center and the Department of Biochemistry, McGill University, McIntyre Medical Sciences Building, 3655 Promenade Sir-William-Osler, Montréal, Québec, Canada, H3G 1Y6.[1]
Institute of Biological Chemistry, Academia Sinica, 128 Academia Road, Section 2, Nankang, 105 Taipei, Taiwan, ROC.[2]
* Co-corresponding authors.
Mailing address for M. L. Tremblay: McGill Cancer Center, McGill University, 3655 Promenade Sir-William-Osler, Room 701, Montréal, Québec H3G 1Y6, Canada.
Phone: +1 (514) 398-8480. Fax: (514) 398-6769.
Email: michel.tremblay@mcgill.ca.
Mailing address for T.-C. Meng: Institute of Biological Chemistry, Academia Sinica, 128 Academia Road, Section 2, Nankang 115, Taipei, Taiwan.
Phone: +886-2-2785-5696 ext 6140. Fax: +886-2-2788-9759,
Email: tcmeng@gate.sinica.edu.tw.

5.1.1 Abstract

Apoptosis is a precisely controlled physiological mechanism that is required for the elimination of cells during embryonic development, in response to stress and infection as well as in the maintenance of homeostasis. Since the outcome of several of these biological processes is regulated by signaling events involving tyrosine phosphorylation, members of the protein tyrosine phosphatase (PTP) gene family are expected to be of primary importance. Here, we summarize the current literature linking the activities of classical PTPs with the regulation of apoptosis. The recent discovery of caspase-cleavage mediated modulation of a member of this family, PTP-PEST, indicates that other PTPs could be modulated in a similar manner. In light of this, we present an analysis of all murine and human PTPs gene for the presence of putative caspase cleavage motifs. Additional studies linking the activity of PTPs to their own regulation during programmed cell death initiation should provide important insight into the understanding of this fundamental physiological phenomenon.

5.1.2 Introduction

Apoptosis is a form of cell suicide that is subjected to several signaling regulators and necessary in normal conditions for embryogenesis, tissue homeostasis, and hematopoiesis. Unbalanced apoptosis contributes to a variety of pathologies such as cancer, neurodegenerative and cardiovascular disorders, acquired immune deficiency syndrome (AIDS), and transplant rejection (279). Two principal pathways propagate the apoptotic signal: the extrinsic and the intrinsic pathway. Death receptors of the Tumour Necrosis Factor (TNF) superfamily trigger the extrinsic pathway (92) while proteins sensing various intracellular stresses initiate the intrinsic pathway (2). Members of the Bcl-2 family of proteins play crucial roles in the tight control of the apoptotic response. While Bcl-2 and related antiapoptotic family members promote cell survival, both the BH3-only and the Bax/Bak subfamily proteins act to propagate the apoptotic signal and to release pro-apoptotic factors such as cytochrome c from mitochondria (2, 274). The recruitment of initiator caspases to an activated death receptor and the cytochrome c induced oligomerization of Apaf-1 are both followed by activation of the caspase cascade, which amplifies the death signal (267). The significance of caspases as signaling proteases resides in their high specificity, and their property to generate protein fragments with modified functions rather than causing a general degradation of their substrates (267). The cleavage of caspase substrates, particularly those that are organizers of the cytoskeletal network, gives rise to morphological changes characteristic of apoptotic cells including cellular detachment, shrinkage of the cell body, cell rounding, and membrane blebbing (77).

Tyrosine phosphorylation initiates or participates in a wide array of signal transduction pathways essential for the proper control of several cellular activities, including motility, metabolism, differentiation, cell growth and proliferation. This reversible modification is added by protein tyrosine kinases (PTKs) and is removed predominantly by the protein tyrosine phosphatases (PTPs). The catalytic domain of

PTPs contains approximately 280 residues and is defined by the signature motif [I/V]HCXXGXXR[S/T], in which the invariant cysteine residue serves in the nucleophilic attack of the phosphorylated substrates (10). PTPs possess additional domains or motifs that can enhance their substrate specificity or restrict them to a specific cellular compartment. The classical PTPs can be further subdivided into two groups: the non-receptor and the receptor-like PTPs (RPTPs) (332). Consistent with the diversity of mammalian PTPs, modified signal transduction resulting from PTP deficiency causes several physiologic abnormalities such as embryonic developmental defect, impairment of the immune system, cancer susceptibility and others (31, 178, 305). A contributing factor to these phenotypes are in many cases a dysregulated apoptosis. Indeed, the determinant role of tyrosine phosphorylation in both extrinsic and intrinsic apoptotic pathways is now recognized (91, 261), implying a fundamental function for PTPs in the balance between cell survival and cell death. Recently, our laboratory reported the direct cleavage and regulation of a PTP, PTP-PEST, via the executioner caspase-3 (138). This proteolysis facilitates cellular detachment as programmed cell death progresses, a hallmark of apoptosis (138). While other PTPs have been shown to affect the apoptotic outcome, this type of caspase-dependent modulation of a PTP had not been previously explored. In this review, we first examine the reported effect of various PTPs on apoptosis, focusing on the classical tyrosine specific PTPs. We then explore two potential mechanisms for the regulation of PTPs in the context of apoptosis: oxidation and caspase cleavage. Moreover, we present an amino acid sequence analysis of putative caspase-cleavage sites in members of the classical PTP family.

5.1.3 PTPs IN THE REGULATION OF APOPTOSIS

5.1.3.1 PTP-PEST

The established role of PTP-PEST involves modulation of cell motility via regulation of the actin cytoskeletal network and cell adhesion (11, 172, 286, 287).

Recently, Hallé and colleagues (138) observed that expression of active PTP-PEST sensitized cells to anti-Fas and TNFα apoptotic stimuli. Their observations implied that PTP-PEST acts on an unidentified substrate—upstream of caspase-3 activation—to potentiate the cell death signal. Importantly, caspase-3 directly cleaves PTP-PEST, which enhances its catalytic activity and alters its scaffolding properties. Moreover, the proteolysis of PTP-PEST facilitates cellular detachment during apoptosis. Noteworthy, the catalytically active fragment of PTP-PEST maintains the ability to interact with a subset of binding partners including paxillin, a regulator of cell adhesion (38, 138). The altered substrate specificity, as well as the presence of PTP-PEST at the edge of retracting lamellipodia during apoptosis, could weaken cytoskeletal anchorage structures, reducing cell adhesion. This regulation of PTP-PEST may participate in the conversion of cellular morphology occurring during programmed cell death, and may even play an important role in embryogenesis as PTP-PEST homozygous deletion leads to embryonic lethality (305). Identification of specific cell death associated substrates of PTP-PEST will provide more insight into tyrosine phosphorylation-regulated apoptotic signaling.

5.1.3.2 PTP-1B

PTP-1B, was the first PTP to be identified and consequently it has been extensively investigated with respect to its function in insulin signaling and obesity (102). Additionally, increasing evidence suggests a requirement for PTP-1B in various apoptotic pathways. It was recently observed that the peroxisome proliferator-activated receptor-γ (PPARγ) agonist troglitazone leads to PTP-1B processing and activation (4). Activated PTP-1B subsequently contributes to STAT3 dephosphorylation and favors apoptosis of human glioma cells (4). The cleavage of PTP-1B by calpain was previously described in platelets (116), but little is known regarding its effect on the regulation of cell survival/cell death programs. Interestingly, PTP-1B does not contain caspases cleavage

sites (see Table 3) and it is not cleaved by caspases during apoptosis (138), further supporting calpain as a unique regulator of PTP-1B integrity. Future studies using the calpain deficient mouse models may confirm the role of this protease in troglitazone induced PTP-1B proteolysis (193). The presence of PTP-1B on the endoplasmic reticulum (ER) makes it an attractive candidate for the regulation of the unfolded protein response. Indeed, PTP-1B and its catalytic activity are required for efficient inositol-requiring kinase 1 (IRE1) signaling that activates c-Jun N-terminal kinase (JNK) and p38 mitogen-activated protein kinase (MAPK), X-box-binding protein 1 (XBP-1) splicing, and ER degradation-enhancing α-mannosidase-like protein (EDEM) transcription (129). As expected, ER-stress-induced apoptosis was attenuated in cells lacking PTP-1B (129). Also, PTP-1B null mice are resistant to Fas-induced liver damage due to the absence of PTP-1B-mediated suppression of pro-survival NF-κB and extracellular related kinase (ERK) signaling (284). In this context, the receptor for hepatocyte growth factor, the tyrosine kinase Met, was identified as a potential PTP-1B substrate (284). Dephosphorylation of Met would inhibit its pro-survival effects, thereby facilitating the transmission of the cell death signal. The level of PTP-1B expression was recently correlated with the sensitivity of hepatocytes to growth factor deprivation-induced apoptosis (124). The pro-survival PI3K/Akt cascade (known to be regulated by PTP-1B) was shown to influence the nuclear localization of Foxo1, a transcription factor that regulates the expression of several pro-apoptotic genes (124, 128). Interestingly, hepatocytes lacking PTP-1B were resistant to apoptosis induced by a constitutively active mutant of Foxo1, which implicates an alternate Akt independent, pathway (124). Finally, PTP-1B was recently identified as a pro-oncogenic molecule (23, 101, 178), which implies an anti-apoptotic function for this enzyme. From these studies, it is clear that PTP-1B plays diverse functions regulated in accord with cell types and cellular contexts. However, a definitive mechanism by which PTP-1B balances pro- and anti-apoptotic signaling remains obscure at this time.

5.1.3.3 TC-PTP

Comparative studies using cell lines that are positive and negative for p53 expression suggest that p53 is required for apoptosis induced by TC-PTP overexpression (259). In MCF-7 cells (breast epithelial adenocarcinoma), accumulation of p53 in response to TC-PTP overexpression directs increased expression of Apaf-1 and the pro-apoptotic α-isoform of caspase-1 (132). Moreover, TC-PTP induces Ipaf expression, which also contributes to caspase-1 initiated apoptosis through promotion of cytochrome-c and Omi release from the mitochondria (328). These studies reveal a pro-apoptotic role for TC-PTP in the context of transformed cells. The impact of TC-PTP expression on the commitment of tumourigenic cells to apoptosis with respect to p53 signaling still needs to be examined *in vivo*.

5.1.3.4 SHPs

Studies performed on viable motheaten (me^v/me^v) mice demonstrate a requirement for SHP-1 to transmit the Fas apoptotic signal into lymphoid cells (315). Upon death receptor stimulation, SHP-1 disrupts anti-apoptotic pathways through the regulation of Lyn, Tyk2 and the p85 subunit of PI3K (377). SHP-1 is recruited on Y291 of FAS, an association likely regulated by tyrosine phosphorylation of the receptor. A Y291A mutated version of the FAS receptor is much less efficient at promoting cell death (93). Interestingly, FAP-1 was proposed to dephosphorylate FAS (Y275), but no mutagenesis studies were done to exclude that other residues are dephosphorylated (114). As dephosphorylation of FAS by FAP-1 was proposed to down-regulate the death signal, it is attractive to speculate that FAP-1 could be involved in regulating the recruitment of SHP-1 to FAS. In sympathetic neurons, SHP-1 favors Bim/Bod expression and c-jun phosphorylation, which results in increased apoptosis (221). Specifically, SHP-1 dephosphorylates TrkA on sites required for its activity (Y674/Y675), which in turn

inhibits NGF-mediated PLC-γ1 and Akt phosphorylation, antagonizing the TrkA survival signal (221). These studies implicate SHP-1 in both the regulation of receptor-mediated apoptosis and in the termination of the survival signal promoted by receptor tyrosine kinase. However, the interconnection between these two functions of SHP-1 is not understood.

In hematopoietic cells, overexpression of SHP-2 accelerates growth factor-deprivation-mediated apoptosis through dephosphorylation of STAT-5 (63). In contrast, studies performed on fibroblasts suggest that SHP-2 activity is required for activation of the anti-apoptotic PI3K/Akt pathway (169). SHP-2 also provides protection against p73 mediated apoptosis induced by the green tea polyphenol epigallocatechin-3-gallate (EGCG) (6). Importantly, genetic studies performed with mice identified SHP-2 as an essential factor for peri-implantation. This developmental defect was attributed to apoptosis of trophoblast stem cells in which the SHP-2 gene was disrupted (366). Activation of MAPK in the SHP-2/SFK/Ras/ERK cascade triggers the phosphorylation and degradation of the pro-apoptotic protein Bim and thereby ensures cell survival (366). Interestingly, reduced Akt activation was also observed in cells lacking SHP-2 (366). It appears that SHP-2 is implicated in multiple aspects of the regulation of apoptosis. Future investigations using the targeted floxed SHP-2 mouse will clarify the relative contribution of SHP-2 as a pro- or an anti-apoptotic PTP in hematopoietic cells. Recently, SHP-2 activation following treatment with the neutrophil-derived protease Cathepsin G was shown to facilitate cardiomyocytes anoikis through the dephosphorylation of FAK (260). In addition, PTP-1B and PTP-PEST were involved in the regulation of cell adhesion and in the modulation of FAK phosphorylation (11, 67, 300, 381). However, the participation of these two phosphatases in FAK-inactivation-mediated anoikis has yet to be investigated. Apoptosis can also be initiated by disturbance of the cytoskeleton (a process termed amorphosis) (222). Several PTPs have been linked to the regulation of cytoskeletal architecture and organization, but their contribution to amorphosis remains to be evaluated.

5.1.3.5 FAP-1

PTPs have been implicated in the regulation of Fas (APO-1 and CD95) mediated apoptosis. Several reports link the Fas-associated phosphatase (FAP-1), also called PTPL1 or PTP-BAS, with the regulation of the cellular apoptotic response. FAP-1 has been found to interact with the cytosolic domain of the Fas receptor, and the level of expression of FAP-1 is proportional to resistance to Fas-mediated apoptosis (288). FAP-1 also interacts with the C-terminal portion of the neurotrophin receptor $p75^{NTR}$, another member of the TNF receptor superfamily, and was proposed, in this context, to attenuate the cell death response to tamoxifen (165). In addition, tumor cell lines lacking FAP-1 expression were sensitive to Fas-induced cell death, whereas tumor cell lines expressing FAP-1 were resistant (288). Expression of FAP-1 was reported in a variety of human tumors and cell lines not sensitive to Fas-induced apoptosis (114, 229, 373). The correlation between FAP-1 expression and cellular resistance to Fas-mediated apoptosis, as well as the high level of expression of this PTP in transformed cells, suggest that FAP-1 could have oncogenic properties, accentuating transformation and participating in the progression of cancer. Tumors of the Ewing's Sarcoma family are characterized by a chromosomal translocation, which fuses the ews gene with the ets family transcription factor fli1, thereby generating the oncogenic transcription factor EWS-FLI1 (1). This abnormal fusion protein regulates specific genes in order to promote cancer (1). Interestingly, high FAP-1 levels were observed in Ewing's Sarcoma, as a result of the activity of EWS-FLI1 (1). Notably, FAP-1 participates in oncogenesis by conferring resistance to etoposide induced caspase-3-mediated cell death (1). NF-κB, another transcriptional regulator that promotes cell survival, also enhances the transcription of the FAP-1 gene (167). Down-regulation of FAP-1 expression during IL-2 mediated activation of T cells correlates with their increased sensitivity to Fas (383). Importantly, association of FAP-1 with the intracellular C-terminal domain of Fas inhibits its trafficking and presentation at the surface of the cells, which attenuates the death signal emanating from Fas (166). Although an antiapoptotic role for FAP-1 has been clearly demonstrated, it has also been

associated with the pro-apoptotic response of breast cancer cells to 4-hydroxytamoxyfen by antagonizing the IRS-1/PI3-K/AKT survival pathway (30). Altogether, these reports identify FAP-1 as an important regulator of the cell death program.

5.1.3.6 Potential Regulation of Fas Ligand Expression by PTPs

Some hematopoietic cells, including cytotoxic T cells and natural killer cells, can eliminate virally infected or transformed target cells via the presentation of the Fas ligand (FasL), also called CD95L, on their surface (173). Due to the potential of FasL to induce cell death, cell surface presentation of this molecule requires tight regulation. FasL can interact with the SH3 domain of the tyrosine kinases Fyn, Lyn and Fgr, and its phosphorylation dictates its cellular distribution (385). The recently identified FasL/PSTPIP/PTP-PEST complex (21) may be involved in balancing the effect of tyrosine kinases on FasL. Notably, the association of PSTPIP with FasL retains it in the cytoplasm, and significantly reduces its cytotoxicity in co-culture assays (21). In addition to its interaction with PTP-PEST, the coiled-coil domain of PSTPIP can bind PTP-HSCF and PTP-PEP (85, 307), two PTPs expressed in the hematopoietic cell lineage. Therefore, through its binding to the SH3 domain of PSTPIP, FasL could become available for regulation by PEST-type PTPs. Interestingly, PSTPIP was characterized as an adaptor for PTP-PEST-mediated dephosphorylation of Abl and WASP (79, 85). However, the dephosphorylation of FasL via PSTPIP bound PTP-PEST has not been investigated. Also, PTP-PEST acts as a scaffolding molecule linking PSTPIP to additional partners (138). The contribution of these protein complexes associated to PTP-PEST to the presentation of FasL at the surface of immune cells is still unknown. Taken together, this evidence suggests a potential role for PTPs in the regulation of the trafficking of death receptor ligands.

5.1.3.7 Effect of PTPs on Differentiation Related Apoptosis

Apoptosis is a central phenomenon linked with the selection, turnover and maturation of developing hematopoietic cells. During interleukin-6 induced differentiation of murine leukemia cells, a reduction in membrane bound PTPε (PTPεM) and an increase in cytosolic PTPε (PTPεC) expression was reported (324). This exchange in PTPε isoform expression suggests a particular role for each species in IL-6 regulating cell differentiation and death. Indeed, overexpression of PTPεM enhanced terminal differentiation and apoptosis, whereas forced expression of PTPεC inhibited cell death in response to IL-6 or leukemia inhibitory factor (LIF) (325). These results reveal a functional significance for the subcellular localization of PTPε (325). These effects of PTPε were dependent on its catalytic activity and involved the regulation of Jak1, Tyk2, gp130 and Stat3 phosphorylation (325). In histiocytic lymphoma cells, PTP-U2 (also named GLEPP1) expression was induced following treatment with 12-*O*-tetradecanoylphorbol-13-acetate (TPA) and favored monocytic differentiation (296). In addition, over-expression of the long form of PTP-U2 (PTP-U2L) induced hypersensitivity to TPA treatment, enhancing the apoptotic response (296). Pim-1, which phosphorylates PTP-U2 and decreases its catalytic activity, was also implicated in the modulation of lymphoma differentiation (350). Along with increased PTP-U2 expression, the amount of the T-cell (TC)-PTP expression has been observed to decrease during the differentiation of lymphoma cells (296). This indicates that a reduction in TC-PTP expression may favor the commitment of cells to apoptosis. Recently, Bourdeau et al (2007) reported that bone marrow stromal cells from TC-PTP -/- mice abnormally secrete interferon-γ (31). This leads to an increase in apoptosis of pre B cells, thus affecting their differentiation program and reducing the population of immature bone marrow B cells (31). Inactivation of the PTP-1B gene, a close homologue of TC-PTP, perturbs myeloid differentiation causing an abnormal monocyte/granulocyte ratio (145, 146). The enhanced sensitivity of monocytes to CSF-1 provides a potential mechanism for their resistance to apoptosis (145). The PTP-PEP, exclusively expressed in hematopoietic cells

(360), is involved in B cell receptor induced growth arrest and programmed cell death (143). Interestingly, PTP-PEP mRNA is significantly increased following anti-IgM stimulation of immature B lymphocytes, while expression of PTP-PEST remains constant (143). More importantly, antisense-mediated suppression of PTP-PEP expression significantly reduces apoptosis and the growth inhibitory effect of anti-IgM (143). Substrates and partners allowing PTP-PEP to promote apoptosis following BCR stimulation still remain to be identified. The above studies on hematopoietic cells point toward a functional significance of PTPs in the regulation of apoptosis during cell differentiation. Programmed cell death and differentiation are also crucial for proper embryonic development. Evidence that these enzymes specifically regulate programmed cell death during embryogenesis could provide an explanation for the functional impact of PTP deficiency on embryonic development.

5.1.3.8 Receptor-PTPs and Apoptosis

Cumulative evidence also supports a role for the Receptor-PTPs (R-PTPs) in the control of apoptosis. Pioneering studies using LAR-overexpressing cells were the first to implicate an R-PTP in the regulation of apoptosis (355). Overexpression and antisense experiments performed in various cell types revealed a cytotoxic function for LAR that involved caspase-mediated, p53 independent, apoptosis (331, 355). It was proposed that LAR induces apoptosis through the dephosphorylation and destabilization of p130Cas, thereby interfering with an anchorage-mediated cell survival signal (354). The dephosphorylation of p130Cas has also been implicated in growth factor activation of Erk, negative regulation of cell spreading by stomach cancer-associated protein-tyrosine phosphatase-1 (SAP-1), and colony formation (244), suggesting a potential role for this PTP in the control of cell growth and survival. It was then proposed that the inactivation of AKT and ILK by SAP-1 contributes to SAP-1inducted apoptosis (318). In contrast, the

osteoclastic PTP (PTP-oc) protects cells against apoptosis by promoting c-Src-mediated activation of NFκB and JNK (7).

Expression of R-PTPs in cells of the heamopoietic lineage was also linked with the control of cell death program. In lymphoma cells, expression and catalytic activity of the truncated-PTPRO inhibit ERK and cell proliferation, and induces apoptosis (64). CD45, or leukocyte common antigen, another R-PTP specifically expressed in the hematopoietic lineage, regulates antigen receptor signal transduction in T and B lymphocytes (327). Inactivation of the murine CD45 gene leads to an increase in the number of B cells and a reduction in the number T cells in the spleen (45). This alteration in the amount and ratio of lymphocytes suggests a role for CD45 in cellular proliferation and differentiation as well as in efficient selection. In support of this hypothesis, CD45 null thymocytes had increased resistance to antigen (anti-CD3) induced apoptosis (45). In addition, CD45 was identified as a candidate galectin-1 receptor, and is required for galectin-1-mediated induction of apoptosis in T-cells (254). Interestingly, splenic B cells from $CD45^{-/-}$ mice fail to undergo PI(3)K, ERK and NF-κB signaling following BCR ligation, which leads to reduced expression of anti-apoptotic members of the Bcl-2 family (160). These cells therefore undergo increased apoptosis, pointing to a survival function for CD45 in B cells (160). A central feature of human immunodeficiency virus type 1 (HIV-1) infection is a reduction in the $CD4^{+}$ lymphocyte population. GP120-mediated apoptosis is one of the several processes accounting for elimination of these cells by HIV-1. Importantly, both the extra-cellular domain and the catalytic activity of CD45 were observed to be necessary for GP120-promoted cell death (8). Molecular analysis of this pathway revealed that GP120 enhances the phosphatase activity of CD45, which translates to the dephosphorylation of Lck (8). CD45 was also observed to enhance the induction of FasL expression in cells treated with GP120; nonetheless, it did not promote Fas-mediated cell death (8, 45). Interestingly, CD45 is required for GP120 initiated inactivation of AKT and caspase-3 processing (8). The impact of other PTPs involved in the regulation of AKT in HIV-infection associated cell death has yet to be investigated.

5.1.3.9 Impact of Prokaryotic PTPs on apoptosis

PTPs have also been implicated in bacterial infection strategies. The protein tyrosine phosphatase YopH, a virulence factor of *Yersinia pestis*, induces apoptosis via a loss of mitochondrial membrane potential (40). Interestingly, the action of YopH appears to depend on the presence of Lck, as Lck-deficient cells display resistance to YopH-induced apoptosis (40). As a defense mechanism in response to infection with microbial pathogens, plant cells undergo a form of programmed cell death termed the hypersensitive response (144). *Pseudomonas syringae* suppresses this response by secreting HopPtoD2, whose PTP activity contributes to the inhibition of the host's MAPK pathway (105). Further studies focused on the interaction between pathogenic microorganisms and their target cells should clarify the virulence functions of various phosphatases and could suggest new therapeutic avenues.

5.1.4 Regulation of PTPs Activity and Functions during Apoptosis

5.1.4.1 ROS Dependent Modulation of Phosphatases during Apoptosis

The generation of reactive oxygen species (ROS) in hyperoxia condition as well as following exposure to TNF actively participates in signaling leading to cell death (51, 299). One of the effects of ROS production, is oxidation of the cysteine residue within the signature motif of PTPs (334). This blocks its nucleophilic activity and inactivates the PTP in a reversible manner (334). A recent study demonstrates that in response to TNFα stimulation, ROS generation inhibits the JNK inactivating MAPK phosphatases (MKPs) (181). This favors the sustained activation of JNK leading to caspase activation and cell death (181). In addition to the dual-specificity phosphatases MKPs, other PTPs are likely modulated by ROS, and this modulation may participate in the induction of apoptosis. Nevertheless, little information is currently available with respect to this phenomenon.

5.1.4.2 Regulation of PTPs by Caspases

A number of proteins with phosphatase activity, including calcineurin (238), PP2A (285), PTEN (338), and MKP-3 (R. Pulido, personal communication), were described as caspase substrate. Recently, the first example of caspase-substrate being a tyrosine specific phosphatase was reported (PTP-PEST) (138). In addition to the classical DXXD motifs, other examples of caspase cleavage sites were identified previously (112). The murine PTP-PEST sequence contains four putative caspase-cleavage motifs (see Table 1) (138). These include the ^{423}EHID and ^{604}DDSD sequences, which act as caspase cleavage sites in HIP-55 (66) and Yin Yang 1 (YY1, a transcriptional regulator) (192), respectively. Despite their presence in the amino acid sequence of PTP-PEST, only the ^{549}DSPD sequence is important for PTP-PEST processing during apoptosis as mutation of this sequence was sufficient to confer resistance to caspase activity. The DSPD sequence is processed by caspases in other proteins including p130Cas and RAD21 (62, 189). Analysis of human PTP-PEST reveals that the site corresponding to the murine ^{549}DSPD (^{580}DLVD) is targeted by caspase in Hef1 (245). Both immunoblots and in gel phosphatase assay did not reveal additional PTPs candidate other than PTP-PEST for caspase processing (138). Nonetheless, we are aware that the experimental procedures used previously have some intrinsic limitations and recognize that PTP-PEST may not be the only PTP modulated by caspases. Therefore, we investigated whether putative caspase cleavage sites are present within the amino acid sequence of all PTPs. We also verified the conservation of these sites between two extensively studied mammalian species: *Mus musculus* and *Homo sapiens*. Our bioinformatics analysis revealed that a large number of PTPs, of both non-receptor and receptor types, contain putative caspase cleavage motifs (see Tables 1 and 2). Interestingly, certain non-receptor PTPs (PTP-PEST, PTP-BAS [FAP-1], SHP-1 and SHP-2), and R-PTPs (LAR, PTPε, PTP-U2 [GLEPP1], SAP-1, and CD45), were all previously implicated in the regulation of apoptosis and all contain putative caspase cleavage motifs. SHP-2, which actively participates in the regulation of apoptosis (6, 63, 169, 260, 366), contains a potential caspase recognition motif but is not degraded

following *in vitro* activation of caspases (138). It is possible that the putative caspase cleavage site within SHP-2 is located in an area that is not accessible in the folded protein. Of note, and in support of a potential functional role for caspase cleavage of PTPs, the presence of caspase-cleavage motifs is conserved between the murine and human sequence of several enzymes (see Tables 1 and 2). In addition, cleavage of PTPs by other proteases such as calpain has been involved in the modulation of their activities (130). Despite the presence of caspase cleavage-sites, the efficient digestion of these candidate PTPs by caspase still need to be experimentally confirmed. The group of potential caspase substrates identified on Table 1 and 2 suggests that the cleavage of PTPs by caspase could be an underestimated mechanism of regulation for these enzymes. Together, both previously published results (138) and the analysis presented herein, suggest that caspases may selectively cleave PTP family members, and that the resulting cleavage products may play a role in the progression of apoptosis.

5.1.5 Conclusions

Apoptosis is a tightly regulated physiologic process of genetically programmed cell death conserved among organisms. As fundamental modulators of signal transduction, PTPs have recently been implicated in the control of apoptotic pathways. Disregulation of apoptosis can result in cellular immortalization and transformation. Various PTPs have been identified as either oncogenes or tumor suppressors (248); which is consistent with the physiologic role for these enzymes in the modulation of apoptosis. Interestingly, the role of PTPs as the regulators of pro-survival signals is widely reported. Individual PTPs were proposed to either enhance or counteract a variety of cell survival signals, ultimately favoring either cell growth or apoptosis. In laboratory model systems, the modulation of particular signaling proteins, such as the JAKs, STATs, MAPKs, receptor tyrosine kinases (RTKs), PI3K and AKT, is commonly mediated by a number of enzymes; not by a single PTP. The mechanism coordinating the modulation of a common substrate by multiple PTPs requires further investigation. The advancement of phospho-proteomics may reveal the physiological importance of particular enzymes as well as novel PTPs substrates that control apoptosis. While PTPs indirectly regulate apoptosis through pro-survival signals, the recent findings that caspase-8 and -9 are directly modulated by Src and Abl PTKs respectively (91, 261), implies that PTPs could play a more direct role than anticipated in the caspase cascade. Although the major characterized activities of PTPs occur upstream of caspase activation, a function for caspase processing of PTP-PEST during apoptosis (138) offers insight into PTP activities downstream of caspase activation. Indeed, we have observed that several members of this family contain putative caspase-cleavage sites. As previously validated with PTP-PEST (138), the proteolysis of these identified potential caspase-substrates and their participation in the completion of apoptosis requires experimental confirmation. Future investigation focusing on the mutual regulation of

apoptotic signaling pathways and PTPs should give rise to promising discoveries that may find applications in avant-garde therapies.

5.1.6 Keywords

Apoptosis, caspase, phosphatase, protein tyrosine phosphatase (PTP), reactive oxygen species (ROS), tyrosine phosphorylation

5.1.7 Acknowledgments

We thank Matthew Stuible, Annie Bourdeau, and Hannah Heath-Engel for critical reviews of the manuscript and for helpful discussions. We are grateful to Martin Calille for its generous assistance with computer software. We also wish to apologize to authors of studies that were not cited due to space limitation. M.H. is recipient of a Rolande and Marcel Gosselin Graduate Studentship. This work was supported by Taiwan National Science Council Grants NSC95-2311-B-001-051-MY3 and NSC95-3112-B-002-028 to T.C.M and by a CIHR operating grant (MOP-12466) to M.L.T. MLT is a holder of the Jeanne et Jean-Louis Lévesque Chair in Cancer Research and a Chercheur National of the Fonds de la Recherche en Santé du Québec.

Table 1 Presence of putative caspase cleavage sites within the amino acid sequence of non-receptor PTPs

Name	Accession number	Species	Sites found
SHP1	NP_002822	*Homo sapiens*	^{59}DFYD, ^{401}DNGD
SHP1	NP_038573	*Mus musculus*	^{59}DFYD, ^{401}DNGD
SHP2	NP_002825	*Homo sapiens*	^{61}DYYD
SHP2	NP_035332	*Mus musculus*	^{61}DYYD
MEG2	NP_002824	*Homo sapiens*	^{133}YLLD, ^{220}SEVT, ^{259}DPFD
MEG2	NP_062625	*Mus musculus*	^{133}YLLD, ^{220}SEVT, ^{259}DPFD
PTP-PEST	NP_002826	*Homo sapiens*	^{481}LSSD, ^{580}DLVD, ^{604}DDSD
PTP-PEST	NP_035333	*Mus musculus*	^{423}EHID, ^{549}DSPD, ^{604}DDSD, ^{740}DKKD
MEG1	NP_002821	*Homo sapiens*	^{77}DSTD, ^{657}TQFD, ^{826}DSSD, ^{829}DFLD
MEG1	NP_064317	*Mus musculus*	^{77}DSTD, ^{826}DSSD, ^{829}DFLD
hPTPH1	NP_002820	*Homo sapiens*	^{77}DSVD, ^{471}DGVD, ^{499}DKND, ^{502}DNGD, ^{760}DPPD, ^{817}DSSD
mPTPH1	XP_143789	*Mus musculus*	^{56}DSSD, ^{129}SLLD, ^{153}DPVD, ^{292}DQND, ^{590}DGVD, ^{618}DKSD, ^{621}DDGD, ^{875}DPPD, ^{878}DIMD, ^{932}DSSD
hPTPD1	NP_008970	*Homo sapiens*	^{151}DFGD, ^{159}ESQD, ^{577}STPD, ^{713}EEED, ^{797}SESD
mPTPRL10	NP_036007	*Mus musculus*	^{151}DFGD, ^{159}ESQD, ^{577}STPD, ^{799}SESD
hPTPD2	NP_005392	*Homo sapiens*	^{149}DFGD, ^{157}DSQD, ^{457}LHTD, ^{578}STPD, ^{593}SSPD, ^{1076}DWPD
mPTP36	NP_033002	*Mus musculus*	^{149}DFGD, ^{578}STPD, ^{593}SSPD
hPTPBAS	NP_006255	*Homo sapiens*	^{218}DLVD, ^{248}DTQD, ^{376}SALD, ^{424}SESD, ^{596}DVFD, ^{879}DAQD, ^{1292}DVTD, ^{1295}DYSD, ^{1298}DRGD, ^{1530}DVGD, ^{1640}GEDD, ^{1794}YVHD, ^{2028}DIYD, ^{2041}SLLD, ^{2044}DVVD, ^{2187}GLLD, ^{2416}DISD
mPTPBL	NP_035334	*Mus musculus*	^{218}DALD, ^{248}DTRD, ^{251}DEED, ^{371}SALD, ^{419}SESD, ^{543}VSLD, ^{589}DVFD, ^{643}AAVD, ^{679}DLLD, ^{872}DAQD, ^{1150}AAVD, ^{1306}DCAD, ^{1311}DKDD, ^{1538}DVGD, ^{1649}GEDD, ^{1788}YVHD, ^{1894}AAVD, ^{2021}DIYD, ^{2034}SLLD, ^{2037}DVVD, ^{2128}DGED, ^{2172}GLLD, ^{2401}DISD,
hPTPTyp	NP_056420	*Homo sapiens*	^{65}DYED
mPTPTyp	NP_033004	*Mus musculus*	^{74}LESD, ^{84}DVSD, ^{161}EELD, ^{176}TLPD
hHDPTP	NP_056281	*Homo sapiens*	^{275}SALD, ^{406}ETVD, ^{409}DNLD, ^{448}VFTD, ^{458}DIRD, ^{1483}DSQD, ^{1625}SLLD
mHDPTP	AAH22721	*Mus musculus*	^{343}DSQD, ^{485}SLLD
mPTPN23/mHDPTP	NP_001074512	*Mus musculus*	^{275}SALD, ^{406}ETVD, ^{409}DNLD, ^{448}VFTD, ^{458}DIRD, ^{647}SELD, ^{1539}DSQD, ^{1681}SLLD

Table 2 Presence of putative caspase cleavage sites within the amino acid sequence of RPTPs

Name	Accession number	Species	Sites found
hCD45	NP_002829	*Homo sapiens*	^{43}LSSD, ^{74}LSPD, ^{86}DSLD, ^{729}ETVD, ^{1005}DDSD, ^{1087}DLKD
mCD45	NP_035340	*Mus musculus*	^{45}ASTD, ^{85}DLKD, ^{331}DRPD, ^{579}ETVD, ^{855}DDSD, ^{1040}DVVD
hLAR	NP_002831	*Homo sapiens*	^{198}EESD, ^{647}EAVD, ^{650}DGED, ^{1033}EVPD, ^{1053}VEVD, ^{1214}LSPD, ^{1336}DLAD, ^{1786}DARD
mLAR	NP_035343	*Mus musculus*	^{198}EESD, ^{647}EAVD, ^{650}DGED, ^{945}VYRD, ^{1024}EVPD, ^{1044}VEVD, ^{1205}LSPD, ^{1327}DLAD, ^{1777}DARD
hPTPdelta	NP_002830	*Homo sapiens*	^{198}EESD, ^{278}PEDD, ^{503}LSSD, ^{653}DGED, ^{654}GEDD, ^{1061}EEVD, ^{1118}TNLD, ^{1159}ESPD, ^{1164}MELD, ^{1791}DARD
mPTPdelta	1083477	*Mus musculus*	^{70}PEDD, ^{295}LSSD, ^{441}AAVD, ^{444}DGED, ^{562}DAQD, ^{843}EEVD, ^{900}TNLD, ^{941}ESPD, ^{946}MELD, ^{1571}DARD
hPTPsigma	NP_002841	*Homo sapiens*	^{207}EETD, ^{287}PEDD, ^{302}DVKD, ^{1269}DNPD, ^{1827}DARD
mPTPsigma	NP_035348	*Mus musculus*	^{198}EETD, ^{274}PEDD, ^{289}DVKD, ^{1244}DNPD, ^{1783}DARD
hPTPlamda	NP_005695	*Homo sapiens*	^{593}DYAD, ^{1096}IVLD, ^{1349}DTPD, ^{1362}AEVD
mPTPlamda	NP_035344	*Mus musculus*	^{593}DYAD, ^{1086}IVLD, ^{1339}DTPD, ^{1352}AEVD
hPTPkappa	NP_002835	*Homo sapiens*	^{50}DLYD, ^{81}DSSD, ^{441}DCLD, ^{595}TLPD
mPTPkappa	NP_033009	*Mus musculus*	^{49}DLYD, ^{82}SNHD, ^{440}DCLD
mPTPmu	NP_033010	*Mus musculus*	^{42}DEDD, ^{224}DVRD, ^{665}FPAD, ^{1433}DLLD
hPTPS31	AAD50277	*Homo sapiens*	^{125}DFVD
hGLEPP1	NP_109592	*Homo sapiens*	^{656}DTTD, ^{921}DDFD
mPTPphi	NP_035346	*Mus musculus*	^{931}DDFD, ^{1082}EEED
hPTPbeta	NP_002828	*Homo sapiens*	^{1285}DWTD, ^{1289}DYND, ^{1496}DGSD, ^{1925}DSKD, ^{1928}DSVD
mPTPbeta	NP_084204	*Mus musculus*	^{96}VSLD, ^{107}LQTD, ^{250}DRRD, ^{1287}DWTD, ^{1290}DYND, ^{1497}DSMD, ^{1536}ESPD, ^{1710}DLKD, ^{1926}DSKD, ^{1929}DSVD
hDEP1	NP_002834	*Homo sapiens*	^{437}VLGD, ^{1160}DYGD, ^{1210}DTTD, ^{1221}LVRD
mDEP1	NP_033008	*Mus musculus*	^{193}EVPD, ^{217}VSVD, ^{658}DSWD, ^{1061}DYGD, ^{1111}DTTD, ^{1122}LVRD
hSAP1	NP_002833	*Homo sapiens*	^{51}EVPD, ^{54}DGLD, ^{140}EVPD, ^{143}DGPD, ^{229}EVPD, ^{232}DGTD, ^{318}EVPD, ^{321}DGPD, ^{407}EVPD, ^{804}DFAD, ^{991}SSPD
mSAP1	BAC37443	*Mus musculus*	^{18}DGLD, ^{111}DGLD, ^{282}DFAD
mPTPESP	NP_031981	*Mus musculus*	^{24}SSLD, ^{519}DLVD, ^{552}LSSD, ^{1416}DASD
hPTPalpha	NP_002827	*Homo sapiens*	^{142}DSKD, ^{145}DRRD
hPTPepsilon	NP_006495	*Homo sapiens*	^{179}SQLD, ^{654}GLLD, ^{688}DFID
mPTPepsilon	NP_035342	*Mus musculus*	^{653}GLLD, ^{687}DFID
hPTPgamma	NP_002832	*Homo sapiens*	^{87}DILD, ^{102}LQLD, ^{105}DGFD, ^{182}DDFD, ^{212}SALD, ^{329}DMTD, ^{1393}VFTD, ^{1433}DESD
mPTPgamma	NP_033007	*Mus musculus*	^{87}DILD, ^{102}LQLD, ^{105}DGFD, ^{182}DDFD, ^{212}SALD, ^{237}ILRD, ^{329}DLAD, ^{332}DFLD, ^{1390}VFTD, ^{1430}EESD
hPTPzeta	NP_002842	*Homo sapiens*	^{242}DTVD, ^{354}DGED, ^{656}SSTD, ^{704}SVTD, ^{812}SSYD, ^{1417}EDGD, ^{1420}DTDD, ^{1423}DDGD, ^{1424}DGDD, ^{1426}DDDD, ^{1427}DDDD, ^{1428}DDDD, ^{1778}KLTD, ^{1944}IVLD
mPTPzeta	NM_011219	*Mus musculus*	^{712}SVTD, ^{820}SSYD, ^{963}DVSD, ^{1369}SSTD, ^{1425}EDGD, ^{1426}DGDD, ^{1428}DDYD, ^{1429}DYDD, ^{1431}DDDD, ^{1433}DDYD, ^{1434}DYDD, ^{1436}DDID, ^{1474}DQSD, ^{1566}SFPD
hPCPTP1	NP_002840	*Homo sapiens*	^{100}DGQD, ^{121}LQMD
hSTEP	NP_116170	*Homo sapiens*	^{204}DFLD, ^{345}DPDD, ^{379}TVAD
mSTEP	NP_038671	*Mus musculus*	^{180}DFLD, ^{321}DPED, ^{355}TVAD
IA2 receptor-like subtype			
hIA2beta	NP_002838	*Homo sapiens*	^{235}SGVD, ^{294}DSED, ^{375}SFPD, ^{383}DDDD, ^{543}AFAD, ^{576}DNKD, ^{608}EQED, ^{826}TVAD, ^{922}SLLD
mPTPNP	AAB06945	*Mus musculus*	^{287}DAKD, ^{311}SEVD, ^{369}DVDD, ^{562}DNKD, ^{594}EQED, ^{812}TVAD, ^{908}SLLD

Table 3 Absence of putative caspase cleavage sequence within various PTPs

Name	Accession number	Species
PTP1B	NP_002818	*Homo sapiens*
PTP1B	NP_035331	*Mus musculus*
TCPTP	NP_033003	*Mus musculus*
TCPTP	NP_002819	*Homo sapiens*
LyPTP	NP_057051	*Homo sapiens*
PTP-PEP	NP_033005	*Mus musculus*
BDP1	NP_055184	*Homo sapiens*
PTPK1	NP_035336	*Mus musculus*
hPTPrho	NP_008981	*Homo sapiens*
mPTPrho	NP_067439	*Mus musculus*
mPTPalpha	NP_033006	*Mus musculus*
mPTPzeta	XP_133009	*Mus musculus*
mPTPSL	NP_035347	*Mus musculus*
hHePTP	NP_002823	*Homo sapiens*
mHePTP	NP_796055	*Mus musculus*
hIA2	NP_002837	*Homo sapiens*
mIA2	NP_033011	*Mus musculus*

5.2 How PTP-PEST is integrated in cellular signalling?

The assembly, disassembly and reorganization of actin fibres plays a critical role in multiple biologic phenomena, including cell motility, phagocytosis, invasion by pathogenic microorganisms, maintenance of cell morphology, cell survival and apoptosis. The interacting partners and substrates of PTP-PEST link this enzyme to the machinery controlling cytoskeletal architecture and to adhesion promoted survival signalling. In 2001, over 50 proteins had already been shown to play a role in linking the cytoskeleton to the extracellular matrix (378). In view of the extreme complexity of the signalling involved in elongation of actin fibres and in their anchorage within adhesion structures, I will focus here on the aspects most relevant to PTP-PEST.

Members of the small GTPase family Rho appear to be key regulators of the dynamic reorganisation of the actin network. Experiments involving growth factor-mediated activation and/or, protein overexpression led to the development of the classic model in which the activation of Cdc42 by bradykinin, of Rac by PDGF and of Rho (RhoA, RhoB, RhoC) by LPA promotes the formation of actin containing structures, respectively: microspikes and filopodia, membrane ruffles and lamellipodia, and stress fibers (Fig. 3) (136, 190, 252). During migration of adherent cells, the projection of membrane protrusions such as filopodia acts to organelles sense the environment in order to establish cell polarity, and to promote the growth of membrane ruffles extending into lamellipodia at the leading edge (190, 266). Anchoring of actin stress fibres between focal adhesions provides a framework on which contractile force facilitates cell body contraction and tail retraction (252). To generate these structures, Rho GTPases stimulate a variety of effectors. Members of the Wiskott-Aldrich syndrome protein family (WASP, neural WASP [N-WASP] and WASP verprolin homologous [WAVE/Scar]) of scaffolding molecules translate the signal from the small GTPase into de-novo actin polymerization from pre-existing filaments (322). The binding of Cdc42 triggers a conformational change within N-WASP that exposes its VCA region (verprolin-

homology [V], cofilin-homology domain [C], acidic domain [A]), which binds to actin monomers (G-actin) and to the Arp2/3 complex to promote actin polymerization, resulting in the formation of filopodia (232, 273). Membrane ruffles and lamellipodia are produced in a similar manner; via the formation of a Rac-IRSp53-WAVE complex that supports actin polymerization (233). Rho stimulates the bundling of actomyosin stress fibres by activating the serine/threonine kinase ROCK (Rho-associated coiled-coil-containing protein kinase) and the actin binding protein mDia (diaphanous-related formin) (24, 252). The phosphorylation of myosin light chain 2 (MLC2), a substrate of ROCK, increases stress fibre contractility (252). This effect is further amplified through ROCK phosphorylation, and through inhibition of the enzymatic activity of the myosin light chain phosphatase (MLC phosphatase). This indirectly amplifies the phosphorylation of MLC2, and therefore increases fibre contraction (252). In addition, activation of mDia promotes filaments elongation by stimulating actin nucleation at the barbed end of growing filaments (137, 252). Rho proteins cycle between GDP and GTP bound forms; or between inactive and active conformations (137). Guanine nucleotide exchange factors (GEFs) of the DH/PH (Dbl homology/pleckstrin homology) domain containing family (for example VAV2 and αPIX) and of the DOCK180 (dedicator of cytokinesis 180)-related family convert the GDP-bound (inactive) form into the GTP-bound (active) form (87, 137). Since they have intrinsic GTPase activity, RhoGTPases can self inactivate (137). However, GTPase-activating proteins (GAPs) such as p190RhoGAP, enhance this intrinsic activity; thereby favouring the GDP-bound conformation (inactive) (137). As exemplified below, several lines of evidence suggest that PTP-PEST is involved the control of upstream regulators and downstream effectors of RhoGTPases.

Figure 3. Stimuli inducing the activity of RhoGTPases promote the formation of specific F-actin containing structures. Swiss 3T3 cells are a good model for the study of induced formation of actin structures because, under starvation conditions, they contain very few organized actin filaments. Stimulation with bradykinin activates Cdc42, which triggers the formation of microspikes and filopodia (190), while PDGF mediates the activation of Rac, which stimulate membrane ruffle formation, and LPA activates Rho, which, in turn, promotes reorganization of F-actin into stress fibres anchored in focal adhesions (136). Since serum contains a "cocktail" of growth factors, it promotes a variety of pathways which lead to the formation of membrane ruffles and stress fibres. As the formation of filopodia is a transient phenomenon, this type of structure is difficult to observe in serum stimulated cells, and is therefore not clearly shown in this picture. The formation of similar structures composed of F-actin was observed in P-MEFs (data not shown). Pictures were acquired as follows: quiescent or serum-starved Swiss 3T3 cells were incubated with PDGF (15 min), LPA (30 min), or serum (15 min), and serum-starved *PTP-PEST* -/- cells were incubated with bradykinin for 15 min. Cells were fixed, permeabilized, and stained for polymerized actin (F-actin) and vinculin as previously described (11). Radom field images were acquired by confocal microscopy (Zeiss LSM 510-NLO). In *PTP-PEST* -/-: white: F-actin. In Swiss 3T3: Red: F-actin; green: vinculin. Phenotypes presented here are similar to those shown previously (136, 190).

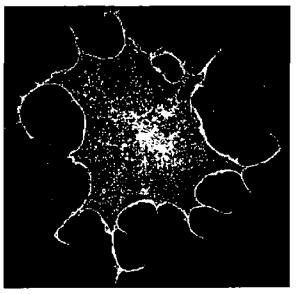

Bradykinin

↓

Cdc42

↓

Microspikes
Filopodia

↓

PDGF

↓

Rac

↓

Membrane ruffles
Lamellipodia

↓

LPA

↓

Rho

↓

Stress fibres
Focal adhesions

↓

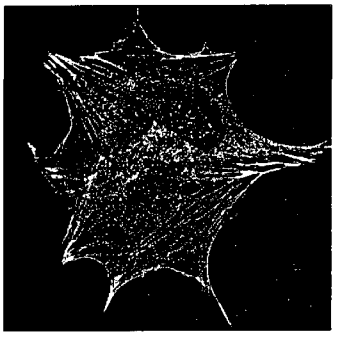

Serum 15 min

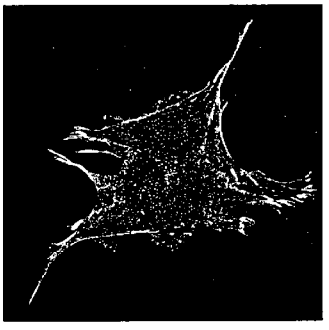

FIG. 3

Engagement of receptors for growth factors, LPA, and extracellular matrix, triggers the phosphorylation of p130Cas SD and the recruitment of Crk (70, 246, 348). In this complex, Crk also associates with DOCK180, which results in the activation of Rac and the generation of protrusions stimulating cell motility (70, 71, 187). In addition, integrin-mediated coupling of p130Cas-Nck, which facilitates the recruitment of the GEF αPIX, was proposed to induce Rac (376). PTP-PEST has been shown to dephosphorylate p130Cas, thereby acting to balance tyrosine phosphorylation-dependent signalling (118, 305). I have now shown that expression of cytosolic PTP-PEST is sufficient to impair the interaction between p130Cas and Crk, as well as the interaction of p130Cas with the SH2 domains of Nck and of Src (Chapter 2). These results imply that PTP-PEST regulates multiple phosphotyrosine sites on this substrate, thereby presumably blocking signalling initiated at this level (Chapter 2). Moreover, PTP-PEST inhibited the production of GTP loaded Rac in cells stimulated with either fibronectin or PDGF (286). These results suggest that PTP-PEST functions upstream of Rac to filter signals leading to its activation.

The expression and post-translational modification of p130Cas not only participates in reshaping of the cytoskeleton, but is also involved in promoting cell survival, proliferation and transformation (46, 153, 344). The data provided within this thesis indicates that cytosolic PTP-PEST significantly attenuates p130Cas-phospho-dependent interactions induced by LPA, a phospholipid that induces cell proliferation and is involve in promoting the progression of various types of cancers (Chapter 2) (234). Interestingly, p130Cas/Crk can signal either to JNK through DOCK180 and Rac (99), or to C3G, which guides the activation of Rap1 toward the MAPKs Erk (110). These molecular mechanisms may account for the role of the p130Cas/Crk interactome in sustaining cell survival and proliferation (71, 110). In accordance with the above described results, we recently observed that growth of *PTP-PEST* -/- cells was accelerated as compared to that of cells expressing WT proteins (Hidehisa Shimizu, Maxime Hallé and Michel L. Tremblay, un-published data). Expression of PTP-PEST in un-stimulated cells, however, did not

induce apoptosis (chapter 4). These observations indicate that PTP-PEST may play a role in restricting signals promoting oncogenic transformation, without inducing apoptosis.

Phosphorylation of the adaptor protein Shc is critical for the transmission of survival signals and to sustain cell proliferation (262). Upon activation of RTKs, recruitment of Shc to the receptor induces the formation of a receptor/Shc/Grb-2/Sos interacting network at the plasma membrane, which acts to initiate the Ras-MAPK cascade (262). Herein, I provide data showing that PTP-PEST and Shc associate primarily in the cytosol, but also interact significantly in cellular membrane fractions (Chapter 2). The dephosphorylation of Shc by PTP-PEST has been correlated with the ability of PTP-PEST to inactivate the Ras-MAPK pathway, which, in that particular study, was associated with impaired lymphocytes activation (95). In addition, the binding of Grb-2 to PTP-PEST assists in the recruitment of PTP-PEST to RTKs (54). Whether this plays a role in downregulation of RTKs, or in preventing the recruitment of Shc to RTKs, or in allowing the targeting of PTP-PEST to Shc in complex with receptors, is still speculative. The possible contribution of these signalling modules to the regulation of the Ras-MAPK cascade and to cell proliferation therefore requires additional examination.

The adaptor protein paxillin is a PTP-PEST binding partner that functions in the propagation of adhesion/growth factor-induced signalling (38, 86). This scaffolding molecule facilitates the reorganisation of the cytoskeleton, which translates into cell movement (38). The LIM3 and LIM4 domains of paxillin bind PTP-PEST (86), and expression of these two domains in tandem may act in a dominant negative fashion; via sequestration of the PTP from other paxillin interacting proteins. The over-expression of a construct encoding both the LIM3 and LIM4 domains stimulated cell spreading and formation of polarized lamellipodia (39). This suggested that paxillin may represent an alternative route through which PTP-PEST can modulate cytoskeletal changes. Experiments using both *paxillin* -/- and *PTP-PEST* -/- cells confirmed this hypothesis, and demonstrated that paxillin is necessary for PTP-PEST to suppress the adhesion-

stimulated activation of Rac, cell spreading and membrane protrusion (172). Interestingly, paxillin couples PTP-PEST with PKL (paxillin kinase linker) (172). The assembly of this complex is crucial for the dephosphorylation of PKL and for the regulation of cellular spreading by PTP-PEST (172). Sastry et al. (2002, 2006) also observed that PTP-PEST could modulate RhoGTPase activity, but via a different mechanism (286, 287). In cells plated on fibronectin, PTP-PEST was observed to directly dephosphorylate and inhibit the Rac-GEF VAV2 and the Rho-GAP p190RhoGAP (287). Therefore, in the absence of PTP-PEST, increased GEF activity of VAV2 (arising from hyperphosphorylation) leads to increased Rac activity and abnormally developed lamellipodia (287). In addition, the loss of PTP-PEST leads to increased p190RhoGAP activity, which inactivates RhoA, and thereby results in a tail retraction defect (287). The above results studies illustrate different mechanisms by which PTP-PEST inhibits signalling leading to RhoGTPases activation, and thereby modulates both the extension of membrane protrusion at the leading edge, and posterior tail retraction.

Although paxillin was proposed to target PTP-PEST to focal adhesions (86), the majority of the paxillin/PTP-PEST association was found to be in the cytosol (chapter 2). Interestingly, mutations within the LIM3 domain of paxillin, which is necessary for binding to PTP-PEST, significantly diminished its localization to focal adhesions (39). Moreover, we observed that expression of a membrane targeted form of PTP-PEST (PTP-PEST-K-Ras 4B tag) increased the association of paxillin with the membrane fraction (Maxime Hallé and Michel L. Tremblay, un-published data). Although experimentally characterized focal adhesions and membrane fractions may not correspond precisely to identical subsellular microenvironment, these data implicate that PTP-PEST could influence the localization of paxillin. A similar effect of PTP-PEST was reported with respect to PSTPIP (85). In this case, PSTPIP, which normally displays a fibrous pattern overlapping with the actin cytoskeleton (307), co-distributes with PTP-PEST when the two proteins are co-expressed (85). These observations suggest that PTP-PEST could play a role in modulating the cellular distribution of its interacting partners.

In addition to regulation of signalling up-stream of RhoGTPases, PTP-PEST has also been shown to be in the regulation of some of their effectors. A variety of stimuli lead to the activation of Cdc42 and its interaction with N-WASP, and thereby to the generation of actin filaments and the production of filopodia (232, 273). Dependent on its interaction with active Cdc42, the phosphorylation of N-WASP tyrosine 291 (Y291) decreases the affinity of its VCA region for its autoinhibitory domain and augments N-WASP actin polymerization promoting activity (337). In addition, phosphorylation of N-WASP Y291 further increases the formation of filopodia (83). Interestingly, WASP was found to associate with PTP-PEST in a trimolecular complex requiring PSTPIP (85). The assembly of this complex allows the phosphatase to target WASP for dephosphorylation, which reduces its ability to stimulate actin polymerization (18, 85). As the N-WASP homologue likely binds PSTPIP, it is attractive to speculate that PTP-PEST could dephosphorylate, and thereby inhibit, N-WASP-driven actin polymerization and filopodia formation. The polymerization of actin at the extremity of intracellular pathogens forms an actin comet tail that acts as a propulsion mechanism (309). Interestingly, expression of N-WASP is essential for the locomotion *Shigella* and EPEC (enteropathogenic *Escherichia coli*) bacteria, as well as vaccinia virus, within host cells (213, 306). Moreover, Abl-mediated tyrosine phosphorylation of N-WASP is required to maximise actin comet tail formation and motility of *Shigella* (42). Importantly, PTP-PEST dephosphorylates and inhibits Abl kinase activity through binding to PSTPIP (79). The above evidence suggests that PTP-PEST is involved in control of the movement of intracellular pathogens; via regulation of both N-WASP and Abl. With respect to protozoan pathogens, Cdc42 is required for the entry of *Leishmania* into CHO cells, and the Cdc42 effector WASP co-localizes with F-actin around endocytosed parasites to form a protective actin cup (212, 237). In chapter 3, I present data demonstrating that *Leishmania* induces the cleavage of PTP-PEST during infection. This proteolysis could allow the parasite to destabilize WASP negative regulatory machinery, which would promote the actin polymeraization necessary for engulfment and the formation of a

protective shell. Additional studies are required to fully delineate the potential role of PTP-PEST in the regulation of intracellular pathogen-driven actin polymerization. In summary, the above observations suggest that PTP-PEST could be an important regulator of WASP and N-WASP, and that this effect, could have broad implications: from cell motility to infectious disease.

The tyrosine kinase Abl has been proposed to play a role in the cytoskeletal reorganization required for the morphological changes associated with cell motility. In contrast with *PTP-PEST* -/- cells, which display hyperprotrusive activity (172, 287), *Abl* -/- cells are defective in the formation of membrane ruffles following PDGF stimulation (256). This impaired Rac-dependent phenotype was linked with the ability of Abl to phosphorylate WAVE, which promotes its actin polymerization inducing activity and the associated plasma membrane reorganization (204, 311). Since PSTPIP couples PTP-PEST with Abl in a platform promoting the dephosphorylation and inactivation of the PTK, one could propose that this mechanism may contribute to the cytoskeletal abnormalities associated with altered PTP-PEST expression.

The different routes through which PTP-PEST acts in signal transduction are illustrated on figure 4.

Figure 4. Proposed PTP-PEST signalling network. PTP-PEST interacts with a variety of signalling and cytoskeletal molecules, and is therefore involved in numerous pathways. In presence of a chemotractant gradient, cells activate a variety of pathways involving RhoGTPases, their upstream regulators, and their downstream effectors. PTP-PEST may regulate this signalling pathway via the modulation of several regulators and effectors. This function of PTP-PEST would likely affect the organization of the actin cytoskeleton, leading to the formation of filopodia, membrane ruffles and actin contractile stress fibres. PTP-PEST may also play a role in the modulation of cell survival signalling.

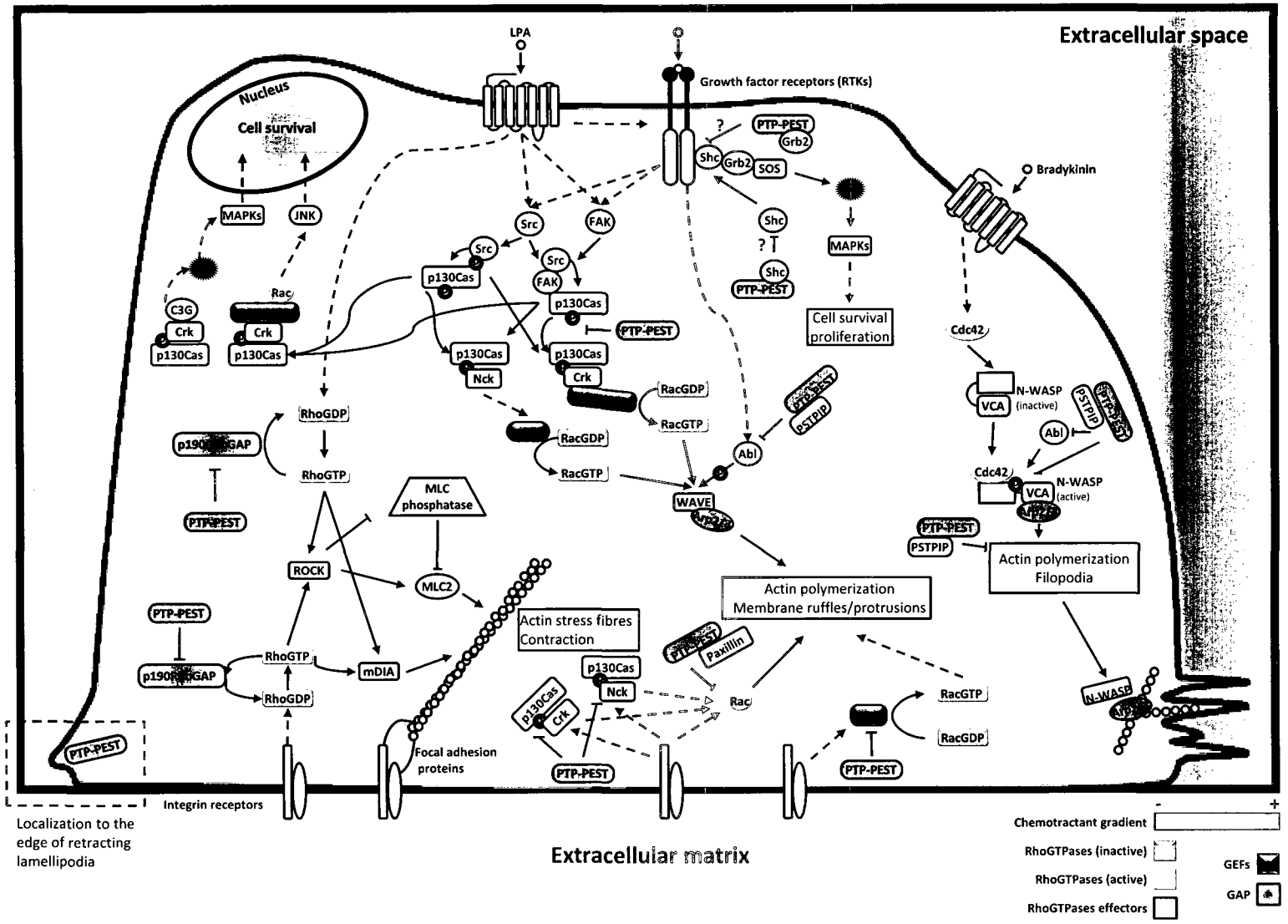
Extracellular space
LPA
Growth factor receptors (RTKs)
Nucleus
Cell survival
MAPKs
JNK
Src
FAK
p130Cas
Crk
C3G
Rac
PTP-PEST
Grb2
Shc
SOS
Cell survival proliferation
Bradykinin
Cdc42
N-WASP
VCA
(inactive)
(active)
PSTPIP
Abl
RhoGDP
RhoGTP
RacGDP
RacGTP
WAVE
MLC phosphatase
MLC2
ROCK
mDIA
Actin polymerization
Membrane ruffles/protrusions
Actin polymerization
Filopodia
Actin stress fibres
Contraction
Paxillin
Nck
Focal adhesion proteins
Integrin receptors
Localization to the edge of retracting lamellipodia
Extracelluiar matrix
Chemotractant gradient
RhoGTPases (inactive)
RhoGTPases (active)
RhoGTPases effectors
GEFs
GAP

FIG. 4

5.3 Is PTP-PEST a positive or a negative regulator of signal transduction?

As described above, PTP-PEST acts primarily to inhibit intracellular signalling. It does not, however, exclude the possibility that in some situations, PTP-PEST acts to stimulate signal transduction.

The tyrosine kinase Abl can phosphorylate Crk on tyrosine 221 (Y221), which leads to intramolecular folding of Crk involving the binding of its SH2 domain to the phosphorylated site (180). The phosphorylation of Crk was proposed to uncouple it from p130Cas, inhibit cell migration, and sensitise cells to apoptosis (71, 151, 180). PTPs involved in the regulation of either Crk or Abl could further modulate this interaction. For example, PTP-1B can catalyze the tyrosine dephosphorylation of Crk, thus maintaining its interaction with p130Cas (323). In addition, PTP-1B/Crk co-expression was found to promote cell migration (323). Also, PTP-PEST can down-regulate Abl via binding to PSTPIP (79); which would presumably result in an increased interaction with p130Cas. As shown here (chapter 2), and previously (11, 120), PTP-PEST expression significantly decreases the stability of p130Cas/Crk complexes. The regulation of this interaction depends on the dephosphorylation of p130Cas by PTP-PEST (chapter 2) (118, 120), and seems to prevail over its potential inhibition of Abl catalytic activity. The blockage of Abl-mediated phosphorylation of Crk by PTP-PEST could therefore, under certain conditions, increase its association with p130Cas, or, alternatively, could be involved in modulating Crk functions independent of p130Cas.

PTP-PEST was found to play a positive role in signalling during receptor-mediated apoptosis. In fact, clones stably expressing PTP-PEST, as well as HeLa299 cells transiently overexpressing PTP-PEST, both displayed increased levels of TNFα/anti-Fas-induced apoptosis, as compared to controls (Chapter 4). The magnitude of the response to TNFα was directly proportional to the level of PTP-PEST expression. Additionally, only

catalytically active PTP-PEST was able to enhance caspase activation following anti-Fas stimulation, and this effect did not require PTP-PEST processing by caspase-3. These observations, as presented in chapter 4, therefore suggest that PTP-PEST acts as a positive regulator of apoptotic signalling downstream of TNFα and anti-Fas, via dephosphorylation of an unknown target.

Taken together, the data presented herein, as well as that previously published, clearly demonstrates negative regulatory roles for PTP-PEST, and illustrates situations in which this enzyme promotes signal transduction. Additional studies are required to fully elucidate the potential roles of PTP-PEST in positive regulation of signalling pathways.

5.4 How is PTP-PEST regulated?

As reported here and elsewhere, PTP-PEST is involved in a variety of biologic phenomena, including cell migration (11, 120, 172, 287), immune responses (18, 95), parasitic infection (chapter 3), apoptosis (138, 139) and embryogenesis (305). As would be expected based on the fundamental importance of this enzyme, a number of mechanisms are involved in its regulation.

Early studies suggested that the expression of the *PTP-PEST* gene is sensitive to stimuli. In support of this hypothesis, exposure of a muscle-derived cell line to insulin led to increased expression of PTP-PEST mRNA (365). Also, treatment of thryroid carcinoma cells with two different agonists of the peroxisome proliferator-activated receptor γ (PPARγ), ciglitazone and 15-deoxy-$\Delta^{12,14}$-prostaglandin J2, augmented PTP-PEST protein levels (65). Although PTP-PEST transcripts and proteins were found to be ubiquitous, higher levels of expression were detected in tissues and cells of the hematopoietic system (85, 94, 95, 321, 375). These reports indicate that *PTP-PEST* gene expression is transcriptionally regulated.

PTP-PEST was found to be a substrate of PKA (cAMP-dependent protein kinase) and PKC (protein kinase C), which catalyze phosphorylation at Ser39 and Ser435 (119). The phosphorylation of Ser39 was sufficient to down-regulate PTP-PEST catalytic activity (119). Also, serine phosphorylation of PTP-PEST was observed in osteoclasts adhering to osteopontin, an agonist for the integrin $\alpha_v\beta_3$ receptor (60). This implies that the phosphorylation of PTP-PEST could be relevant to adhesion signalling leading to cytoskeletal rearrangements. Interestingly, PKA localizes to the leading pseudopod, where it phosphorylates and inhibits PTP-PEST within cells undergoing chemotaxis; correlating with increased p130Cas phosphorylation and increased RacGTP loading (155). Moreover, the serine-threonine kinase MST3 (mammalian sterile 20-like kinase 3) phosphorylates and inactivates PTP-PEST, and was proposed to play a mechanistic role in the control of cell motility (215). These reports illustrate the importance of post-translational modifications in the modulation of PTP-PEST activity, and therefore in the control of cellular processes.

The targeting of PTPs to a particular subcellular compartment is an important element in the regulation of their function (330). PTP-PEST was previously shown to be primarily cytosolic (56). However, subsequent analysis demonstrated the presence of PTP-PEST in focal adhesion-like structures, in membrane ruffles, and in the crude membrane fraction (chapter 2) (11, 215). Interestingly, in cells responding to fibronectin stimulation, the relocalization of PTP-PEST at the periphery and at the extremity of membrane protrusions was correlated with increased catalytic activity (286). Moreover, in healthy control cells (COS cells not microinjected with recombinant caspase-3 or untreated HeLa cells), EGFP-PTP-PEST consistently accumulated at the edge of retracting lamellipodia of motile cells (Maxime Hallé and Michel L. Tremblay, un-published results). Importantly, EGFP-PTP-PEST was localized at the periphery of retracting membrane ruffles in cells undergoing apoptosis (chapter 4). The correlation between accumulation of PTP-PEST in a particular membrane protrusion and its subsequent retraction, as well

as the increased PTP activity seen during that period (286), emphasize the importance of this phosphatase in destabilization of cellular adhesion to the substratum. Although PTP-PEST binding to Grb-2 was shown to target the phosphatase to RTKs (54), the exact mechanism by which PTP-PEST translocates to retracting lamella remains unknown. However, as membrane retraction is an integral part of both cell migration and apoptosis, it is possible that similar molecular mechanisms operate in both processes.

PTP-PEST was observed to interact with diverse cellular proteins. In several cases, the protein regions involved have been narrowed-down to specific motifs and domains. For example, the recruitment of Shc PTB domain to PTP-PEST is mediated by a NPLH motif (53, 133). Interestingly, the protein kinase C (PKC) activator, phorbol 12-myristate 13-acetate (PMA), induced the phosphorylation of Shc (mainly on serine), which correlated with increased formation of Shc-PTP-PEST complexes (133). An increase in Shc-PTP-PEST association also occurs in response to B-cell receptor stimulation (95). Although the cellular context leading to increased or decreased association of PTP-PEST with several of its binding partners remains unknown, the above studies suggest that these interactions might be subject to specific mechanisms of regulation. In fact, Faisal et al (2002) determined that the phosphorylation of Shc at Ser29 was essential for its binding to PTP-PEST (107). Within the current study, I have observed that the localization of PTP-PEST affects complex assembly. Accordingly, while some PTP-PEST-mediated interactions in the membrane fraction were identical to those found in the cytosol, others were unique to one compartment. In addition, I have provided data illustrating the regulation of PTP-PEST interactions by proteolysis. Specifically, caspase-3-mediated cleavage of PTP-PEST at the ^{549}DSPD motif regulates its scaffolding functions. Furthermore, in vitro experiments indicated that, in the presence of caspase-3, even though the integrity of the Pro2 domain (paxillin binding site on PTP-PEST) was maintained, the binding affinity of paxillin proteins for PTP-PEST was decreased. These results indicate that caspase-3 regulates the assembly of PTP-PEST protein complexes at two levels: through the direct cleavage of PTP-PEST, and by processing some of its

interacting partners. In summary, stimuli promoting or restraining PTP-PEST interactions undoubtedly regulates its functions by changing the amount of PTP-PEST targeted to specific protein complexes.

Herein, the cleavage of PTP-PEST by caspase-3 was observed to increase its phosphatase activity (chapter 4). Truncation of other PTPs such as TC-PTP was demonstrated to promote their activity (80, 382). This implies that, in addition to targeting the enzyme to various subcellular compartments/specific protein complexes, the extra-catalytic domains of PTPs may play a role in regulating their catalytic activity. Indeed, SHPs are regulated via an autoinhibitory mechanism involving intramolecular interactions (242). Interestingly, the expression of the myc-ECFP-PTP-PEST-EYFP construct resulted in an intense FRET (fluorescence resonance energy transfer) signal (Maxime Hallé and Michel L. Tremblay, un-published observations). This may reflect the existence of a conformation in which the PTP-PEST catalytic domain is in close proximity to the non-enzymatic C-terminal segment, which may act in both substrate targeting and regulation of catalysis. Structural studies on PTP-PEST will confirm or refute this hypothesis.

PTP-PEST cleavage was found to promote its catalytic activity, and to modulate its interaction (chapter 4). The classical PTP gene family, in humans, consists of 38 genes, with great diversity in their non-enzymatic domains (5). Surprisingly, no PTPs in addition to PTP-PEST were seen to be cleaved following the caspase activation, as determined by both in immunoblotting and in gel phosphatase experiments (138). However, due to technical limitations, caspase cleavage of additional PTPs could not be excluded. I therefore analyzed the amino acid sequences of over 76 human and murine PTPs, and found putative caspase cleavage sites in the sequences of several, but not all, enzymes (139). The above data indicates that caspases may regulate a subset of PTPs, including PTP-PEST, in order to promote apoptosis. In addition, calpain mediated proteolysis has also been implicated in the regulation of PTPs activity (130). The study of regulatory

mechanisms governing PTP-PEST will likely provide additional insight into the modulation of other members of this family of enzymes.

PTP-PEST was also cleaved by GP63 during *L. major* infection. Although the exact site of cleavage has not yet been mapped, PTP-PEST amino acid sequence contains several putative GP63 cleavage sites (^{7}LRR, ^{35}LRR, ^{58}NVKK, ^{139}GRK, ^{216}MRK, ^{286}VHR and ^{436}EIKK) (Maxime Hallé, Matthew Stuible and Michel L. Tremblay, un-published data) (34). GP63 may therefore mediate either inhibition or activation of PTP-PEST. As the proteolysis of PTP-PEST is seen during two distinct biological processes, it is likely that the maintenance of its integrity is physiologically significant. Of note, *L. donovani* infection was recently found to induce a general activation of PTPs in macrophages (123), and was correlated with the dephosphorylation of several proteins in cells exposed to this parasite (27). Since *Leishmania* infection does not induce the degradation of either PTP-1B (chapter 3) or SHP-1 (27), and a high degree of structural homology is seen in the catalytic domain of PTPs (10), it would be surprising if GP63 leads to inactivation of PTP-PEST via cleavage within the catalytic domain. It is possible that processing by GP63 modifies, as opposed to inhibits, PTP function.

The decreased stability of PTP-PEST observed in cells exposed to different species of *Leishmania* underscores the importance of PTP-PEST regulation in infectious disease. However, as PTP-PEST modulates proteins involved in cellular transformation, the aberrant regulation of this PTP may be relevant to physiological process in addition to those associated with microorganism induced illness. Abnormal transcripts of PTP-PEST have, in fact, been detected in colorectal carcinomas (320). A missense mutation (Lys61Arg), as well as two deletions (both resulting in a frame shift), were identified, and led to the expression of at least one truncated form of PTP-PEST (320). Although the deletions were thought to arise from irregular splicing events, the precise function of this shorter form of PTP-PEST in cellular transformation remains unknown (320). A more recent study reported the presence of three PTP-PEST variants in human breast cancer

cell lines and tumour samples (310). The Val322Ile and Glu709Lys mutations caused, respectively, a small increase and a small decrease in PTP-PEST phosphatase activity. Interestingly, the Thr573Ala substitution resulted in a marked increase in PTP-PEST catalytic activity (310), possibly indicating that phosphorylation at this site impacts enzymatic activity. Taken together, the above investigations point to a potential role for loss of normal PTP-PEST function in pathologies including parasitic infection and tumourigenesis.

The different cellular processes controlling PTP-PEST functions are depicted in figure 5. In conclusion, numerous studies have confirmed that PTP-PEST is subjected to multiple regulatory mechanisms.

Figure 5. Modes of PTP-PEST regulation. PTP-PEST participates in several biological phenomena including cell migration, apoptosis, embryonic development and parasitic infections. The expression, activity, localization, protein interactions and integrity of this enzyme are regulated by a variety of mechanisms.

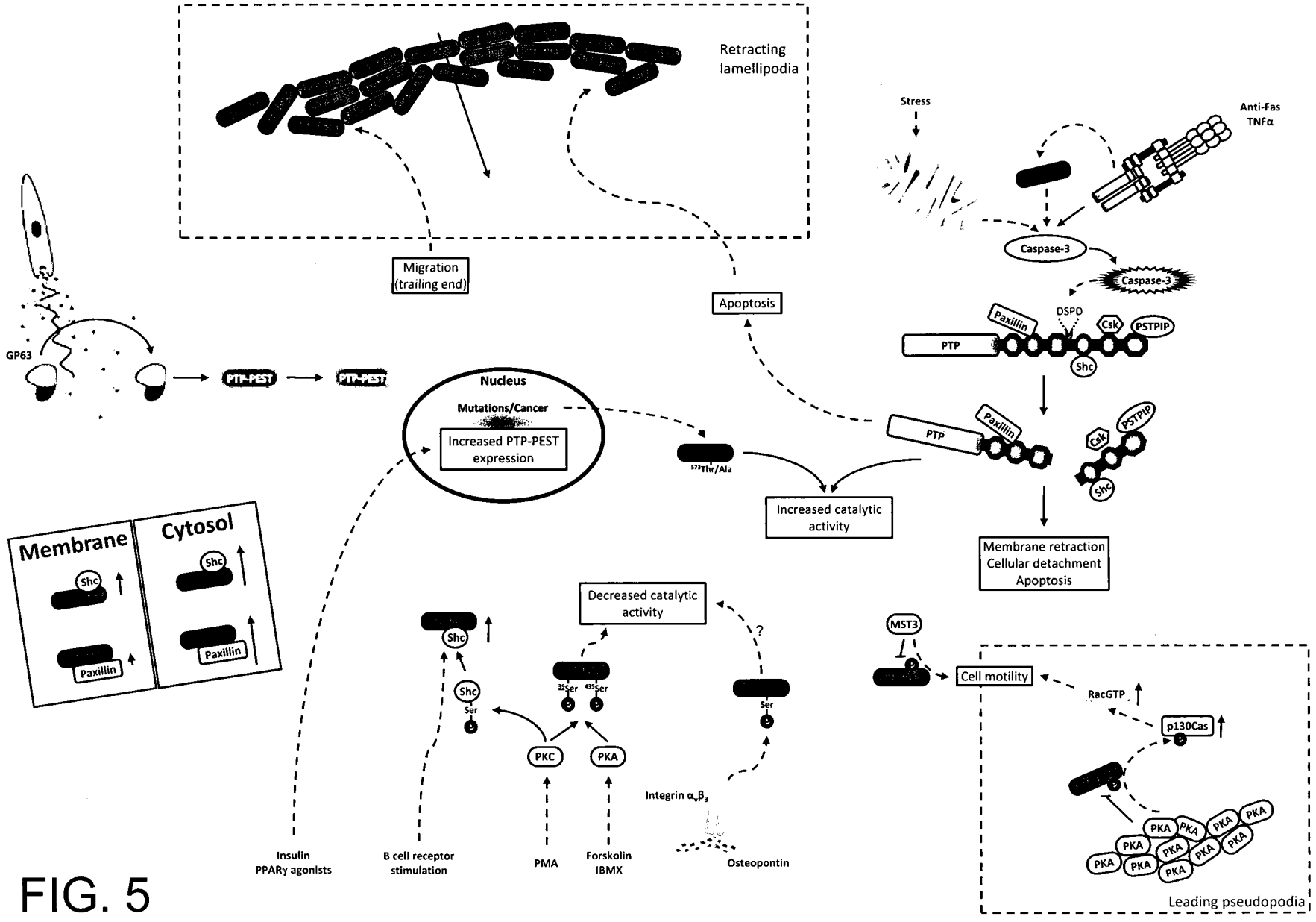
Retracting lamellipodia
Migration (trailing end)
Apoptosis
Stress
Anti-Fas TNFα
Caspase-3
Caspase-3
Paxillin
DSPD
Csk
PSTPIP
PTP
Shc
GP63
PTP-PEST
PTP-PEST
Nucleus
Mutations/Cancer
Increased PTP-PEST expression
573Thr/Ala
Increased catalytic activity
Membrane retraction
Cellular detachment
Apoptosis
Membrane
Cytosol
Shc
Paxillin
Decreased catalytic activity
Shc
Ser
PKC
PKA
Integrin αvβ3
Osteopontin
Insulin
PPARγ agonists
B cell receptor stimulation
PMA
Forskolin
IBMX
MST3
Cell motility
RacGTP
p130Cas
PKA
Leading pseudopodia

FIG. 5

5.5 Is PTP-PEST an active regulator or a housekeeping gene?

Constitutively expressed housekeeping genes are involved in fundamental processes required to maintain cellular homeostasis (43). A true housekeeping phosphatase would be expected to show little substrate specificity and to be constitutively active, in order to maintain a basal cellular level of phosphorylation. The different mechanisms of regulation of PTP-PEST, as well as its involvement in a variety of physiologic phenomena, suggest that this enzyme can occupy both housekeeping and pro-active roles.

Several aspects of the regulation and function of PTP-PEST point to a housekeeping role for this enzyme. PTP-PEST displays a ubiquitous pattern of expression in adult organisms and can be detected at early stages of embryogenesis (56, 305, 321, 375). Additionally, this enzyme is necessary for the completion of embryonic development, for cell migration, and for increased sensitivity to apoptotic inducers (11, 305) (chapter 4). Thus, a titrating effect, in which constitutive PTP-PEST activity would keep vital signalling components inactive in a broad range of cell types, may explain the regulatory functions of PTP-PEST. The expression and phosphorylation of the PTP-PEST substrate p130Cas plays a pro-oncogenic role by promoting cell migration, survival and transformation (15, 35, 118, 153, 188). In addition, uncoupling of the p130Cas/Crk complex was recently proposed to enhance apoptosis induced by proteasome inhibition (151). The investigations presented here show that PTP-PEST is required to abrogate p130Cas-phospho-dependent interactions with SH2 containing molecules in resting cells, and that it further limits this association following LPA stimulation (chapter 2). In addition, we observed that expression of PTP-PEST reduces cell proliferation (Hidehisa Shimizu, Maxime Hallé and Michel L. Tremblay, un-published results). The maintenance of p130Cas in a dephosphorylated state by PTP-PEST presumably blocks associated signaling pathways. Nevertheless, the expression of PTP-PEST alone did not induce

apoptosis in resting cells (chapter 4). This indicates that the negative effect of PTP-PEST on cell proliferation is not due to activation of cell death. The above evidence suggests that PTP-PEST could play an essential housekeeping role via prevention of transformation through stabilization of cells in a differentiated state, inhibition of oncogenic signalling, and maintenance of sensitivity to apoptotic signals.

As described above, PTP-PEST is also involved in the regulation of a variety of substrates influencing the polymerization and organisation of actin filaments. For example, by limiting p130Cas/Crk interactions, by maintaining Rac, WASP and N-WASP activities at low levels, and by modulating the localization of paxillin and PSTPIP in resting cells (chapter 2 and data not shown) (18, 85, 120, 286), PTP-PEST could prevent aberrant signals from increasing production of membrane protrusions. Accordingly, *PTP-PEST -/-* cells displayed defective polarity, and transient over-expression of PTP-PEST prevented the formation of membrane protrusion, dependent on catalytic activity (286, 287). The titration of signalling molecules by PTP-PEST could thereby prevent the inappropriate projection of pseudopods. In cells expressing physiological levels of PTP-PEST, p130Cas/Crk assembly and protrusive activity are augmented in response to various stimuli (chapter 2 and data not shown) (172, 286), and PTP-PEST may therefore act as a filter that selectively allows the transmission of specific signals. This effect might be particularly important in sensing a chemotactic gradient and in activation of site directed migration.

Although the qualifying term "housekeeping" may seem "unglamorous", this function of PTP-PEST could be fundamental in preventing adverse effects caused by hyperphosphorylated substrates, and in transduction of signals to the appropriate target in a spatiotemporal manner.

Certain data with respect to PTP-PEST indicate dynamic functions and modes of regulation. Even though the PTP-PEST expression pattern is ubiquitous, increased levels

were found in haemopoietic cells (85, 94, 95), suggesting that PTP-PEST may have discrete functions in specific cell types. Interestingly, in cells stimulated with anti-Fas, as well as in migrating cells, PTP-PEST was observed to specifically relocalize at the edge of retracting lamellipodia (chapter 4, Maxime Hallé and Michel L. Tremblay un-published results). Also, the activity of PTP-PEST was correlated with its translocation to the cell periphery (286). This dynamic regulation of PTP-PEST was associated with a positive role in cellular detachment during apoptosis, and in tail retraction of migrating cells (chapter 4) (287). Additionally, the involvement of regulatory mechanisms including phosphorylation, cleavage and recruitment of signalling molecules (chapter 3, 4, (54, 60, 95, 107, 133, 155), in response to various agonists, supports the existence of dynamic functions of PTP-PEST. Importantly, PTP-PEST has great substrate specificity. In fact, the overexpression of PTP-PEST reduces the phosphorylation of only a small subset of proteins (p150, p130, p125, p115 and p54) (95, 120), and only three proteins are hyperphosphorylated in *PTP-PEST* -/- cells (p180, p130 and p97) (84). Moreover, only a single band, corresponding to p130Cas, showed increased phosphorylation in total cell lysates from *PTP-PEST* -/- embryos (305). Notably, the PTP-PEST relocalization and interaction with WASP at the immune synapse inhibits immune synapse formation and actin polymerization (18). As the presence of PTP-PEST at the membrane correlates with retraction, intracellular parasites, which depend of the projection of membrane sheets to trigger their entry (250), may target PTP-PEST to enhance this process. Interestingly, early cleavage of PTP-PEST was observed during cellular infection with *Leishmania* (chapter 3). It is possible that this cleavage dissociates PTP-PEST from WASP proteins, increasing their phosphorylation and promoting actin polymerization activity. This effect would support both the engulfment of the protozoa and synthesis of a protective actin cup (chapter 3) (212, 237). The above evidence points to the existence of pro-active functions for PTP-PEST.

Collectively, the ubiquitous pattern of expression of PTP-PEST, as well as its fundamental importance in basic biologic phenomena, indicates that this enzyme has

housekeeping features. In contrast, its tight regulation, some of its functional characteristics, and its substrate specificity, point to non-housekeeping roles. Additional studies are required to determine how this functional duality of PTP-PEST is physiologically balanced.

6 CONCLUSION

The requirement for PTP-PEST to complete embryogenesis demonstrates its fundamental physiological importance (305). At a mechanistic level, the majority of studies on PTP-PEST have focussed on its regulation of the cytoskeleton and associated cellular functions. Herein, I present data linking PTP-PEST with various biologically relevant processes, including LPA signalling, host-pathogen interaction, and apoptosis. Importantly, these studies illustrates two complementary levels at which PTP-PEST regulates, and is itself regulated by, diverse stimuli. First, the integration of PTP-PEST in different pathways was explored. Specifically, PTP-PEST was found to modulate the cellular response to both LPA-induced signalling and receptor-mediated apoptosis. Second, the effect of external stimuli on PTP-PEST was investigated. PTP-PEST was found to relocalize to retracting membrane ruffles in cells stimulated with anti-Fas, and was cleaved in response to two independent and unrelated inducers.

PEST sequences have been proposed to reduce protein stability (272). The irreversible nature of proteolytic modification represents a unique regulatory mechanism. The presence of PEST sequences in a PTP isolated by Yang et al (1993) was proposed to be of paramount importance in the modulation of this enzyme, hence named "PTP-PEST":

"... If a similar role applies to this segment of PTP-PEST, one could envisage a situation in which the activity of the enzyme may be controlled by physical displacement to a distinct intracellular location away from its normal pool of substrates, following proteolytic cleavage of the C-terminal domain."

Yang et al. 1993, J. Biol. Chem. 268: 6622-6628.

Subsequent pulse-chase analysis, however, underscored the stability of PTP-PEST (56). Consequently, the importance of proteolytic regulation of PTP-PEST has, until recently, been underappreciated.

In this thesis, *Leishmania* infection was found to induce the cleavage of both PTP-PEST and p130Cas, and of caspase-3, cortactin, TC-PTP and TAB1, and to inactivate p38. These events were dependent on expression of the parasitic surface metalloprotease GP63, and coincided with early transfer of this protein to the host intracellular space during the infection process.

Another physiological process involving regulated proteolysis leading to major cytoskeletal rearrangements is apoptosis. Importantly, PTP-PEST is cleaved by caspase-3, which affects both its phosphatase activity and scaffolding properties. The expression of PTP-PEST promotes receptor-mediated caspase activation, and cleavage at the ^{549}DSPD motif is essential for efficient cellular detachment in response to apoptotic stimuli.

Several infectious agents in addition to *Leishmania* target cytoskeletal components during their pathogenesis (239). Also, rearrangement of the actin network and inhibition of apoptosis, are crucial events leading to cellular transformation and the dissemination of metastatic cells, which both sustain cancer progression. Further studies evaluating putative tumour-suppressor or pro-oncogenic roles for PTP-PEST, as well as its involvement in various infectious diseases, should be promising. In summary, this work presents novel mechanisms of PTP-PEST regulation, which are integrated in fundamental biological processes.

7 REFERENCES

1. **Abaan, O. D., A. Levenson, O. Khan, P. A. Furth, A. Uren, and J. A. Toretsky.** 2005. PTPL1 is a direct transcriptional target of EWS-FLI1 and modulates Ewing's Sarcoma tumorigenesis. Oncogene **24:**2715-22.
2. **Adams, J. M.** 2003. Ways of dying: multiple pathways to apoptosis. Genes Dev. **17:**2481-95.
3. **Aga, E., D. M. Katschinski, G. van Zandbergen, H. Laufs, B. Hansen, K. Muller, W. Solbach, and T. Laskay.** 2002. Inhibition of the spontaneous apoptosis of neutrophil granulocytes by the intracellular parasite *Leishmania major*. J. Immunol. **169:**898-905.
4. **Akasaki, Y., G. Liu, H. H. Matundan, H. Ng, X. Yuan, Z. Zeng, K. L. Black, and J. S. Yu.** 2006. A peroxisome proliferator-activated receptor-gamma agonist, troglitazone, facilitates caspase-8 and -9 activities by increasing the enzymatic activity of protein-tyrosine phosphatase-1B on human glioma cells. J Biol Chem **281:**6165-74.
5. **Alonso, A., J. Sasin, N. Bottini, I. Friedberg, A. Osterman, A. Godzik, T. Hunter, J. Dixon, and T. Mustelin.** 2004. Protein tyrosine phosphatases in the human genome. Cell **117:**699-711.
6. **Amin, A. R., V. S. Thakur, R. K. Paul, G. S. Feng, C. K. Qu, H. Mukhtar, and M. L. Agarwal.** 2007. SHP-2 tyrosine phosphatase inhibits p73-dependent apoptosis and expression of a subset of p53 target genes induced by EGCG. Proc Natl Acad Sci U S A **104:**5419-24.
7. **Amoui, M., M. H. Sheng, S. T. Chen, D. J. Baylink, and K. H. Lau.** 2007. A transmembrane osteoclastic protein-tyrosine phosphatase regulates osteoclast activity in part by promoting osteoclast survival through c-Src-dependent activation of NFkappaB and JNK2. Arch Biochem Biophys **463:**47-59.
8. **Anand, A. R., and R. K. Ganju.** 2006. HIV-1 gp120-mediated apoptosis of T cells is regulated by the membrane tyrosine phosphatase CD45. J Biol Chem **281:**12289-99.
9. **Andersen, J. N., A. Elson, R. Lammers, J. Romer, J. T. Clausen, K. B. Moller, and N. P. Moller.** 2001. Comparative study of protein tyrosine phosphatase-epsilon isoforms: membrane localization confers specificity in cellular signalling. Biochem. J. **354:**581-90.
10. **Andersen, J. N., O. H. Mortensen, G. H. Peters, P. G. Drake, L. F. Iversen, O. H. Olsen, P. G. Jansen, H. S. Andersen, N. K. Tonks, and N. P. Moller.** 2001. Structural and evolutionary relationships among protein tyrosine phosphatase domains. Mol Cell Biol **21:**7117-36.
11. **Angers-Loustau, A., J. F. Côté, A. Charest, D. Dowbenko, S. Spencer, L. A. Lasky, and M. L. Tremblay.** 1999. Protein tyrosine phosphatase-PEST regulates focal adhesion disassembly, migration, and cytokinesis in fibroblasts. J. Cell Biol. **144:**1019-31.
12. **Angers-Loustau, A., J. F. Côté, and M. L. Tremblay.** 1999. Roles of protein tyrosine phosphatases in cell migration and adhesion. Biochem. Cell Biol. **77:**493-505.
13. **Ashford, R. W., P. Desjeux, and P. Deraadt.** 1992. Estimation of population at risk of infection and number of cases of Leishmaniasis. Parasitol Today **8:**104-5.
14. **Astier, A., S. N. Manie, H. Avraham, H. Hirai, S. F. Law, Y. Zhang, E. A. Golemis, Y. Fu, B. J. Druker, N. Haghayeghi, A. S. Freedman, and S. Avraham.** 1997. The related adhesion focal tyrosine kinase differentially phosphorylates p130Cas and the Cas-like protein, p105HEF1. J Biol Chem **272:**19719-24.

15. **Auvinen, M., A. Paasinen-Sohns, H. Hirai, L. C. Andersson, and E. Holtta.** 1995. Ornithine decarboxylase- and ras-induced cell transformations: reversal by protein tyrosine kinase inhibitors and role of pp130CAS. Mol Cell Biol **15**:6513-25.
16. **Avraham, H. K., T. H. Lee, Y. Koh, T. A. Kim, S. Jiang, M. Sussman, A. M. Samarel, and S. Avraham.** 2003. Vascular endothelial growth factor regulates focal adhesion assembly in human brain microvascular endothelial cells through activation of the focal adhesion kinase and related adhesion focal tyrosine kinase. J Biol Chem **278**:36661-8.
17. **Awasthi, A., R. Mathur, A. Khan, B. N. Joshi, N. Jain, S. Sawant, R. Boppana, D. Mitra, and B. Saha.** 2003. CD40 signaling is impaired in L. major-infected macrophages and is rescued by a p38MAPK activator establishing a host-protective memory T cell response. J. Exp. Med. **197**:1037-43.
18. **Badour, K., J. Zhang, F. Shi, Y. Leng, M. Collins, and K. A. Siminovitch.** 2004. Fyn and PTP-PEST-mediated regulation of Wiskott-Aldrich syndrome protein (WASp) tyrosine phosphorylation is required for coupling T cell antigen receptor engagement to WASp effector function and T cell activation. J. Exp. Med. **199**:99-112.
19. **Balaraman, S., V. K. Singh, P. Tewary, and R. Madhubala.** 2005. Leishmania lipophosphoglycan activates the transcription factor activating protein 1 in J774A.1 macrophages through the extracellular signal-related kinase (ERK) and p38 mitogen-activated protein kinase. Mol. Biochem. Parasitol. **139**:117-27.
20. **Barrett, D. M., S. M. Black, H. Todor, R. K. Schmidt-Ullrich, K. S. Dawson, and R. B. Mikkelsen.** 2005. Inhibition of protein-tyrosine phosphatases by mild oxidative stresses is dependent on S-nitrosylation. J. Biol. Chem. **280**:14453-61.
21. **Baum, W., V. Kirkin, S. B. Fernandez, R. Pick, M. Lettau, O. Janssen, and M. Zornig.** 2005. Binding of the Intracellular Fas Ligand (FasL) Domain to the Adaptor Protein PSTPIP Results in a Cytoplasmic Localization of FasL. J. Biol. Chem. **280**:40012-24.
22. **Belle, E. A.** 1958. Cultivation of *Leishmania donovani* in human amnion epithelial cell tissue cultures: a preliminary report. Can. Med. Assoc. J. **79**:726-8.
23. **Bentires-Alj, M., and B. G. Neel.** 2007. Protein-tyrosine phosphatase 1B is required for HER2/Neu-induced breast cancer. Cancer Res **67**:2420-4.
24. **Bishop, A. L., and A. Hall.** 2000. Rho GTPases and their effector proteins. Biochem J **348 Pt 2**:241-55.
25. **Blanchetot, C., M. Chagnon, N. Dubé, M. Hallé, and M. L. Tremblay.** 2005. Substrate-trapping techniques in the identification of cellular PTP targets. Methods **35**:44-53.
26. **Blanchetot, C., L. G. Tertoolen, and J. den Hertog.** 2002. Regulation of receptor protein-tyrosine phosphatase alpha by oxidative stress. EMBO J. **21**:493-503.
27. **Blanchette, J., N. Racette, R. Faure, K. A. Siminovitch, and M. Olivier.** 1999. Leishmania-induced increases in activation of macrophage SHP-1 tyrosine phosphatase are associated with impaired IFN-gamma-triggered JAK2 activation. Eur. J. Immunol. **29**:3737-44.
28. **Boatright, K. M., and G. S. Salvesen.** 2003. Mechanisms of caspase activation. Curr. Opin. Cell Biol. **15**:725-31.
29. **Bogdan, C., N. Donhauser, R. Doring, M. Rollinghoff, A. Diefenbach, and M. G. Rittig.** 2000. Fibroblasts as host cells in latent leishmaniosis. J. Exp. Med. **191**:2121-30.
30. **Bompard, G., C. Puech, C. Prebois, F. Vignon, and G. Freiss.** 2002. Protein-tyrosine phosphatase PTPL1/FAP-1 triggers apoptosis in human breast cancer cells. J Biol Chem **277**:47861-9.

31. **Bourdeau, A., N. Dubé, K. M. Heinonen, J. F. Théberge, K. M. Doody, and M. L. Tremblay.** 2007. TC-PTP-deficient bone marrow stromal cells fail to support normal B lymphopoiesis due to abnormal secretion of interferon-{gamma}. Blood **109**:4220-4228.
32. **Bouton, A. H., R. B. Riggins, and P. J. Bruce-Staskal.** 2001. Functions of the adapter protein Cas: signal convergence and the determination of cellular responses. Oncogene **20**:6448-58.
33. **Bouvier, J., R. J. Etges, and C. Bordier.** 1985. Identification and purification of membrane and soluble forms of the major surface protein of Leishmania promastigotes. J. Biol. Chem. **260**:15504-9.
34. **Bouvier, J., P. Schneider, R. Etges, and C. Bordier.** 1990. Peptide substrate specificity of the membrane-bound metalloprotease of *Leishmania*. Biochemistry **29**:10113-9.
35. **Brinkman, A., S. van der Flier, E. M. Kok, and L. C. Dorssers.** 2000. BCAR1, a human homologue of the adapter protein p130Cas, and antiestrogen resistance in breast cancer cells. J Natl Cancer Inst **92**:112-20.
36. **Brittingham, A., G. Chen, B. S. McGwire, K. P. Chang, and D. M. Mosser.** 1999. Interaction of Leishmania gp63 with cellular receptors for fibronectin. Infect. Immun. **67**:4477-84.
37. **Brittingham, A., C. J. Morrison, W. R. McMaster, B. S. McGwire, K. P. Chang, and D. M. Mosser.** 1995. Role of the Leishmania surface protease gp63 in complement fixation, cell adhesion, and resistance to complement-mediated lysis. J. Immunol. **155**:3102-11.
38. **Brown, M. C., and C. E. Turner.** 2004. Paxillin: adapting to change. Physiol Rev **84**:1315-39.
39. **Brown, M. C., and C. E. Turner.** 2002. Roles for the tubulin- and PTP-PEST-binding paxillin LIM domains in cell adhesion and motility. Int J Biochem Cell Biol **34**:855-63.
40. **Bruckner, S., S. Rhamouni, L. Tautz, J. B. Denault, A. Alonso, B. Becattini, G. S. Salvesen, and T. Mustelin.** 2005. Yersinia phosphatase induces mitochondrially dependent apoptosis of T cells. J. Biol. Chem. **280**:10388-94.
41. **Burridge, K., S. K. Sastry, and J. L. Sallee.** 2006. Regulation of cell adhesion by protein-tyrosine phosphatases. I. Cell-matrix adhesion. J Biol Chem **281**:15593-6.
42. **Burton, E. A., T. N. Oliver, and A. M. Pendergast.** 2005. Abl kinases regulate actin comet tail elongation via an N-WASP-dependent pathway. Mol Cell Biol **25**:8834-43.
43. **Butte, A. J., V. J. Dzau, and S. B. Glueck.** 2001. Further defining housekeeping, or "maintenance," genes Focus on "A compendium of gene expression in normal human tissues". Physiol Genomics **7**:95-6.
44. **Button, L. L., G. Wilson, C. R. Astell, and W. R. McMaster.** 1993. Recombinant *Leishmania* surface glycoprotein GP63 is secreted in the baculovirus expression system as a latent metalloproteinase. Gene **134**:75-81.
45. **Byth, K. F., L. A. Conroy, S. Howlett, A. J. Smith, J. May, D. R. Alexander, and N. Holmes.** 1996. CD45-null transgenic mice reveal a positive regulatory role for CD45 in early thymocyte development, in the selection of CD4+CD8+ thymocytes, and B cell maturation. J Exp Med **183**:1707-18.
46. **Cabodi, S., A. Tinnirello, P. Di Stefano, B. Bisaro, E. Ambrosino, I. Castellano, A. Sapino, R. Arisio, F. Cavallo, G. Forni, M. Glukhova, L. Silengo, F. Altruda, E. Turco, G. Tarone, and P. Defilippi.** 2006. p130Cas as a new regulator of mammary epithelial cell proliferation, survival, and HER2-neu oncogene-dependent breast tumorigenesis. Cancer Res **66**:4672-80.

47. **Caenepeel, S., G. Charydczak, S. Sudarsanam, T. Hunter, and G. Manning.** 2004. The mouse kinome: discovery and comparative genomics of all mouse protein kinases. Proc Natl Acad Sci U S A **101:**11707-12.
48. **Campbell, D. A., U. Kurath, and J. Fleischmann.** 1992. Identification of a gp63 surface glycoprotein in *Leishmania tarentolae*. FEMS Microbiol. Lett. **75:**89-92.
49. **Carmen, J. C., and A. P. Sinai.** 2007. Suicide prevention: disruption of apoptotic pathways by protozoan parasites. Mol. Microbiol. **64:**904-16.
50. **Casamassima, A., and E. Rozengurt.** 1997. Tyrosine phosphorylation of p130(cas) by bombesin, lysophosphatidic acid, phorbol esters, and platelet-derived growth factor. Signaling pathways and formation of a p130(cas)-Crk complex. J Biol Chem **272:**9363-70.
51. **Chandel, N. S., and G. R. Budinger.** 2007. The cellular basis for diverse responses to oxygen. Free Radic Biol Med **42:**165-74.
52. **Charbonneau, H., N. K. Tonks, K. A. Walsh, and E. H. Fischer.** 1988. The leukocyte common antigen (CD45): a putative receptor-linked protein tyrosine phosphatase. Proc Natl Acad Sci U S A **85:**7182-6.
53. **Charest, A., J. Wagner, S. Jacob, C. J. McGlade, and M. L. Tremblay.** 1996. Phosphotyrosine-independent binding of SHC to the NPLH sequence of murine protein-tyrosine phosphatase-PEST. Evidence for extended phosphotyrosine binding/phosphotyrosine interaction domain recognition specificity. J. Biol. Chem. **271:**8424-9.
54. **Charest, A., J. Wagner, M. Kwan, and M. L. Tremblay.** 1997. Coupling of the murine protein tyrosine phosphatase PEST to the epidermal growth factor (EGF) receptor through a Src homology 3 (SH3) domain-mediated association with Grb2. Oncogene **14:**1643-51.
55. **Charest, A., J. Wagner, E. S. Muise, H. H. Heng, and M. L. Tremblay.** 1995. Structure of the murine MPTP-PEST gene: genomic organization and chromosomal mapping. Genomics **28:**501-7.
56. **Charest, A., J. Wagner, S. H. Shen, and M. L. Tremblay.** 1995. Murine protein tyrosine phosphatase-PEST, a stable cytosolic protein tyrosine phosphatase. Biochem. J. **308 (Pt 2):**425-32.
57. **Chaudhuri, G., and K. P. Chang.** 1988. Acid protease activity of a major surface membrane glycoprotein (gp63) from Leishmania mexicana promastigotes. Mol. Biochem. Parasitol. **27:**43-52.
58. **Chaudhuri, G., M. Chaudhuri, A. Pan, and K. P. Chang.** 1989. Surface acid proteinase (gp63) of *Leishmania mexicana*. A metalloenzyme capable of protecting liposome-encapsulated proteins from phagolysosomal degradation by macrophages. J. Biol. Chem. **264:**7483-9.
59. **Chay, K. O., S. S. Park, and J. F. Mushinski.** 2002. Linkage of caspase-mediated degradation of paxillin to apoptosis in Ba/F3 murine pro-B lymphocytes. J. Biol. Chem. **277:**14521-9.
60. **Chellaiah, M. A., R. S. Biswas, D. Yuen, U. M. Alvarez, and K. A. Hruska.** 2001. Phosphatidylinositol 3,4,5-trisphosphate directs association of Src homology 2-containing signaling proteins with gelsolin. J. Biol. Chem. **276:**47434-44.
61. **Chen, D. Q., B. K. Kolli, N. Yadava, H. G. Lu, A. Gilman-Sachs, D. A. Peterson, and K. P. Chang.** 2000. Episomal expression of specific sense and antisense mRNAs in Leishmania amazonensis: modulation of gp63 level in promastigotes and their infection of macrophages in vitro. Infect. Immun. **68:**80-6.

62. **Chen, F., M. Kamradt, M. Mulcahy, Y. Byun, H. Xu, M. J. McKay, and V. L. Cryns.** 2002. Caspase proteolysis of the cohesin component RAD21 promotes apoptosis. J. Biol. Chem. **277**:16775-81.
63. **Chen, J., W. M. Yu, K. D. Bunting, and C. K. Qu.** 2004. A negative role of SHP-2 tyrosine phosphatase in growth factor-dependent hematopoietic cell survival. Oncogene **23**:3659-69.
64. **Chen, L., P. Juszczynski, K. Takeyama, R. C. Aguiar, and M. A. Shipp.** 2006. Protein tyrosine phosphatase receptor-type O truncated (PTPROt) regulates SYK phosphorylation, proximal B-cell-receptor signaling, and cellular proliferation. Blood **108**:3428-33.
65. **Chen, Y., S. M. Wang, J. C. Wu, and S. H. Huang.** 2006. Effects of PPARgamma agonists on cell survival and focal adhesions in a Chinese thyroid carcinoma cell line. J. Cell. Biochem. **98**:1021-35.
66. **Chen, Y. R., R. Kori, B. John, and T. H. Tan.** 2001. Caspase-mediated cleavage of actin-binding and SH3-domain-containing proteins cortactin, HS1, and HIP-55 during apoptosis. Biochem. Biophys. Res. Commun. **288**:981-9.
67. **Cheng, A., G. S. Bal, B. P. Kennedy, and M. L. Tremblay.** 2001. Attenuation of adhesion-dependent signaling and cell spreading in transformed fibroblasts lacking protein tyrosine phosphatase-1B. J. Biol. Chem. **276**:25848-55.
68. **Chiang, G. G., and B. M. Sefton.** 2001. Specific dephosphorylation of the Lck tyrosine protein kinase at Tyr-394 by the SHP-1 protein-tyrosine phosphatase. J Biol Chem **276**:23173-8.
69. **Cho, S. Y., and R. L. Klemke.** 2000. Extracellular-regulated kinase activation and CAS/Crk coupling regulate cell migration and suppress apoptosis during invasion of the extracellular matrix. J Cell Biol **149**:223-36.
70. **Cho, S. Y., and R. L. Klemke.** 2002. Purification of pseudopodia from polarized cells reveals redistribution and activation of Rac through assembly of a CAS/Crk scaffold. J Cell Biol **156**:725-36.
71. **Chodniewicz, D., and R. L. Klemke.** 2004. Regulation of integrin-mediated cellular responses through assembly of a CAS/Crk scaffold. Biochim Biophys Acta **1692**:63-76.
72. **Chong, Y. P., T. D. Mulhern, and H. C. Cheng.** 2005. C-terminal Src kinase (CSK) and CSK-homologous kinase (CHK)--endogenous negative regulators of Src-family protein kinases. Growth Factors **23**:233-44.
73. **Choy, E., V. K. Chiu, J. Silletti, M. Feoktistov, T. Morimoto, D. Michaelson, I. E. Ivanov, and M. R. Philips.** 1999. Endomembrane trafficking of ras: the CAAX motif targets proteins to the ER and Golgi. Cell **98**:69-80.
74. **Cloutier, J. F., and A. Veillette.** 1996. Association of inhibitory tyrosine protein kinase p50csk with protein tyrosine phosphatase PEP in T cells and other hemopoietic cells. EMBO J. **15**:4909-18.
75. **Coburn, B., I. Sekirov, and B. B. Finlay.** 2007. Type III secretion systems and disease. Clin. Microbiol. Rev. **20**:535-49.
76. **Cohen, S., H. Ushiro, C. Stoscheck, and M. Chinkers.** 1982. A native 170,000 epidermal growth factor receptor-kinase complex from shed plasma membrane vesicles. J Biol Chem **257**:1523-31.
77. **Coleman, M. L., and M. F. Olson.** 2002. Rho GTPase signalling pathways in the morphological changes associated with apoptosis. Cell Death Differ. **9**:493-504.

78. **Coleman, M. L., E. A. Sahai, M. Yeo, M. Bosch, A. Dewar, and M. F. Olson.** 2001. Membrane blebbing during apoptosis results from caspase-mediated activation of ROCK I. Nat. Cell Biol. **3**:339-45.
79. **Cong, F., S. Spencer, J. F. Côté, Y. Wu, M. L. Tremblay, L. A. Lasky, and S. P. Goff.** 2000. Cytoskeletal protein PSTPIP1 directs the PEST-type protein tyrosine phosphatase to the c-Abl kinase to mediate Abl dephosphorylation. Mol. Cell **6**:1413-23.
80. **Cool, D. E., N. K. Tonks, H. Charbonneau, E. H. Fischer, and E. G. Krebs.** 1990. Expression of a human T-cell protein-tyrosine-phosphatase in baby hamster kidney cells. Proc Natl Acad Sci U S A **87**:7280-4.
81. **Cool, D. E., N. K. Tonks, H. Charbonneau, K. A. Walsh, E. H. Fischer, and E. G. Krebs.** 1989. cDNA isolated from a human T-cell library encodes a member of the protein-tyrosine-phosphatase family. Proc Natl Acad Sci U S A **86**:5257-61.
82. **Corradin, S., A. Ransijn, G. Corradin, M. A. Roggero, A. A. Schmitz, P. Schneider, J. Mauel, and G. Vergeres.** 1999. MARCKS-related protein (MRP) is a substrate for the Leishmania major surface protease leishmanolysin (gp63). J. Biol. Chem. **274**:25411-8.
83. **Cory, G. O., R. Garg, R. Cramer, and A. J. Ridley.** 2002. Phosphorylation of tyrosine 291 enhances the ability of WASp to stimulate actin polymerization and filopodium formation. Wiskott-Aldrich Syndrome protein. J Biol Chem **277**:45115-21.
84. **Côté, J. F., A. Charest, J. Wagner, and M. L. Tremblay.** 1998. Combination of gene targeting and substrate trapping to identify substrates of protein tyrosine phosphatases using PTP-PEST as a model. Biochemistry **37**:13128-37.
85. **Côté, J. F., P. L. Chung, J. F. Théberge, M. Hallé, S. Spencer, L. A. Lasky, and M. L. Tremblay.** 2002. PSTPIP is a substrate of PTP-PEST and serves as a scaffold guiding PTP-PEST toward a specific dephosphorylation of WASP. J. Biol. Chem. **277**:2973-86.
86. **Côté, J. F., C. E. Turner, and M. L. Tremblay.** 1999. Intact LIM 3 and LIM 4 domains of paxillin are required for the association to a novel polyproline region (Pro 2) of protein-tyrosine phosphatase-PEST. J. Biol. Chem. **274**:20550-60.
87. **Côté, J. F., and K. Vuori.** 2007. GEF what? Dock180 and related proteins help Rac to polarize cells in new ways. Trends Cell Biol. **17**:383-93.
88. **Cousin, H., and D. Alfandari.** 2004. A PTP-PEST-like protein affects alpha5beta1-integrin-dependent matrix assembly, cell adhesion, and migration in Xenopus gastrula. Dev. Biol. **265**:416-32.
89. **Croft, D. R., M. L. Coleman, S. Li, D. Robertson, T. Sullivan, C. L. Stewart, and M. F. Olson.** 2005. Actin-myosin-based contraction is responsible for apoptotic nuclear disintegration. J. Cell Biol. **168**:245-55.
90. **Cunningham, A. C.** 2002. Parasitic adaptive mechanisms in infection by leishmania. Exp. Mol. Pathol. **72**:132-41.
91. **Cursi, S., A. Rufini, V. Stagni, I. Condo, V. Matafora, A. Bachi, A. P. Bonifazi, L. Coppola, G. Superti-Furga, R. Testi, and D. Barila.** 2006. Src kinase phosphorylates Caspase-8 on Tyr380: a novel mechanism of apoptosis suppression. EMBO J **25**:1895-905.
92. **Curtin, J. F., and T. G. Cotter.** 2003. Live and let die: regulatory mechanisms in Fas-mediated apoptosis. Cell Signal **15**:983-92.
93. **Daigle, I., S. Yousefi, M. Colonna, D. R. Green, and H. U. Simon.** 2002. Death receptors bind SHP-1 and block cytokine-induced anti-apoptotic signaling in neutrophils. Nat Med **8**:61-7.

94. **Davidson, D., J. F. Cloutier, A. Gregorieff, and A. Veillette.** 1997. Inhibitory tyrosine protein kinase p50csk is associated with protein-tyrosine phosphatase PTP-PEST in hemopoietic and non-hemopoietic cells. J. Biol. Chem. **272:**23455-62.
95. **Davidson, D., and A. Veillette.** 2001. PTP-PEST, a scaffold protein tyrosine phosphatase, negatively regulates lymphocyte activation by targeting a unique set of substrates. EMBO J. **20:**3414-26.
96. **Defilippi, P., P. Di Stefano, and S. Cabodi.** 2006. p130Cas: a versatile scaffold in signaling networks. Trends Cell Biol. **16:**257-63.
97. **Demeter, J., and S. Sazer.** 1998. imp2, a new component of the actin ring in the fission yeast Schizosaccharomyces pombe. J Cell Biol **143:**415-27.
98. **den Hertog, J., C. E. Pals, L. J. Jonk, and W. Kruijer.** 1992. Differential expression of a novel murine non-receptor protein tyrosine phosphatase during differentiation of P19 embryonal carcinoma cells. Biochem. Biophys. Res. Commun. **184:**1241-9.
99. **Dolfi, F., M. Garcia-Guzman, M. Ojaniemi, H. Nakamura, M. Matsuda, and K. Vuori.** 1998. The adaptor protein Crk connects multiple cellular stimuli to the JNK signaling pathway. Proc Natl Acad Sci U S A **95:**15394-9.
100. **Dowbenko, D., S. Spencer, C. Quan, and L. A. Lasky.** 1998. Identification of a novel polyproline recognition site in the cytoskeletal associated protein, proline serine threonine phosphatase interacting protein. J. Biol. Chem. **273:**989-96.
101. **Dubé, N., A. Cheng, and M. L. Tremblay.** 2004. The role of protein tyrosine phosphatase 1B in Ras signaling. Proc. Natl. Acad. Sci. USA **101:**1834-9.
102. **Dubé, N., and M. L. Tremblay.** 2005. Involvement of the small protein tyrosine phosphatases TC-PTP and PTP1B in signal transduction and diseases: from diabetes, obesity to cell cycle, and cancer. Biochim Biophys Acta **1754:**108-17.
103. **Ellis, M., D. K. Sharma, J. D. Hilley, G. H. Coombs, and J. C. Mottram.** 2002. Processing and trafficking of Leishmania mexicana GP63. Analysis using GP18 mutants deficient in glycosylphosphatidylinositol protein anchoring. J. Biol. Chem. **277:**27968-74.
104. **Erikson, R. L., M. S. Collett, E. Erikson, and A. F. Purchio.** 1979. Evidence that the avian sarcoma virus transforming gene product is a cyclic AMP-independent protein kinase. Proc Natl Acad Sci U S A **76:**6260-4.
105. **Espinosa, A., M. Guo, V. C. Tam, Z. Q. Fu, and J. R. Alfano.** 2003. The Pseudomonas syringae type III-secreted protein HopPtoD2 possesses protein tyrosine phosphatase activity and suppresses programmed cell death in plants. Mol Microbiol **49:**377-87.
106. **Etges, R., J. Bouvier, and C. Bordier.** 1986. The major surface protein of Leishmania promastigotes is a protease. J Biol Chem **261:**9098-101.
107. **Faisal, A., M. el-Shemerly, D. Hess, and Y. Nagamine.** 2002. Serine/threonine phosphorylation of ShcA. Regulation of protein-tyrosine phosphatase-pest binding and involvement in insulin signaling. J. Biol. Chem. **277:**30144-52.
108. **Falschlehner, C., C. H. Emmerich, B. Gerlach, and H. Walczak.** 2007. TRAIL signalling: decisions between life and death. Int J Biochem Cell Biol **39:**1462-75.
109. **Fearnhead, H. O., J. Rodriguez, E. E. Govek, W. Guo, R. Kobayashi, G. Hannon, and Y. A. Lazebnik.** 1998. Oncogene-dependent apoptosis is mediated by caspase-9. Proc. Natl. Acad. Sci. USA **95:**13664-9.
110. **Feller, S. M.** 2001. Crk family adaptors-signalling complex formation and biological roles. Oncogene **20:**6348-71.
111. **Fink, S. L., and B. T. Cookson.** 2005. Apoptosis, pyroptosis, and necrosis: mechanistic description of dead and dying eukaryotic cells. Infect Immun **73:**1907-16.

112. **Fischer, U., R. U. Janicke, and K. Schulze-Osthoff.** 2003. Many cuts to ruin: a comprehensive update of caspase substrates. Cell Death Differ. **10:**76-100.
113. **Flint, A. J., T. Tiganis, D. Barford, and N. K. Tonks.** 1997. Development of "substrate-trapping" mutants to identify physiological substrates of protein tyrosine phosphatases. Proc Natl Acad Sci U S A **94:**1680-5.
114. **Foehr, E. D., G. Lorente, V. Vincent, K. Nikolich, and R. Urfer.** 2005. FAS associated phosphatase (FAP-1) blocks apoptosis of astrocytomas through dephosphorylation of FAS. J Neurooncol **74:**241-8.
115. **Frangioni, J. V., P. H. Beahm, V. Shifrin, C. A. Jost, and B. G. Neel.** 1992. The nontransmembrane tyrosine phosphatase PTP-1B localizes to the endoplasmic reticulum via its 35 amino acid C-terminal sequence. Cell **68:**545-60.
116. **Frangioni, J. V., A. Oda, M. Smith, E. W. Salzman, and B. G. Neel.** 1993. Calpain-catalyzed cleavage and subcellular relocation of protein phosphotyrosine phosphatase 1B (PTP-1B) in human platelets. EMBO J. **12:**4843-56.
117. **Garton, A. J., M. R. Burnham, A. H. Bouton, and N. K. Tonks.** 1997. Association of PTP-PEST with the SH3 domain of p130cas; a novel mechanism of protein tyrosine phosphatase substrate recognition. Oncogene **15:**877-85.
118. **Garton, A. J., A. J. Flint, and N. K. Tonks.** 1996. Identification of p130(cas) as a substrate for the cytosolic protein tyrosine phosphatase PTP-PEST. Mol. Cell. Biol. **16:**6408-18.
119. **Garton, A. J., and N. K. Tonks.** 1994. PTP-PEST: a protein tyrosine phosphatase regulated by serine phosphorylation. EMBO J. **13:**3763-71.
120. **Garton, A. J., and N. K. Tonks.** 1999. Regulation of fibroblast motility by the protein tyrosine phosphatase PTP-PEST. J. Biol. Chem. **274:**3811-8.
121. **Ge, B., H. Gram, F. Di Padova, B. Huang, L. New, R. J. Ulevitch, Y. Luo, and J. Han.** 2002. MAPKK-independent activation of p38alpha mediated by TAB1-dependent autophosphorylation of p38alpha. Science **295:**1291-4.
122. **Ghosh, D., and P. Chakraborty.** 2002. Involvement of protein tyrosine kinases and phosphatases in uptake and intracellular replication of virulent and avirulent *Leishmania donovani* promastigotes in mouse macrophage cells. Biosci. Rep. **22:**395-406.
123. **Gomez, M. A., S. Li, M. L. Tremblay, and M. Olivier.** 2007. NRAMP-1 expression modulates protein-tyrosine phosphatase activity in macrophages: impact on host cell signaling and functions. J Biol Chem **282:**36190-8.
124. **Gonzalez-Rodriguez, A., O. Escribano, J. Alba, C. M. Rondinone, M. Benito, and A. M. Valverde.** 2007. Levels of protein tyrosine phosphatase 1B determine susceptibility to apoptosis in serum-deprived hepatocytes. J Cell Physiol **212:**76-88.
125. **Gouin, E., M. D. Welch, and P. Cossart.** 2005. Actin-based motility of intracellular pathogens. Curr. Opin. Microbiol. **8:**35-45.
126. **Gregorieff, A., J. F. Cloutier, and A. Veillette.** 1998. Sequence requirements for association of protein-tyrosine phosphatase PEP with the Src homology 3 domain of inhibitory tyrosine protein kinase p50(csk). J Biol Chem **273:**13217-22.
127. **Gregory, D. J., M. Godbout, I. Contreras, G. Forget, and M. Olivier.** 2008. A novel form of NF-kappaB is induced by Leishmania infection: involvement in macrophage gene expression. Eur. J. Immunol. **38:**1071-81.
128. **Gu, F., N. Dubé, J. W. Kim, A. Cheng, J. Ibarra-Sanchez Mde, M. L. Tremblay, and Y. R. Boisclair.** 2003. Protein tyrosine phosphatase 1B attenuates growth hormone-mediated JAK2-STAT signaling. Mol. Cell. Biol. **23:**3753-62.

129. **Gu, F., D. T. Nguyen, M. Stuible, N. Dubé, M. L. Tremblay, and E. Chevet.** 2004. Protein-tyrosine phosphatase 1B potentiates IRE1 signaling during endoplasmic reticulum stress. J. Biol. Chem. **279:**49689-93.
130. **Gulati, P., B. Markova, M. Gottlicher, F. D. Bohmer, and P. A. Herrlich.** 2004. UVA inactivates protein tyrosine phosphatases by calpain-mediated degradation. EMBO Rep. **5:**812-7.
131. **Gupta, A., B. S. Lee, M. A. Khadeer, Z. Tang, M. Chellaiah, Y. Abu-Amer, J. Goldknopf, and K. A. Hruska.** 2003. Leupaxin is a critical adaptor protein in the adhesion zone of the osteoclast. J. Bone Miner. Res. **18:**669-85.
132. **Gupta, S., V. Radha, C. Sudhakar, and G. Swarup.** 2002. A nuclear protein tyrosine phosphatase activates p53 and induces caspase-1-dependent apoptosis. FEBS Lett. **532:**61-6.
133. **Habib, T., R. Herrera, and S. J. Decker.** 1994. Activators of protein kinase C stimulate association of Shc and the PEST tyrosine phosphatase. J. Biol. Chem. **269:**25243-6.
134. **Hagel, M., E. L. George, A. Kim, R. Tamimi, S. L. Opitz, C. E. Turner, A. Imamoto, and S. M. Thomas.** 2002. The adaptor protein paxillin is essential for normal development in the mouse and is a critical transducer of fibronectin signaling. Mol Cell Biol **22:**901-15.
135. **Hajmova, M., K. P. Chang, B. Kolli, and P. Volf.** 2004. Down-regulation of gp63 in Leishmania amazonensis reduces its early development in Lutzomyia longipalpis. Microbes Infect **6:**646-9.
136. **Hall, A.** 1998. Rho GTPases and the actin cytoskeleton. Science **279:**509-14.
137. **Hall, A.** 2005. Rho GTPases and the control of cell behaviour. Biochem Soc Trans **33:**891-5.
138. **Hallé, M., Y. C. Liu, S. Hardy, J. F. Théberge, C. Blanchetot, A. Bourdeau, T. C. Meng, and M. L. Tremblay.** 2007. Caspase-3 regulates catalytic activity and scaffolding functions of the protein tyrosine phosphatase PEST, a novel modulator of the apoptotic response. Mol. Cell. Biol. **27:**1172-90.
139. **Hallé, M., M. L. Tremblay, and T. C. Meng.** 2007. Protein tyrosine phosphatases: emerging regulators of apoptosis. Cell Cycle **6:**2773-81.
140. **Hao, L., T. Tiganis, N. K. Tonks, and H. Charbonneau.** 1997. The noncatalytic C-terminal segment of the T cell protein tyrosine phosphatase regulates activity via an intramolecular mechanism. J Biol Chem **272:**29322-9.
141. **Hardy, S., W. El-Assaad, E. Przybytkowski, E. Joly, M. Prentki, and Y. Langelier.** 2003. Saturated fatty acid-induced apoptosis in MDA-MB-231 breast cancer cells. A role for cardiolipin. J. Biol. Chem. **278:**31861-70.
142. **Harte, M. T., J. D. Hildebrand, M. R. Burnham, A. H. Bouton, and J. T. Parsons.** 1996. p130Cas, a substrate associated with v-Src and v-Crk, localizes to focal adhesions and binds to focal adhesion kinase. J Biol Chem **271:**13649-55.
143. **Hasegawa, K., H. Yajima, T. Katagiri, M. Ogimoto, Y. Arimura, K. Mitomo, K. Mashima, K. Mizuno, and H. Yakura.** 1999. Requirement of PEST domain tyrosine phosphatase PEP in B cell antigen receptor-induced growth arrest and apoptosis. Eur. J. Immunol. **29:**887-96.
144. **Heath, M. C.** 2000. Hypersensitive response-related death. Plant Mol Biol **44:**321-34.
145. **Heinonen, K. M., N. Dubé, A. Bourdeau, W. S. Lapp, and M. L. Tremblay.** 2006. Protein tyrosine phosphatase 1B negatively regulates macrophage development through CSF-1 signaling. Proc Natl Acad Sci U S A **103:**2776-81.

146. **Heinonen, K. M., and M. L. Tremblay.** 2006. Protein tyrosine phosphatase 1B in hematopoiesis. Cell Cycle **5**:1053-6.
147. **Hepburn, N. C.** 2000. Cutaneous leishmaniasis. Clin. Exp. Dermatol. **25**:363-70.
148. **Herwaldt, B. L.** 1999. Leishmaniasis. Lancet **354**:1191-9.
149. **Hespanhol, R. C., C. S. M. de Nazare, M. B. Meuser, S. L. M. M. de Nazareth, and S. Corte-Real.** 2005. The expression of mannose receptors in skin fibroblast and their involvement in *Leishmania* (*L.*) *amazonensis* invasion. J. Histochem. Cytochem. **53**:35-44.
150. **Higgs, H. N., and T. D. Pollard.** 2001. Regulation of actin filament network formation through ARP2/3 complex: activation by a diverse array of proteins. Annu. Rev. Biochem. **70**:649-76.
151. **Holcomb, M., A. Rufini, D. Barila, and R. L. Klemke.** 2006. Deregulation of proteasome function induces Abl-mediated cell death by uncoupling p130CAS and c-CrkII. J Biol Chem **281**:2430-40.
152. **Honda, H., T. Nakamoto, R. Sakai, and H. Hirai.** 1999. p130(Cas), an assembling molecule of actin filaments, promotes cell movement, cell migration, and cell spreading in fibroblasts. Biochem Biophys Res Commun **262**:25-30.
153. **Honda, H., H. Oda, T. Nakamoto, Z. Honda, R. Sakai, T. Suzuki, T. Saito, K. Nakamura, K. Nakao, T. Ishikawa, M. Katsuki, Y. Yazaki, and H. Hirai.** 1998. Cardiovascular anomaly, impaired actin bundling and resistance to Src-induced transformation in mice lacking p130Cas. Nat Genet **19**:361-5.
154. **Hoon Kim, D., S. Jeon Choi, S. Kook, W. Kim, and W. Keun Song.** 2003. Phosphorylation-dependent cleavage of p130cas in apoptotic rat-1 cells. Biochem. Biophys. Res. Commun. **300**:141-8.
155. **Howe, A. K., L. C. Baldor, and B. P. Hogan.** 2005. Spatial regulation of the cAMP-dependent protein kinase during chemotactic cell migration. Proc Natl Acad Sci U S A **102**:14320-5.
156. **Hsiao, C. H., C. Yao, P. Storlie, J. E. Donelson, and M. E. Wilson.** 2008. The major surface protease (MSP or GP63) in the intracellular amastigote stage of Leishmania chagasi. Mol. Biochem. Parasitol. **157**:148-59.
157. **Huang, J., H. Hamasaki, T. Nakamoto, H. Honda, H. Hirai, M. Saito, T. Takato, and R. Sakai.** 2002. Differential regulation of cell migration, actin stress fiber organization, and cell transformation by functional domains of Crk-associated substrate. J Biol Chem **277**:27265-72.
158. **Hunter, T.** 1989. Protein-tyrosine phosphatases: the other side of the coin. Cell **58**:1013-6.
159. **Hunter, T.** 1987. A thousand and one protein kinases. Cell **50**:823-9.
160. **Huntington, N. D., Y. Xu, H. Puthalakath, A. Light, S. N. Willis, A. Strasser, and D. M. Tarlinton.** 2006. CD45 links the B cell receptor with cell survival and is required for the persistence of germinal centers. Nat Immunol **7**:190-8.
161. **Hussain, N. K., S. Jenna, M. Glogauer, C. C. Quinn, S. Wasiak, M. Guipponi, S. E. Antonarakis, B. K. Kay, T. P. Stossel, N. Lamarche-Vane, and P. S. McPherson.** 2001. Endocytic protein intersectin-l regulates actin assembly via Cdc42 and N-WASP. Nat Cell Biol **3**:927-32.
162. **Ibarra-Sanchez, M. J., J. Wagner, M. T. Ong, C. Lampron, and M. L. Tremblay.** 2001. Murine embryonic fibroblasts lacking TC-PTP display delayed G1 phase through defective NF-kappaB activation. Oncogene **20**:4728-39.

163. **Ingley, E.** 2008. Src family kinases: regulation of their activities, levels and identification of new pathways. Biochim Biophys Acta **1784**:56-65.
164. **Irby, R. B., W. Mao, D. Coppola, J. Kang, J. M. Loubeau, W. Trudeau, R. Karl, D. J. Fujita, R. Jove, and T. J. Yeatman.** 1999. Activating SRC mutation in a subset of advanced human colon cancers. Nat Genet **21**:187-90.
165. **Irie, S., T. Hachiya, S. Rabizadeh, W. Maruyama, J. Mukai, Y. Li, J. C. Reed, D. E. Bredesen, and T. A. Sato.** 1999. Functional interaction of Fas-associated phosphatase-1 (FAP-1) with p75(NTR) and their effect on NF-kappaB activation. FEBS Lett **460**:191-8.
166. **Ivanov, V. N., P. Lopez Bergami, G. Maulit, T. A. Sato, D. Sassoon, and Z. Ronai.** 2003. FAP-1 association with Fas (Apo-1) inhibits Fas expression on the cell surface. Mol. Cell. Biol. **23**:3623-35.
167. **Ivanov, V. N., Z. Ronai, and T. K. Hei.** 2006. Opposite roles of FAP-1 and dynamin in the regulation of Fas (CD95) translocation to the cell surface and susceptibility to Fas ligand-mediated apoptosis. J Biol Chem **281**:1840-52.
168. **Ivens, A. C., C. S. Peacock, E. A. Worthey, L. Murphy, G. Aggarwal, M. Berriman, E. Sisk, M. A. Rajandream, E. Adlem, R. Aert, A. Anupama, Z. Apostolou, P. Attipoe, N. Bason, C. Bauser, A. Beck, S. M. Beverley, G. Bianchettin, K. Borzym, G. Bothe, C. V. Bruschi, M. Collins, E. Cadag, L. Ciarloni, C. Clayton, R. M. Coulson, A. Cronin, A. K. Cruz, R. M. Davies, J. De Gaudenzi, D. E. Dobson, A. Duesterhoeft, G. Fazelina, N. Fosker, A. C. Frasch, A. Fraser, M. Fuchs, C. Gabel, A. Goble, A. Goffeau, D. Harris, C. Hertz-Fowler, H. Hilbert, D. Horn, Y. Huang, S. Klages, A. Knights, M. Kube, N. Larke, L. Litvin, A. Lord, T. Louie, M. Marra, D. Masuy, K. Matthews, S. Michaeli, J. C. Mottram, S. Muller-Auer, H. Munden, S. Nelson, H. Norbertczak, K. Oliver, S. O'Neil, M. Pentony, T. M. Pohl, C. Price, B. Purnelle, M. A. Quail, E. Rabbinowitsch, R. Reinhardt, M. Rieger, J. Rinta, J. Robben, L. Robertson, J. C. Ruiz, S. Rutter, D. Saunders, M. Schafer, J. Schein, D. C. Schwartz, K. Seeger, A. Seyler, S. Sharp, H. Shin, D. Sivam, R. Squares, S. Squares, V. Tosato, C. Vogt, G. Volckaert, R. Wambutt, T. Warren, H. Wedler, J. Woodward, S. Zhou, W. Zimmermann, D. F. Smith, J. M. Blackwell, K. D. Stuart, B. Barrell, et al.** 2005. The genome of the kinetoplastid parasite, Leishmania major. Science **309**:436-42.
169. **Ivins Zito, C., M. I. Kontaridis, M. Fornaro, G. S. Feng, and A. M. Bennett.** 2004. SHP-2 regulates the phosphatidylinositide 3'-kinase/Akt pathway and suppresses caspase 3-mediated apoptosis. J Cell Physiol **199**:227-36.
170. **Iwanicki, M. P., T. Vomastek, R. W. Tilghman, K. H. Martin, J. Banerjee, P. B. Wedegaertner, and J. T. Parsons.** 2008. FAK, PDZ-RhoGEF and ROCKII cooperate to regulate adhesion movement and trailing-edge retraction in fibroblasts. J Cell Sci **121**:895-905.
171. **Jaffe, C. L., and D. M. Dwyer.** 2003. Extracellular release of the surface metalloprotease, gp63, from Leishmania and insect trypanosomatids. Parasitol. Res. **91**:229-37.
172. **Jamieson, J. S., D. A. Tumbarello, M. Hallé, M. C. Brown, M. L. Tremblay, and C. E. Turner.** 2005. Paxillin is essential for PTP-PEST-dependent regulation of cell spreading and motility: a role for paxillin kinase linker. J. Cell Sci. **118**:5835-47.
173. **Janssen, O., J. Qian, A. Linkermann, and D. Kabelitz.** 2003. CD95 ligand--death factor and costimulatory molecule? Cell Death Differ **10**:1215-25.
174. **Jeong, S. Y., and D. W. Seol.** 2008. The role of mitochondria in apoptosis. BMB Rep **41**:11-22.

175. **Jin, J., T. Shirogane, L. Xu, G. Nalepa, J. Qin, S. J. Elledge, and J. W. Harper.** 2003. SCFbeta-TRCP links Chk1 signaling to degradation of the Cdc25A protein phosphatase. Genes Dev **17**:3062-74.
176. **Joshi, P. B., B. L. Kelly, S. Kamhawi, D. L. Sacks, and W. R. McMaster.** 2002. Targeted gene deletion in *Leishmania major* identifies leishmanolysin (GP63) as a virulence factor. Mol. Biochem. Parasitol. **120**:33-40.
177. **Joshi, P. B., D. L. Sacks, G. Modi, and W. R. McMaster.** 1998. Targeted gene deletion of Leishmania major genes encoding developmental stage-specific leishmanolysin (GP63). Mol. Microbiol. **27**:519-30.
178. **Julien, S. G., N. Dubé, M. Read, J. Penney, M. Paquet, Y. Han, B. P. Kennedy, W. J. Muller, and M. L. Tremblay.** 2007. Protein tyrosine phosphatase 1B deficiency or inhibition delays ErbB2-induced mammary tumorigenesis and protects from lung metastasis. Nat Genet **39**:338-46.
179. **Junghae, M., and J. G. Raynes.** 2002. Activation of p38 mitogen-activated protein kinase attenuates Leishmania donovani infection in macrophages. Infect. Immun. **70**:5026-35.
180. **Kain, K. H., and R. L. Klemke.** 2001. Inhibition of cell migration by Abl family tyrosine kinases through uncoupling of Crk-CAS complexes. J Biol Chem **276**:16185-92.
181. **Kamata, H., S. Honda, S. Maeda, L. Chang, H. Hirata, and M. Karin.** 2005. Reactive oxygen species promote TNFalpha-induced death and sustained JNK activation by inhibiting MAP kinase phosphatases. Cell **120**:649-61.
182. **Kamhawi, S.** 2006. Phlebotomine sand flies and *Leishmania* parasites: friends or foes? Trends Parasitol. **22**:439-45.
183. **Karachi, Z. Z.** 2005. Leishmaniasis--an impending epidemic. J Pak Med Assoc **55**:468-9.
184. **Kerr, J. F., A. H. Wyllie, and A. R. Currie.** 1972. Apoptosis: a basic biological phenomenon with wide-ranging implications in tissue kinetics. Br J Cancer **26**:239-57.
185. **Kim, W., S. Kook, D. J. Kim, C. Teodorof, and W. K. Song.** 2004. The 31-kDa caspase-generated cleavage product of p130cas functions as a transcriptional repressor of E2A in apoptotic cells. J. Biol. Chem. **279**:8333-42.
186. **Kima, P. E.** 2007. The amastigote forms of Leishmania are experts at exploiting host cell processes to establish infection and persist. Int. J. Parasitol. **37**:1087-96.
187. **Kiyokawa, E., Y. Hashimoto, S. Kobayashi, H. Sugimura, T. Kurata, and M. Matsuda.** 1998. Activation of Rac1 by a Crk SH3-binding protein, DOCK180. Genes Dev **12**:3331-6.
188. **Klemke, R. L., J. Leng, R. Molander, P. C. Brooks, K. Vuori, and D. A. Cheresh.** 1998. CAS/Crk coupling serves as a "molecular switch" for induction of cell migration. J Cell Biol **140**:961-72.
189. **Kook, S., S. R. Shim, S. J. Choi, J. Ahnn, J. I. Kim, S. H. Eom, Y. K. Jung, S. G. Paik, and W. K. Song.** 2000. Caspase-mediated cleavage of p130cas in etoposide-induced apoptotic Rat-1 cells. Mol. Biol. Cell **11**:929-39.
190. **Kozma, R., S. Ahmed, A. Best, and L. Lim.** 1995. The Ras-related protein Cdc42Hs and bradykinin promote formation of peripheral actin microspikes and filopodia in Swiss 3T3 fibroblasts. Mol Cell Biol **15**:1942-52.
191. **Kranenburg, O., and W. H. Moolenaar.** 2001. Ras-MAP kinase signaling by lysophosphatidic acid and other G protein-coupled receptor agonists. Oncogene **20**:1540-6.
192. **Krippner-Heidenreich, A., G. Walsemann, M. J. Beyrouthy, S. Speckgens, R. Kraft, H. Thole, R. V. Talanian, M. M. Hurt, and B. Luscher.** 2005. Caspase-dependent regulation

and subcellular redistribution of the transcriptional modulator YY1 during apoptosis. Mol Cell Biol **25:**3704-14.

193. **Kuchay, S. M., N. Kim, E. A. Grunz, W. P. Fay, and A. H. Chishti.** 2007. Double Knockouts reveal that Protein Tyrosine Phosphatase 1B is a Physiological Target of Calpain-1 in Platelets. Mol Cell Biol **In press.**
194. **Kulkarni, M. M., E. A. Jones, W. R. McMaster, and B. S. McGwire.** 2008. Fibronectin binding and proteolytic degradation by Leishmania and effects on macrophage activation. Infect. Immun. **76:**1738-47.
195. **Kulkarni, M. M., W. R. McMaster, E. Kamysz, W. Kamysz, D. M. Engman, and B. S. McGwire.** 2006. The major surface-metalloprotease of the parasitic protozoan, Leishmania, protects against antimicrobial peptide-induced apoptotic killing. Mol. Microbiol. **62:**1484-97.
196. **Kumar, S.** 2007. Caspase function in programmed cell death. Cell Death Differ. **14:**32-43.
197. **Kurenova, E., L. H. Xu, X. Yang, A. S. Baldwin, Jr., R. J. Craven, S. K. Hanks, Z. G. Liu, and W. G. Cance.** 2004. Focal adhesion kinase suppresses apoptosis by binding to the death domain of receptor-interacting protein. Mol. Cell. Biol. **24:**4361-71.
198. **Kyaw, M., M. Yoshizumi, K. Tsuchiya, S. Kagami, Y. Izawa, Y. Fujita, N. Ali, Y. Kanematsu, K. Toida, K. Ishimura, and T. Tamaki.** 2004. Src and Cas are essentially but differentially involved in angiotensin II-stimulated migration of vascular smooth muscle cells via extracellular signal-regulated kinase 1/2 and c-Jun NH2-terminal kinase activation. Mol. Pharmacol. **65:**832-41.
199. **Lai, K. M., and T. Pawson.** 2000. The ShcA phosphotyrosine docking protein sensitizes cardiovascular signaling in the mouse embryo. Genes Dev **14:**1132-45.
200. **Lai, Y. J., C. S. Chen, W. C. Lin, and F. T. Lin.** 2005. c-Src-mediated phosphorylation of TRIP6 regulates its function in lysophosphatidic acid-induced cell migration. Mol Cell Biol **25:**5859-68.
201. **Lai, Y. J., W. C. Lin, and F. T. Lin.** 2007. PTPL1/FAP-1 negatively regulates TRIP6 function in lysophosphatidic acid-induced cell migration. J Biol Chem **282:**24381-7.
202. **Lamarche, N., N. Tapon, L. Stowers, P. D. Burbelo, P. Aspenstrom, T. Bridges, J. Chant, and A. Hall.** 1996. Rac and Cdc42 induce actin polymerization and G1 cell cycle progression independently of p65PAK and the JNK/SAPK MAP kinase cascade. Cell **87:**519-29.
203. **Larsen, M., M. L. Tremblay, and K. M. Yamada.** 2003. Phosphatases in cell-matrix adhesion and migration. Nat. Rev. Mol. Cell Biol. **4:**700-11.
204. **Leng, Y., J. Zhang, K. Badour, E. Arpaia, S. Freeman, P. Cheung, M. Siu, and K. Siminovitch.** 2005. Abelson-interactor-1 promotes WAVE2 membrane translocation and Abelson-mediated tyrosine phosphorylation required for WAVE2 activation. Proc Natl Acad Sci U S A **102:**1098-103.
205. **Lengyel, E., K. Sawada, and R. Salgia.** 2007. Tyrosine kinase mutations in human cancer. Curr Mol Med **7:**77-84.
206. **Lerm, M., A. Holm, A. Seiron, E. Sarndahl, K. E. Magnusson, and B. Rasmusson.** 2006. *Leishmania donovani* requires functional Cdc42 and Rac1 to prevent phagosomal maturation. Infect. Immun. **74:**2613-8.
207. **Levinson, A. D., H. Oppermann, L. Levintow, H. E. Varmus, and J. M. Bishop.** 1978. Evidence that the transforming gene of avian sarcoma virus encodes a protein kinase associated with a phosphoprotein. Cell **15:**561-72.

208. **Lin, Y., A. C. Ceacareanu, and A. Hassid.** 2003. Nitric oxide-induced inhibition of aortic smooth muscle cell motility: role of PTP-PEST and adaptor proteins p130cas and Crk. Am. J. Physiol. Heart Circ. Physiol. **285:**H710-21.

209. **Liu, F., D. E. Hill, and J. Chernoff.** 1996. Direct binding of the proline-rich region of protein tyrosine phosphatase 1B to the Src homology 3 domain of p130(Cas). J. Biol. Chem. **271:**31290-5.

210. **Liu, L., L. Wang, Y. Zhao, Y. Wang, Z. Wang, and Z. Qiao.** 2006. Testosterone attenuates p38 MAPK pathway during *Leishmania donovani* infection of macrophages. Parasitol. Res. **99:**189-93.

211. **Lockshin, R. A., and Z. Zakeri.** 2001. Programmed cell death and apoptosis: origins of the theory. Nat Rev Mol Cell Biol **2:**545-50.

212. **Lodge, R., and A. Descoteaux.** 2005. Leishmania donovani promastigotes induce periphagosomal F-actin accumulation through retention of the GTPase Cdc42. Cell. Microbiol. **7:**1647-58.

213. **Lommel, S., S. Benesch, K. Rottner, T. Franz, J. Wehland, and R. Kuhn.** 2001. Actin pedestal formation by enteropathogenic Escherichia coli and intracellular motility of Shigella flexneri are abolished in N-WASP-defective cells. EMBO Rep **2:**850-7.

214. **Lowry, W. E., J. Huang, Y. C. Ma, S. Ali, D. Wang, D. M. Williams, M. Okada, P. A. Cole, and X. Y. Huang.** 2002. Csk, a critical link of g protein signals to actin cytoskeletal reorganization. Dev Cell **2:**733-44.

215. **Lu, T. J., W. Y. Lai, C. Y. Huang, W. J. Hsieh, J. S. Yu, Y. J. Hsieh, W. T. Chang, T. H. Leu, W. C. Chang, W. J. Chuang, M. J. Tang, T. Y. Chen, T. L. Lu, and M. D. Lai.** 2006. Inhibition of cell migration by autophosphorylated mammalian sterile 20-like kinase 3 (MST3) involves paxillin and protein-tyrosine phosphatase-PEST. J Biol Chem **281:**38405-17.

216. **Lyons, P. D., J. M. Dunty, E. M. Schaefer, and M. D. Schaller.** 2001. Inhibition of the catalytic activity of cell adhesion kinase beta by protein-tyrosine phosphatase-PEST-mediated dephosphorylation. J. Biol. Chem. **276:**24422-31.

217. **Macdonald, M. H., C. J. Morrison, and W. R. McMaster.** 1995. Analysis of the active site and activation mechanism of the Leishmania surface metalloproteinase GP63. Biochim Biophys Acta **1253:**199-207.

218. **MacKeigan, J. P., L. O. Murphy, and J. Blenis.** 2005. Sensitized RNAi screen of human kinases and phosphatases identifies new regulators of apoptosis and chemoresistance. Nat. Cell Biol. **7:**591-600.

219. **Manning, G., D. B. Whyte, R. Martinez, T. Hunter, and S. Sudarsanam.** 2002. The protein kinase complement of the human genome. Science **298:**1912-34.

220. **Markova, B., P. Herrlich, L. Ronnstrand, and F. D. Bohmer.** 2003. Identification of protein tyrosine phosphatases associating with the PDGF receptor. Biochemistry **42:**2691-9.

221. **Marsh, H. N., C. I. Dubreuil, C. Quevedo, A. Lee, M. Majdan, G. S. Walsh, S. Hausdorff, F. A. Said, O. Zoueva, M. Kozlowski, K. Siminovitch, B. G. Neel, F. D. Miller, and D. R. Kaplan.** 2003. SHP-1 negatively regulates neuronal survival by functioning as a TrkA phosphatase. J Cell Biol **163:**999-1010.

222. **Martin, S. S., and K. Vuori.** 2004. Regulation of Bcl-2 proteins during anoikis and amorphosis. Biochim. Biophys. Acta **1692:**145-57.

223. **Mathew, S., S. P. George, Y. Wang, M. R. Siddiqui, K. Srinivasan, L. Tan, and S. Khurana.** 2008. Potential molecular mechanism for c-Src kinase mediated regulation of intestinal cell migration. J Biol Chem.
224. **Mathur, R. K., A. Awasthi, P. Wadhone, B. Ramanamurthy, and B. Saha.** 2004. Reciprocal CD40 signals through p38MAPK and ERK-1/2 induce counteracting immune responses. Nat. Med. **10:**540-4.
225. **Mauro, L., D. Sisci, M. Bartucci, M. Salerno, J. Kim, T. Tam, M. A. Guvakova, S. Ando, and E. Surmacz.** 1999. SHC-alpha5beta1 integrin interactions regulate breast cancer cell adhesion and motility. Exp Cell Res **252:**439-48.
226. **McGarrigle, D., D. Shan, S. Yang, and X. Y. Huang.** 2006. Role of tyrosine kinase Csk in G protein-coupled receptor- and receptor tyrosine kinase-induced fibroblast cell migration. J. Biol. Chem. **281:**10583-8.
227. **McGwire, B. S., K. P. Chang, and D. M. Engman.** 2003. Migration through the extracellular matrix by the parasitic protozoan Leishmania is enhanced by surface metalloprotease gp63. Infect. Immun. **71:**1008-10.
228. **McGwire, B. S., W. A. O'Connell, K. P. Chang, and D. M. Engman.** 2002. Extracellular release of the glycosylphosphatidylinositol (GPI)-linked Leishmania surface metalloprotease, gp63, is independent of GPI phospholipolysis: implications for parasite virulence. J. Biol. Chem. **277:**8802-9.
229. **Meinhold-Heerlein, I., F. Stenner-Liewen, H. Liewen, S. Kitada, M. Krajewska, S. Krajewski, J. M. Zapata, A. Monks, D. A. Scudiero, T. Bauknecht, and J. C. Reed.** 2001. Expression and potential role of Fas-associated phosphatase-1 in ovarian cancer. Am J Pathol **158:**1335-44.
230. **Meng, T. C., T. Fukada, and N. K. Tonks.** 2002. Reversible oxidation and inactivation of protein tyrosine phosphatases in vivo. Mol. Cell **9:**387-99.
231. **Meng, T. C., S. F. Hsu, and N. K. Tonks.** 2005. Development of a modified in-gel assay to identify protein tyrosine phosphatases that are oxidized and inactivated in vivo. Methods **35:**28-36.
232. **Miki, H., T. Sasaki, Y. Takai, and T. Takenawa.** 1998. Induction of filopodium formation by a WASP-related actin-depolymerizing protein N-WASP. Nature **391:**93-6.
233. **Miki, H., H. Yamaguchi, S. Suetsugu, and T. Takenawa.** 2000. IRSp53 is an essential intermediate between Rac and WAVE in the regulation of membrane ruffling. Nature **408:**732-5.
234. **Mills, G. B., and W. H. Moolenaar.** 2003. The emerging role of lysophosphatidic acid in cancer. Nat Rev Cancer **3:**582-91.
235. **Moffitt, K. L., S. L. Martin, and B. Walker.** 2007. The emerging role of serine proteases in apoptosis. Biochem Soc Trans **35:**559-60.
236. **Moore, K. J., and G. Matlashewski.** 1994. Intracellular infection by *Leishmania donovani* inhibits macrophage apoptosis. J. Immunol. **152:**2930-7.
237. **Morehead, J., I. Coppens, and N. W. Andrews.** 2002. Opsonization modulates Rac-1 activation during cell entry by *Leishmania amazonensis*. Infect. Immun. **70:**4571-80.
238. **Mukerjee, N., K. M. McGinnis, Y. H. Park, M. E. Gnegy, and K. K. Wang.** 2000. Caspase-mediated proteolytic activation of calcineurin in thapsigargin-mediated apoptosis in SH-SY5Y neuroblastoma cells. Arch Biochem Biophys **379:**337-43.
239. **Münter, S., M. Way, and F. Frischknecht.** 2006. Signaling during pathogen infection. Sci. STKE **2006:**re5.

240. **Nakamoto, T., R. Sakai, K. Ozawa, Y. Yazaki, and H. Hirai.** 1996. Direct binding of C-terminal region of p130Cas to SH2 and SH3 domains of Src kinase. J Biol Chem **271:**8959-65.
241. **Nandan, D., T. Yi, M. Lopez, C. Lai, and N. E. Reiner.** 2002. Leishmania EF-1alpha activates the Src homology 2 domain containing tyrosine phosphatase SHP-1 leading to macrophage deactivation. J. Biol. Chem. **277:**50190-7.
242. **Neel, B. G., H. Gu, and L. Pao.** 2003. The 'Shp'ing news: SH2 domain-containing tyrosine phosphatases in cell signaling. Trends Biochem. Sci. **28:**284-93.
243. **Nishiya, N., Y. Iwabuchi, M. Shibanuma, J. F. Côté, M. L. Tremblay, and K. Nose.** 1999. Hic-5, a paxillin homologue, binds to the protein-tyrosine phosphatase PEST (PTP-PEST) through its LIM 3 domain. J. Biol. Chem. **274:**9847-53.
244. **Noguchi, T., M. Tsuda, H. Takeda, T. Takada, K. Inagaki, T. Yamao, K. Fukunaga, T. Matozaki, and M. Kasuga.** 2001. Inhibition of cell growth and spreading by stomach cancer-associated protein-tyrosine phosphatase-1 (SAP-1) through dephosphorylation of p130cas. J Biol Chem **276:**15216-24.
245. **O'Neill, G. M., and E. A. Golemis.** 2001. Proteolysis of the docking protein HEF1 and implications for focal adhesion dynamics. Mol. Cell. Biol. **21:**5094-108.
246. **Ojaniemi, M., and K. Vuori.** 1997. Epidermal growth factor modulates tyrosine phosphorylation of p130Cas. Involvement of phosphatidylinositol 3'-kinase and actin cytoskeleton. J Biol Chem **272:**25993-8.
247. **Oliveira, S. H., S. G. Fonseca, P. R. Romao, F. Figueiredo, S. H. Ferreira, and F. Q. Cunha.** 1998. Microbicidal activity of eosinophils is associated with activation of the arginine-NO pathway. Parasite Immunol. **20:**405-12.
248. **Östman, A., C. Hellberg, and F. D. Böhmer.** 2006. Protein-tyrosine phosphatases and cancer. Nat Rev Cancer **6:**307-20.
249. **Pandey, S., P. Chakraborti, R. Sharma, S. Bandyopadhyay, D. Sarkar, and S. Adhya.** 2004. Involvement of Leishmania donovani major surface glycoprotein gp63 in promastigote multiplication. J Biosci **29:**15-22.
250. **Patel, J. C., and J. E. Galan.** 2005. Manipulation of the host actin cytoskeleton by Salmonella--all in the name of entry. Curr Opin Microbiol **8:**10-5.
251. **Pelicci, G., L. Lanfrancone, A. E. Salcini, A. Romano, S. Mele, M. Grazia Borrello, O. Segatto, P. P. Di Fiore, and P. G. Pelicci.** 1995. Constitutive phosphorylation of Shc proteins in human tumors. Oncogene **11:**899-907.
252. **Pellegrin, S., and H. Mellor.** 2007. Actin stress fibres. J Cell Sci **120:**3491-9.
253. **Pellegrini, M., S. Pacini, and C. T. Baldari.** 2005. p66SHC: the apoptotic side of Shc proteins. Apoptosis **10:**13-8.
254. **Perillo, N. L., K. E. Pace, J. J. Seilhamer, and L. G. Baum.** 1995. Apoptosis of T cells mediated by galectin-1. Nature **378:**736-9.
255. **Peschard, P., and M. Park.** 2007. From Tpr-Met to Met, tumorigenesis and tubes. Oncogene **26:**1276-85.
256. **Plattner, R., L. Kadlec, K. A. DeMali, A. Kazlauskas, and A. M. Pendergast.** 1999. c-Abl is activated by growth factors and Src family kinases and has a role in the cellular response to PDGF. Genes Dev. **13:**2400-11.
257. **Playford, M. P., P. D. Lyons, S. K. Sastry, and M. D. Schaller.** 2006. Identification of a filamin docking site on PTP-PEST. J Biol Chem **281:**34104-12.
258. **Privé, C., and A. Descoteaux.** 2000. *Leishmania donovani* promastigotes evade the activation of mitogen-activated protein kinases p38, c-Jun N-terminal kinase, and

extracellular signal-regulated kinase-1/2 during infection of naive macrophages. Eur. J. Immunol. **30:**2235-44.

259. **Radha, V., C. Sudhakar, and G. Swarup.** 1999. Induction of p53 dependent apoptosis upon overexpression of a nuclear protein tyrosine phosphatase. FEBS Lett. **453:**308-12.
260. **Rafiq, K., M. A. Kolpakov, M. Abdelfettah, D. N. Streblow, A. Hassid, L. J. Dell'Italia, and A. Sabri.** 2006. Role of protein-tyrosine phosphatase SHP2 in focal adhesion kinase down-regulation during neutrophil cathepsin G-induced cardiomyocytes anoikis. J Biol Chem **281:**19781-92.
261. **Raina, D., P. Pandey, R. Ahmad, A. Bharti, J. Ren, S. Kharbanda, R. Weichselbaum, and D. Kufe.** 2005. c-Abl tyrosine kinase regulates caspase-9 autocleavage in the apoptotic response to DNA damage. J. Biol. Chem. **280:**11147-51.
262. **Ravichandran, K. S.** 2001. Signaling via Shc family adapter proteins. Oncogene **20:**6322-30.
263. **Ray, D., Y. Terao, D. Nimbalkar, L. H. Chu, M. Donzelli, T. Tsutsui, X. Zou, A. K. Ghosh, J. Varga, G. F. Draetta, and H. Kiyokawa.** 2005. Transforming growth factor beta facilitates beta-TrCP-mediated degradation of Cdc25A in a Smad3-dependent manner. Mol Cell Biol **25:**3338-47.
264. **Rengan, R., H. D. Ochs, L. I. Sweet, M. L. Keil, W. T. Gunning, N. A. Lachant, L. A. Boxer, and G. M. Omann.** 2000. Actin cytoskeletal function is spared, but apoptosis is increased, in WAS patient hematopoietic cells. Blood **95:**1283-92.
265. **Reuther, G. W., J. E. Buss, L. A. Quilliam, G. J. Clark, and C. J. Der.** 2000. Analysis of function and regulation of proteins that mediate signal transduction by use of lipid-modified plasma membrane-targeting sequences. Methods Enzymol **327:**331-50.
266. **Ridley, A. J., M. A. Schwartz, K. Burridge, R. A. Firtel, M. H. Ginsberg, G. Borisy, J. T. Parsons, and A. R. Horwitz.** 2003. Cell migration: integrating signals from front to back. Science **302:**1704-9.
267. **Riedl, S. J., and G. S. Salvesen.** 2007. The apoptosome: signalling platform of cell death. Nat Rev Mol Cell Biol **8:**405-13.
268. **Riedl, S. J., and Y. Shi.** 2004. Molecular mechanisms of caspase regulation during apoptosis. Nat Rev Mol Cell Biol **5:**897-907.
269. **Rizvi, F. S., M. A. Ouaissi, B. Marty, F. Santoro, and A. Capron.** 1988. The major surface protein of *Leishmania* promastigotes is a fibronectin-like molecule. Eur. J. Immunol. **18:**473-6.
270. **Roberts, L. S., J. Janovy, and G. D. Schmidt.** 2000. Gerald D. Schmidt & Larry S. Roberts' foundations of parasitology, Sixth Edition, 6th ed. McGraw-Hill, Boston.
271. **Rodriguez, J., and Y. Lazebnik.** 1999. Caspase-9 and APAF-1 form an active holoenzyme. Genes Dev **13:**3179-84.
272. **Rogers, S., R. Wells, and M. Rechsteiner.** 1986. Amino acid sequences common to rapidly degraded proteins: the PEST hypothesis. Science **234:**364-8.
273. **Rohatgi, R., L. Ma, H. Miki, M. Lopez, T. Kirchhausen, T. Takenawa, and M. W. Kirschner.** 1999. The interaction between N-WASP and the Arp2/3 complex links Cdc42-dependent signals to actin assembly. Cell **97:**221-31.
274. **Roset, R., L. Ortet, and G. Gil-Gomez.** 2007. Role of Bcl-2 family members on apoptosis: what we have learned from knock-out mice. Front Biosci **12:**4722-30.
275. **Roskoski, R., Jr.** 2005. Src kinase regulation by phosphorylation and dephosphorylation. Biochem. Biophys. Res. Commun. **331:**1-14.

276. **Rottner, K., S. Lommel, J. Wehland, and T. E. Stradal.** 2004. Pathogen-induced actin filament rearrangement in infectious diseases. J. Pathol. **204**:396-406.
277. **Ruest, P. J., N. Y. Shin, T. R. Polte, X. Zhang, and S. K. Hanks.** 2001. Mechanisms of CAS substrate domain tyrosine phosphorylation by FAK and Src. Mol Cell Biol **21**:7641-52.
278. **Ruhland, A., N. Leal, and P. E. Kima.** 2007. *Leishmania* promastigotes activate PI3K/Akt signalling to confer host cell resistance to apoptosis. Cell. Microbiol. **9**:84-96.
279. **Rupinder, S. K., A. K. Gurpreet, and S. Manjeet.** 2007. Cell suicide and caspases. Vascul Pharmacol **46**:383-93.
280. **Russello, S. V., and S. K. Shore.** 2004. SRC in human carcinogenesis. Front Biosci **9**:139-44.
281. **Sacks, D. L.** 2001. Leishmania-sand fly interactions controlling species-specific vector competence. Cell Microbiol **3**:189-96.
282. **Sakai, R., A. Iwamatsu, N. Hirano, S. Ogawa, T. Tanaka, H. Mano, Y. Yazaki, and H. Hirai.** 1994. A novel signaling molecule, p130, forms stable complexes in vivo with v-Crk and v-Src in a tyrosine phosphorylation-dependent manner. Embo J **13**:3748-56.
283. **Salazar, E. P., I. Hunger-Glaser, and E. Rozengurt.** 2003. Dissociation of focal adhesion kinase and paxillin tyrosine phosphorylation induced by bombesin and lysophosphatidic acid from epidermal growth factor receptor transactivation in Swiss 3T3 cells. J Cell Physiol **194**:314-24.
284. **Sangwan, V., G. N. Paliouras, A. Cheng, N. Dubé, M. L. Tremblay, and M. Park.** 2006. Protein-tyrosine Phosphatase 1B Deficiency Protects against Fas-induced Hepatic Failure. J. Biol. Chem. **281**:221-228.
285. **Santoro, M. F., R. R. Annand, M. M. Robertson, Y. W. Peng, M. J. Brady, J. A. Mankovich, M. C. Hackett, T. Ghayur, G. Walter, W. W. Wong, and D. A. Giegel.** 1998. Regulation of protein phosphatase 2A activity by caspase-3 during apoptosis. J Biol Chem **273**:13119-28.
286. **Sastry, S. K., P. D. Lyons, M. D. Schaller, and K. Burridge.** 2002. PTP-PEST controls motility through regulation of Rac1. J. Cell Sci. **115**:4305-16.
287. **Sastry, S. K., Z. Rajfur, B. P. Liu, J. F. Cote, M. L. Tremblay, and K. Burridge.** 2006. PTP-PEST couples membrane protrusion and tail retraction via VAV2 and p190RhoGAP. J. Biol. Chem. **281**:11627-36.
288. **Sato, T., S. Irie, S. Kitada, and J. C. Reed.** 1995. FAP-1: a protein tyrosine phosphatase that associates with Fas. Science **268**:411-5.
289. **Schaller, M. D., and J. T. Parsons.** 1995. pp125FAK-dependent tyrosine phosphorylation of paxillin creates a high-affinity binding site for Crk. Mol Cell Biol **15**:2635-45.
290. **Schlaepfer, D. D., M. A. Broome, and T. Hunter.** 1997. Fibronectin-stimulated signaling from a focal adhesion kinase-c-Src complex: involvement of the Grb2, p130cas, and Nck adaptor proteins. Mol Cell Biol **17**:1702-13.
291. **Schlagenhauf, E., R. Etges, and P. Metcalf.** 1998. The crystal structure of the Leishmania major surface proteinase leishmanolysin (gp63). Structure **6**:1035-46.
292. **Schlein, Y.** 1993. Leishmania and Sandflies: interactions in the life cycle and transmission. Parasitol Today **9**:255-8.
293. **Schlessinger, J., and M. A. Lemmon.** 2003. SH2 and PTB domains in tyrosine kinase signaling. Sci STKE **2003**:RE12.
294. **Seay, M. B., P. L. Heard, and G. Chaudhuri.** 1996. Surface Zn-proteinase as a molecule for defense of *Leishmania mexicana amazonensis* promastigotes against cytolysis inside macrophage phagolysosomes. Infect. Immun. **64**:5129-37.

295. **Sebbagh, M., C. Renvoize, J. Hamelin, N. Riche, J. Bertoglio, and J. Breard.** 2001. Caspase-3-mediated cleavage of ROCK I induces MLC phosphorylation and apoptotic membrane blebbing. Nat. Cell Biol. **3:**346-52.

296. **Seimiya, H., and T. Tsuruo.** 1998. Functional involvement of PTP-U2L in apoptosis subsequent to terminal differentiation of monoblastoid leukemia cells. J Biol Chem **273:**21187-93.

297. **Selbach, M., and S. Backert.** 2005. Cortactin: an Achilles' heel of the actin cytoskeleton targeted by pathogens. Trends Microbiol. **13:**181-9.

298. **Seufferlein, T., and E. Rozengurt.** 1994. Lysophosphatidic acid stimulates tyrosine phosphorylation of focal adhesion kinase, paxillin, and p130. Signaling pathways and cross-talk with platelet-derived growth factor. J Biol Chem **269:**9345-51.

299. **Shen, H. M., and S. Pervaiz.** 2006. TNF receptor superfamily-induced cell death: redox-dependent execution. Faseb J **20:**1589-98.

300. **Shen, Y., G. Schneider, J. F. Cloutier, A. Veillette, and M. D. Schaller.** 1998. Direct association of protein-tyrosine phosphatase PTP-PEST with paxillin. J. Biol. Chem. **273:**6474-81.

301. **Shi, J., and J. E. Casanova.** 2006. Invasion of host cells by *Salmonella typhimurium* requires focal adhesion kinase and p130Cas. Mol. Biol. Cell **17:**4698-708.

302. **Shim, S. R., S. Kook, J. I. Kim, and W. K. Song.** 2001. Degradation of focal adhesion proteins paxillin and p130cas by caspases or calpains in apoptotic rat-1 and L929 cells. Biochem. Biophys. Res. Commun. **286:**601-8.

303. **Sibilia, M., R. Kroismayr, B. M. Lichtenberger, A. Natarajan, M. Hecking, and M. Holcmann.** 2007. The epidermal growth factor receptor: from development to tumorigenesis. Differentiation **75:**770-87.

304. **Silverman, J. M., S. K. Chan, D. P. Robinson, D. M. Dwyer, D. Nandan, L. J. Foster, and N. E. Reiner.** 2008. Proteomic analysis of the secretome of *Leishmania donovani*. Genome Biol. **9:**R35.

305. **Sirois, J., Côté, J-F., Charest, A., Uetani, N., Bourdeau, A., Duncan, S.A., Daniels, E. and Tremblay, M.L.** 2006. Essential function of PTP-PEST during mouse embryonic vascularization, mesenchyme formation, neurogenesis and early liver development. Mech Dev **123:**869-880.

306. **Snapper, S. B., F. Takeshima, I. Anton, C. H. Liu, S. M. Thomas, D. Nguyen, D. Dudley, H. Fraser, D. Purich, M. Lopez-Ilasaca, C. Klein, L. Davidson, R. Bronson, R. C. Mulligan, F. Southwick, R. Geha, M. B. Goldberg, F. S. Rosen, J. H. Hartwig, and F. W. Alt.** 2001. N-WASP deficiency reveals distinct pathways for cell surface projections and microbial actin-based motility. Nat Cell Biol **3:**897-904.

307. **Spencer, S., D. Dowbenko, J. Cheng, W. Li, J. Brush, S. Utzig, V. Simanis, and L. A. Lasky.** 1997. PSTPIP: a tyrosine phosphorylated cleavage furrow-associated protein that is a substrate for a PEST tyrosine phosphatase. J. Cell Biol. **138:**845-60.

308. **Stamm, L. M., M. A. Pak, J. H. Morisaki, S. B. Snapper, K. Rottner, S. Lommel, and E. J. Brown.** 2005. Role of the WASP family proteins for Mycobacterium marinum actin tail formation. Proc. Natl. Acad. Sci. U. S. A. **102:**14837-42.

309. **Stevens, J. M., E. E. Galyov, and M. P. Stevens.** 2006. Actin-dependent movement of bacterial pathogens. Nat. Rev. Microbiol. **4:**91-101.

310. **Streit, S., J. E. Ruhe, P. Knyazev, T. Knyazeva, S. Iacobelli, S. Peter, H. Hoefler, and A. Ullrich.** 2006. PTP-PEST phosphatase variations in human cancer. Cancer Genet Cytogenet **170:**48-53.

311. **Stuart, J. R., F. H. Gonzalez, H. Kawai, and Z. M. Yuan.** 2006. c-Abl interacts with the WAVE2 signaling complex to induce membrane ruffling and cell spreading. J Biol Chem **281:**31290-7.
312. **Stuart, L. M., S. A. Bell, C. R. Stewart, J. M. Silver, J. Richard, J. L. Goss, A. A. Tseng, A. Zhang, J. B. El Khoury, and K. J. Moore.** 2007. CD36 signals to the actin cytoskeleton and regulates microglial migration via a p130Cas complex. J. Biol. Chem. **282:**27392-401.
313. **Stuible, M., K. M. Doody, and M. L. Tremblay.** 2008. PTP1B and TC-PTP: regulators of transformation and tumorigenesis. Cancer Metastasis Rev **27:**215-30.
314. **Stupack, D. G., and D. A. Cheresh.** 2002. Get a ligand, get a life: integrins, signaling and cell survival. J. Cell Sci. **115:**3729-38.
315. **Su, X., T. Zhou, Z. Wang, P. Yang, R. S. Jope, and J. D. Mountz.** 1995. Defective expression of hematopoietic cell protein tyrosine phosphatase (HCP) in lymphoid cells blocks Fas-mediated apoptosis. Immunity **2:**353-62.
316. **Suzuki, J., and T. Shishido.** 2007. Regulation of cellular transformation by oncogenic and normal Abl kinases. J Biochem **141:**453-8.
317. **Tabernero, L., A. R. Aricescu, E. Y. Jones, and S. E. Szedlacsek.** 2008. Protein tyrosine phosphatases: structure-function relationships. Febs J **275:**867-82.
318. **Takada, T., T. Noguchi, K. Inagaki, T. Hosooka, K. Fukunaga, T. Yamao, W. Ogawa, T. Matozaki, and M. Kasuga.** 2002. Induction of apoptosis by stomach cancer-associated protein-tyrosine phosphatase-1. J. Biol. Chem. **277:**34359-66.
319. **Takeda, H., T. Matozaki, Y. Fujioka, T. Takada, T. Noguchi, T. Yamao, M. Tsuda, F. Ochi, K. Fukunaga, S. Narumiya, T. Yamamoto, and M. Kasuga.** 1998. Lysophosphatidic acid-induced association of SHP-2 with SHPS-1: roles of RHO, FAK, and a SRC family kinase. Oncogene **16:**3019-27.
320. **Takekawa, M., F. Itoh, Y. Hinoda, M. Adachi, T. Ariyama, J. Inazawa, K. Imai, and A. Yachi.** 1994. Chromosomal localization of the protein tyrosine phosphatase G1 gene and characterization of the aberrant transcripts in human colon cancer cells. FEBS Lett **339:**222-8.
321. **Takekawa, M., F. Itoh, Y. Hinoda, Y. Arimura, M. Toyota, M. Sekiya, M. Adachi, K. Imai, and A. Yachi.** 1992. Cloning and characterization of a human cDNA encoding a novel putative cytoplasmic protein-tyrosine-phosphatase. Biochem. Biophys. Res. Commun. **189:**1223-30.
322. **Takenawa, T., and H. Miki.** 2001. WASP and WAVE family proteins: key molecules for rapid rearrangement of cortical actin filaments and cell movement. J Cell Sci **114:**1801-9.
323. **Takino, T., M. Tamura, H. Miyamori, M. Araki, K. Matsumoto, H. Sato, and K. M. Yamada.** 2003. Tyrosine phosphorylation of the CrkII adaptor protein modulates cell migration. J Cell Sci **116:**3145-55.
324. **Tanuma, N., K. Nakamura, and K. Kikuchi.** 1999. Distinct promoters control transmembrane and cytosolic protein tyrosine phosphatase epsilon expression during macrophage differentiation. Eur J Biochem **259:**46-54.
325. **Tanuma, N., K. Nakamura, H. Shima, and K. Kikuchi.** 2000. Protein-tyrosine phosphatase PTPepsilon C inhibits Jak-STAT signaling and differentiation induced by interleukin-6 and leukemia inhibitory factor in M1 leukemia cells. J Biol Chem **275:**28216-21.
326. **Taylor, R. C., S. P. Cullen, and S. J. Martin.** 2008. Apoptosis: controlled demolition at the cellular level. Nat Rev Mol Cell Biol **9:**231-41.

327. **Tchilian, E. Z., and P. C. Beverley.** 2006. Altered CD45 expression and disease. Trends Immunol **27**:146-53.
328. **Thalappilly, S., S. Sadasivam, V. Radha, and G. Swarup.** 2006. Involvement of caspase 1 and its activator Ipaf upstream of mitochondrial events in apoptosis. Febs J **273**:2766-78.
329. **Thiakaki, M., B. Kolli, K. P. Chang, and K. Soteriadou.** 2006. Down-regulation of gp63 level in *Leishmania amazonensis* promastigotes reduces their infectivity in BALB/c mice. Microbes Infect. **8**:1455-63.
330. **Tiganis, T., and A. M. Bennett.** 2007. Protein tyrosine phosphatase function: the substrate perspective. Biochem J **402**:1-15.
331. **Tisi, M. A., Y. Xie, T. T. Yeo, and F. M. Longo.** 2000. Downregulation of LAR tyrosine phosphatase prevents apoptosis and augments NGF-induced neurite outgrowth. J. Neurobiol. **42**:477-86.
332. **Tonks, N. K.** 2006. Protein tyrosine phosphatases: from genes, to function, to disease. Nat Rev Mol Cell Biol **7**:833-46.
333. **Tonks, N. K.** 2003. PTP1B: from the sidelines to the front lines! FEBS Lett. **546**:140-8.
334. **Tonks, N. K.** 2005. Redox redux: revisiting PTPs and the control of cell signaling. Cell **121**:667-70.
335. **Tonks, N. K., H. Charbonneau, C. D. Diltz, E. H. Fischer, and K. A. Walsh.** 1988. Demonstration that the leukocyte common antigen CD45 is a protein tyrosine phosphatase. Biochemistry **27**:8695-701.
336. **Tonks, N. K., C. D. Diltz, and E. H. Fischer.** 1988. Purification of the major protein-tyrosine-phosphatases of human placenta. J Biol Chem **263**:6722-30.
337. **Torres, E., and M. K. Rosen.** 2003. Contingent phosphorylation/dephosphorylation provides a mechanism of molecular memory in WASP. Mol Cell **11**:1215-27.
338. **Torres, J., J. Rodriguez, M. P. Myers, M. Valiente, J. D. Graves, N. K. Tonks, and R. Pulido.** 2003. Phosphorylation-regulated cleavage of the tumor suppressor PTEN by caspase-3: implications for the control of protein stability and PTEN-protein interactions. J Biol Chem **278**:30652-60.
339. **Totpal, K., S. Agarwal, and B. B. Aggarwal.** 1992. Phosphatase inhibitors modulate the growth-regulatory effects of human tumor necrosis factor on tumor and normal cells. Cancer Res. **52**:2557-62.
340. **Tsujita, K., S. Suetsugu, N. Sasaki, M. Furutani, T. Oikawa, and T. Takenawa.** 2006. Coordination between the actin cytoskeleton and membrane deformation by a novel membrane tubulation domain of PCH proteins is involved in endocytosis. J Cell Biol **172**:269-79.
341. **Tsutsumi, R., H. Higashi, M. Higuchi, M. Okada, and M. Hatakeyama.** 2003. Attenuation of Helicobacter pylori CagA x SHP-2 signaling by interaction between CagA and C-terminal Src kinase. J Biol Chem **278**:3664-70.
342. **Turk, B., and V. Stoka.** 2007. Protease signalling in cell death: caspases versus cysteine cathepsins. FEBS Lett **581**:2761-7.
343. **Turk, B. E.** 2007. Manipulation of host signalling pathways by anthrax toxins. Biochem. J. **402**:405-17.
344. **van der Flier, S., A. Brinkman, M. P. Look, E. M. Kok, M. E. Meijer-van Gelder, J. G. Klijn, L. C. Dorssers, and J. A. Foekens.** 2000. Bcar1/p130Cas protein and primary breast cancer: prognosis and response to tamoxifen treatment. J Natl Cancer Inst **92**:120-7.

345. **van Zandbergen, G., M. Klinger, A. Mueller, S. Dannenberg, A. Gebert, W. Solbach, and T. Laskay.** 2004. Cutting edge: neutrophil granulocyte serves as a vector for *Leishmania* entry into macrophages. J. Immunol. **173**:6521-5.

346. **Victoir, K., J. Arevalo, S. De Doncker, D. C. Barker, T. Laurent, E. Godfroid, A. Bollen, D. Le Ray, and J. C. Dujardin.** 2005. Complexity of the major surface protease (msp) gene organization in Leishmania (Viannia) braziliensis: evolutionary and functional implications. Parasitology **131**:207-14.

347. **Voth, B. R., B. L. Kelly, P. B. Joshi, A. C. Ivens, and W. R. McMaster.** 1998. Differentially expressed *Leishmania major* gp63 genes encode cell surface leishmanolysin with distinct signals for glycosylphosphatidylinositol attachment. Mol. Biochem. Parasitol. **93**:31-41.

348. **Vuori, K., H. Hirai, S. Aizawa, and E. Ruoslahti.** 1996. Introduction of p130cas signaling complex formation upon integrin-mediated cell adhesion: a role for Src family kinases. Mol Cell Biol **16**:2606-13.

349. **Wade, R., J. Bohl, and S. Vande Pol.** 2002. Paxillin null embryonic stem cells are impaired in cell spreading and tyrosine phosphorylation of focal adhesion kinase. Oncogene **21**:96-107.

350. **Wang, Z., N. Bhattacharya, M. K. Meyer, H. Seimiya, T. Tsuruo, J. A. Tonani, and N. S. Magnuson.** 2001. Pim-1 negatively regulates the activity of PTP-U2S phosphatase and influences terminal differentiation and apoptosis of monoblastoid leukemia cells. Arch Biochem Biophys **390**:9-18.

351. **Webb, J. R., L. L. Button, and W. R. McMaster.** 1991. Heterogeneity of the genes encoding the major surface glycoprotein of Leishmania donovani. Mol Biochem Parasitol **48**:173-84.

352. **Wei, L., Y. Yang, X. Zhang, and Q. Yu.** 2002. Anchorage-independent phosphorylation of p130(Cas) protects lung adenocarcinoma cells from anoikis. J Cell Biochem **87**:439-49.

353. **Weidow, C. L., D. S. Black, J. B. Bliska, and A. H. Bouton.** 2000. CAS/Crk signalling mediates uptake of Yersinia into human epithelial cells. Cell. Microbiol. **2**:549-60.

354. **Weng, L. P., X. Wang, and Q. Yu.** 1999. Transmembrane tyrosine phosphatase LAR induces apoptosis by dephosphorylating and destabilizing p130Cas. Genes Cells **4**:185-96.

355. **Weng, L. P., J. Yuan, and Q. Yu.** 1998. Overexpression of the transmembrane tyrosine phosphatase LAR activates the caspase pathway and induces apoptosis. Curr Biol **8**:247-56.

356. **Wincker, P., C. Ravel, C. Blaineau, M. Pages, Y. Jauffret, J. P. Dedet, and P. Bastien.** 1996. The Leishmania genome comprises 36 chromosomes conserved across widely divergent human pathogenic species. Nucleic Acids Res **24**:1688-94.

357. **Wise, C. A., J. D. Gillum, C. E. Seidman, N. M. Lindor, R. Veile, S. Bashiardes, and M. Lovett.** 2002. Mutations in CD2BP1 disrupt binding to PTP PEST and are responsible for PAPA syndrome, an autoinflammatory disorder. Hum. Mol. Genet. **11**:961-9.

358. **Woelbing, F., S. L. Kostka, K. Moelle, Y. Belkaid, C. Sunderkoetter, S. Verbeek, A. Waisman, A. P. Nigg, J. Knop, M. C. Udey, and E. von Stebut.** 2006. Uptake of *Leishmania major* by dendritic cells is mediated by Fcgamma receptors and facilitates acquisition of protective immunity. J. Exp. Med. **203**:177-88.

359. **World Health Organization** 2008. http://www.who.int/leishmaniasis/disease_epidemiology/en/index.html. [Online.]

360. **Wu, J., A. Katrekar, L. A. Honigberg, A. M. Smith, M. T. Conn, J. Tang, D. Jeffery, K. Mortara, J. Sampang, S. R. Williams, J. Buggy, and J. M. Clark.** 2006. Identification of substrates of human protein-tyrosine phosphatase PTPN22. J Biol Chem **281:**11002-10.

361. **Wu, J. J., and A. M. Bennett.** 2005. Essential role for mitogen-activated protein (MAP) kinase phosphatase-1 in stress-responsive MAP kinase and cell survival signaling. J. Biol. Chem. **280:**16461-6.

362. **Wu, W. S., J. R. Wu, and C. T. Hu.** 2008. Signal cross talks for sustained MAPK activation and cell migration: the potential role of reactive oxygen species. Cancer Metastasis Rev **27:**303-14.

363. **Wu, Y., D. Dowbenko, and L. A. Lasky.** 1998. PSTPIP 2, a second tyrosine phosphorylated, cytoskeletal-associated protein that binds a PEST-type protein-tyrosine phosphatase. J. Biol. Chem. **273:**30487-96.

364. **Wu, Y., S. D. Spencer, and L. A. Lasky.** 1998. Tyrosine phosphorylation regulates the SH3-mediated binding of the Wiskott-Aldrich syndrome protein to PSTPIP, a cytoskeletal-associated protein. J Biol Chem **273:**5765-70.

365. **Yang, Q., D. Co, J. Sommercorn, and N. K. Tonks.** 1993. Cloning and expression of PTP-PEST. A novel, human, nontransmembrane protein tyrosine phosphatase. J. Biol. Chem. **268:**17650.

366. **Yang, W., L. D. Klaman, B. Chen, T. Araki, H. Harada, S. M. Thomas, E. L. George, and B. G. Neel.** 2006. An Shp2/SFK/Ras/Erk signaling pathway controls trophoblast stem cell survival. Dev Cell **10:**317-27.

367. **Yang, Z., D. M. Mosser, and X. Zhang.** 2007. Activation of the MAPK, ERK, following Leishmania amazonensis infection of macrophages. J Immunol **178:**1077-85.

368. **Yao, C., J. E. Donelson, and M. E. Wilson.** 2007. Internal and Surface-Localized Major Surface Proteases of *Leishmania* spp. and Their Differential Release from Promastigotes. Eukaryot. Cell **6:**1905-12.

369. **Yao, C., J. E. Donelson, and M. E. Wilson.** 2003. The major surface protease (MSP or GP63) of Leishmania sp. Biosynthesis, regulation of expression, and function. Mol. Biochem. Parasitol. **132:**1-16.

370. **Yao, C., K. G. Leidal, A. Brittingham, D. E. Tarr, J. E. Donelson, and M. E. Wilson.** 2002. Biosynthesis of the major surface protease GP63 of Leishmania chagasi. Mol. Biochem. Parasitol. **121:**119-28.

371. **Yao, C., J. Luo, C. Hsiao, J. E. Donelson, and M. E. Wilson.** 2005. Internal and surface subpopulations of the major surface protease (MSP) of Leishmania chagasi. Mol Biochem Parasitol **139:**173-83.

372. **Yao, C., J. Luo, P. Storlie, J. E. Donelson, and M. E. Wilson.** 2004. Multiple products of the *Leishmania chagasi* major surface protease (MSP or GP63) gene family. Mol. Biochem. Parasitol. **135:**171-83.

373. **Yao, H., E. Song, J. Chen, and P. Hamar.** 2004. Expression of FAP-1 by human colon adenocarcinoma: implication for resistance against Fas-mediated apoptosis in cancer. Br J Cancer **91:**1718-25.

374. **Yeung, Y. G., S. Soldera, and E. R. Stanley.** 1998. A novel macrophage actin-associated protein (MAYP) is tyrosine-phosphorylated following colony stimulating factor-1 stimulation. J Biol Chem **273:**30638-42.

375. **Yi, T., J. L. Cleveland, and J. N. Ihle.** 1991. Identification of novel protein tyrosine phosphatases of hematopoietic cells by polymerase chain reaction amplification. Blood **78:**2222-8.

376. **Yoshii, S., M. Tanaka, Y. Otsuki, D. Y. Wang, R. J. Guo, Y. Zhu, R. Takeda, H. Hanai, E. Kaneko, and H. Sugimura.** 1999. alphaPIX nucleotide exchange factor is activated by interaction with phosphatidylinositol 3-kinase. Oncogene **18:**5680-90.
377. **Yousefi, S., and H. U. Simon.** 2003. SHP-1: a regulator of neutrophil apoptosis. Semin. Immunol. **15:**195-9.
378. **Zamir, E., and B. Geiger.** 2001. Molecular complexity and dynamics of cell-matrix adhesions. J. Cell Sci. **114:**3583-90.
379. **Zandi, R., A. B. Larsen, P. Andersen, M. T. Stockhausen, and H. S. Poulsen.** 2007. Mechanisms for oncogenic activation of the epidermal growth factor receptor. Cell Signal **19:**2013-23.
380. **Zarubin, T., and J. Han.** 2005. Activation and signaling of the p38 MAP kinase pathway. Cell Res. **15:**11-8.
381. **Zhang, Z., S. Y. Lin, B. G. Neel, and B. Haimovich.** 2006. Phosphorylated alpha-actinin and protein-tyrosine phosphatase 1B coregulate the disassembly of the focal adhesion kinase x Src complex and promote cell migration. J Biol Chem **281:**1746-54.
382. **Zhao, Z., N. F. Zander, D. A. Malencik, S. R. Anderson, and E. H. Fischer.** 1992. Continuous spectrophotometric assay of protein tyrosine phosphatase using phosphotyrosine. Anal Biochem **202:**361-6.
383. **Zhou, Y. W., Y. Komada, H. Inaba, E. Azuma, and M. Sakurai.** 1998. Down-regulation of Fas-associated phosphatase-1 (FAP-1) in interleukin-2-activated T cells. Cell Immunol **186:**103-10.
384. **Zimmermann, K. C., C. Bonzon, and D. R. Green.** 2001. The machinery of programmed cell death. Pharmacol Ther **92:**57-70.
385. **Zuccato, E., E. J. Blott, O. Holt, S. Sigismund, M. Shaw, G. Bossi, and G. M. Griffiths.** 2007. Sorting of Fas ligand to secretory lysosomes is regulated by mono-ubiquitylation and phosphorylation. J Cell Sci **120:**191-9.

8 APPENDIX

5. RESEARCH PERSONNEL: (attach additional sheets if preferred)

Name	Department	Job Title/Classification	Trained in the safe use of biological safety cabinets within the last 3 years? If yes, indicate training date.
Michel Tremblay	Cancer Centre	Principal Invesetigator	
Maxime Halle	Cancer Centre	PhD student	
Serge Hardy	cancer Centre	Post Doc	
Jean Francois Theberge	Cancer Centre	Research Assistant	
Jacinthe Sirois	Cancer Centre	Research Assistant	

6. Briefly describe:

i) the biohazardous material involved (e.g. bacteria, viruses, human tissues, toxins of biological origin) & designated biosafety risk group

cell and tissue culture, use of retroviral DNA, risk group 2 containmnet level 2
use of bacterial culture , risk group 1

ii) the procedures involving biohazards

all cell and tissue culture is done in the biological safetty cabinet which is located in our lab, Rm 715 and in the tissue culture room for the cancer centre, Rm 729. Working surfaces are cleaned and/or decontaminated with disinfecting agent or 70%EtOH both before or after spills. All media is aspirated into containers with inactivating detergent (Diversol BX/A). Contaminated disposable materials (eg plastic tissue culture supplies) are collected in biohazard bags and sealed, before transporting to another room to be autoclaved in a leak-proof container. Contaminated re-usable supplies (eg glass piptettes) are chemically disinfected with Diversol BX/A or bleach before removing from the cell culture room for washing.

iii) the protocol for decontaminating spills

Spills are decontaminated with Diverol BX/A or bleach.

7. Does the protocol present conditions (e.g. handling of large volumes or high concentrations of pathogens) that could increase the hazards?

7. Does the protocol present conditions (e.g. handling of large volumes or high concentrations of pathogens) that could increase the hazards?

No

8. Do the specific procedures to be employed involving genetically engineered organisms have a history of safe use?

yes

9. What precautions will be taken to reduce production of infectious droplets and aerosols?

biological safetly cabinets are used or all infectous agents

10. Will the biohazardous materials in this project expose members of the research team to any risks that might require special training, vaccination or other protective measures? If yes, please explain.

no

11. Will this project produce combined hazardous waste – i.e. radioactive biohazardous waste, biohazardous animal carcasses contaminated with toxic chemicals, etc.? If yes, please explain how disposal will be handled.

no

12. List the biological safety cabinets to be used.

Building	Room No.	Manufacturer	Model No.	Serial No.	Date Certified
McIntyre	715	Nuair	NU-425-300	26052XX	Feb 1, 2005 ~~Nov 10, 2003~~
"	729	Baker Company		SP6952V	Feb 1, 2005
"	"	"		SP11714V	Feb 1, 2005